

ATTACHMENT 1

AR # 2

Revised Underground Injection Control
Permit Applications for FutureGen 2.0



Underground Injection Control Permit Applications for FutureGen 2.0 Morgan County Class VI UIC Wells 1, 2, 3, and 4

SUPPORTING DOCUMENTATION

March 2013

**(Revised May 2013 in accordance with the U.S. Environmental Protection
Agency's Completeness Review)**



Acknowledgment: This material is based upon work supported by the Department of Energy under Award Number DE-FE0001882.

Disclaimer: This report was prepared as an account of work sponsored by an agency of the United States Government. Neither the United States Government nor any agency thereof, nor any of their employees, makes any warranty, express or implied, or assumes any legal liability or responsibility for the accuracy, completeness, or usefulness of any information, apparatus, product, or process disclosed, or represents that its use would not infringe privately owned rights. Reference herein to any specific commercial product, process, or service by trade name, trademark, manufacturer, or otherwise does not necessarily constitute or imply its endorsement, recommendation, or favoring by the United States Government or any agency thereof. The views and opinions of authors expressed herein do not necessarily state or reflect those of the United States Government or any agency thereof.

Contact Information:

FutureGen Industrial Alliance, Inc.
73 Central Park Plaza East
Jacksonville, IL 62650
Telephone: 217/243-8215
Email: info@FutureGenAlliance.org
Homepage: www.FutureGenAlliance.org

COPYRIGHT © 2013 FUTUREGEN INDUSTRIAL ALLIANCE, INC.

ALL RIGHTS RESERVED. NO PART OF THIS REPORT MAY BE REPRODUCED OR TRANSMITTED IN ANY FORM BY ANY MEANS, ELECTRONIC OR MECHANICAL, INCLUDING PHOTOCOPYING, RECORDING OR ANY INFORMATION STORAGE AND RETRIEVAL SYSTEM, WITHOUT PERMISSION FROM THE FUTUREGEN INDUSTRIAL ALLIANCE, INC.

**Underground Injection Control Class VI Permit
Applications for FutureGen 2.0
Morgan County Class VI UIC Wells 1, 2, 3, and 4**

SUPPORTING DOCUMENTATION

Prepared by
FutureGen Industrial Alliance, Inc.
73 Central Park Plaza East
Jacksonville, IL 62650

Prepared for
U.S. Environmental Protection Agency, Region 5
77 West Jackson Boulevard
Chicago, IL 60604

March 2013
(Revised May 2013 in accordance with the U.S. Environmental Protection Agency's
Completeness Review)

Summary

The FutureGen Industrial Alliance (Alliance) prepared this supporting documentation for its Underground Injection Control (UIC) Class VI permit applications for the construction and operation of four injection wells in Morgan County, Illinois, for the injection of carbon dioxide (CO₂). The Alliance is a non-profit membership organization created to benefit the public interest and the interests of science through research, development, and demonstration of near-zero emissions coal technology. It is partnering with the U.S. Department of Energy (DOE) on the FutureGen 2.0 Project.

The Alliance proposes to construct and operate four wells for the injection of CO₂. Permit applications have been prepared for each of the proposed injection wells, with the supporting documentation for each of the wells collectively provided within this document. This supporting documentation was prepared in accordance with the U.S. Environmental Protection Agency's (EPA's) *UIC Control Program for Carbon Dioxide Geologic Sequestration Wells* (The Geological Sequestration [GS] Rule, codified in Title 40 of the Code of Federal Regulations [40 CFR 146.81 et seq.]). The applications and supporting documentation are based on currently available data, including regional data and site-specific data derived from a stratigraphic well drilled by the Alliance in late 2011 near the site of the proposed injection wells.

The proposed Morgan County CO₂ storage site is 11 mi (18 km) northeast of the City of Jacksonville (see Figure S.1), and is located under agricultural land. The Alliance plans to inject approximately 1.1 million metric tons (MMT) of CO₂ annually into the Mount Simon Sandstone over 20 years, for a total of 22 MMT. The CO₂ for injection will be captured from the nearby Meredosia, Illinois, coal-fueled power plant, which will be repowered with oxy-combustion and carbon capture technology. The CO₂ will be captured from the power plant and then piped underground approximately 30 mi to the storage site for injection and permanent storage. Figure S.2 is a schematic of the FutureGen 2.0 Project showing the integration of the repowered oxy-combustion power plant, transport of CO₂ by buried pipeline, and injection of CO₂ for permanent storage.

Figure S.3 shows the stratigraphy at the Morgan County CO₂ storage site. The four injection wells will be directionally drilled from a single well pad and completed within a permeable layer of the Cambrian-aged Mount Simon Sandstone approximately 4,000 ft below ground surface (bgs) (the "injection zone"). The Alliance proposes this injection zone because it is of sufficient depth, thickness, porosity, and permeability to contain the proposed 22 MMT of CO₂. This proposed injection zone has demonstrated reservoir capacity in natural-gas storage facilities elsewhere in the Illinois Basin and contains a hypersaline aquifer that is in excess of recommended Safe Drinking Water Act standards and is not considered to be of beneficial use.

The injection zone is overlain by the Eau Claire Formation, a thick regional layer of predominantly sandstone that is of sufficient thickness, lateral continuity, and has low enough permeabilities to serve as the primary confining zone or caprock. No faults or fractures were identified based on geophysical well logs of the stratigraphic well and seismic analysis of the site. The Eau Claire Formation is a carbonate and shale unit that has been proven to be an effective confining zone at 38 natural-gas storage reservoirs in Illinois. The Morgan County CO₂ storage site affords a secondary confining zone – the Franconia Formation – for additional protection of underground sources of drinking water (USDWs).

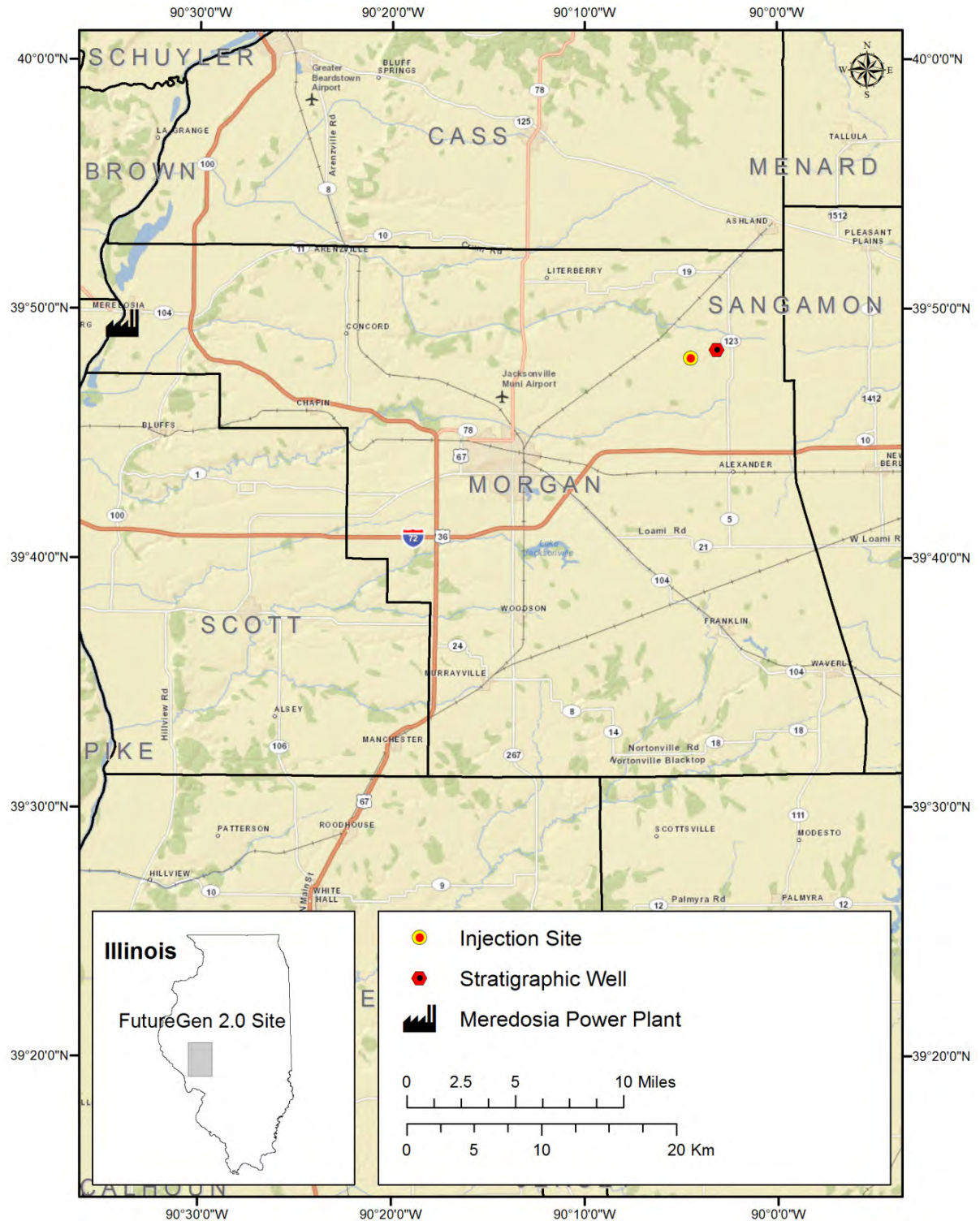


Figure S.1. Illinois Map Showing Morgan County and the Location of the Injection Well Pad

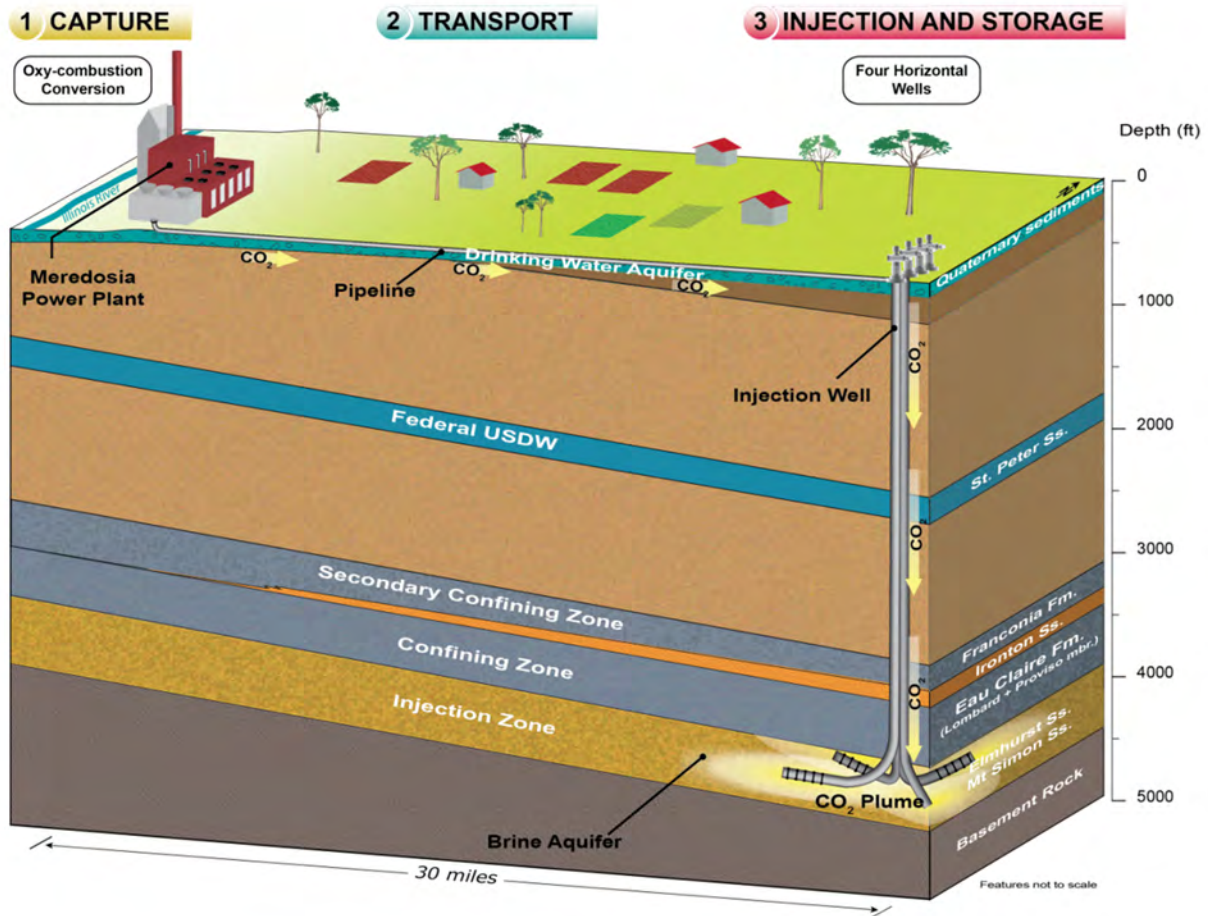


Figure S.2. Graphical Overview of the Conceptual Design of the CO₂ Storage Site

At the proposed Morgan County site, all known water-supply wells are completed in the surficial sediments (<150 ft bgs). For the purpose of the permit applications and supporting documentation, the deeper St. Peter Sandstone is considered the lowermost USDW based on a water sample collected at the stratigraphic well that was 3,700 ppm of total dissolved solids, and below the federal regulatory upper limit of 10,000 ppm for drinking water aquifers. While recognized as a federal USDW, the St. Peter Sandstone is not recognized by the State of Illinois as a suitable source for potable water at the Morgan County storage site.

The supporting documentation that accompanies the Alliance’s UIC permit applications demonstrates that the injection zone is of sufficient capacity and the confining zone is of sufficient thickness and integrity for the site to permanently store the CO₂ in a manner that is protective of USDWs. The application is based on regional and site-specific data derived from the stratigraphic well that was specifically drilled in support of this UIC application in late 2011 near the site of the proposed injection wells. These data were used as input to a numerical model that was used to delineate the Area of Review (AoR) and to optimize the storage site design.

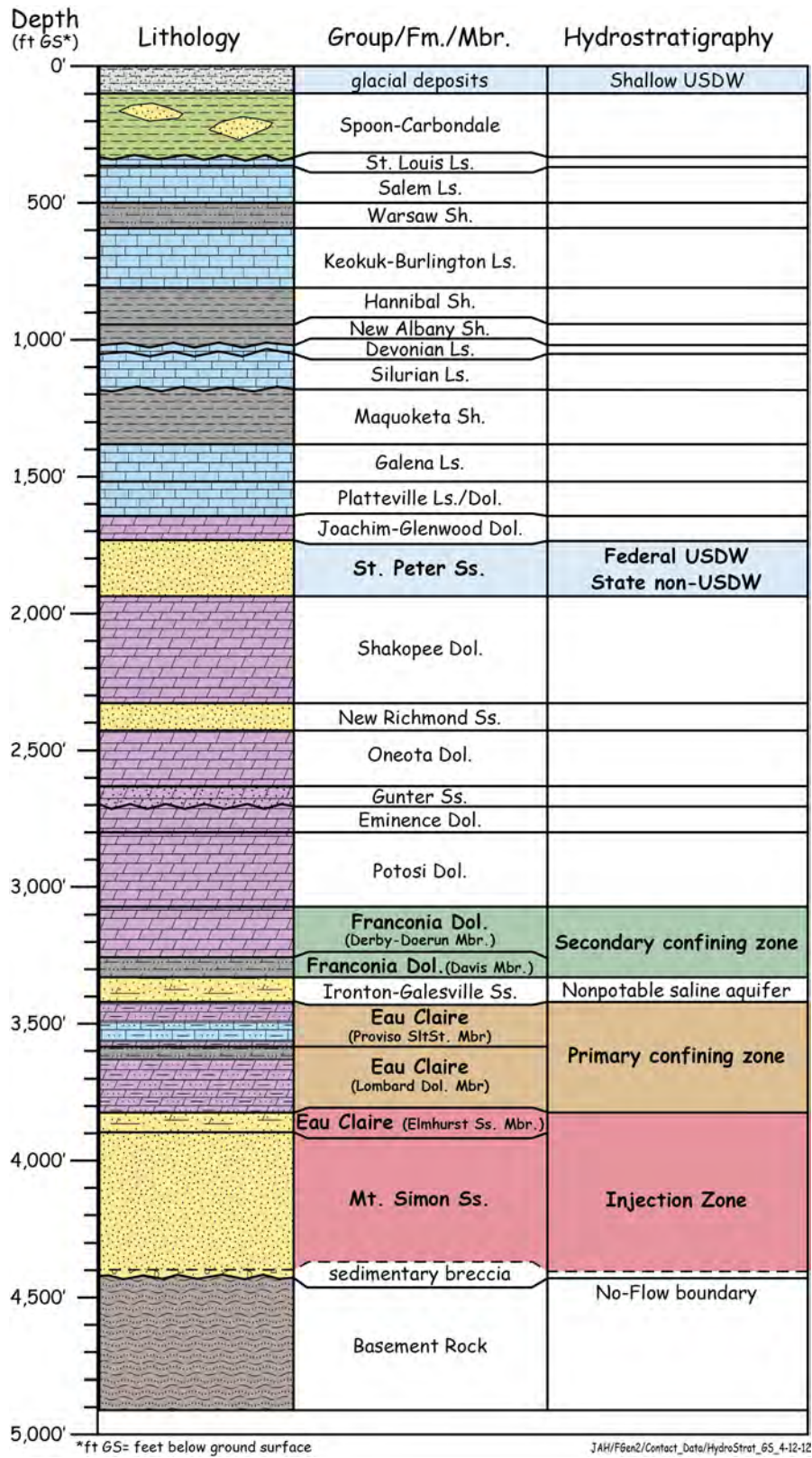


Figure S.3. Stratigraphy and Proposed Injection and Confining Zones at the Morgan County CO₂ Storage Site

Area of Review

The Alliance has defined the AoR (the region encompassing the CO₂ storage site where particular attention must be paid to USDW protection) as the projected lateral and vertical migration of the CO₂ plume from the start of injection until the lateral spread of the plume ends (approximately 5 years after injection stops). To identify this plume area, the Alliance used the STOMP-CO₂ simulator to model the coupled hydrologic, chemical, thermal processes, and chemical interactions with aqueous fluids and rock minerals. The plume is identified as the volume in which 99 percent of the mass resides. This volume is determined from the numerical model and the resulting map area is displayed in Figure S.4.

Also shown in Figure S.4 is a larger 25-mi² (65-km²) area that represents an expanded survey area used to identify the existence of any confining zone penetrations (i.e., existing wells that may penetrate the caprock). Although numerous wells are located within the expanded survey area that includes the AoR, none other than the Alliance's stratigraphic well penetrates the injection zone, the confining zone, or the secondary confining zone. Within the AoR itself, there are three other existing deep wells, none of which penetrates beyond the Maquoketa Shale (see Figure S.3). Because no wells within the AoR could serve as conduits for the movement of fluids from the injection zone into USDWs, no corrective actions on existing wells will need to be taken.

Surface bodies of water and other pertinent surface features (including structures intended for human occupancy), administrative boundaries, and roads within the AoR and the expanded survey area are shown in Figure S.4. There are no subsurface cleanup sites, mines, quarries, or Tribal lands within this area.

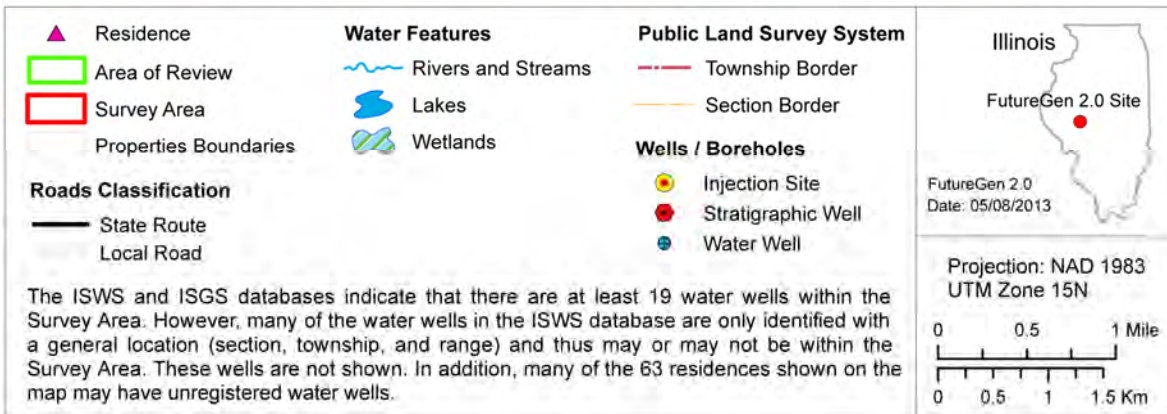
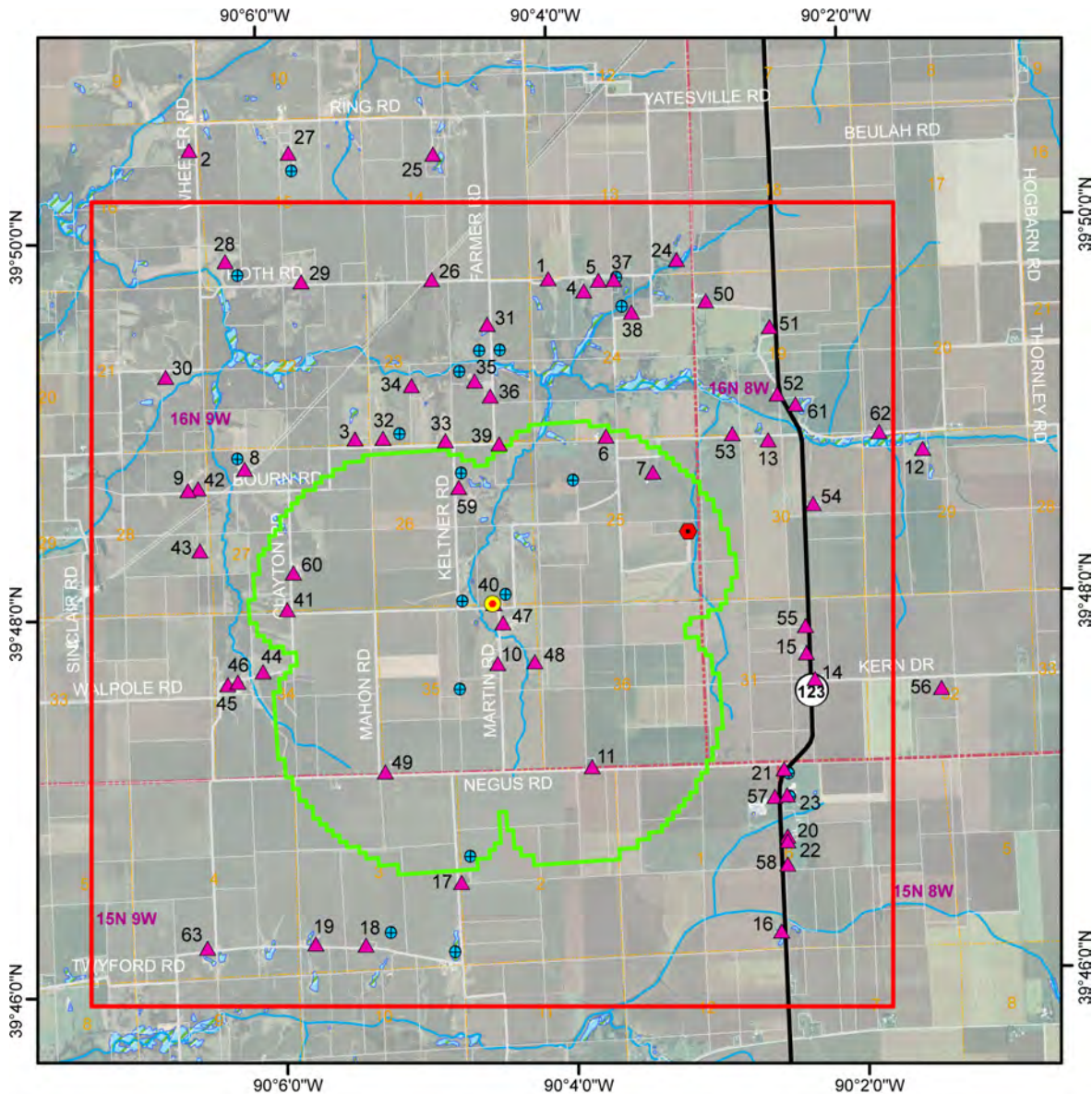


Figure S.4. Map of Residences, Water Wells, and Surface Water Features Within the Delineated AoR and Survey Area

Construction and Operations Plan

At the Meredosia Power Plant, the captured CO₂ will be purified (at least 97 percent purity), dehydrated, and compressed to 2,100 psig before entering the CO₂ pipeline. At these conditions, the CO₂ will be in a dense fluid phase, non-corrosive and non-flammable. The CO₂ pressure will decrease as the CO₂ travels the length of the pipeline to the CO₂ storage site. At the injection wellhead, the pressure is estimated to be between 1,100 and 1,900 psi. The approximately 30-mile (48-km) pipeline will be 10 to 12 in. (25 to 30 cm) in diameter and have a design flow rate of 1.1 MMT/yr (57.3 mmscf/d).

The storage site design was optimized for receiving the CO₂ at a rate of 1.1 MMT/yr. The four horizontal injection well design affords a number of advantages over the more common vertical injection well design. The horizontal wells will minimize the required injection pressures, which for this design will be less than 450 psi above the natural formation pressures. This provides additional protection of the confining layer and eliminates the need for some surface infrastructure such as booster pumps. The “thin” CO₂ plume that results from horizontal wells will also stabilize faster than if the CO₂ were to be injected over a longer vertical interval.

The injection wells will be built with a protection system that will control the injection of the CO₂ and provide a means to safely halt CO₂ injection in the event of an injection well or equipment failure. The injection process will be monitored by an integrated system of equipment and instrumentation that will be capable of detecting whether injection conditions are out of acceptable limits and responding by either adjusting conditions or halting injection. The system is designed to operate automatically with manual overrides.

Testing and Monitoring Plan

An extensive monitoring, verification, and accounting system will be implemented to verify that injected CO₂ is effectively contained within the injection zone. The objectives of the monitoring program are to track the lateral extent of CO₂ within the injection zone, characterize any geochemical or geomechanical changes that occur within the injection and confining zones that may affect containment, and to track the areal extent of the injected CO₂ through indirect monitoring techniques such as geophysical and surveillance methods. The monitoring network, shown in Figure S.5, will be designed to account for and verify the location of all CO₂ injected into the ground. It will include three monitoring wells in the injection zone and a monitoring well above the confining zone to verify CO₂ has not migrated into that zone. In addition, a groundwater monitoring well will be completed in the St. Peter Formation to be protective of this lowermost federal USDW. Monitoring of the site will continue for 50 years after injection has ceased.

A *vertical well* is drilled from the ground surface to a specified completion depth in a straight line.

A *horizontal well* is drilled from the ground surface to a specified depth and then curved to proceed in a horizontal direction. The curved section is referred to as a lateral.

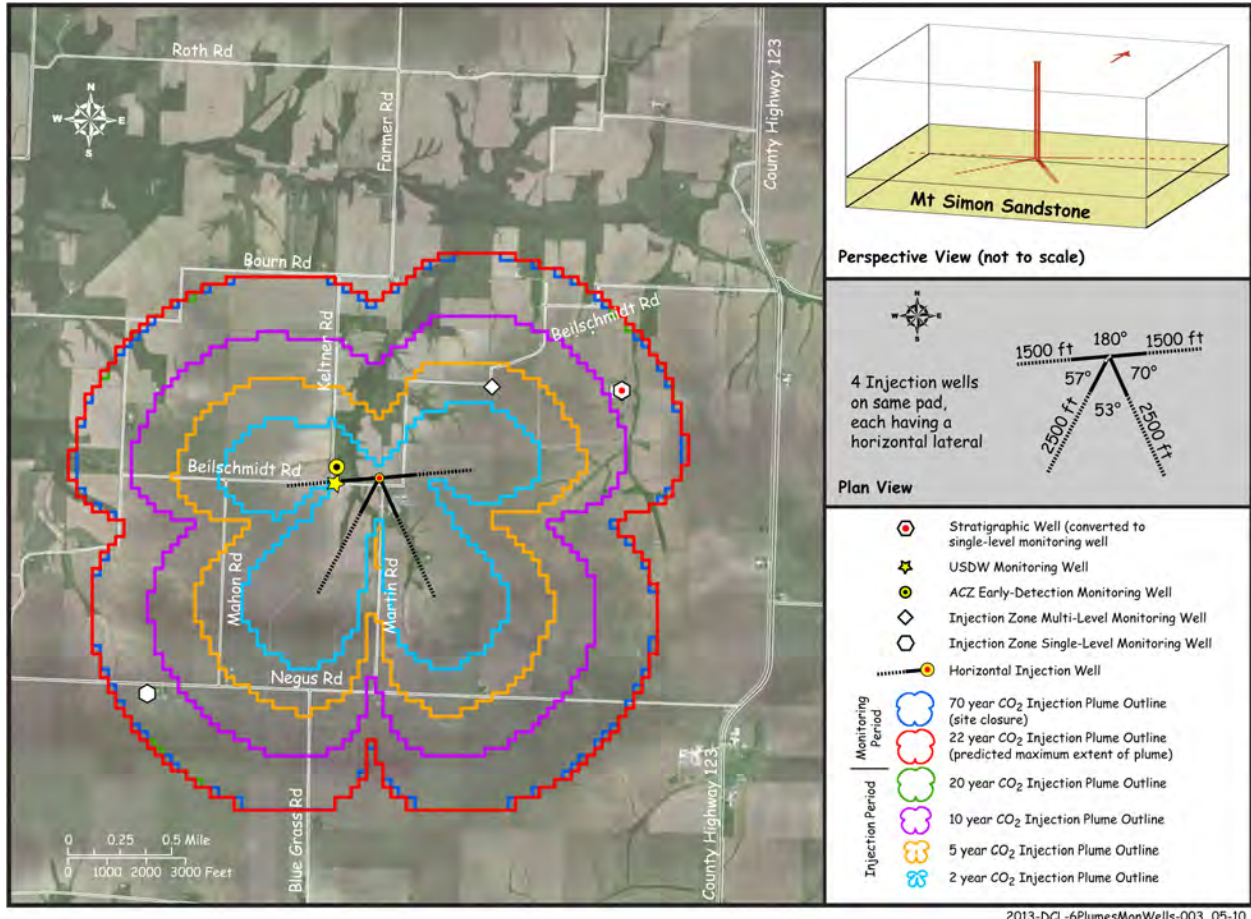


Figure S.5. Nominal Well Network Layout

Injection Well Plugging Plan

After injection ceases, the injection wells will be plugged with cement to ensure that they do not provide a conduit from the injection zone to a USDW or the ground surface. Post-injection monitoring will include a combination of groundwater monitoring, storage zone pressure monitoring, and geophysical monitoring of the Morgan County CO₂ storage site. The monitoring locations, methods, and schedule will be designed to show the position of the CO₂ plume and demonstrate that USDWs are not being endangered.

Post-Injection Site Care and Site Closure Plan

Post-injection monitoring will include a combination of groundwater monitoring, storage zone pressure monitoring, and geophysical monitoring of the Morgan County CO₂ storage site. The monitoring locations, methods, and schedule are designed to show the position of the CO₂ plume and demonstrate that USDWs are not being endangered.

After the active injection phase, the surface infrastructure will be reduced and the remaining areas reclaimed and returned to their pre-development condition. All unneeded gravel pads, access roads, and surface facilities will be removed, and the land will be reclaimed for agricultural or other pre-development uses.

Site closure will occur at the end of the post-injection site care period. Site closure activities will include decommissioning remaining surface equipment, plugging monitoring wells, restoring the site, and preparing and submitting site closure reports. All remaining surface facilities will be removed, including buildings, access roads and parking areas, sidewalks, underground electric and telecommunication facilities, and fencing. The land will be reclaimed for agricultural or other pre-development uses.

Emergency and Remedial Response Plan

The Alliance will develop a comprehensive Emergency and Remedial Response Plan for its Morgan County CO₂ storage site, indicating what actions would be necessary in the unlikely event of an emergency at the site. The plan will ensure that site operators know which entities and individuals are to be notified and what actions need to be taken to expeditiously mitigate any emergency situation and protect human health and safety and the environment, including USDWs. If an adverse event occurred, a variety of emergency or remedial responses would be deployed depending on the circumstances (e.g., the location, type, and volume of a release) to protect USDWs.

The entire CO₂ storage project is focused on retention of the CO₂ in the injection zone.

Financial Responsibility Plan

The Alliance has developed a plan to maintain financial responsibility for the construction, operation, closure, and monitoring of the proposed injection wells and to undertake any emergency or remedial actions that may be necessary. To ensure that sufficient funds will be available, the Alliance has obtained an estimate of the cost of hiring a third party to undertake any necessary actions to protect USDWs within the AoR. Funding for performing any needed corrective actions will be deposited in a CO₂ Storage Trust Fund that will be available during all phases of the project. The Alliance will also obtain a third-party insurance policy that would be available for conducting any emergency or remedial response actions.

Conclusion

The Alliance prepared its Class VI UIC permit applications and supporting documentation to demonstrate that 1) the proposed Morgan County CO₂ storage site comprises an injection zone of sufficient areal extent, thickness, porosity, and permeability to receive up to 22 MMT of CO₂ over 20 years; and 2) the confining zone and secondary confining zone are free of faults and fractures and are of sufficient areal extent and integrity to contain the injected CO₂, allowing the injection of CO₂ at the proposed pressures and volumes without initiating or propagating fractures in the confining zones. These findings are supported by the results of the drilling of a stratigraphic well that provided site-specific geologic data as well as available regional data from sources such as the Illinois State Geological Survey.

The Alliance has developed comprehensive construction and operations, testing and monitoring, injection well plugging, and post-injection site care and site closure plans, as well as an emergency and remedial response plan, to protect USDWs. To ensure that sufficient funds are available to undertake these actions, the Alliance has also developed a financial responsibility plan.

The Alliance is confident that its permit applications and supporting documentation demonstrate compliance with EPA’s GS Rule. Table S.1 provides a crosswalk between the regulatory requirements in that rule and the organization of the Alliance’s supporting documentation.

Table S.1. Crosswalk Between Applicable Regulatory Provisions in the GS Rule and the Alliance UIC Permit Application Supporting Documentation

GS Rule – Regulatory Requirements	Alliance UIC Permit Application
40 CFR 146.82, Required Class VI permit information	Chapter 1, Introduction Chapter 2, Conceptual Model of the Site Based on Geology and Hydrology
40 CFR 146.83, Minimum criteria for siting	Chapter 2, Conceptual Model of the Site Based on Geology and Hydrology
40 CFR 146.84, Area of review and corrective action	Chapter 3, Area of Review and Corrective Action Plan
40 CFR 146.85, Financial responsibility	Chapter 9, Financial Responsibility
40 CFR 146.86, Injection well construction requirements	Chapter 4, Construction and Operations Plan
40 CFR 146.87, Logging, sampling, and testing prior to injection well operation	Chapter 4, Construction and Operations Plan
40 CFR 146.88, Injection well operating requirements	Chapter 4, Construction and Operations Plan
40 CFR 146.89, Mechanical integrity	Chapter 5, Testing and Monitoring Plan
40 CFR 146.90, Testing and monitoring requirements	Chapter 5, Testing and Monitoring Plan
40 CFR 146.91, Reporting requirements	throughout
40 CFR 146.92, Injection well plugging	Chapter 6, Injection Well-Plugging Plan
40 CFR 146.93, Post-injection site care and site closure	Chapter 7, Post-Injection Site Care and Site Closure Plan
40 CFR 146.94, Emergency and remedial response	Chapter 8, Emergency and Remedial Response Plan
40 CFR 146.95, Class VI injection depth waiver requirements	Not applicable

Acronyms and Abbreviations

°C	degrees Celsius (or Centigrade)
°F	degree(s) Fahrenheit
2D	two-dimensional
3C	three-component
3D	three-dimensional
ac	acre(s)
ACZ	Above Confining Zone
ADM	Archer Daniels Midland
AFL	Annular Flow Log
AIC	Akaike information criterion
Al	aluminum
Alliance	FutureGen Industrial Alliance, Inc.
AoR	Area of Review
API	American Petroleum Institute
APT	annular pressure test
As	arsenic
ASTM	American Society for Testing and Materials
ASU	air separation unit
B	boron
bbl	barrel(s)
bgs	below ground surface
bkb	below the kelly bushing
BTC	buttress thread coupling
C	carbon
Ca	calcium
CAA	Clean Air Act
CAAPP	Clean Air Act Permit Program
CaCl ₂	calcium chloride
CBL	cement bond log
CCS	carbon capture and storage
Cd	cadmium
CFR	Code of Federal Regulations

CH ₄	methane
Cl	chlorine
cm	centimeter(s)
cm/sec	centimeter(s) per second
CMR	compensated magnetic resonance
CO	carbon monoxide
CO ₂	carbon dioxide
cP	centipoise
CPU	compression unit
Cr	chromium
CRDS	cavity ring-down laser spectroscopy
CSIRO	Commonwealth Scientific and Industrial Research Organisation
CWA	Clean Water Act
d	day(s)
DCS	Distributed Control System
DIC	dissolved inorganic carbon
DIS	discriminator
DO	dissolved oxygen
DOE	U.S. Department of Energy
Dol	dolomite
DST	drill-stem test
DTS	distributed temperature sensing
ECD	electron capture detector
EIS	environmental impact statement
ELAN	Elemental Analysis
EPA	U.S. Environmental Protection Agency
ERT	electrical resistivity tomography
ESP	electrostatic precipitator or electric submersible pump
EUE	external upset end
F	fluorine
FBP	Formation Break-Down Pressure
FCP	fracture closure pressure
Fe	iron
FEED	Front-End Engineering Design
FG1	FutureGen stratigraphic well

FGD	flue-gas desulphurization
FIT	Formation Integrity Test
FL	Flux Leakage
FPP	fracture propagation pressure
FR	Federal Register
ft	foot(feet)
ft/min	foot(feet) per minute
ft ³	cubic foot(feet)
FTS	Flow-Through Sampler
$\mu\text{g}/\text{m}^3$	microgram(s) per cubic meter
G	ground acceleration
g	gram(s)
g/cc	gram(s) per cubic centimeter
g/cm ³	gram(s) per cubic centimeter
gal	gallon(s)
GAP	U.S. Geological Survey Gap Analysis Program
GIE	Gulf Interstate Engineering
gpd	gallon(s) per day
gpm	gallon(s) per minute
GPS	global positioning systems
GR	gamma ray survey log
GS	geological sequestration
H ₂ S	hydrogen sulfide
ha	hectare(s)
HCl	hydrochloric (acid)
HCO ₃	bicarbonate
HDPE	high-density polyethylene
Hg	mercury
HMI	Human Machine Interface
hp	horse power
hr	hour(s)
I.D.	inner diameter
ICL	imaging caliper tool
ICP	inductively coupled plasma
ID	identification

IDNR	Illinois Department of Natural Resources
IEPA	Illinois Environmental Protection Agency
ILCS	Illinois Compiled Statutes
ILOIL	Illinois Oil and Gas Resources (Internet Map Service)
in.	inch(es)
InSAR	Interferometric Synthetic Aperture Radar
INW	Instrumentation Northwest
IRMS	isotope ratio mass spectrometry
ISGS	Illinois State Geological Survey
ISIP	Instantaneous Shut-In Pressure
ISWS	Illinois State Water Survey
K	potassium (or thousand)
KB	kelly bushing
KCl	potassium chloride
kg/m ³	kilogram(s) per cubic meter
Kh	horizontal permeability; permeability parallel to sedimentary layering
km	kilometer(s)
ksi	kilopound(s) per square inch
k-s-p	permeability-saturation-capillary pressure
Kv	vertical permeability; permeability perpendicular to sedimentary layering
kW	kilowatt(s)
L	liter(s)
lb	pound(s)
lbm	pound-mass
LC/MS	liquid chromatography/mass spectrometry
LOP	Leak-Off Pressure
Ls	limestone
LT	Limit Test
LTC	long thread coupling
μMHOS/cm	micromho(s) per centimeter
mBq	millibecquerel(s)
Mbr	geologic member (unit)
MD	measured depth
mD	millidarcy(ies)
mD-ft	millidarcy foot(feet)

MDNR	Missouri Department of Natural Resources
MDT	Modular Formation Dynamics Tester
MESPOP	maximum extent of the separate-phase plume or pressure
Mg	magnesium
mg	milligram(s)
mg/kg	milligram(s) per kilogram
mg/m ³	milligram(s) per cubic meter
Mgd	million gallons per day
mi	mile(s)
mi ²	square mile(s)
MICP	mercury injection capillary pressure
mGal	milliGal(s)
min	minute(s)
MIP	maximum injection pressure
MIT	mechanical integrity test(ing) or Massachusetts Institute of Technology
mmscf	million standard cubic (foot)feet
mmscfd	million standard cubic (foot)feet per day
MMT	million metric ton(s)
MMT/yr	million metric ton(s) per year
MMTA	million metric tons per annum
Mn	manganese
MPa	megapascal(s)
mph	mile(s) per hour
ms	millisecond(s)
MS	microseismic or mass spectrometry
MSL	mean sea level
MT	magnetotelluric or metric ton(nes)
MTC	metal to metal seal
mV	millivolt(s)
MVA	Monitoring, Verification, and Accounting
MW(e)	megawatt electric
N	nitrogen
N ²	nitrogen
NA	not applicable
Na	sodium
NACE	National Association of Corrosion Engineers
NaCl	sodium chloride

NAD	North American Datum
NaAlCO ₃ (OH) ₂)	dawsonite
NEPA	National Environmental Policy Act of 1969, as amended
NETL	National Environmental Technology Laboratory
Ni	nickel
NO ₂	nitrogen oxide
NOG	naturally occurring gas
NO _x	nitrogen oxides
NPDES	National Pollutant Discharge Elimination System
NPT	National Pipe Threads
O ₂	oxygen
O.D.	outside diameter
OES	optical emission spectrometry
OG	(IDNR's) Division of Oil and Gas
OGW	oil and gas well
OPID	Operator Identification Number
P	phosphorus
Pb	lead
PBTD	plugged-back depth
PDC	polycrystalline diamond compact drilling bit
PDCB	perfluorodimethylcyclobutane
PDCH	perfluoro-1,2-dimethylcyclohexane
PEB	plain-end and beveled
PETE	polyethylene terephthalate
PFBA	pentafluorobenzoic acid
PFT	referred to as perfluorinated tracers
PIGN	Gamma-Neutron Porosity (Schlumberger ELAN porosity log/survey)
PHIT	Total Porosity (Schlumberger ELAN porosity log/survey)
PIGE	Effective Porosity (Schlumberger ELAN porosity log/survey)
PLC	programmable logic controller
PLL	Pollution Legal Liability
PM	particulate matter
PM ₁₀	particulate matter with an aerodynamic diameter of less than 10 microns
PM _{2.5}	particulate matter with an aerodynamic diameter of less than 2.5 microns
PNNL	Pacific Northwest National Laboratory
PNWD	(Battelle-) Pacific Northwest Division
ppb	parts per billion

ppbv	parts per billion on a volumetric basis
ppg	pound(s) per gallon
ppm	parts per million
pptv	parts per trillion on a volumetric basis
psi	pounds per square inch
psia	pounds per square inch, absolute
psig	pound-force per square inch gauge (or pounds per square inch gauge)
PTCH	perfluorotrimethylcyclohexane
PVC	polyvinyl chloride
QA	Quality Assurance
QMC	quasi Monte Carlo
RAT	radioactive tracer
RCI	(Tool and Baker's) Reservoir Characterization Instrument
RCRA	Resource Conservation and Recovery Act
RH	relative humidity
Rn	radon
RTU	remote terminal unit
Rwa	water resistivity
$\mu\text{S/cm}$	microsiemen(s) per centimeter
s	second(s)
S	sulfur
SAR	synthetic aperture radars
Sb	antimony
SBT	segmented bond tool
scCO ₂	supercritical carbon dioxide
SCMT	slim cement mapping tool
SDWA	Safe Drinking Water Act
Se	selenium
sec	second(s)
SEM	scanning electron microscopy
SEM/EDX	scanning electron microscopy with energy dispersive x-ray (analysis)
SF ₆	sulfur hexafluoride
SG	shallow gas (collector)
Sh	shale
SIC	Standard Industrial Classification

SltSt	siltstone
SO _x	sulfur oxides
SpC	specific conductance
Sr	strontium
Ss	sandstone
STOMP	Subsurface Transport Over Multiple Phases
STP	standard temperature and pressure
SWC	side-wall core
SWPPP	Storm Water Pollution Prevention Plan
TD	total depth
TDAS	Tubular Design and Analysis System
TDS	total dissolved solids
THPO	Tribal Historic Preservation Office
TI	thallium
TOC	total organic carbon
TVD	total vertical depth
UCI	Ultrasonic Casing Imager
UIC	Underground Injection Control
USDW	underground sources of drinking water
USI	ultrasonic Imager
UTM	Universal Transverse Mercator
V	vanadium
VdB	vibration decibel(s)
VDL	variable-density log
VIM	vertically integrated mass
VIMPA	vertically integrated mass per unit area
VSP	vertical seismic profile(ing)
W	watt(s)
WAPMMS	well annular pressure maintenance and monitoring system
WGNHS	Wisconsin Geological and Natural History Survey
WS-CRDS	wavelength-scanned cavity ring-down spectroscopy
XRD	x-ray diffraction
X-Z	cross-section

yd ³	cubic yard(s)
yr	year(s)
Zn	zinc

Contents

Summary	iii
Area of Review	vii
Construction and Operations Plan	ix
Testing and Monitoring Plan	ix
Injection Well Plugging Plan.....	x
Post-Injection Site Care and Site Closure Plan.....	x
Emergency and Remedial Response Plan.....	xi
Financial Responsibility Plan	xi
Conclusion	xi
Acronyms and Abbreviations	xiii
1.0 Introduction	1.1
1.1 Project Overview.....	1.1
1.1.1 FutureGen Alliance	1.1
1.1.2 The FutureGen 2.0 Project	1.3
1.1.3 Proposed CO ₂ Storage System	1.3
1.2 Required Administrative Information	1.7
1.3 Supporting Documentation Contents and Organization.....	1.9
1.4 References	1.11
2.0 Geology and Hydrology	2.1
2.1 Geology	2.1
2.1.1 Regional Geology.....	2.3
2.1.2 Major Stratigraphic Units.....	2.8
2.1.3 Site Geology.....	2.13
2.2 Injection Zone Water Chemistry	2.21
2.3 Geologic Structure.....	2.22
2.3.1 Site Geologic Structure	2.22
2.4 Geomechanical Information.....	2.30
2.4.1 Karst	2.30
2.4.2 Local Crustal Stress Conditions	2.31
2.4.3 Elastic Moduli and Fracture Gradient	2.32
2.5 Seismic History of Region	2.35
2.5.1 Regional Topography and Geomorphology	2.36
2.5.2 Site Surface Topography	2.37
2.6 Groundwater.....	2.38
2.6.1 Surficial Aquifer System.....	2.38
2.6.2 Upper-Bedrock Aquifer System.....	2.42

2.6.3	Lower-Bedrock Aquifer System	2.43
2.7	Site Evaluation of Mineral Resources	2.49
2.8	Wells Within the Survey Area	2.50
2.9	Conclusion.....	2.54
2.10	References	2.55
3.0	Area of Review and Corrective Action Plan	3.1
3.1	Area of Review	3.1
3.1.1	Description of Simulator	3.2
3.1.2	Physical Processes Modeled.....	3.3
3.1.3	Conceptual Model	3.3
3.1.4	Numerical Model Implementation	3.23
3.1.5	Representative Case Scenario Description.....	3.26
3.1.6	Computational Model Results	3.27
3.1.7	Method for Delineating the AoR from Model Results	3.37
3.1.8	Delineation of the AoR	3.38
3.1.9	Periodic Reevaluation of AoR.....	3.39
3.1.10	Parameter Sensitivity and Uncertainty	3.41
3.2	Corrective Action Plan	3.43
3.2.1	Identification of Primary Confining Zone Penetrations	3.43
3.2.2	Corrective Actions.....	3.45
3.3	References	3.47
4.0	Construction and Operations Plan	4.1
4.1	Operating Data	4.1
4.1.1	Source of CO ₂	4.1
4.1.2	Chemical and Physical Characteristics of the CO ₂ Stream	4.2
4.1.3	Daily Rate and Volume and/or Mass and Total Anticipated Volume and/or Mass of the CO ₂ Stream	4.2
4.1.4	Pressure and Temperature of CO ₂ Delivered to the Storage Site	4.2
4.2	Well Design.....	4.3
4.2.1	Average and Maximum Wellhead Injection Pressure	4.3
4.2.2	Casing and Tubing Program.....	4.6
4.2.3	Cementing Program.....	4.11
4.2.4	Packer	4.12
4.2.5	Annular Fluid	4.13
4.2.6	Wellhead.....	4.13
4.2.7	Well Openings to Formation	4.15
4.2.8	Schematic of the Subsurface Construction Details of the Well	4.16
4.2.9	Pre-Operational Formation Testing.....	4.19
4.2.10	Wireline Logging	4.19

4.2.11	Coring.....	4.21
4.3	Demonstrating the Well’s Mechanical Integrity Prior to Injection	4.21
4.4	Stimulation Program	4.22
4.5	References	4.22
5.0	Testing and Monitoring Plan	5.1
5.1	Conceptual Monitoring Network Design	5.2
5.1.1	Environmental Monitoring Considerations	5.3
5.1.2	Numerical Modeling	5.4
5.1.3	Defining the Area of Review.....	5.5
5.1.4	Monitoring Well Network.....	5.5
5.2	Monitoring Activities	5.9
5.2.1	Monitoring Program Summary	5.9
5.2.2	Groundwater Quality and Geochemistry Monitoring.....	5.17
5.2.3	Injection Zone Monitoring	5.23
5.2.4	CO ₂ Injection Process Monitoring	5.26
5.3	Injection Well Testing and Monitoring	5.27
5.3.1	Pressure Fall-Off Testing	5.27
5.3.2	Mechanical Integrity Testing During Service Life of Well.....	5.28
5.3.3	Well Annulus Pressure Maintenance and Monitoring System.....	5.33
5.3.4	Injection Well Control and Alarm System.....	5.34
5.4	Monitoring, Verification, and Accounting	5.34
5.5	Schedule	5.35
5.6	Data Management	5.35
5.7	Testing and Monitoring Plan Maintenance	5.37
5.8	Quality Assurance and Surveillance Plan	5.37
5.9	References	5.37
6.0	Injection Well Plugging Plan.....	6.1
6.1	Injection Well Tests	6.1
6.1.1	Tests or Measures for Determining Bottom-Hole Reservoir Pressure	6.1
6.1.2	Injection Well Testing to Ensure External Mechanical Integrity	6.1
6.2	Plugging Plan	6.2
6.3	References	6.6
7.0	Post-Injection Site Care and Site Closure Plan.....	7.1
7.1	Computational Modeling for the Post-Injection Period	7.1
7.1.1	Pressure Differential.....	7.1
7.1.2	Predictions of CO ₂ Migration During the Post-Injection Site Care Period	7.1
7.1.3	Predicted Extent of the CO ₂ Plume at Site Closure.....	7.4
7.2	Post-Injection Monitoring Plan	7.5
7.2.1	Groundwater-Quality Monitoring	7.5

7.2.2	Carbon Dioxide Storage Zone and Pressure Monitoring	7.5
7.2.3	Geophysical Monitoring for CO ₂ Plume Tracking.....	7.6
7.2.4	Post-Injection Monitoring Locations, Methods, and Schedule	7.7
7.2.5	Reporting Schedule	7.7
7.2.6	Monitoring Plan Review and Maintenance	7.7
7.3	Site Closure Plan	7.8
7.3.1	Surface Equipment Decommissioning	7.8
7.3.2	Monitoring Well Plugging	7.8
7.3.3	Site Restoration/Remedial Activities	7.9
7.3.4	Site Closure Reporting	7.9
7.4	References	7.10
8.0	Class VI Emergency and Remedial Response Plan.....	8.1
8.1	Development of a Comprehensive Emergency and Remedial Response Plan.....	8.1
8.1.1	Identification of Adverse Events.....	8.2
8.1.2	Resources or Infrastructure Potentially Affected	8.3
8.2	Emergency and Remedial Response Actions to Protect USDWs	8.5
8.3	Amending the Emergency and Remedial Response Plan.....	8.12
8.4	Staff Training and Exercise Procedures	8.12
8.5	Emergency Contacts.....	8.12
8.6	Communications with Adjacent Landowners and Emergency Response Personnel	8.13
8.7	Communications Plan and Emergency Notification Procedures.....	8.14
8.8	References	8.14
9.0	Financial Responsibility	9.1
9.1	Alliance Financial Requirements Compliance Approach	9.1
9.2	Detailed Cost Estimate	9.2
9.3	CO ₂ Storage Trust Fund	9.3
9.3.1	Trustee Selection	9.3
9.3.2	Trust Agreement.....	9.4
9.3.3	Financial Strength of the Trustee	9.4
9.4	Third-Party Insurance.....	9.4
9.4.1	Selection of Third-Party Insurer.....	9.4
9.4.2	Insurance Estimate and Application.....	9.5
9.4.3	Proof of Insurance	9.7
9.4.4	Financial Strength of Insurer.....	9.7
9.5	References	9.7
Appendix A	– Requirements Matrices.....	A.1
Appendix B	– Known Wells Within the Survey Area	B.1
Appendix C	– Cost Estimate to Demonstrate Financial Responsibility for Class VI UIC Permit.....	C.1
Appendix D	– Insurance Review to Support Futuregen Alliance’s UIC Permit Application.....	D.1

Figures

1.1	Map Showing Morgan County and the Location of the Injection Wells	1.2
1.2	Location Maps of the Stratigraphic Well and the Proposed Storage Site's Injection Wells.....	1.5
1.3	Graphical Overview of the Conceptual Design of the CO ₂ Storage Site	1.6
2.1	Stratigraphy and Proposed Injection and Confining Zones at the Morgan County CO ₂ Storage Site	2.2
2.2	The Illinois Structural Basin Within the Midwestern United States	2.4
2.3	Regional East-West Cross Section Across the Western Half of Illinois	2.5
2.4	Regional North-South Cross Section	2.6
2.5	Structure and Lithology of the Precambrian Basement in Wells in Western Illinois and Portions of Iowa and Missouri	2.7
2.6	Structure on Top of the Mount Simon Sandstone in West-Central Illinois and Portions of Iowa and Missouri.....	2.10
2.7	Thickness of the Mount Simon Sandstone in West-Central Illinois and Portions of Iowa and Missouri	2.11
2.8	Structure-Contour Map for the Top of the Eau Claire Formation in West-Central Illinois and Portions of Iowa and Missouri	2.12
2.9	Stratigraphic Column for the Recently Drilled Stratigraphic Well at the Proposed Morgan County CO ₂ Storage Site.....	2.14
2.10	Slabbed Whole Core from the Lowermost Lombard Member Mudstones and Siltstones, the Elmhurst Sandstones, and the Lower Mount Simon Sandstones from the Stratigraphic Well ...	2.16
2.11	Lithology, Mineralogy, and Hydrologic Units of the Proposed Injection Zone and Lower Primary Confining Zone, as Encountered Within the Stratigraphic Well.....	2.17
2.12	Relationship Between Lithology, Mineralogy, Side-Wall Core and Wireline Log Computed Permeability for the Eau Claire Formation and Uppermost Mount Simon Intervals in the Stratigraphic Well	2.19
2.13	Structural Features of Illinois	2.23
2.14	Location of the two 2D seismic survey lines, L101 and L201, at the proposed Morgan County CO ₂ storage site	2.24
2.15	Reprocessed West-East 2D Seismic Line L201	2.25
2.16	Reprocessed South-North 2D Seismic Line L101	2.25
2.17	Gravity and GPS Stations for the 2011 Survey.....	2.27
2.18	Overlay of Local Bouguer Gravity with USGS Regional Survey	2.28
2.19	Regional WE Bouguer Anomaly Profile.....	2.29
2.20	Regional Historic Earthquakes	2.35
2.21	Earthquake Risk for Illinois Given as Maximum Accelerations with a 2 Percent Probability of Being Exceeded Within 50 Years	2.36
2.22	Surficial Quaternary Deposits of Illinois	2.37
2.23	Surface Topography and Drainage.....	2.38
2.24	Thickness of Unconsolidated Pleistocene Glacial Drift in Morgan and Adjacent Counties	2.39

2.25	Variability of Quaternary Sediments and Shallow Pennsylvanian Rocks in the Vicinity of the Proposed Morgan County CO ₂ Storage Site	2.40
2.26	Locations of Private/Domestic Water Wells Within 1.5 Mi of the Stratigraphic Well	2.41
2.27	Thickness and Distribution of Mississippian Aquifers and the Boundary for 10,000 mg/L TDS in the Middle Mississippian Rocks.....	2.43
2.28	Regional Map Showing Limits of Freshwater in the Ironton-Galesville Sandstone Relative to the Proposed Morgan County CO ₂ Storage Site	2.45
2.29	Pressure vs. Depth Profile Relationships Within the FutureGen Stratigraphic Well	2.47
2.30	Observed Hydraulic Head Comparison Between the Unconsolidated Quaternary Aquifer, St. Peter Sandstone, and Mount Simon Sandstone Within the FutureGen Stratigraphic Well ...	2.48
2.31	Map of Oil and Gas Wells Located Near the Proposed Morgan County CO ₂ Storage Site	2.49
2.32	Wells Located Within the Survey Area.....	2.53
3.1	EarthVision® Solid Earth Model for the Proposed Morgan County CO ₂ Storage Site	3.4
3.2	Division of Stratigraphic Layers to Create Computational Model Layers.....	3.5
3.3	Horizontal Permeability Versus Depth in Each Model Layer.....	3.8
3.4	Kv/Kh Assigned to Each Model Layer Versus Depth	3.10
3.5	Comparison of SWC Porosity Measurements and Associated ELAN Porosity Log Values	3.11
3.6	Comparison of SWC Porosity Measurements and Associated ELAN Porosity Log Values: <38 Gamma API Units.....	3.12
3.7	Comparison of SWC Porosity Measurements and Associated ELAN Porosity Log Values: 38 to 64 Gamma API Units	3.12
3.8	Comparison of SWC Porosity Measurements and Associated ELAN Porosity Log Values: >64 Gamma API Units.....	3.13
3.9	Comparison of SWC Porosity Measurements and Regression-Calibrated ELAN Log Porosities: ≤64 Gamma API Units	3.14
3.10	Porosity Versus Depth in Each Model Layer.....	3.14
3.11	Grain Density Versus Depth in Each Model Layer.....	3.15
3.12	Aqueous Saturation Versus Capillary Pressure Based on Mercury Injection Data from the Hazen No. 5 Well at the Manlove Gas Field in Champagne County, Illinois	3.16
3.13	Static Fluid Temperature Profile Performed on February 9, 2012 in the Stratigraphic Well.....	3.21
3.14	Numerical Model Grid for a) Full Domain, and b) Finer Resolution Area Containing the Injection Wells	3.23
3.15	Permeability Assigned to Numerical Model a) Horizontal Permeability; b) Vertical Permeability	3.24
3.16	CO ₂ Plume Area Versus Time Relative to Plume Extent at End of Injection Period	3.25
3.17	Pressure Differential Versus Time at the Injection Well	3.26
3.18	Operational Well Design for Representative Case Scenario as Implemented in the Numerical Model	3.27
3.19	Mass of Injected CO ₂ over Time Integrated over the Entire Model Domain.....	3.28
3.20	Injection Pressure Versus Time for All Four Injection Wells.....	3.28
3.21	CO ₂ -Rich Phase Saturation for the Representative Case Scenario Simulations Shown at Selected Times	3.30

3.22	Cutaway View of CO ₂ -Rich Phase Saturation Along A-A' for Selected Times	3.32
3.23	Cutaway View CO ₂ -Rich Phase Saturation Along B-B' for Selected Times	3.34
3.24	Cross-Sectional View of Pressure Differential at Selected Times	3.36
3.25	Area of Review for the Morgan County CO ₂ Storage Site	3.39
3.26	AoR Correction Action Plan Flowchart	3.41
3.27	Scatter Plots of Monte Carlo, Latin-Hypercube, and QMC Samples.....	3.42
3.28	Location of the Well Penetrations in the Area Surrounding the Storage Site	3.44
3.29	Well Construction Diagram for a Deep Borehole (API# 121370034900) in Morgan County that Penetrates the Target Reservoir for CO ₂ Sequestration	3.46
3.30	Well Construction Diagram for a Deep Borehole (API# 121370034601) in Morgan County that Penetrates the Target Reservoir for CO ₂ Sequestration	3.47
4.1	CO ₂ Wellhead Injection Pressure for Various Outside Diameter Tubing Sizes (with heat transfer)	4.5
4.2	CO ₂ Wellhead Injection Pressure for Various Outside Diameter Tubing Sizes (adiabatic)	4.6
4.3	Illustration of the Wellhead and Christmas Tree.....	4.14
4.4	Injection Well Schematic – Cased-Hole Completion	4.17
4.5	Injection Well Schematic – Open-Hole Completion	4.18
5.1	Conceptual Injection and Monitoring Well Network Layout with Predicted CO ₂ Lateral Extent over Time.....	5.6
5.2	Cross-Sectional View of Injection and Monitoring Well Network.....	5.7
6.1	Diagram of Cased Injection Well After Plugging and Abandonment.....	6.4
6.2	Diagram of Non-Cased Injection Well After Plugging and Abandonment	6.5
7.1	Simulated Pressure Differential Versus Time at Monitoring Well Locations	7.3
7.2	Simulated Plume Area over Time	7.3
7.3	Simulated Areal Extent of the CO ₂ Plume at the Time of Site Closure	7.4
7.4	Layout of the Horizontal Injection Wells and the Monitoring Wells and the Predicted Plume Boundaries at Different Years.....	7.6
8.1	Map of Residences, Water Wells, and Surface-Water Features Within the Delineated AoR and Survey Area.....	8.4

Tables

1.1	General Class VI Waste Injection Well Permits Application Information	1.8
1.2	Permits Required for the FutureGen 2.0 Project	1.8
1.3	Summary of UIC Permit Applications Supporting Documentation.....	1.10
1.4	Crosswalk Between Applicable Regulatory Provisions in the GS Rule and the Alliance UIC Permit Application Supporting Documentation	1.10
2.1	Published Physical Properties for Precambrian Basement Rocks in the Illinois Basin	2.8
2.2	Intervals of Geophysical Wireline Characterization Logs and Side-Wall Cores Collected in the Stratigraphic Well	2.15
2.3	Whole-Core Intervals Collected from the Stratigraphic Well.....	2.15
2.4	Hydrogeology of the Injection and Confining Zones Within the Stratigraphic Well	2.15
2.5	Permeabilities from Proviso Member Rotary Side-Wall Cores	2.20
2.6	Rotary Side-Wall Core Permeabilities from the Secondary Confining Zone	2.21
2.7	Data from Fluid Samples Collected with the MDT Sampler from the Mount Simon Sandstone in the CCS#1 Well at the Decatur Site	2.21
2.8	Lithostatic Pressure at Important Interfaces.....	2.31
2.9	Relation of Principal Stresses to Fault Types	2.32
2.10	Elastic Moduli Parameters from Triaxial Tests on Vertical Core Plugs in the Injection Interval and Precambrian Basement.....	2.33
2.11	Minimum Horizontal Stress and Fracture Gradient Calculated from Triaxial Tests	2.33
2.12	Range of Geomechanical Properties	2.33
2.13	Elastic Moduli Parameters from Triaxial Tests of Core from the Lowermost Part of the Lombard Member.....	2.34
2.14	Minimum Horizontal Stress and Fracture Gradient Calculated from Triaxial Tests	2.34
2.15	Range of Eau Claire Geomechanical Properties in the CCS#1 Well, Decatur Illinois	2.35
2.16	Analyses of Two Formation Fluid Samples from the Mount Simon Sandstone in the Stratigraphic Well	2.46
2.17	List of Wells Located Within the AoR.....	2.51
3.1	Comparison of Results from Hydraulic Field Tests and ELAN Data.....	3.7
3.2	Summary of the Scaling Factors Applied for the Modeling	3.7
3.3	Lithology-Specific Permeability Anisotropy Averages from Literature.....	3.9
3.4	Summary of the Kv/Kh Ratios Applied to Model Layers.....	3.9
3.5	Permeability Ranges Used to Assign Brooks-Corey Parameters to Model Layers.....	3.16
3.6	Values for Constants a and b for Different Lithologies	3.16
3.7	Formation Compressibility Values Selected from Available Sources	3.17
3.8	Summary of the Hydrologic Properties Assigned to Each Model Layer	3.18
3.9	Pressure Data Obtained from the Mount Simon Formation Using the MDT Tool.....	3.20
3.10	Summary of Initial Conditions.....	3.24
3.11	Mass Rate of CO ₂ Injection for Each of the Four Lateral Injection Wells.....	3.27

3.12	Scaling Factors Evaluated for Parameter Sensitivity Analysis	3.42
4.1	CO ₂ Acceptance Specifications.....	4.2
4.2	Pipeline Design Assumptions and Results	4.3
4.3	Flow Rates and Limiting Pressures for Hydraulic Calculations	4.4
4.4	Load Scenarios Evaluated	4.7
4.5	Minimum Design Factors and Corresponding Scenarios for Conductor Casing String.....	4.8
4.6	Minimum Design Factors and Corresponding Scenarios for Surface Casing String	4.8
4.7	Minimum Design Factors and Corresponding Scenarios for Intermediate Casing String	4.8
4.8	Minimum Design Factors and Corresponding Scenarios for Long-String Casing.....	4.9
4.9	Minimum Design Factors and Corresponding Scenarios for Tubing-String.....	4.9
4.10	Borehole and Casing and Tubing Program for the Horizontal CO ₂ Injection Wells	4.10
4.11	Properties of Well Casing and Tubing Materials	4.10
4.12	Cementing Program	4.11
4.13	Material Classes from API 6A	4.15
4.14	Wireline Logging Program	4.19
5.1	Summary of Planned Testing and Monitoring Activities.....	5.11
5.2	Additional Monitoring Activities Under Consideration.....	5.12
5.3	Monitoring Frequencies by Method and Project Phase for both Planned and Considered Monitoring Activities	5.14
5.4	Aqueous Sampling Requirements	5.20
5.5	Analytical Requirements	5.21
5.6	Examples of Wireline Tools for Monitoring Corrosion of Casing and Tubing	5.31
5.7	Examples of Wireline Tools for Evaluating Cement Behind Casing.....	5.32
6.1	Intervals to Be Plugged and Materials/Methods Used.....	6.3
7.1	Pressure Differential to Baseline Conditions at Well Location at the Base of the Ironton Formation for Well 3 and at the Top of the Injection Zone for the Rest of the Wells During and After Injection	7.2
7.2	Summary of Post-Injection Site Care Monitoring Schedule	7.7
8.1	Potential Adverse Events	8.3
8.2	Adverse Events Potentially Affecting USDWs.....	8.6
8.3	Outside Emergency Response.....	8.13
8.4	Agency Emergency Response.....	8.13
9.1	Approach to Meeting Financial Responsibility Requirements.....	9.2
9.2	FutureGen 2.0 Third-Party Cost Estimate for Planned Activities.....	9.2
9.3	FutureGen 2.0 Third-Party Cost Estimate for Emergency and Remedial Response Actions	9.3

1.0 Introduction

The FutureGen Industrial Alliance, Inc. (Alliance) prepared this documentation to support its Underground Injection Control (UIC) Class VI permit applications to the U.S. Environmental Protection Agency (EPA), Region 5, for the construction and operation of four wells for the injection of carbon dioxide (CO₂) in Morgan County, Illinois. The four injection wells will be drilled from a single well pad. Figure 1.1 shows the location of the proposed injection wells. This supporting documentation was prepared in accordance with the UIC Control Program for Carbon Dioxide Geologic Sequestration Wells (The GS [Geological Sequestration] Rule, published on December 10, 2010 [75 FR 77230] and codified in Title 40 of the Code of Federal Regulations [40 CFR 146.81 et seq.].¹

The Alliance has prepared separate application forms (EPA Forms 7520-6 and 7520-14) for each proposed injection well (referred to as Morgan County Class VI UIC Wells 1, 2, 3, and 4). Because the four injection wells will be similarly constructed and drilled from a single well pad, the CO₂ injected through the four wells will form one co-mingled CO₂ plume. Therefore, this supporting documentation applies to all four proposed injection wells.² The applications and supporting documentation are based on currently available data, including regional data and site-specific data derived from a stratigraphic well drilled by the Alliance in late 2011 near the site of the proposed injection wells.

A project overview, administrative information required by 40 CFR 144.31(e)(1) through (6), and a description of the remaining chapters of this supporting documentation are presented in the following sections. Appendix A contains a table listing where each regulatory requirement in the GS Rule, including the minimum criteria for siting, is addressed.

1.1 Project Overview

This section provides a description of the Alliance, the FutureGen 2.0 Project, and the Alliance's proposed CO₂ storage system.

1.1.1 FutureGen Alliance

The Alliance is a non-profit corporation created to benefit the public interest and the interests of science through research, development, and demonstration of near-zero emissions coal technology. It is partnering with the U.S. Department of Energy (DOE) on the FutureGen 2.0 Project. Members of the Alliance include some of the largest coal producers, coal users, and coal equipment suppliers in the world. The active role of industry in this project ensures that the public and private sector share the cost and risk of developing the advanced technologies necessary to commercialize the FutureGen 2.0 concept.

¹ The injection well permit applications and this supporting documentation were prepared at the Alliance's direction by Battelle's Pacific Northwest Division.

² Throughout this supporting documentation, the Alliance uses the future tense to refer to the actions the Alliance intends to undertake with respect to its proposed injection wells. The Alliance recognizes that such actions can only be undertaken after the issuance of UIC permits by the EPA.

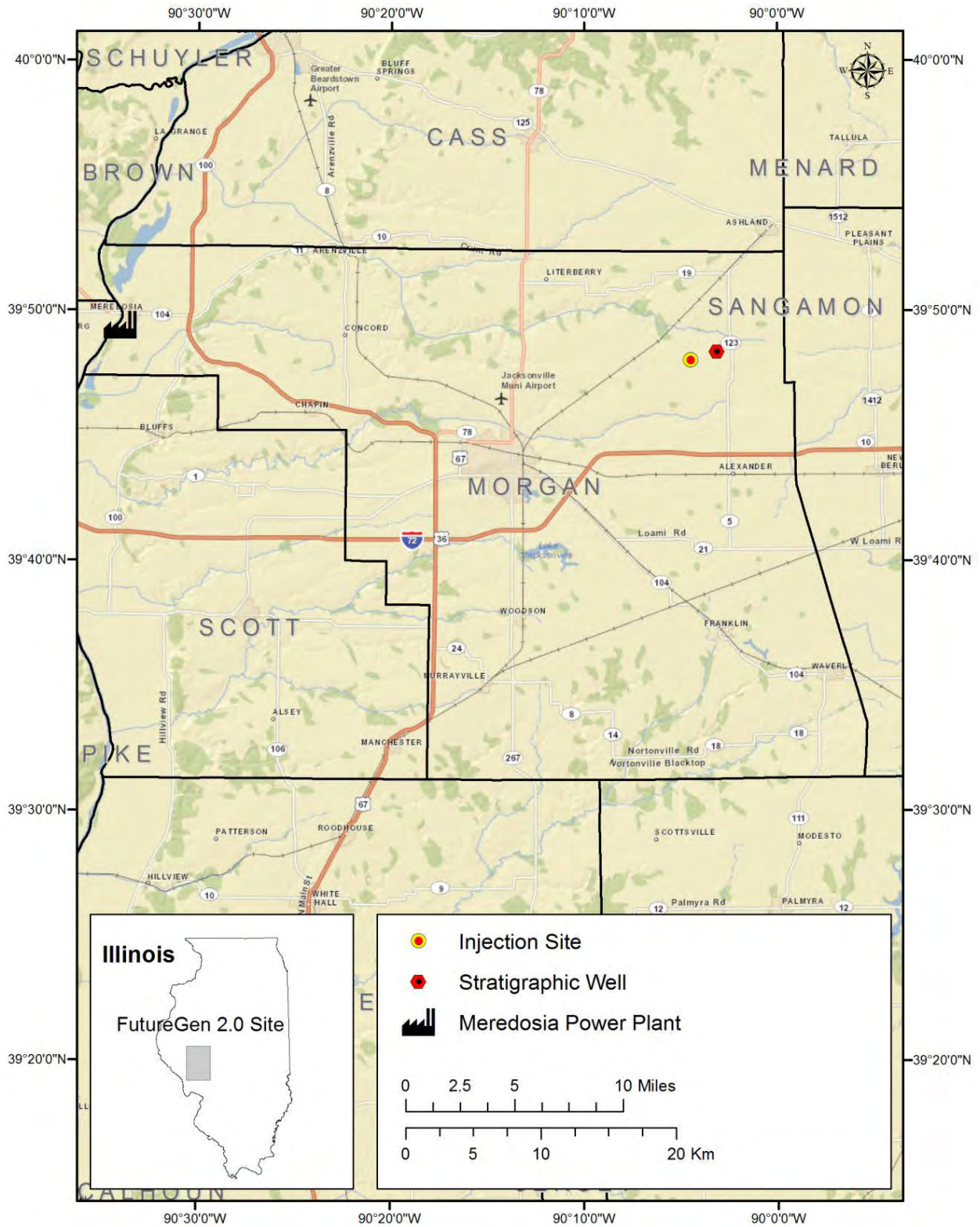


Figure 1.1. Map Showing Morgan County and the Location of the Injection Wells

1.1.2 The FutureGen 2.0 Project

In September 2010, the Alliance signed a Cooperative Agreement (DE-FE0001882) with DOE to develop FutureGen 2.0, a commercial-scale oxy-combustion repowering project that will use carbon capture and storage (CCS) technology. The FutureGen 2.0 Project is a public-private partnership, with costs shared by DOE and the other project partners. The project has been awarded \$1 billion in American Recovery and Reinvestment Act funding through the DOE Office of Fossil Energy.

DOE Cost-Share Phases

- *Phase I:* Project Definition
- *Phase II:* Design and Permitting
- *Phase III:* Construction, and Commissioning
- *Phase IV:* Operations

Pursuant to the Cooperative Agreement, the Alliance is working with Ameren Energy Resources (Ameren), Babcock & Wilcox Company, and Air Liquide Process and Construction, Inc. to develop a near-zero emission, coal-fueled power plant. The Alliance plans to acquire a portion of Ameren's existing Meredosia Power Plant in Meredosia, Illinois, and repower one of its units with oxy-combustion and carbon capture technology. An oxy-combustion system combusts coal in the presence of a mixture of oxygen and CO₂. The heat produced by the combustion process is used to make steam. The steam is used to generate electricity. A byproduct of the oxy-combustion process is an emission stream that has a high concentration of CO₂ that can be captured and passed through a CO₂ purification and compression unit. In combination, these processes result in the capture of at least 90 percent of the power plant's CO₂ emissions and reduction of other conventional emissions to near-zero levels.

The captured CO₂ will be transported from the power plant through an underground pipeline to four injection wells (on a single well pad) drilled into the Mount Simon Sandstone—sandstone that underlies central Illinois—so that the CO₂ can be sequestered within that injection zone, which would serve as a permanent underground CO₂ storage reservoir. The Alliance plans to inject approximately 1.1 MMT of CO₂ annually into the Mount Simon Sandstone where it will be permanently stored. A total of 22 MMT will be injected over 20 years, using four horizontal injection wells. Visitor, research, and training facilities will be located in nearby Jacksonville, Illinois.

In accordance with the National Environmental Policy Act of 1969, as amended, DOE is preparing an environmental impact statement (EIS) to assess the potential environmental impacts of the FutureGen 2.0 Project. DOE issued its Notice of Intent to prepare the EIS in May 2011 (76 FR 29728), and held scoping meetings in the area in June 2011. A draft EIS is expected to be released in spring 2013; additional public hearings will be held at that time.

1.1.3 Proposed CO₂ Storage System

The CCS component of the FutureGen 2.0 Project is a GS demonstration project intended to prove the effectiveness of the GS conceptual design and related CCS technologies. The primary objective is to site, design, construct, and operate a CO₂ pipeline and underground CO₂ storage reservoir with sufficient capacity to accept, transport, and sequester at least 1.1 MMT of CO₂ annually in a deep saline geologic formation.

The proposed CO₂ storage site includes the surface facilities, injection wells, monitoring wells, access roads, and an underground CO₂ injection zone. The surface facilities, wells, and access roads are expected to require no more than 25 surface acres. The area of CO₂ storage is cloverleaf-shaped and is

located on the western margin of the Illinois Basin, an elongated structural basin that is centered in and underlying most of the state of Illinois (see Chapter 2.0, Figure 2.2). The storage site is approximately 6 mi (10 km) north of the unincorporated town of Alexander, 6 mi (10 km) southwest of Ashland, and 11 mi (18 km) northeast of the City of Jacksonville (see Figure 1.2), and is currently agricultural land.

The conceptual design of the CO₂ storage site includes four horizontal injection wells; surface facilities; the subsurface CO₂ injection zone; and monitoring, verification, and accounting systems (including monitoring wells). Figure 1.3 provides a graphical overview of the conceptual design.

1.1.3.1 Stratigraphic Well

In 2011, the Alliance drilled a stratigraphic well (sometimes referred to as the project's "characterization well" and numerically identified in some figures as "FGA #1") near the location of the proposed injection wells to generate site-specific information about geologic, hydrogeologic, and biogeochemical conditions. Figure 1.2 shows the relative locations of the well pad for the four proposed injection wells and the stratigraphic well. The stratigraphic well provided the detailed hydrologic data with which to characterize the below ground surface environment as part of assessing site feasibility and designing the CO₂ storage site. By further revealing the geologic characteristics (injectivity, porosity, etc.) of the proposed injection zone, this well has enabled the project to move from a generalized understanding of the geology of the region to an understanding of the site-specific geology of the proposed injection zone. This supporting documentation reflects the stratigraphic well data and analysis. Once injection begins, the Alliance plans to use the stratigraphic well as one of its monitoring wells, as described more fully in Chapter 5.0, Testing and Monitoring Plan.

1.1.3.2 CO₂ Stream

The Morgan County CO₂ storage site is expected to receive approximately 1.1 MMT of CO₂ annually from the oxy-combustion power plant. The emissions stream from the power plant will be captured at the plant, purified, dehydrated, and compressed to 2,100 psig before the CO₂ is placed into the pipeline for transport to the injection wells. At these conditions, the CO₂ will be in a dense fluid phase, non-corrosive, and non-flammable. Transporting CO₂ as a dense fluid is preferred because it requires smaller diameter pipelines and the CO₂ can be pumped without the need for complex and additional compression equipment along the pipeline route. The estimated length of the pipeline to the UIC injection well site is approximately 30 mi (48 km).

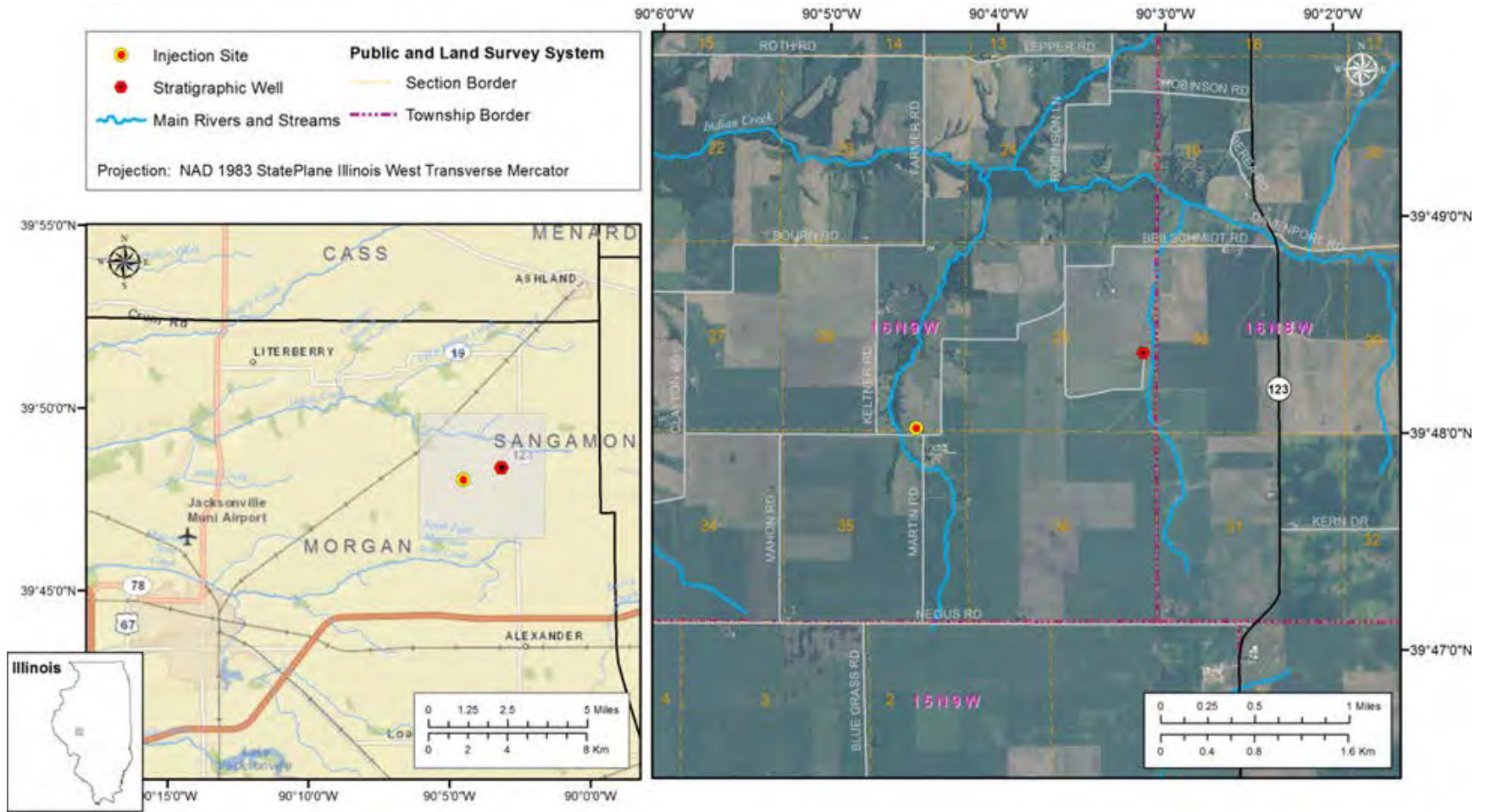


Figure 1.2. Location Maps of the Stratigraphic Well and the Proposed Storage Site's Injection Wells

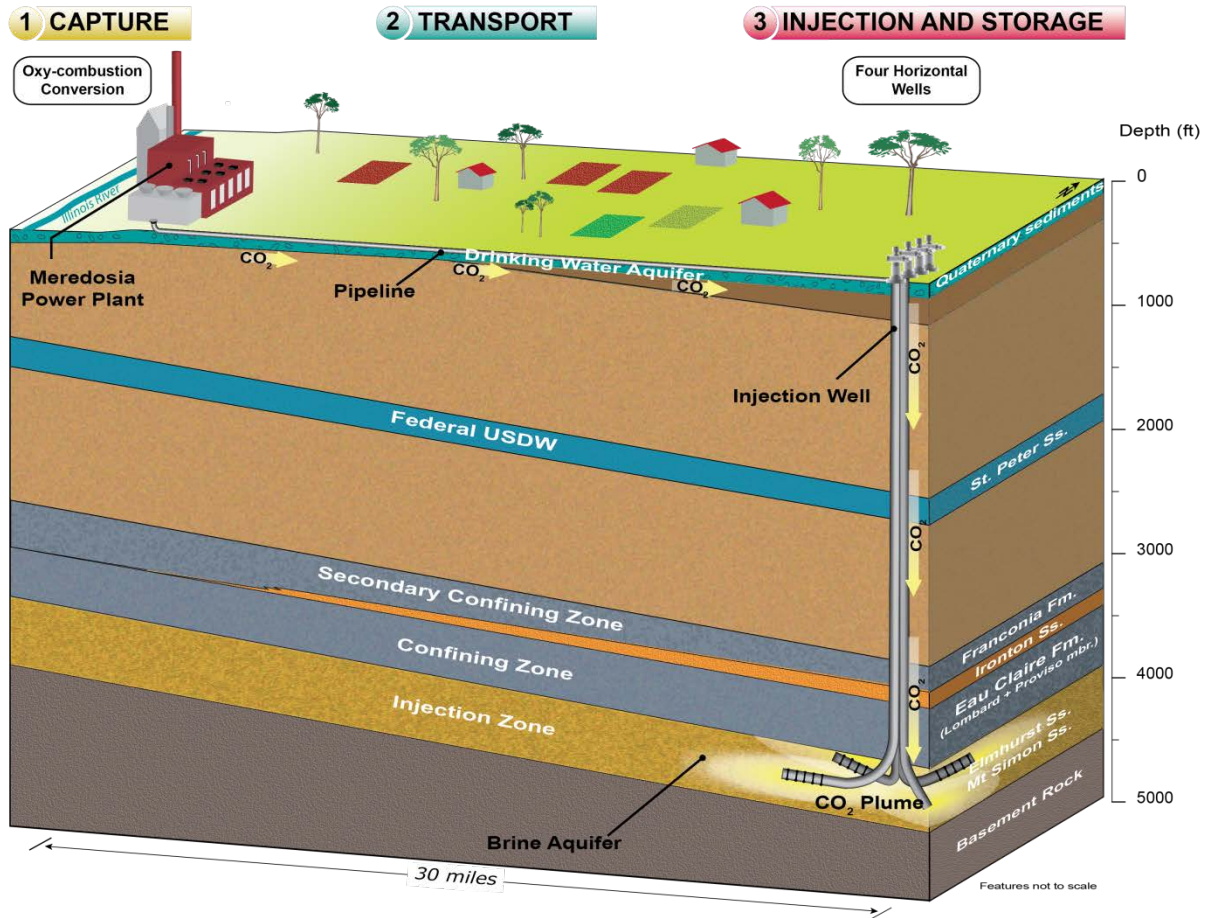


Figure 1.3. Graphical Overview of the Conceptual Design of the CO₂ Storage Site

1.1.3.3 Surface Facilities

The surface area associated with the four injection wells and associated structures is expected to be less than 10 acres. Limited additional acreage will be required for monitoring wells and access roads.

1.1.3.4 Injection Wells

Once permits are issued, four horizontal injection wells will be constructed at the Morgan County CO₂ storage site. Each well will be designed to provide operational flexibility and backup capability. The wells will be approximately 4,000 ft (1,219 m) deep. The wells will be located in the center of Section 26, Township 16N, Range 9W, at approximately latitude 39.800266°N and longitude 90.07469°W (subject to final review and survey), in Morgan County, Illinois (see Figure 1.2).

The Construction and Operations Plan developed by the Alliance to meet the requirements of 40 CFR 146.86 through 146.89 is presented in Chapter 4.0 of this supporting documentation. The Injection Well-Plugging Plan developed to meet the requirements of 40 CFR 146.92 is presented in Chapter 6.0. The Site Closure Plan is described in Chapter 7.0.

1.1.3.5 Injection and Confining Zones

The Alliance proposes to inject CO₂ into the Mount Simon Sandstone and Elmhurst Sandstone member of the Eau Claire Formation (see Figure 1.3). The Alliance proposes this injection zone because of its depth, thickness, porosity, and permeability. The top of the Elmhurst Sandstone member is approximately 3,900 ft (1,190 m) bgs and the injection zone is approximately 565 ft (172 m) thick in the target location. The proposed injection zone consists of quartz sandstone, and it has demonstrated reservoir capacity in natural-gas storage facilities elsewhere in the Illinois Basin. The injection zone contains a hypersaline aquifer with a temperature of approximately 103°F (39.4°C) and total dissolved solids of approximately 40,000 mg/L—well in excess of recommended Safe Drinking Water Act standards.

The injection zone is overlain by the Eau Claire Formation, a thick regional confining zone with low permeability above the Elmhurst Sandstone member. The Franconia Dolomite and Davis member serves as a secondary confining zone for additional protection of underground sources of drinking water.

The geologic setting, along with detailed information about the Morgan County CO₂ storage site, is presented in Chapter 2.0.

1.1.3.6 Monitoring Program

An extensive monitoring, verification, and accounting system will be installed to verify that injected CO₂ is effectively contained within the injection zone. The monitoring network will be designed to account for and verify the location of all CO₂ injected into the ground. It will include monitoring wells in the injection zone, immediately above the primary confining zone, and in the lowermost USDW aquifer. The objectives of the monitoring program are to track the lateral extent of CO₂ within the injection zone, characterize any geochemical or geomechanical changes that occur within the injection and confining zones that may affect containment, and track the extent of the injected CO₂ using direct and indirect monitoring methods. The monitoring program is designed to verify CO₂ retention in the injection zone. In the unlikely event of unintended migration, the monitoring program is intended to detect and quantify the migration through the confining zones, assess the potential to adversely affect underground sources of drinking water, and guide remedial actions.

The Testing and Monitoring Plan developed by the Alliance to meet the requirements of 40 CFR 146.90 is presented in Chapter 5.0 of this supporting documentation. Post-injection site care monitoring is described in Chapter 7.0.

1.2 Required Administrative Information

Table 1.1 provides the administrative information for the Class VI injection well permit applications as required by 40 CFR 144.31(e)(1 through 6).

Table 1.2 lists the permits or construction approvals received or applied for under specific programs listed in 40 CFR 144.31(e)(6). It also includes other relevant state environment permits and permits required for modifications at the Meredosia Power Plant.

Table 1.1. General Class VI Waste Injection Well Permits Application Information

Injection Well Information	
Well Name and Number	Morgan County Class VI UIC Wells 1, 2, 3, and 4
County	Morgan County, Illinois
Section–Township–Range	26–16N–9W
Latitude and Longitude	39.800266°N and 90.07469°W
Applicant Information	
Name	FutureGen Industrial Alliance, Inc.
Address and Phone Number	Washington D.C. Office 1101 Pennsylvania Ave., Sixth Floor Washington, D.C. 20004 Phone: (202) 280-6019
	Morgan County Office 73 Central Park Plaza East Jacksonville, IL 62650 Phone: (217) 243-8215
Ownership Status	Non-stock, non-profit corporation
Status as Federal, State, Private, Public, Or Other Entity	Private entity
Related Standard Industrial Classification (SIC) Codes	
The GS Rule asks for the identification of up to four SIC codes that best reflect the principal products or services provided by the facility. The SIC system is a U.S. government system for classifying industries by a four-digit code. A SIC code has not been established for geologic sequestration of CO ₂ . SIC Code 4922 is Natural Gas Transmission, and includes natural-gas storage (OSHA 2012b, a). Natural-gas storage is similar to CO ₂ storage.	
Federal Government Jurisdiction or Protection	
The injection wells and the storage site are not located on Indian land, as there are no federally recognized Native American tribes located within the State of Illinois.	

Table 1.2. Permits Required for the FutureGen 2.0 Project

Program	Permits	Status
(i) Hazardous Waste Management program under RCRA	Not required	Not applicable
(ii) UIC program under SDWA	(UIC) Class VI Permit Morgan County FutureGen UIC Well 1 (UIC) Class VI Permit Morgan County FutureGen UIC Well 2 (UIC) Class VI Permit Morgan County FutureGen UIC Well 3 (UIC) Class VI Permit Morgan County FutureGen UIC Well 4	Permit Submitted to EPA Region 5 Permit Submitted to EPA Region 5 Permit Submitted to EPA Region 5 Permit Submitted to EPA Region 5
(iii) NPDES program under CWA	Required for stratigraphic well, power plant, pipeline, and injection/monitoring wells	Stratigraphic well construction performed under General NPDES Permit No. ILR10 (issued August 11, 2008, expires July 31, 2013). SWPPP prepared May 4, 2011; Ameren Energy Resources, with the Alliance, submitted an NPDES modification application to IEPA on May 10, 2012 for power plant modifications

Table 1.2. (contd)

Program	Permits	Status
(iv) Prevention of Significant Deterioration (PSD) program under the CAA	Not required	Ameren Energy Resources, with the Alliance, submitted a Construction Permit Application for a Proposed Project at a CAAPP Source to IEPA on February 8, 2012 for power plant modifications. Due to netting, PSD not required
(v) Nonattainment program under the CAA	Not required	Not applicable. Area is in attainment for all criteria pollutants
(vi) National Emission Standards for Hazardous Pollutants (NESHAPS) preconstruction approval under the CAA	Not required	Not applicable
(vii) Ocean dumping permits under the Marine Protection Research and Sanctuaries Act	Not required	Not applicable
(viii) Dredge and fill permits under section 404 of CWA	May be required for power plant and pipeline; well pads will not affect wetlands	Wetlands areas are being avoided at the power plant site and injection/monitoring well pad locations; pipeline route not yet finalized
(ix) Other relevant environmental permits, including state permits		
Drilling Permit	Required for stratigraphic well and injection/monitoring wells	OG-7 permit application for stratigraphic well was delivered to the IDNR on June 28, 2011
Illinois Endangered Species Protection Act (520 ILCS 10; ILCS 2012a)	Incidental take permit may be required for the power plant and pipeline	Consultations with IDNR are ongoing
Illinois' Private Sewage Disposal Licensing Act (225 ILCS 225; ILCS 2012b)	Applicability being determined	

CAA = Clean Air Act; CAAPP = Clean Air Act Permit Program; CWA = Clean Water Act; IDNR = Illinois Department of Natural Resources; IEPA = Illinois Environmental Protection Agency; ILCS = Illinois Compiled Statutes; NPDES = National Pollution Discharge Elimination System; OG = (IDNR) Division of Oil and Gas; RCRA = Resource Conservation and Recovery Act; SDWA = Safe Drinking Water Act; SWPPP = Storm Water Pollution Prevention Plan.

1.3 Supporting Documentation Contents and Organization

The following chapters address proposed injection well activities and responsibilities from the geologic setting and development of the Area of Review (AoR) through post-injection site care and site closure, including emergency and remedial actions and financial responsibility, as described in Table 1.3. Table 1.4 summarizes where the applicable regulatory provisions in the GS Rule are addressed within the supporting documentation.

Table 1.3. Summary of UIC Permit Applications Supporting Documentation

Chapter	Title	Purpose
1	Introduction	This chapter provides an overview of the Alliance and the FutureGen 2.0 Project, a description of the Alliance’s proposed CO ₂ storage system, and administrative information.
2	Conceptual Model of the Site Based on Geology and Hydrology	This chapter provides information about the geology, hydrology, and biogeochemistry of the Morgan County site. This information is used collectively to develop a conceptual model of the site, which will guide the numerical simulations, design, and monitoring of the site. A set of input parameters is presented that will form the basis for the numerical model of the injection and confining zones used to develop the AoR. The conceptual model is based on regional geology, hydrology, and site-specific information from the stratigraphic well.
3	Area of Review and Corrective Action Plan	This chapter describes the AoR and specifies the corrective actions that will be taken to address features that compromise the integrity of the confining zone above the injection zone targeted for CO ₂ storage.
4	Construction and Operations Plan	This chapter describes the injection well design, construction methods, and materials, as well as the proposed conduct of injection operations.
5	Testing and Monitoring Plan	This chapter describes the plan for testing the injection wells during and after construction and the requirements for monitoring the injection zone, performance of the confining zone, and other media to ensure the protection of underground sources of drinking water.
6	Injection Well-Plugging Plan	This chapter describes planned methods for plugging the injection wells after the period of injection is complete.
7	Post-Injection Site Care and Site Closure Plan	This chapter describes the plan for closure of the CO ₂ storage site after the injection period and activities related to long-term site care.
8	Emergency and Remedial Response Plan	This chapter describes the actions that may be required if injection activities cause endangerment to underground sources of drinking water, including notification procedures and identification of emergency contacts.
9	Financial Responsibility	This chapter describes the instruments the Alliance will use to demonstrate and maintain financial responsibility for the operation and closure of the CO ₂ storage site in a manner that will protect underground sources of drinking water.

Table 1.4. Crosswalk Between Applicable Regulatory Provisions in the GS Rule and the Alliance UIC Permit Application Supporting Documentation

GS Rule – Regulatory Requirements	Alliance UIC Permit Application Supporting Documentation
40 CFR 146.82, Required Class VI permit information	Chapter 1, Introduction Chapter 2, Conceptual Model of the Site Based on Geology and Hydrology
40 CFR 146.83, Minimum criteria for siting	Chapter 2, Conceptual Model of the Site Based on Geology and Hydrology
40 CFR 146.84, Area of review and corrective action	Chapter 3, Area of Review and Corrective Action Plan
40 CFR 146.85, Financial responsibility	Chapter 9, Financial Responsibility
40 CFR 146.86, Injection well construction requirements	Chapter 4, Construction and Operations Plan

Table 1.4. (contd)

GS Rule – Regulatory Requirements	Alliance UIC Permit Application Supporting Documentation
40 CFR 146.87, Logging, sampling, and testing prior to injection well operation	Chapter 4, Construction and Operations Plan
40 CFR 146.88, Injection well operating requirements	Chapter 4, Construction and Operations Plan
40 CFR 146.89, Mechanical integrity	Chapter 5, Testing and Monitoring Plan
40 CFR 146.90, Testing and monitoring requirements	Chapter 5, Testing and Monitoring Plan
40 CFR 146.91, Reporting requirements	throughout
40 CFR 146.92, Injection well plugging	Chapter 6, Injection Well-Plugging Plan
40 CFR 146.93, Post-injection site care and site closure	Chapter 7, Post-Injection Site Care and Site Closure Plan
40 CFR 146.94, Emergency and remedial response	Chapter 8, Emergency and Remedial Response Plan
40 CFR 146.95, Class VI injection depth waiver requirements	Not applicable

Appendixes contain supplemental information, as follows:

Appendix A – Requirements Matrices

Appendix B – Known Wells Within the Survey Area

Appendix C – Third-Party Cost Estimate

Appendix D – Memorandum Regarding Insurance Coverage

1.4 References

40 CFR 144.31. Code of Federal Regulations, Title 40, *Protection of the Environment*, Part 144 “Underground Injection Control Program,” Section 31, “Application for a Permit; Authorization by Permit.”

40 CFR 146. Code of Federal Regulations, Title 40, *Protection of Environment*, Part 146, “Underground Injection Control Program: Criteria and Standards.”

75 FR 77230. December 10, 2010. “Federal Requirements Under the Underground Injection Control (UIC) Program for Carbon Dioxide (CO₂) Geologic Sequestration (GS) Wells.” *Federal Register*. U.S. Environmental Protection Agency.

76 FR 29728. May 23, 2011. “Notice of Intent to Prepare an Environmental Impact Statement and Notice of Potential Floodplain and Wetlands Involvement for the FutureGen 2.0 Program.” *Federal Register*. U.S. Department of Energy.

American Recovery and Reinvestment Act of 2009 (ARRA). Public Law 111-5.

Clean Air Act (CAA). 42 U.S.C. § 7401 et seq.

Clean Water Act (CWA)/Federal Water Pollution Control Act. 33 U.S.C. § 1344 et seq.

ILCS (Illinois Compiled Statutes). 2012a. *Illinois Endangered Species Protection Act*. Available online at <http://www.ilga.gov/legislation/ilcs/ilcs3.asp?ActID=1730&ChapterID=43>

ILCS (Illinois Compiled Statutes). 2012b. *Private Sewage Disposal Licensing Act*. Available online at <http://www.ilga.gov/legislation/ilcs/ilcs3.asp?ActID=1337&ChapterID=24>

Marine Protection, Research, and Sanctuaries Act (MPRSA) of 1972, as amended. 16 U.S.C. § 1431 et seq. and 33 USC § 1401 et seq. (1988)

National Environmental Policy Act of 1969, as amended (NEPA). 42 U.S.C. § 4321 et seq.

OSHA (Occupational Health and Safety Administration). 2012a. *Standard Industrial Code 2813; Industrial Gases*. Occupational Safety and Health Administration, Washington D.C. Accessed on 8/30/12 at http://www.osha.gov/pls/imis/sic_manual.display?id=600&tab=description.

OSHA (Occupational Health and Safety Administration). 2012b. *Standard Industrial Code 4619; Pipelines, Not Elsewhere Included*. Occupational Safety and Health Administration, Washington D.C. Accessed on 8/30/12 at http://www.osha.gov/pls/imis/sic_manual.display?id=929&tab=description.

Resource Conservation and Recovery Act of (RCRA). 42 U.S.C. § 6901 et seq.

Safe Drinking Water Act of 1974, as amended. 42 U.S.C. 300f et seq.

2.0 Geology and Hydrology

The geologic and hydrogeologic properties described in this chapter are used to develop a conceptual model of the proposed CO₂ storage site in Morgan County, Illinois. The conceptual model is a fundamental part of this UIC Class VI Permit submitted by the Alliance for the construction and operation of up to four CO₂ injection wells. This chapter provides both regional and local information about the injection zone (the geologic formation that will receive the CO₂) and the confining zones (the geologic formations that will act as a barrier to fluid migration). This information is provided to demonstrate that the proposed Morgan County CO₂ storage site is a suitable geologic system for CO₂ storage, and the confining zones have sufficient extent and integrity to contain the injected CO₂ and displaced formation fluids so as to ensure the protection of nearby underground sources of drinking water (USDWs). This chapter provides background information in support of the conceptual model, which is developed in detail in Chapter 3.0. The information in this chapter is also critical to the design, construction, and operation of the injection and monitoring wells and in the subsequent well plugging after the site has completed CO₂ injections.

The regional geology, including the regional continuity of the proposed injection and confining zones, is described in Section 2.1. A site-specific description of the geology at the Morgan County CO₂ storage site—derived from a stratigraphic well that was drilled near the proposed injection in support of this UIC application—is provided in Section 2.2. This information is supported by results from other nearby wells and the published literature, which together form the basis of the description of the geologic setting of the proposed Morgan County CO₂ storage site described in Section 2.3. Geomechanical data for the proposed injection and confining zones are presented in Section 2.4. The seismic history of the region is described in Section 2.5. Site groundwater is described in Section 2.6. A site evaluation of mineral resources is presented in Section 2.7. A discussion of the wells within the AoR and the one well (stratigraphic well) that penetrates the injection and confining zones follows in Section 2.8. The conclusion in Section 2.9 demonstrates that the proposed Morgan County CO₂ storage site meets the minimum criteria for siting specified in 40 CFR 146.83(a). Note that the detailed physical and chemical properties used as input parameters to the computational model are presented in Chapter 3.0. References for sources cited in the text are contained in the final section of this chapter.

2.1 Geology

The Alliance proposes to inject CO₂ into the Cambrian-age Mount Simon Sandstone and the lower Eau Claire Formation (Elmhurst Sandstone member), which combined make up the injection zone. The Mount Simon Sandstone is the thickest and most widespread potential CO₂ injection formation in Illinois (Leetaru and McBride 2009), and at the Morgan County site (Figure 2.1). The Elmhurst Sandstone, along with the Mount Simon, is an injection zone at a number of natural-gas storage sites in Illinois (Morse and Leetaru 2005). The confining zone for the proposed injection zone consists of the Lombard and Proviso members of the Eau Claire Formation that overlies the Mount Simon and Elmhurst sandstones. The Eau Claire is the most important regional confining zone in Illinois (Leetaru et al. 2005, 2009). The Davis member of the Franconia Formation forms a secondary confining zone above the Eau Claire Formation. Impermeable Precambrian-aged basement rocks underlie the Mount Simon Sandstone and form a no-flow boundary to the conceptual model.

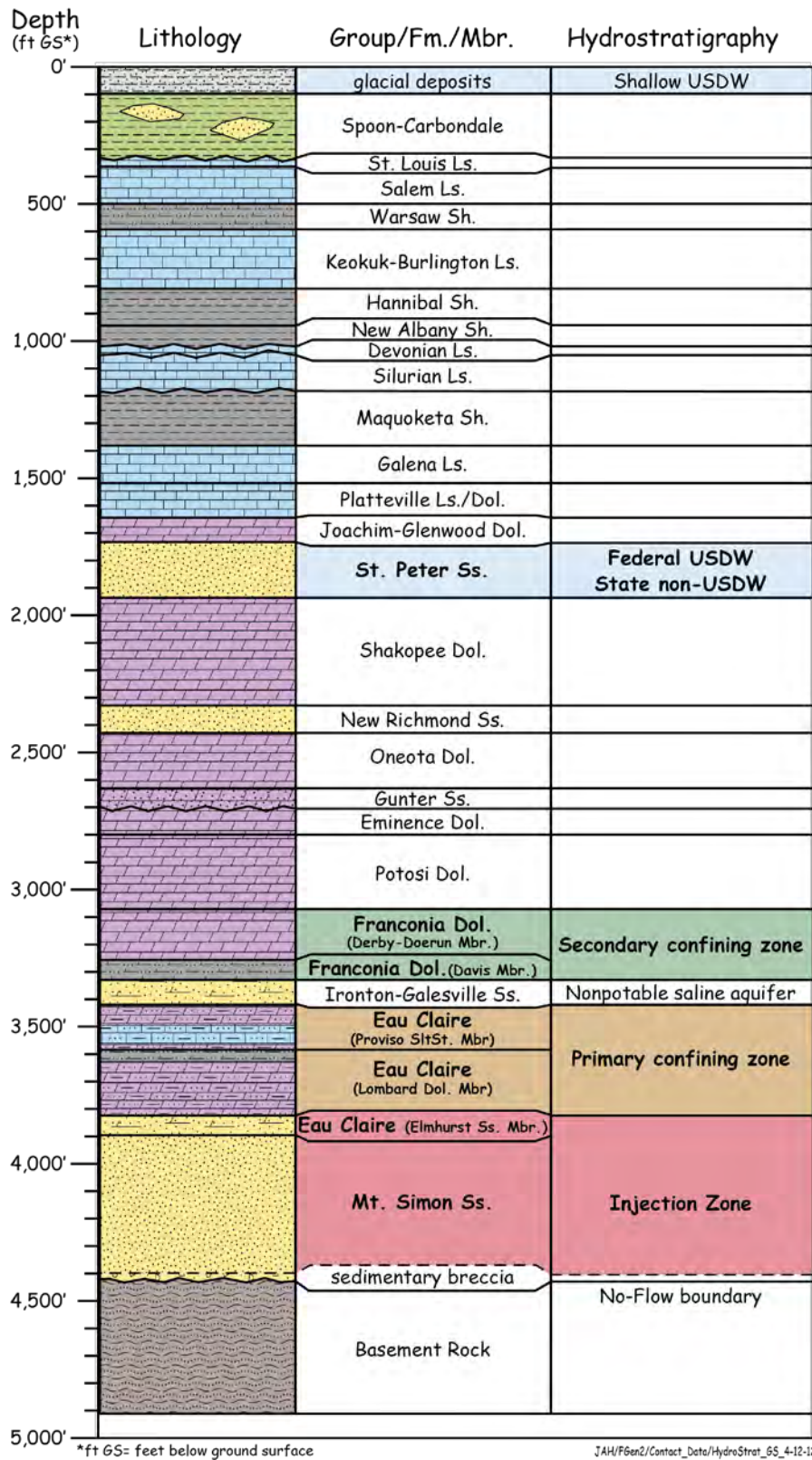


Figure 2.1. Stratigraphy and Proposed Injection and Confining Zones at the Morgan County CO₂ Storage Site

2.1.1 Regional Geology

The regional geology of Illinois is well known from wells and borings drilled in conjunction with hydrocarbon exploration, aquifer development and use, and coal and commercial mineral exploration. Related data are largely publicly available through the Illinois State Geological Survey (ISGS)¹ and the U.S. Geological Survey (USGS).² In addition, the DOE has sponsored a number of studies by the Midwest Geologic Sequestration Consortium³ to evaluate subsurface strata in Illinois and adjacent states as possible targets for the containment of anthropogenic CO₂. This section describes the regional geology, including stratigraphy, structure, and seismicity.

The Mount Simon Sandstone in the Illinois Basin represents a regional target for safe injection of anthropogenic CO₂ (Leetaru et al. 2005). The Illinois Basin covers an area of about 110,000 mi² over Illinois and parts of Indiana and Kentucky (Figure 2.2). The Illinois Basin contains approximately 120,000 mi³ of Cambrian to Pennsylvanian marine and terrestrial sedimentary rocks with a maximum thickness of about 15,000 ft (4,572 m) (Buschbach and Kolata 1991; Goetz et al. 1992; McBride and Kolata 1999). The basin structure across the proposed CO₂ storage site is shown in two regional cross sections in Figure 2.3 and Figure 2.4.

The thickest part of the Cambrian Mount Simon Sandstone is in northeast Illinois, where it exceeds a thickness of 2,600 ft (792 m). A post-Cambrian shift in basin subsidence gradually caused the center of the basin to migrate southeast. As a result, today the deepest part of the Illinois Basin lies in extreme southeastern Illinois. In that area, the top of the Precambrian basement is deeper than 14,000 ft (4,267 m), and the depth to the Mount Simon Sandstone is about 13,500 ft (4,114 m) (Willman et al. 1975). In west-central Illinois the Precambrian basement dips gently to the east-southeast (Figure 2.5).

¹ <http://www.isgs.uiuc.edu/>

² <http://www.usgs.gov/>

³ <http://sequestration.org/>



Figure 2.2. The Illinois Structural Basin Within the Midwestern United States (modified from Buschbach and Kolata 1991)

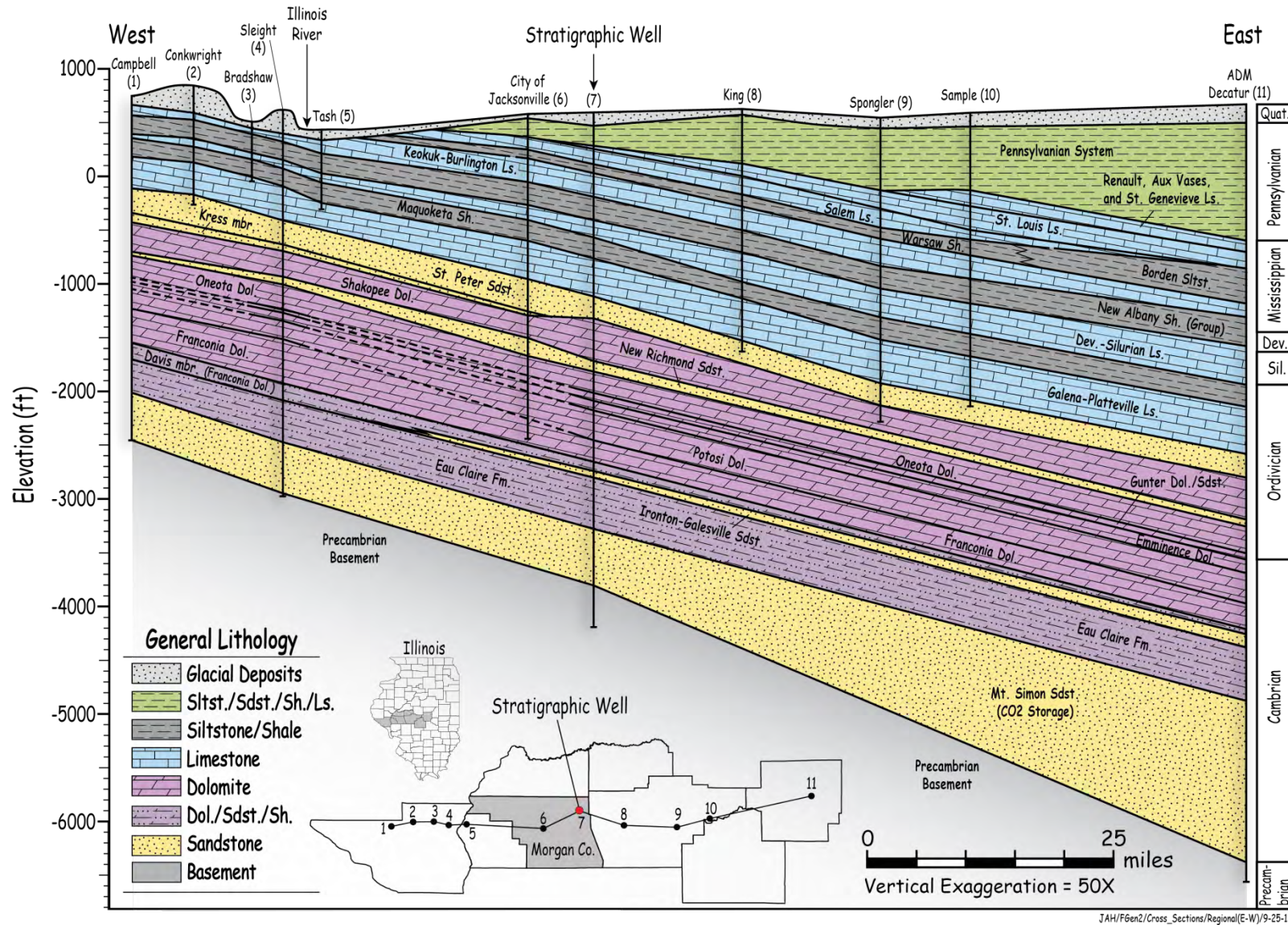
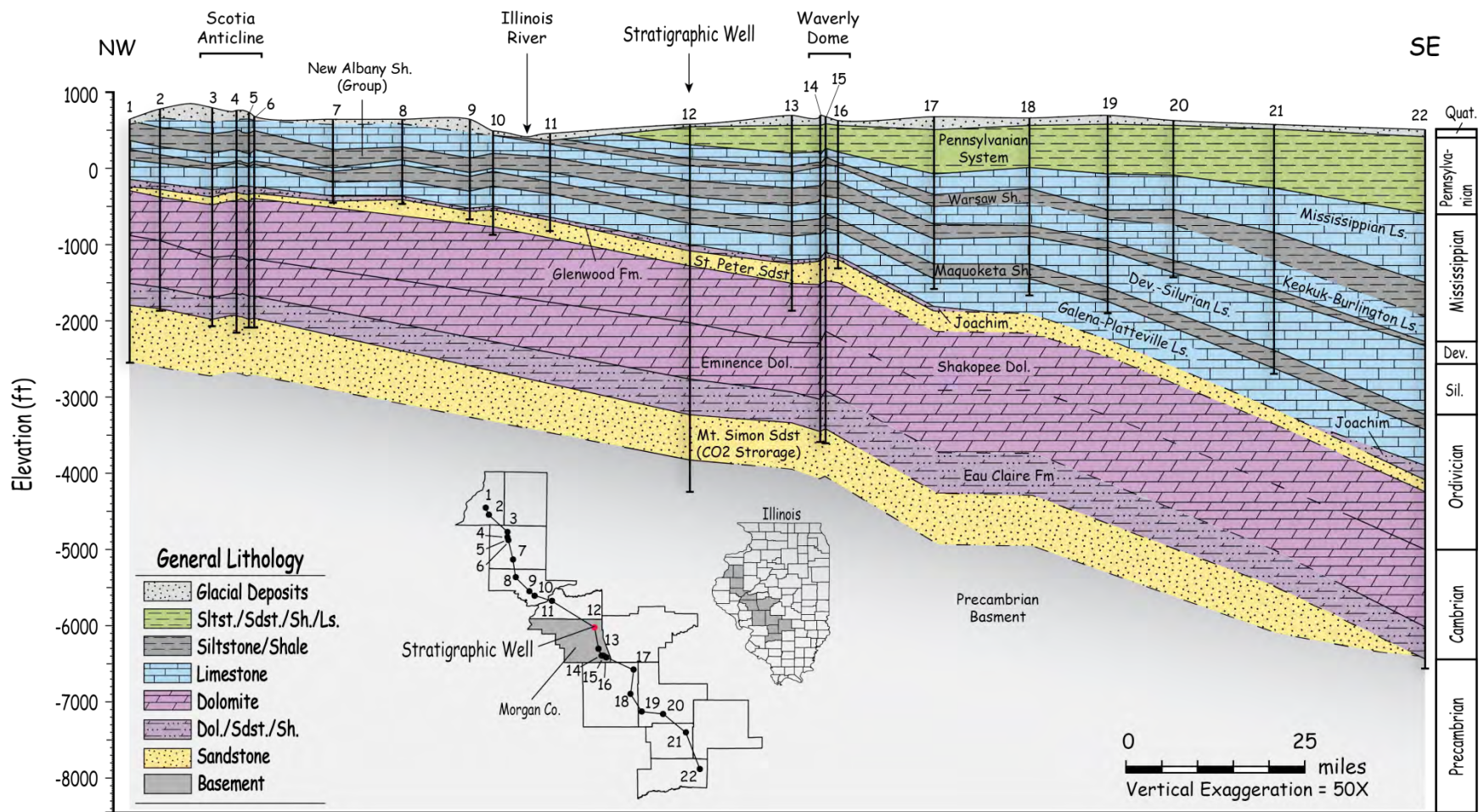


Figure 2.3. Regional East-West Cross Section Across the Western Half of Illinois (based in part on data from ISGS 2011)



Fut6en/N-S_x-sec_KRP_092512

Figure 2.4. Regional North-South Cross Section (based in part on data from ISGS 2011a)

2.1.2 Major Stratigraphic Units

The following discussion includes the regional characteristics of the Precambrian basement that underlies the injection zone, the Mount Simon and Elmhurst sandstones (proposed CO₂ injection zone), the confining zone immediately above the injection zone (upper Eau Claire Formation), and the secondary confining zones.

2.1.2.1 Precambrian Basement

Regionally, the Precambrian basement (see Figure 2.5) that underlies the Mount Simon Sandstone includes silica-rich igneous and metamorphic rock (Bickford et al. 1986; McBride and Kolata 1999). Similar Precambrian rocks also underlie the Mount Simon Sandstone equivalent (the Lamotte Sandstone) in Missouri (Kisvarsanyi 1979; Lidiak 1996). Considerable topographic relief (up to 1,800 ft [549 m]) has been mapped on the Precambrian basement (Leetaru and McBride 2009). Much of this relief is erosional topography created prior to deposition of Cambrian sediments and may exert considerable influence on injection zone thickness, lithology (character of the rock formation), and lithofacies characteristics of the Mount Simon Sandstone (Bowen et al. 2011).

Published analyses of the Precambrian basement rocks regionally within the Illinois Basin indicate they have extremely low porosity and permeability (Table 2.1). Furthermore, wireline log calculations of permeability indicate that fractures in the Precambrian rock are not transmissive. Available data indicate that the basement rock represents a basal confining, no-flow boundary for proposed injection of CO₂ into the Mount Simon Sandstone.

Table 2.1. Published Physical Properties for Precambrian Basement Rocks in the Illinois Basin

Reference	Permeability (mD)	Porosity (%)	Pore Compressibility (Pa ⁻¹)	Hydraulic Conductivity (cm/sec)
EPA (2011)	0.0091			1.8x10 ⁻¹²
Birkholzer et al. (2008)	0.03 in top portion	0.05 in top portion		
Birkholzer et al. (2008)	0.0001	0.05		
Zhou et al. (2010)		0.05		
Zhou et al. (2010)	Kh and Kv = 0.0001E ⁻¹⁵ m ²	0.05	7.42E ⁻¹⁰ and 22.26E ⁻¹⁰	
Sminchak (2011)	0.0008 (ave. of 13 samples)	1.8 (ave. of 13 samples)		

2.1.2.2 Geology of the Injection Zone: Mount Simon and Elmhurst Sandstones

The Mount Simon Sandstone along with the Elmhurst Sandstone member of the Eau Claire Formation is the target zone for the injection of CO₂. The Mount Simon Sandstone has a proven injection-zone capacity, based on a number of natural-gas storage facilities across the Illinois Basin (Buschbach and Bond 1974; Morse and Leetaru 2005) and data from the Archer Daniels Midland (ADM) carbon sequestration site in Macon County, Illinois (Leetaru et al. 2009).

More than 900 wells, mostly pre-1980, have been drilled into the Mount Simon Sandstone in the Illinois Basin (ISGS 2011a); about 50 of these wells in Illinois extend to the Precambrian basement underlying the Mount Simon. Most of the wells drilled into the Mount Simon Sandstone prior to 1980 lack well-log suites suitable for quantitative analysis of porosity and permeability. In north-central

Illinois where the Mount Simon Sandstone is used for natural-gas storage, some detailed analyses of porosity, permeability, and lithofacies connectivity are available, although most gas-storage wells only penetrate the upper part of the Mount Simon (Morse and Leetaru 2005).

The regional structural dip of the Mount Simon Sandstone in Morgan County is to the southeast as shown in Figure 2.6. The thickness of the Mount Simon ranges from less than 500 ft (152 m) in westernmost and southwestern Illinois to more than 2,500 ft (792 m) in the northeastern part of the state (Figure 2.7). The Mount Simon Sandstone thins or is not present over Precambrian structures and paleotopographic highs, such as the Ozark Dome in southeastern Missouri, and localized highs several tens of miles west and south of the proposed Morgan County CO₂ storage site (Figure 2.6 and Figure 2.9).

Regionally, the Mount Simon Sandstone varies in lithology from conglomerate to sandstone to shale. Bowen et al. (2011) recognized six dominant lithofacies in studying the Mount Simon Sandstone from 135 wells over a multi-state area (eastern Illinois, Indiana, northern Kentucky, and Tennessee). These lithofacies include cobble conglomerate, stratified gravel conglomerate, poorly sorted sandstone, well-sorted sandstone, interstratified sandstone and shale, and shale. Diagenetic clay minerals in the Mount Simon Sandstone most commonly include illite and kaolinite. Cements that can occlude porosity include iron oxide, authigenic clay, and quartz overgrowths (Bowen et al. 2011).

The ADM UIC Class 6 Application (EPA 2011) reported that in the ADM carbon capture and storage (CCS) well number 1 (ADM CCS#1 well), poorly sorted sandstone lithofacies, containing intervals of better-sorted finer and coarser sandstone, were the most common lithofacies in the Mount Simon Formation; some thin shale stringers were also present. An arkosic interval was selected as the injection target. The ADM CCS#1 well is closer to the center of the Cambrian Illinois Basin depocenter than is the proposed Morgan County CO₂ storage site. Lithologic variability is expected across the basin, especially in the lower part of the Mount Simon Sandstone, where lithologies can change due to paleotopography and depositional environment.

The Mount Simon Sandstone represents continental and shallow marine environments of deposition that reflect gentle basin subsidence and gradual transgressive marine encroachment over the deeply eroded Precambrian basement rocks (Leetaru et al. 2009). Terrestrial depositional environments such as alluvial fans, braided streams, eolian dunes, and wadi deposits are interpreted in the Mount Simon core from wells and outcrop in Missouri and Wisconsin (Houseknecht 2001; Hunt 2004; Wilkens et al. 2011). Transitional marine depositional environments represented in the Mount Simon Sandstone include barrier islands, deltas, and tidal inlets with shallow marine sands and coastal bars (Sargent and Lasemi 1993; Wilkens et al. 2011; Driese et al. 1981). The continental depositional lithofacies transition upward into marine facies of the Eau Claire Formation. This change is indicative (along with patterns of sediment thickening) of basin subsidence and sea-level rise during a major marine transgressive event (Kolata and Nimz 2010).

Included as part of the proposed injection zone is the Elmhurst Sandstone, the basal (lowest) member of the Eau Claire Formation (see Figure 2.1). The Elmhurst Sandstone consists of fine- to medium-grained, fossil-bearing, white, red, or gray sandstones with irregular interbedded gray shales and minor dolomite (Willman et al. 1975). Regionally, these sandstones are porous, permeable, and in hydrologic communication with the Mount Simon Sandstone (Buschbach and Bond 1974; Hanson 1960; Hunt 2004; Morse and Leetaru 2005).

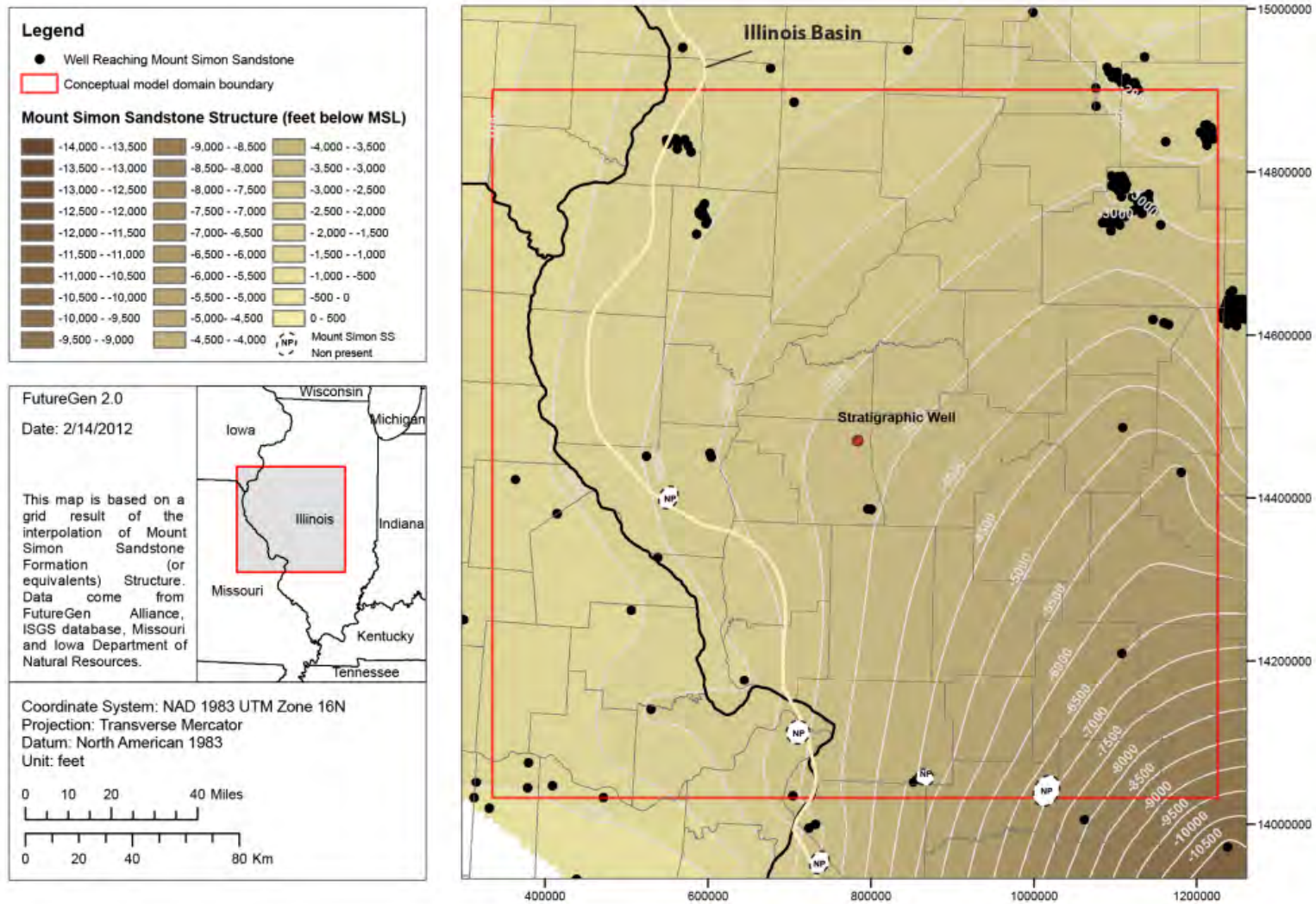


Figure 2.6. Structure on Top of the Mount Simon Sandstone in West-Central Illinois and Portions of Iowa and Missouri (based in part on data from ISGS 2011a, MDNR 2012, and IDNR 2012). White areas represent nondeposition of the Mount Simon Sandstone on Precambrian paleotopographic highs.

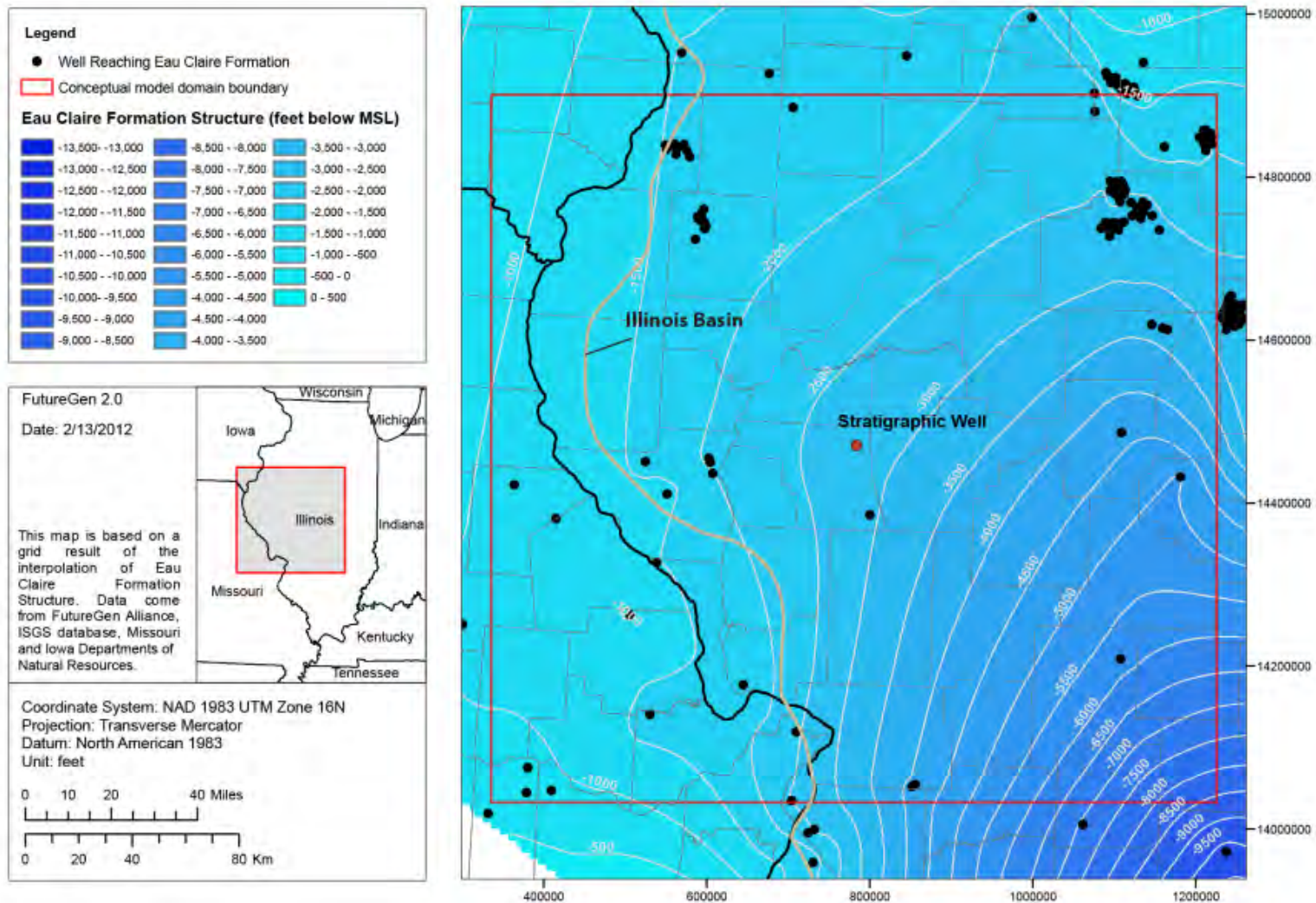


Figure 2.8. Structure-Contour Map for the Top of the Eau Claire Formation in West-Central Illinois and Portions of Iowa and Missouri (based in part on data from ISGS 2011a, MDNR 2012, and IDNR 2012)

2.1.2.3 Geology of the Confining Zone: Eau Claire Formation

The Eau Claire Formation is a widespread, heterolithic carbonate and fine siliciclastic unit present across west-central Illinois (Figure 2.8) and parts of seven adjoining states (Sminchak 2011). The low-permeability Lombard and Proviso members of the Eau Claire form an effective confining layer at 38 natural-gas storage reservoirs in Illinois (Buschbach and Bond 1974; Morse and Leetaru 2005). The confining members of Eau Claire overlie the Elmhurst Sandstone member (see Figure 2.1).

Regionally, the Lombard member of the Eau Claire Formation consists of glauconitic and sandy dolomite interbedded with mudstones and shale; the shale content increases to the south and sand content increases to the west and north (Willman et al. 1975). The Lombard member is overlain by the Proviso member, which is characterized by limestone, dolomite, sandy siltstone, and shale beds. The Lombard and Proviso members are continuous and extend across several buried Precambrian highs in the region.

In addition to the Eau Claire Formation, the widespread, low-permeability Franconia Dolomite Formation (Figure 2.1) (Kolata and Nimz 2010) may be considered a secondary confining zone for the containment of scCO₂ within the region (see Figure 2.1).

2.1.3 Site Geology

The proposed storage site is located approximately 11 mi (18 km) northeast of the City of Jacksonville, 6 mi (9.7 km) north of the unincorporated village of Alexander, and 6 mi (9.7 km) southwest of Ashland (see Figure 2.2). To support the evaluation of the Morgan County site as a potential carbon storage site a deep stratigraphic well (Figure 2.9) was drilled and extensively characterized. The stratigraphic well, located at longitude 90.0528W, latitude 39.8067N, is approximately 1 mi (1.6 km) east of the planned storage site. The results and interpretations of the data from the stratigraphic well are presented in this supporting documentation and used to support the following discussions of site-specific geology and hydrology at the proposed Morgan County CO₂ storage site.

The stratigraphic well reached a total depth of 4,826 ft (1,471 m) bgs within the Precambrian basement. The well penetrated 479 ft (146 m) of the Eau Claire Formation and 512 ft (156 m) of the Mount Simon Sandstone. Contact picks in the stratigraphic well (Figure 2.9) are based on correlations with wells in the ISGS database as well as comparison of the well cuttings with lithologies in drillers logs and published descriptions.

The stratigraphic well was extensively characterized, sampled, and geophysically logged during drilling. These resulting data, together with the regional data, form the basis for developing a conceptual model. Intervals where wireline geophysical logs and rotary side-wall drill cores were acquired are listed in Table 2.2. A total of 177 ft of whole core were collected from the lower Eau Claire-upper Mount Simon Sandstone (Table 2.3) and 34 ft were collected from lower Mount Simon Sandstone-Precambrian basement interval. In addition to whole drill core, a total of 130 side-wall core plugs were obtained from the combined interval of the Eau Claire Formation, Mount Simon Sandstone, and the Precambrian basement. Depths for the primary hydrogeologic units relevant to injection of CO₂ and protection of USDWs are listed in Table 2.4. Slabbed cores from the Lombard and Elmhurst members and the Mount Simon Sandstone are shown in Figure 2.10.

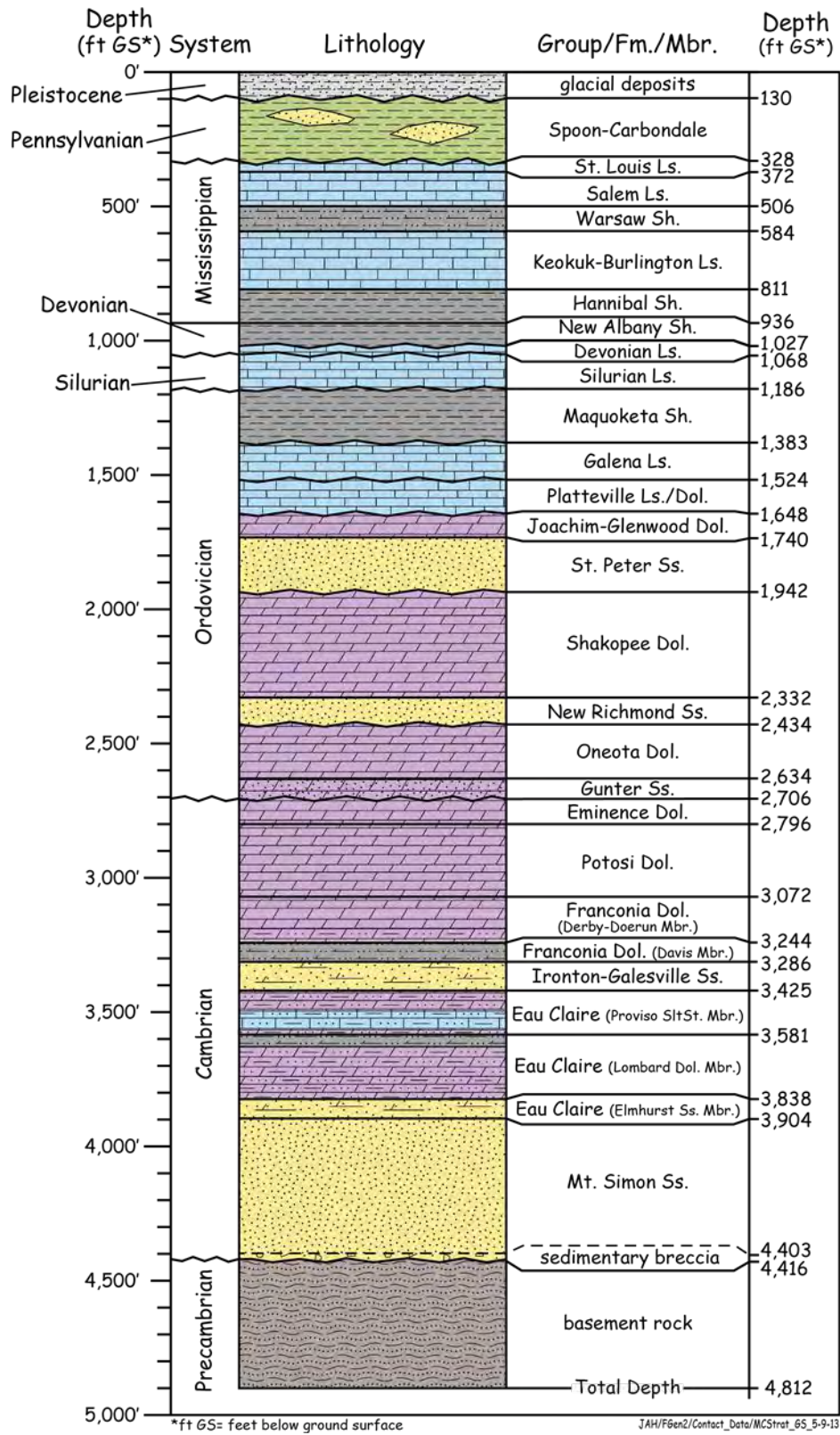


Figure 2.9. Stratigraphic Column for the Recently Drilled Stratigraphic Well at the Proposed Morgan County CO₂ Storage Site. Wavy lines represent major unconformities reported for the Morgan County area by Willman et al. (1975).

Table 2.2. Intervals of Geophysical Wireline Characterization Logs and Side-Wall Cores Collected in the Stratigraphic Well

Log Type	Run #	Log Interval Top (ft bgs)	Log Interval Bottom (ft bgs)
Triple Combo	1	31	2,036
Resistivity	1	31	2,036
Triple Combo (Gamma, Neutron, Density) plus Photoelectric Cross-Section Log	2	553	4,015
Sonic Dipole	2	566	3,962
Resistivity Image	2	564	4,013
Spectral Gamma Ray	2	372	3,978
Elemental Capture Log	2	91	4,014
Rotary Side-Wall Cores	2	Top Sample 684	Bottom Sample 3,968
Triple Combo (Gamma, Neutron, Density) plus Photoelectric Cross-Section Log	3	3,932	4,806
Sonic Dipole	3	3,932	4,806
Resistivity Image	3	3,966	4,810
Ultrasonic Image	3	3,922	4,886
Spectral Gamma Ray	3	3,932	4,806
Elemental Capture Log	3	81	4,024
Nuclear Magnetic Resonance	3	3,932	4,806
Rotary Side-Wall Cores	3	Top Sample 4,020	Bottom Sample 4,782

Table 2.3. Whole-Core Intervals Collected from the Stratigraphic Well

Core Run #	Core Diameter (in.)	Interval Top (ft bgs)	Interval Bottom (ft bgs)	Number of Feet Cored/Recovered	Stratigraphic Unit
1	3.5	3,758	3,868	110/107.8	Eau Claire Lombard and Elmhurst members
2	3.5	3,868	3,908	40/30.0	Eau Claire Elmhurst member
3	3.5	3,910	3,943	33/33.0	Upper Mount Simon Sandstone
4	4.5	4,486	4,420	34/25.9	Lower Mount Simon Sandstone and Precambrian basement
5	4.5	4,420	4,428	8/8.5	Precambrian basement

Table 2.4. Hydrogeology of the Injection and Confining Zones Within the Stratigraphic Well

Stratigraphic Unit	Hydrostratigraphic Unit	Top Depth (ft bgs)	Thickness (ft)
Eau Claire (Proviso member)	Eau Claire Siltstone (Confining zone)	3,425	156
Eau Claire (Lombard member)	Eau Claire Dolomite (Confining zone)	3,581	257
Eau Claire (Elmhurst member)	Eau Claire Sandstone (Injection zone)	3,838	66
Mount Simon Sandstone	Mount Simon Sandstone (Injection zone)	3,904	512
Precambrian basement	(Lower No-Flow Boundary)	4,416	>400



Figure 2.10. Slabbed Whole Core from the Lowermost Lombard Member Mudstones and Siltstones, the Elmhurst Sandstones, and the Lower Mount Simon Sandstones from the Stratigraphic Well

2.1.3.1 Injection Zone

The combined thickness of the proposed injection zone, which includes the Mount Simon and Elmhurst sandstones, is 565 ft (172 m) at the stratigraphic well (Figure 2.9). As observed in cuttings, core logs, and image logs, the Mount Simon Sandstone primarily consists of fine-to-coarse quartz arenite with local granule-rich quartz or arkosic sandstone beds. Based on the computed mineralogy (Elemental Analysis [ELAN]) log, feldspar appears to be considerably more common in the lower part of the Mount Simon Sandstone. In Figure 2.11, cored intervals are indicated with red bars; rotary side-wall core and core-plug locations are indicated to the left of the lithology panel. Standard gamma ray and resistivity curves are shown in the second panel; ELAN-calculated permeability (red curve) is in the third panel, along with two different lab measurements of permeability for each rotary side-wall core. Neutron- and density-crossplot porosity is shown in the fourth panel, along with lab-measured porosity for core plugs and rotary side-wall cores. The proposed injection interval (location of the horizontal wells' injection laterals) is highlighted on the geophysical log panels in Figure 2.11.

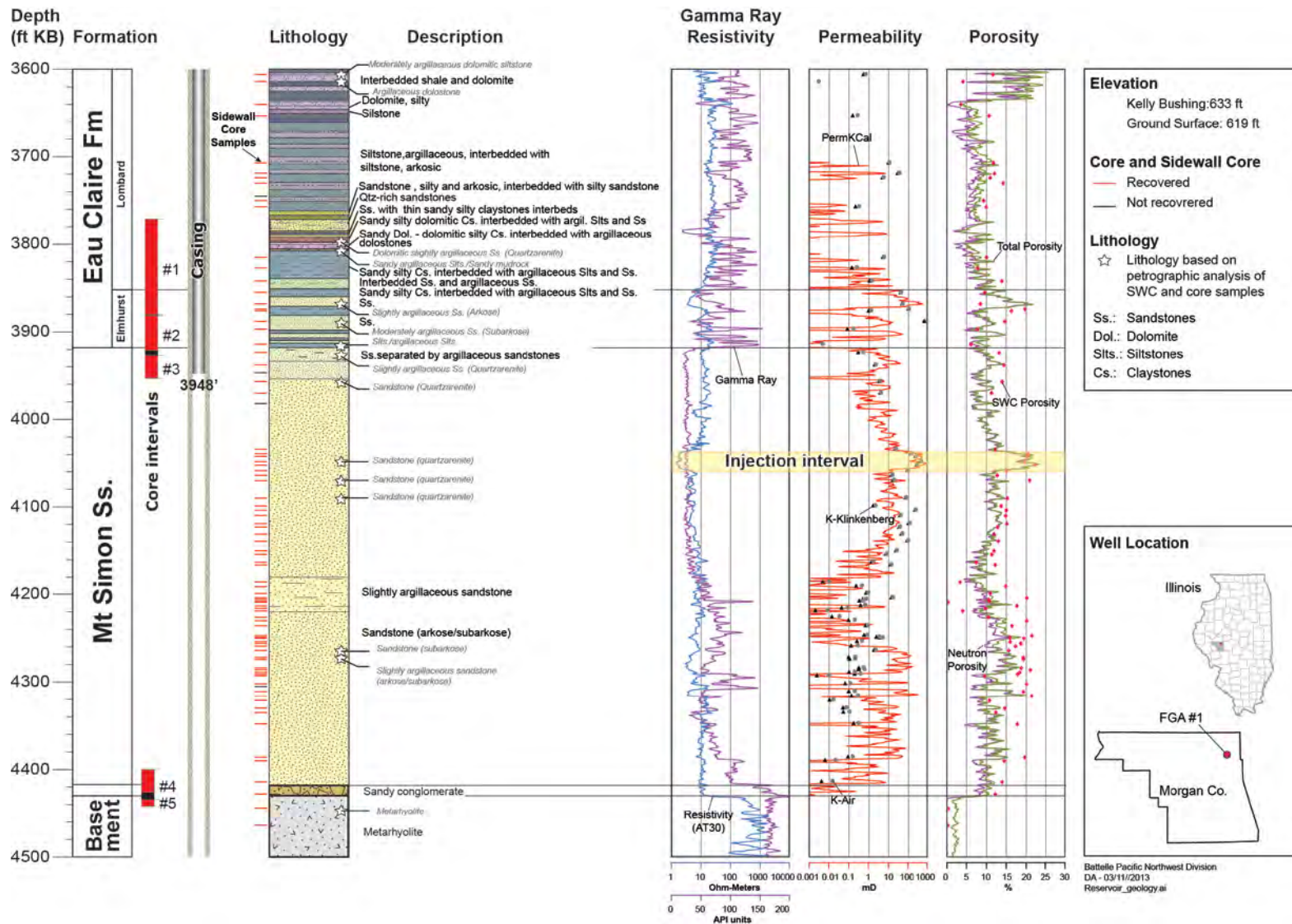


Figure 2.11. Lithology, Mineralogy, and Hydrologic Units of the Proposed Injection Zone (Mt Simon and Elmhurst) and Lower Primary Confining Zone (Lombard), as Encountered Within the Stratigraphic Well. Data are explained in the text.

Permeability in the sandstones, as measured in rotary side-wall cores and plugs from whole core, appears to be dominantly related to grain size and abundance of clay. Horizontal permeability (K_h) data in the stratigraphic well outnumber vertical permeability (K_v) data, because K_h could not be determined from rotary side-wall cores. However, K_v/K_h ratios were successfully determined for 20 vertical/horizontal siliciclastic core-plug pairs cut from intervals of whole core. Within the Mount Simon Sandstone, the horizontal permeabilities of the lower Mount Simon alluvial fan lithofacies range from 0.005 to 0.006 mD and average ratios of vertical to horizontal permeabilities range from 0.635 to 0.722 (at the 4,318–4,388 ft KB depth, Figure 2.11). Horizontal core-plug permeabilities range from 0.032 to 2.34 mD at the 3,852–3,918 ft KB depth; K_v/K_h ratios for these same samples range from 0.081 to 0.833. Details of K_h and K_v by depth and by numerical model layer are covered in Chapter 3.0.

2.1.3.2 Confining Zone

The Proviso and Lombard members of the Eau Claire Formation form the primary confining zone for the proposed Morgan County CO₂ storage site. The combined thickness of these strata is 413 ft (126 m) at the stratigraphic well. Eighty ft (24 m) of whole core were obtained in the Lombard member of the Eau Claire Formation, along with 13 rotary side-wall cores. In addition, 10 rotary side-wall cores were collected in the Proviso member.

Rock cuttings and rotary side-wall core lithologies from the upper Proviso member include tan to light brown, dense, occasionally glauconitic microcrystalline, slightly dolomitic limestone. The lower half of the Proviso member is a tan to cream, argillaceous, and slightly silty microcrystalline dolomite with interbedded siliceous cemented quartz sandstone. The sand grains are very fine- to fine-grained, sub-rounded and clear to white with occasional glauconite.

Thinly bedded to laminated siltstone and mudstone dominate lithologies in the Lombard; whole core and rotary side-wall cores indicate lithologies are extremely heterolithic. Well cuttings include red to light brown, non-calcareous shale near the top of the member with tan to light brown, siliceous, finely crystalline dolomite. Thin bands of dolomite are present in some rotary side-wall cores. Minor abundances of glauconite are present in drill cuttings throughout the section; and trace amounts of oolites were observed in cuttings near the top of the unit. Thin beds of quartz sandstone are present in the Lombard, immediately overlying the Elmhurst member.

Wireline and core-based lithology, porosity, and permeability for the primary confining zone are shown in Figure 2.12. The computed lithology track indicates the upward decrease in quartz silt and increase in carbonate in the Proviso member, along with a decrease in permeability. The permeabilities of the rotary side-wall cores in the Proviso range from 0.000005 mD to 1 mD (Table 2.5); the one sample lower than 0.0001 is not shown in Figure 2.12. Permeabilities in the Lombard member range from 0.001 mD to 28 mD, reflecting the greater abundance of siltstone in this interval, particularly in the lowermost part of the member. The upward decrease in computed log permeability (red curve in the permeability panel) reflects decreasing silt supply and possibly increasing water depths of the original depositional environment.

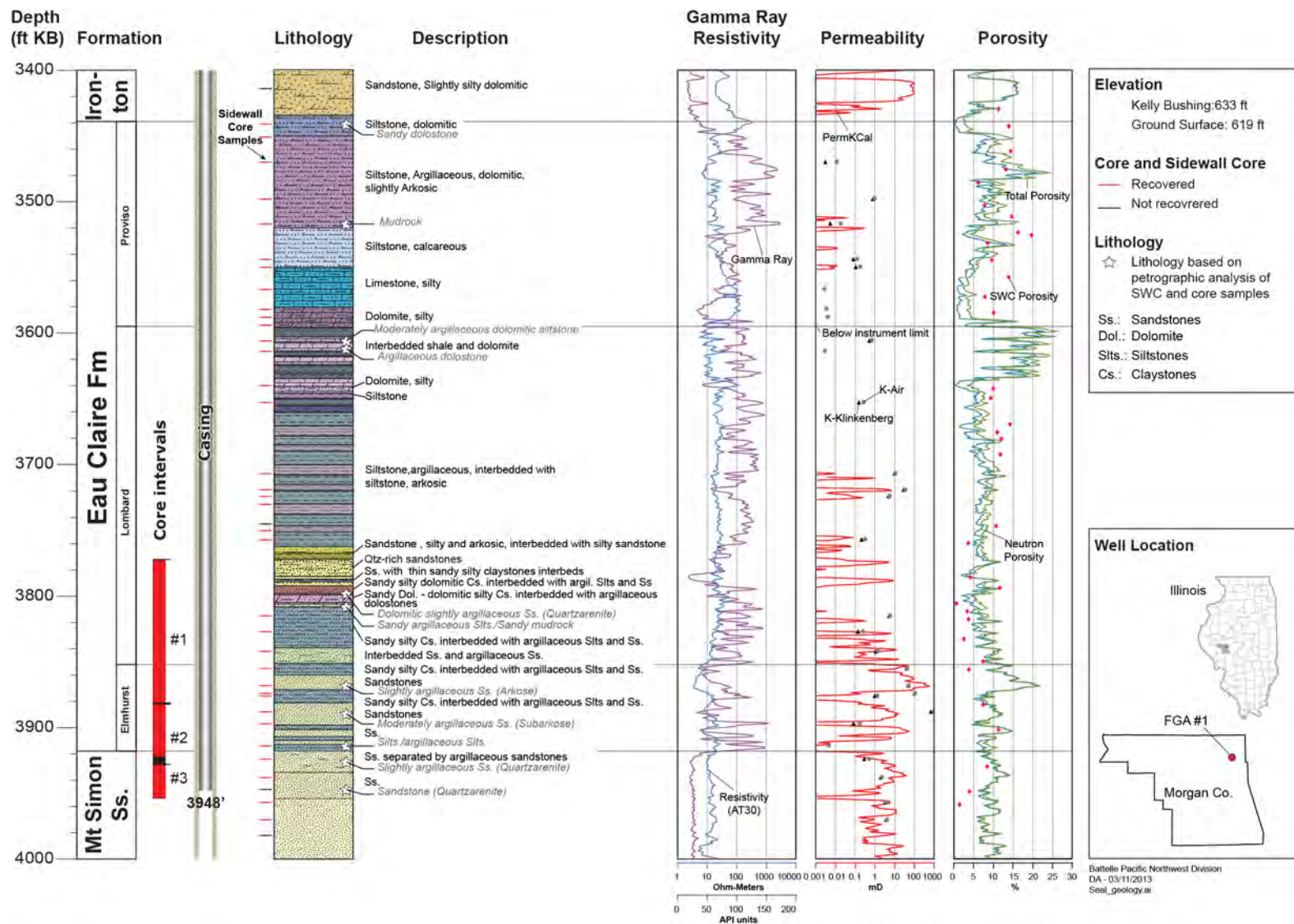


Figure 2.12. Relationship Between Lithology, Mineralogy, Side-Wall Core and Wireline Log Computed (ELAN) Permeability for the Eau Claire Formation and Uppermost Mount Simon Intervals in the Stratigraphic Well. One Proviso sample with permeability below 0.0001 mD is not shown.

Whole core plugs and associated vertical permeabilities are available only from the lowermost part of the Lombard. Thin (few inches/centimeters), high-permeability sandstone streaks resemble the underlying Elmhurst; low-permeability siltstone and mudstone lithofacies have vertical permeabilities of 0.0004-0.465 mD, and Kv/Kh ratios of 0.000 to 0.17.

Table 2.5. Permeabilities from Proviso Member Rotary Side-Wall Cores

Formation	Depth (ft bgs)	Horizontal Permeability (mD)
Eau Claire (Proviso member)	3,427	.0001
Eau Claire (Proviso member)	3,437	.0001
Eau Claire (Proviso member)	3,456	.003
Eau Claire (Proviso member)	3,484	.795
Eau Claire (Proviso member)	3,503	.005
Eau Claire (Proviso member)	3,530	.082
Formation	Depth (ft bgs)	Horizontal Permeability (mD)
Eau Claire (Proviso member)	3,536	.108
Eau Claire (Proviso member)	3,553	.0005
Eau Claire (Proviso member)	3,568	.001
Eau Claire (Proviso member)	3,574	.001
Eau Claire (Proviso member)	3,580	.000005

It is important to note that regional well-log correlations and drilling data indicate that the Lombard and Proviso members of the Eau Claire Formation do not pinch out against paleotopographic highs west of the proposed Morgan County CO₂ storage site. Instead, these confining units are laterally continuous and overstep the Precambrian highs in Pike County.

2.1.3.3 Secondary Confining Zone

The combined 244-ft (74-m) interval of the Franconia Dolomite Formation (Figure 2.9) form a secondary confining zone for the Mount Simon and Elmhurst injection zones. The Franconia lithology, as observed in well cuttings, is dominated by tan to light brown, microcrystalline dolomite. Dolomite in cuttings from the upper part of the Franconia contains minor amounts of fine-grained, clear and sub-rounded quartz sand. The lower part of the Franconia is a slightly pyritic and glauconitic cream to light brown, microcrystalline dolomite with scattered grains of clear, sub-rounded quartz sand.

The underlying Davis member is a low-permeability, light gray to light brown, microcrystalline dolomite and argillaceous (shaley), sandy dolomite. The lowermost part of the unit is a tight argillaceous, dolomitic sandstone that marks the upward transition from the Ironton Sandstone. The Davis member dolomites regionally grade laterally into low-permeability shales (Willman et al. 1975).

The ELAN geophysical logs indicate effective porosities (total porosity minus shale effect or clay-bound water) in the Franconia range from <0.01 to 7 percent, with an average of 3 percent; and effective porosities in the Davis interval range from <0.01 to 3 percent, with an average of 0.1 percent in the upper part of the Davis, and an average effective porosity of 0.79 percent in the lower, more argillaceous (clay-rich) part of the unit.

The ELAN geophysical logs indicated permeabilities are generally less than the wireline tool limit of 0.01 mD throughout the secondary confining zone. Two rotary side-wall cores were taken from the

Franconia, and three side-wall cores were cut in the Davis member. Laboratory-measured rotary side-wall core (horizontal) permeabilities (Table 2.6) are very low (0.001–0.000005 mD). The permeabilities of the two Franconia samples were measured with a special pulse decay permeameter; the sample from 3,140 ft bgs (957 m) has a permeability less than the lower instrument limit of 0.000005 mD. A relatively high porosity (7.8 percent porosity with 12.5-mD permeability) was recorded for one Davis side-wall core. This appears to represent an isolated thin (less than 1 ft [15 cm] sand stringer within the lower Davis member).

Table 2.6. Rotary Side-Wall Core Permeabilities from the Secondary Confining Zone

Formation	Depth (ft bgs)	Horizontal Permeability (mD)
Franconia Dolomite	3,140	<.000005
Franconia Dolomite	3,226	.000006
Davis	3,268	.001
Davis	3,291	0.125
Davis	3,303	12.5

Vertical core plugs are required for directly determining vertical permeability and there are no data from the stratigraphic well for vertical permeability or for determining vertical permeability anisotropy in the secondary confining zone. However, Kv/Kh ratios of 0.007 have been reported elsewhere for Paleozoic carbonate mudstones (Saller et al. 2004).

2.2 Injection Zone Water Chemistry

Analyses of two formation fluid samples from the stratigraphic well, collected at a depth of 4,048 ft (1,234 m) below the kelly bushing (bkb) (Sample 11) using Schlumberger’s Modular Formation Dynamics Tester (MDT) sampler, are shown in Table 2.16. Based on these initial samples, the best estimate total dissolved solids (TDS) concentration selected for initial simulation is a constant 47,500 mg/L throughout the Mount Simon Sandstone. The EPA (2011) reported TDS for eight samples from the Mount Simon Sandstone from the CCS#1 near Decatur, Illinois (Table 2.7). TDS varied with depth yielding a minimum concentration of 164,500 mg/L at 5,772 ft (1,759 m) and a maximum concentration of 228,100 mg/L at 7,045 ft (2,147 m). Note that these depths are 2,000 to 3,000 ft (610 to 914 m) deeper than those encountered at the Morgan County CO₂ storage site and would represent an upper maximum for TDS at the proposed storage site.

Table 2.7. Data from Fluid Samples Collected with the MDT Sampler from the Mount Simon Sandstone in the CCS#1 Well at the Decatur Site (modified after EPA 2011)

Sample ID	Depth (ft)	Formation Pressure (psi)	Formation Temperature (degrees F)	TDS (mg/L)	Brine Density (g/L)
MDT-4	5,772	2,582.9	119.8	164,500	1.09
MDT-3	6,764	3,077.5	125.1	185,600	1.12
MDT-14	6,764	3,077.5	125.1	179,800	Not analyzed
MDT-5	6,840	3,105.9	125.0	182,300	1.12
MDT-9	6,840	3,105.9	125.0	219,800	Not analyzed
MDT-2	6,912	3,141.8	125.8	211,700	1.14
MDT-1	7,045	3,206.1	125.7	228,100	1.12
MDT-8	7,045	3,206.1	125.7	201,500	Not analyzed

2.3 Geologic Structure

Known major geologic structures in Illinois are shown in Figure 2.13. The proposed storage site is on the southern flank of the very broad Sangamon Arch. Structural dips on sedimentary strata within the western part of the Illinois Basin are low—generally less than one degree to the east and southeast, based on regional structure maps (Figure 2.6 and Figure 2.8).

2.3.1 Site Geologic Structure

The geologic structure in the vicinity of the proposed Morgan County CO₂ storage site consists of a very gentle, 0.25-degree dip to the southeast, as determined by the three-dimensional (3D) geologic conceptual model developed for the site that used local and regional well data. Low structural dips are confirmed by the resistivity-based image logs (Formation Microimager) acquired in the stratigraphic well. The principal geologic structure in proximity to Morgan County is the very broad Sangamon Arch (Figure 2.13). Neither this map nor any other published sources (Whiting and Stevenson 1965; Kolata and Nelson 1991) indicate the existence of any mapped faults or fracture zones in the vicinity of the proposed Morgan County CO₂ storage site.

2.3.1.1 Reflection Seismic Profiles

Two two-dimensional (2D) surface seismic lines, shown in Figure 2.14, were acquired in January 2011 along public roads near the proposed Morgan County CO₂ storage site. A seismic survey gives an image of the subsurface based on differences in density and seismic wave velocity of the different geologic layers. It allows one to identify formation depths and thicknesses in addition to discontinuities such as faulting.

Both profiles indicate a thick sequence of Paleozoic-aged rocks. The seismic lines are not of optimal quality due to seismic noise,¹ but they do not indicate the presence of obvious faults or large changes in thickness of the injection or confining zones. Apparent discontinuities in the seismic lines appear to be an artifact of processing lines that were acquired along bends in roads as a straight line.

The seismic data acquired along these two seismic profiles were reprocessed by Exploration Development, Inc. in August 2012 to reduce the noise and improve the interpretation (Figure 2.15 and Figure 2.16). Both profiles indicate a thick sequence of Paleozoic-aged rocks with a contact between Precambrian and Mount Simon at 640 ms and a contact between Eau Claire and Mount Simon at 580 ms. Some vertical disruptions, which extend far below the sedimentary basin, remain and their regular spatial periodicity is unlikely related to faults. These discontinuous reflections could also be discontinuities created by collapse features associated with karsts formations that are known to occur in the Potosi Formation.

¹ Jaqucki P, V Smith, H Leetaru, and M Coueslan. 2011. *Seismic Survey Results and Interpretation – Illinois FutureGen 2.0 Potential Sites*. Schlumberger Carbon Services, Westerville, Ohio. Unpublished report to the FutureGen Industrial Alliance.

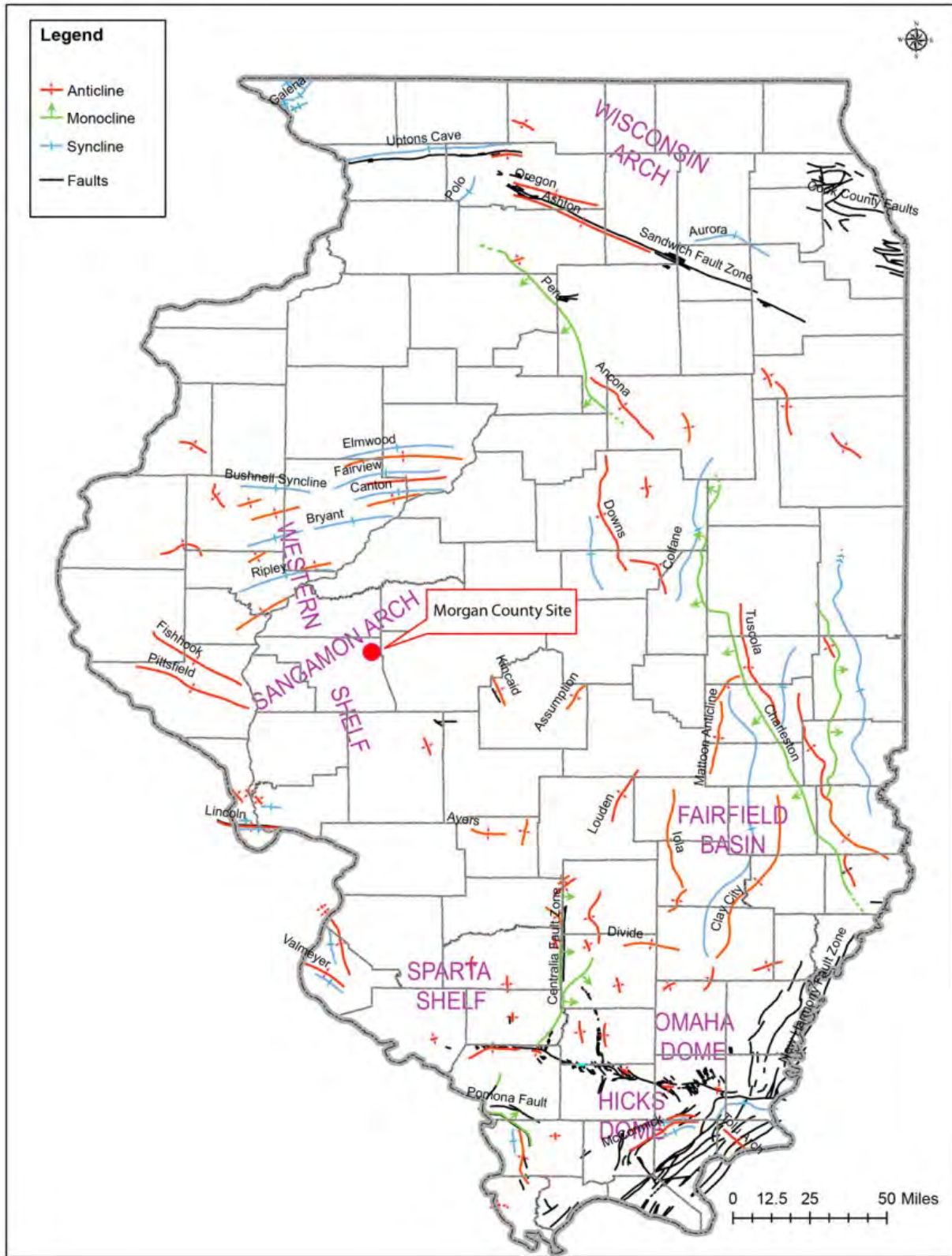


Figure 2.13. Structural Features of Illinois (modified from Nelson 1995)

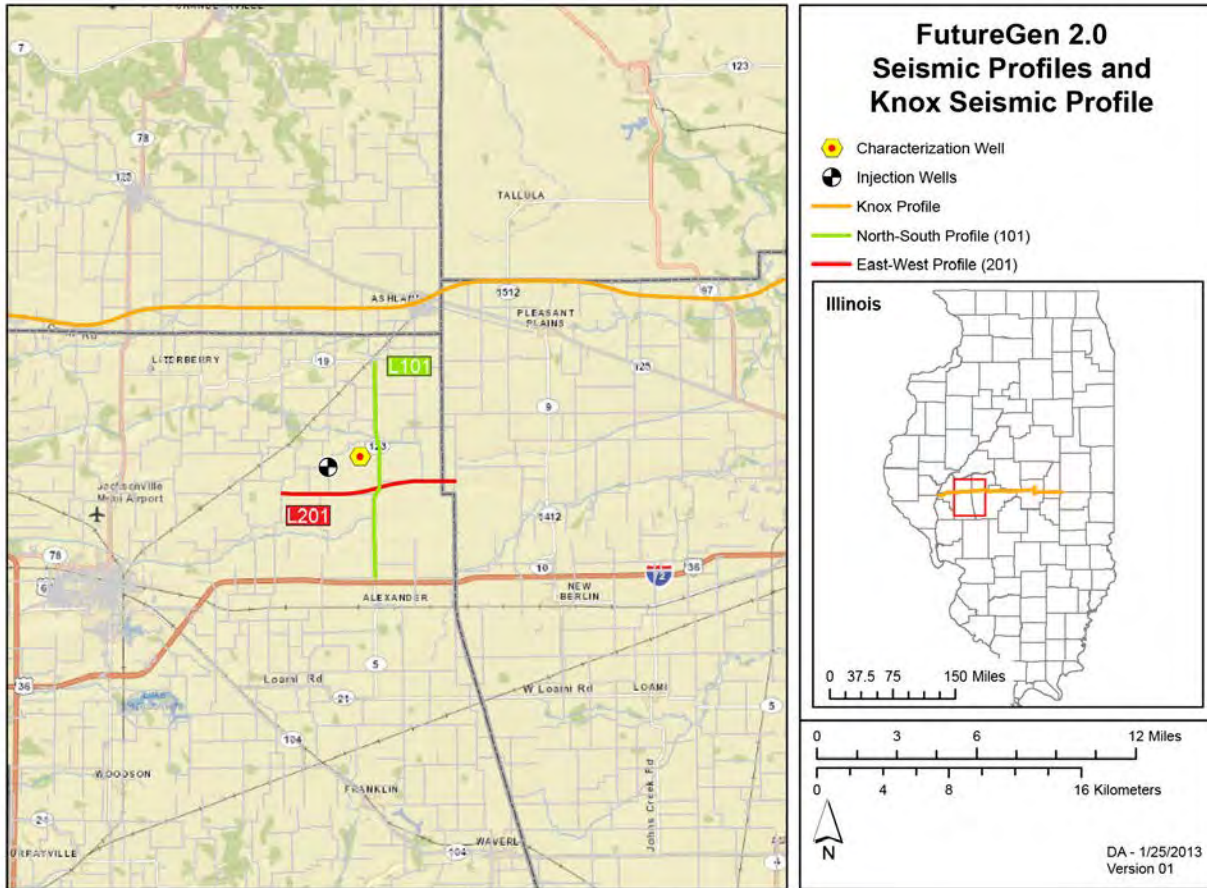


Figure 2.14. Location of the two 2D seismic survey lines, L101 and L201, at the proposed Morgan County CO₂ storage site. The north-south line is along Illinois State Highway 123. The Knox seismic profile completed in 2012 by the ISGS and that passes within 10 miles of the site is also drawn in orange.

A fault can usually be recognized and interpreted in seismic data if it creates a quasi-vertical displacement of 20 ms or more in several successive reflection events. This 20-ms reflector displacement rule represents a reflector discontinuity that most interpreters can see by visual inspection of seismic data. The amount of vertical fault throw that would produce a 20-ms vertical displacement would be $(0.01 \text{ sec}) \times (\text{P-wave interval velocity})$, for whatever interval velocity is appropriate local to a suspected fault. For the interval from the surface down to the Eau Claire at the FutureGen site in Morgan County, the P-wave interval velocity local to seismic lines L101 and L201 ranges from approximately 7,000 ft/s (shallow) to approximately 12,000 ft/s (deep). Thus, faults having vertical throws of 120 ft at the Eau Claire, and perhaps as little as 70 ft at shallow depths, should be detected if they traverse either profile. No faults with a clear vertical displacement have been identified; the only clear observation that can be made is the existence of a growth fault that affects Mount Simon and Eau Claire formations in the eastern part of the L201 profile at offset 28,000 ft (Figure 2.15). This growth fault is more than 1.5 miles away from the outermost edge of the CO₂ plume and does not extend far upward in the overburden. For these reasons, it is highly unlikely that it could affect the integrity of the reservoir.

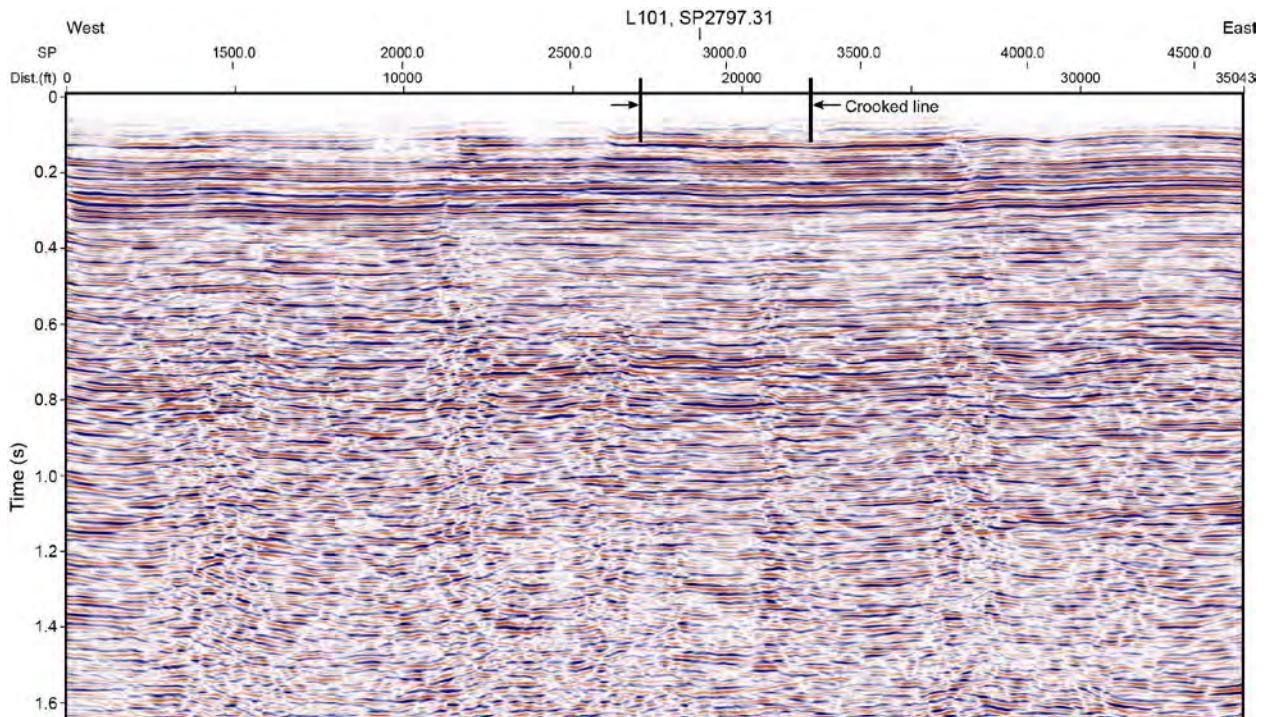


Figure 2.15. Reprocessed West-East 2D Seismic Line L201. Distance along horizontal axis is in feet and time (two-way travel time) along vertical axis is in seconds.

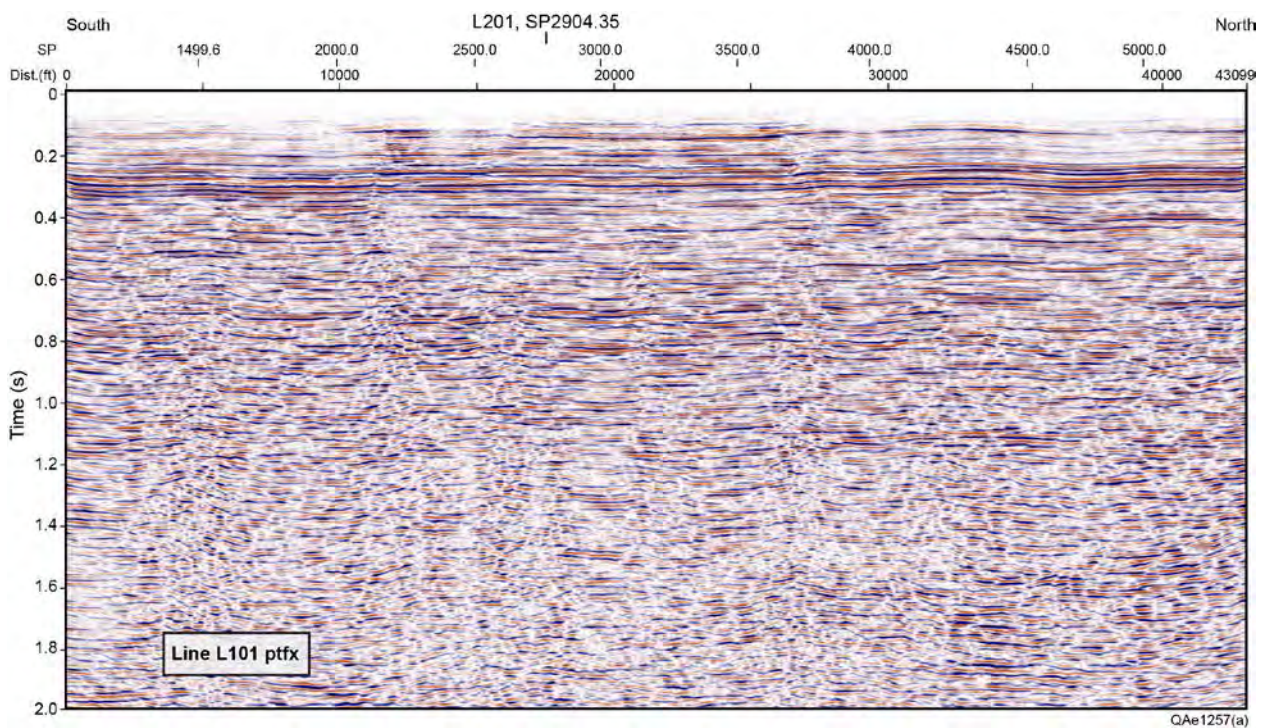


Figure 2.16. Reprocessed South-North 2D Seismic Line L101. Distance along horizontal axis is in feet and time (two-way travel time) along vertical axis is in seconds.

The Illinois State Geological Survey (ISGS) recently acquired a new 120-mi long seismic reflection survey across central Illinois as part of a DOE-sponsored research project to characterize reservoir rocks for geologic storage of carbon dioxide. The continuous east-west line extends from Meredosia to southwestern Champaign County (Figure 2.14). This line, which is currently under re-processing, will supply additional information about the structure of the sedimentary layers which will be correlated to the observations made on both profiles L101 and L201.

Future efforts at Morgan County will also include the acquisition of vertical seismic profiling data in the stratigraphic well to better evaluate the cause of the vertical disruptions in seismic reflections observed on the two existing seismic profiles.

2.3.1.2 Gravity Data

A site-specific surface gravity survey was conducted in November 2011, including 240 regularly spaced stations within a 2-mi by 2-mi area that covers the stratigraphic well site and the proposed storage site (Figure 2.17 and Figure 2.18). This survey will serve as a baseline for time-lapse gravity observations made after the beginning of the injection.

The survey results have a good correlation with the regional gravity maps of Daniels et al. (2008). Located at a minimum between two large-scale 15-mGal positive anomalies, the survey measurements complete the regional survey and allow a better definition of the short wavelength content of the gravity signal above the FutureGen storage site (Figure 2.18). At the scale of the survey, the Bouguer anomaly presents several small undulations (1,000–2,000 m in wavelength and 1–2 mGal in amplitude) that can be interpreted as variations in the topography of the Precambrian basement. There is no indication of any major subsurface discontinuities within the site.

Figure 2.19 presents forward modeling of the Bouguer anomaly along a 250-km-long southwest-northeast (W-SW to E-NE) profile passing through the deepest wells of the region. The observed short wavelength anomalies are well explained by variations in the basement topography ($d = 2.70 \text{ g/cm}^3$) overlaid by a less dense Mount Simon Sandstone ($d = 2.46$); background density being 2.67. The long wavelength anomalies are linked to deep denser mafic intrusions ($d = 2.80$) in the basement as observed in other parts of the Illinois Basin and confirmed by the observed magnetic anomalies (not represented here). Other interpretations could also be valid but this one makes the most of sense especially when one looks at the importance of this phenomenon at the regional scale. Note the thickening of Mount Simon to the east of the stratigraphic well, which is compatible with the growth fault identified on the L100 seismic profile.

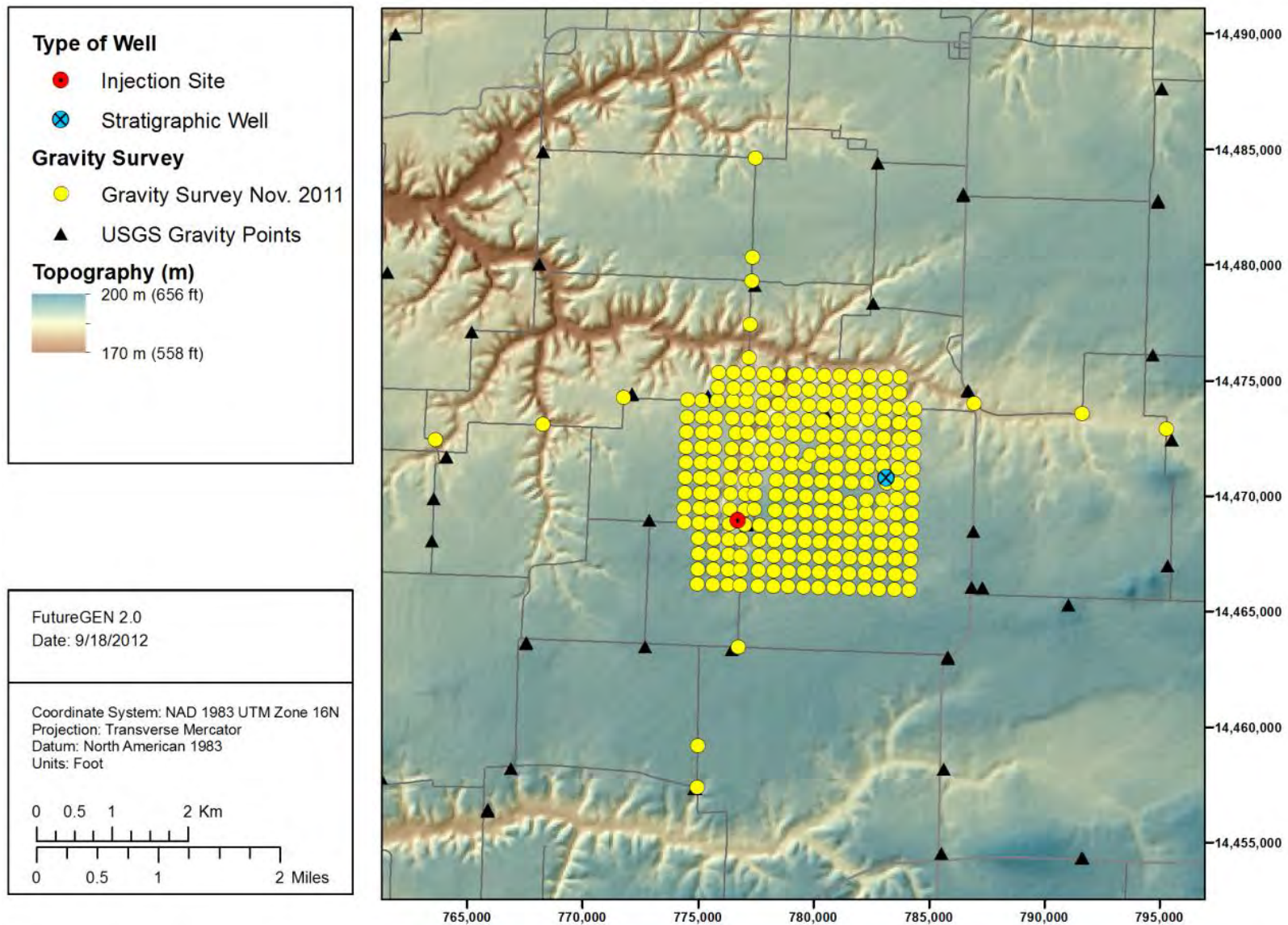


Figure 2.17. Gravity and GPS Stations for the 2011 Survey. Black triangles represent existing USGS gravity stations.

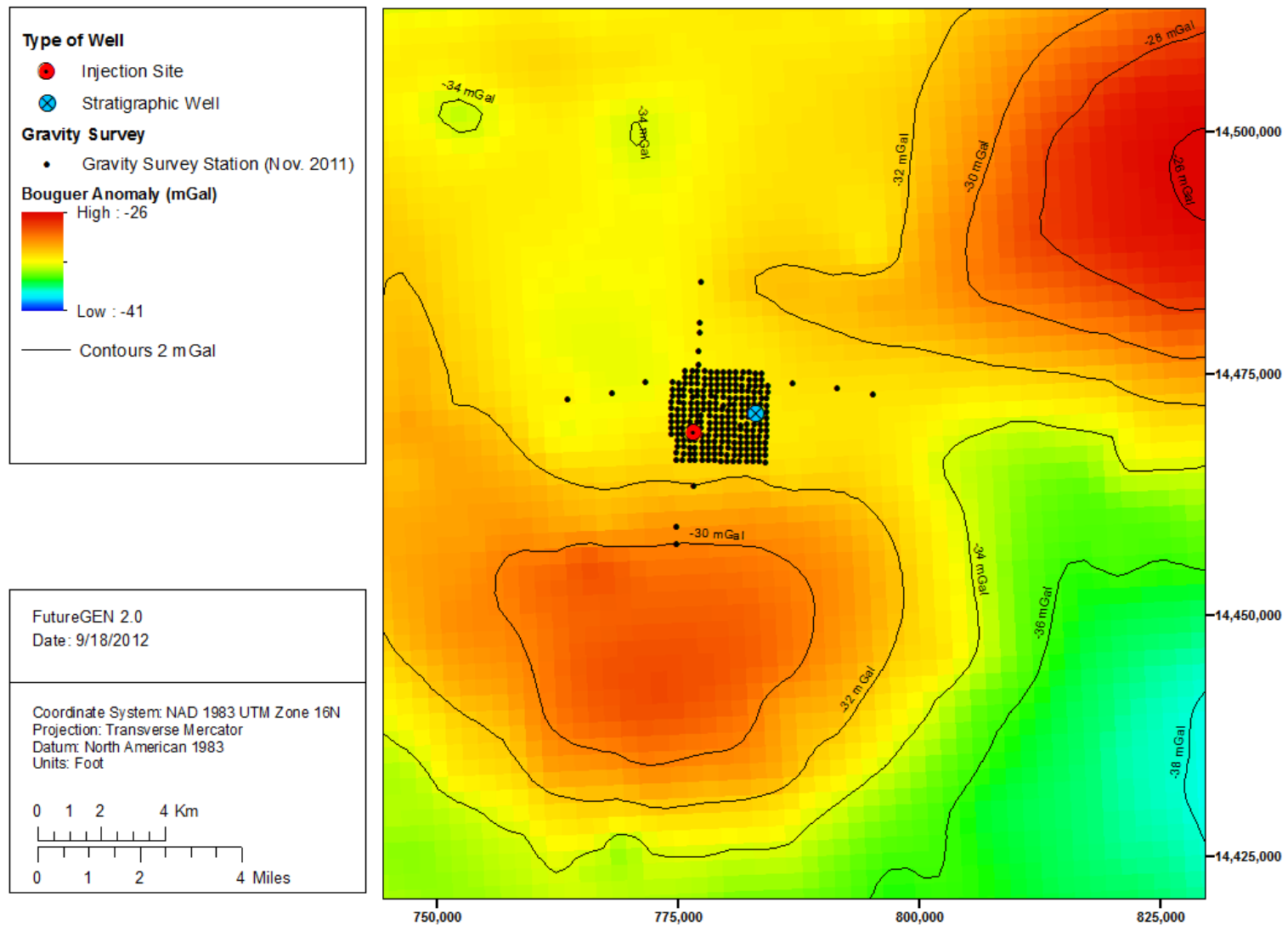


Figure 2.18. Overlay of Local Bouguer Gravity with USGS Regional Survey (regional survey data from Daniels et al. 2008).

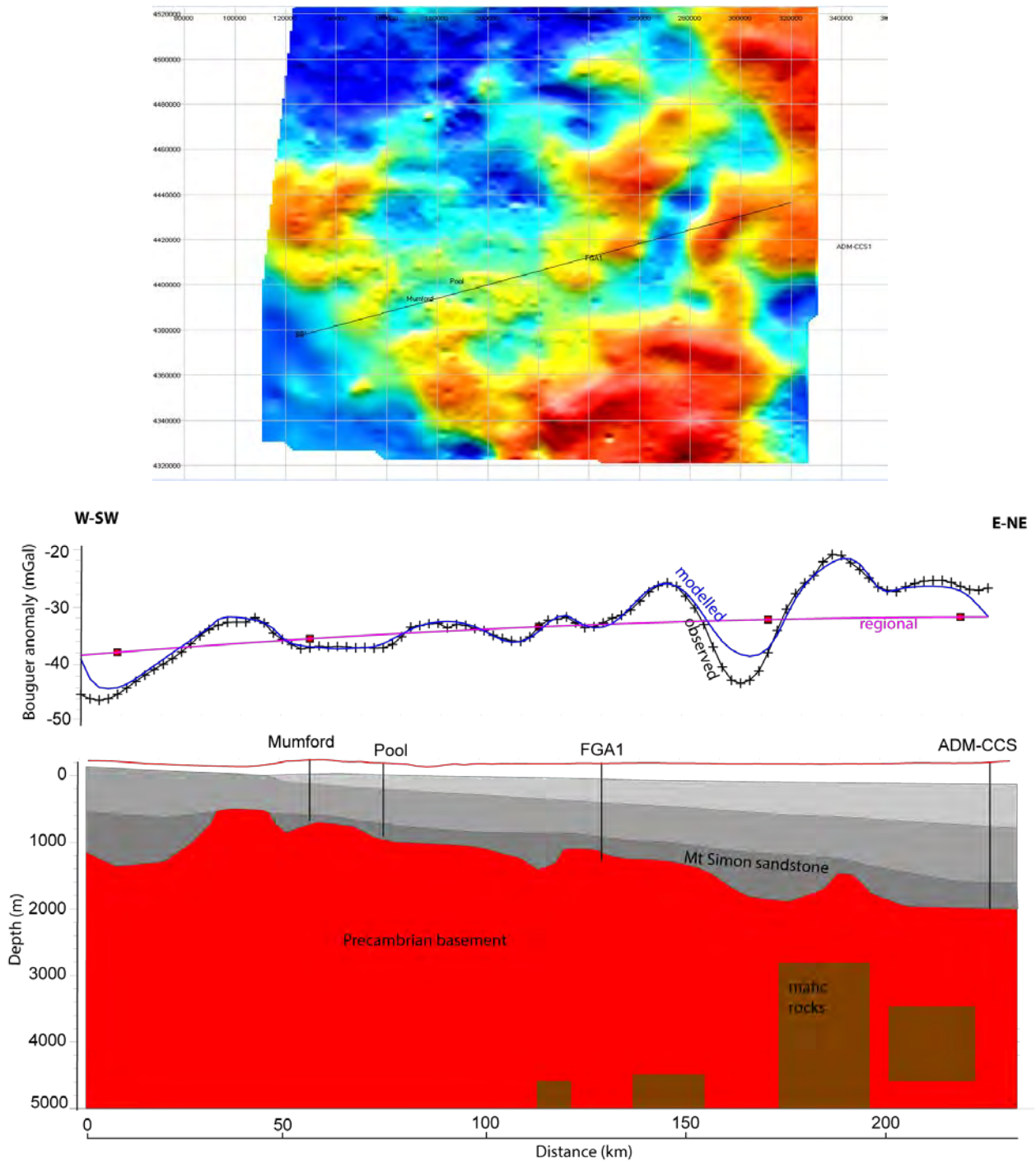


Figure 2.19. Regional WE Bouguer Anomaly Profile. Bottom: modeled depth cross section with Precambrian basement in red and Paleozoic rocks in grays. Middle: Bouguer anomaly in milliGals (black line = observed; blue line = modeled; pink = regional). Top: Bouguer anomaly map with location of the profile and of the deepest wells used to constrain the modeling.

2.4 Geomechanical Information

Geomechanical properties discussed in this section are derived from laboratory analyses of whole core and rotary side-wall cores from the stratigraphic well, as well as from acoustic and density log data, and the azimuth of open fractures, drilling-induced fractures, and well-bore breakout as observed in the resistivity-based image log. Geomechanical well logs, computed from shear and compressional components of the crossed dipole sonic log, provide information about the variability of Young's modulus ("rock stiffness") and Poisson's ratio ("rock compressibility"). Triaxial laboratory tests, conducted on vertical plugs from whole core, provide estimates for elastic moduli, and will be used to calibrate the geomechanical logs calculated from the wireline geophysical logs.

This section first addresses general mechanical properties of the rock layers encountered in the stratigraphic well, including any indications of faults, fractures, fissures, or karst. Next the available information about the stress tensors, or the nature of earth stress, is discussed for the stratigraphic well and how this information compares with regional stresses. Finally, the available geomechanical data are reviewed, specific to the injection zone and confining layers.

Various supportive geomechanical data were collected, but there are no available "mini-frac" or leak-off tests to directly measure fracture pressure in either the injection or confining zones. Mini-frac or leak-off data are required to definitively calculate site-specific fracture gradients, and to produce high-confidence failure plots, fault slip tendency estimates, and critical pore fluid pressure increase estimates. All of these tests will be realized in 2013 during the second phase of the project. However, the log and core data do allow for a determination of site-specific stress orientation and relative magnitudes of stress within the subsurface, a preliminary assessment of geomechanical properties, and provide a good comparison with regional data. Because of the limited quantitative data, regional geomechanical data were used as parameter input for the design and numerical simulations (Chapter 3.0).

2.4.1 Karst

There are no indications of karst topography, sinkholes, or voids in the near surface, but there is evidence of Knox-age karst features (*sensu* Freiburg and Leetaru 2012) in the subsurface Potosi Dolomite between 2,839 and 3,074 ft (865–937 m) bgs. The paleokarst expression includes the development of vuggy porosity, as observed in rotary side-wall cores and in the resistivity-based image log, as well as lost circulation zones during the drilling of the stratigraphic well. This zone is above the Franconia secondary confining layer. The buried Knox paleokarst zone is known regionally and was encountered in the ADM CCS wells at Decatur, Illinois (Freiburg and Leetaru 2012).

There is no evidence of tectonic fracture zones, and there are very few natural fractures intersecting the stratigraphic well bore, as indicated in the resistivity-based image log and in the 211 ft of whole core. The azimuth of the maximum horizontal stress in the stratigraphic well, as indicated by the azimuth of the dipole sonic fast shear wave, and by the azimuth of the sparse natural fractures detected by image logs, is N79.9°E, over the entire sedimentary interval, as logged from 4,416 (1,346 m) to 596 ft (182 m) bgs. Natural fractures that are parallel to the maximum horizontal stress are more likely to be transmissive (Streit and Hillis 2004).

2.4.2 Local Crustal Stress Conditions

Geomechanical analysis of sonic and density log data from the stratigraphic well, together with analysis of natural fractures, drilling-induced fractures, and well-bore breakout as observed in the resistivity-based image log (Schlumberger’s Formation Microimager log) allow a partial determination of earth stress conditions within the well bore. A summary of the findings is as follows: the azimuth of the maximum horizontal stress (S_{hmax}) is N 79.9°E and has a much larger magnitude than the minimum horizontal stress (S_{hmin}). The lithostatic (vertical or S_v) stress is larger than S_{hmin} in both injection zones and confining layers indicating that the stress regime is not inverse. However in the absence of quantitative estimate of S_{hmax} , it is not possible to state whether S_v is greater than S_{hmax} (normal stress regime) or not (strike-slip stress regime). Uncalibrated geomechanical stress properties logs were calculated from the density log and the compressional and shear wave sonic log data. These geomechanical logs indicate there is strong stress anisotropy. These uncalibrated geomechanical logs will later have been calibrated over the cored interval with six triaxial core-plug tests. There are no indications of faults or tectonic fracture zones within the injection zone or in the primary or secondary confining zones, and the normal stress regime appears to be valid for the entire sedimentary logged interval from 4,416 (1,346 m) to 596 ft (182 m). Details of the basic determination of the stress regime follow.

2.4.2.1 Determination of Vertical Stress S_v from Density Measurements

The magnitude of the vertical stress (S_v) can be represented by the weight of the overburden (i.e., lithostatic pressure) and can be calculated by integration of wireline log-derived rock densities from the surface to the depth of interest (Zoback et al. 2003). Where density log data are not available (depth <596 ft [182 m]), Zoback et al. (2003) are followed in assigning a density of 2,300 kg/m³ for siltstones, shales, and sandstones (typical lithologies of the shallow Pennsylvanian section at the site). The overburden gradient, calculated from these data is 1.1 psi/ft. Lithostatic pressures (S_v) at the top of the reservoir (base of primary confining zone), top of primary confining zone, and at the top and base of the secondary seals are shown in Table 2.8.

Table 2.8. Lithostatic Pressure at Important Interfaces

Unit	MPa	psi
Top of Franconia confining zone	3.36	3,388
Top of Ironton Saline Aquifer	25.34	3,675
Top of Proviso confining zone	26.15	3,792
Top of Elmhurst reservoir	29.9	4,249

2.4.2.2 Maximum and Minimum Horizontal Stress Azimuth from Resistivity-Based Image Logs

In vertical wells, the occurrence of breakout or tensile fractures usually implies that S_{hmin} is the minimum principal stress and that there are large differences between the two horizontal stresses S_{Hmax} and S_{hmin} . The azimuths of the maximum and minimum horizontal stresses are indicated by the azimuth of the induced tensile fractures and the borehole breakout, respectively (Zoback et al. 2003).

Both well-bore breakouts and tensile fractures are present in the borehole image logs. The calculated azimuth of borehole breakout minimum horizontal stress (S_{hmin}) is 169.9°N; the azimuth of maximum horizontal stress (S_{Hmax}) is 79.9°N. The azimuth of maximal horizontal stress (S_{Hmax}) in the stratigraphic well is consistent with regional stresses (Helmutz Centre Potsdam – GFZ 2012). However in the absence of quantitative determination of S_{Hmax} , it is impossible to state whether it is greater or not than S_v .

In summary, data from the stratigraphic well indicate that vertical lithostatic stress (S_v) is greater than the minimum horizontal stress (S_{hmin}). This indicates that the site is not in an inverse stress regime, and any undetected faults, if present, would be either normal or strike-slip faults (Table 2.9). The basic stress analysis data did not indicate any change in stress regime from the base of the Mount Simon to the top of the logged interval (4,416 [1,346 m] to 596 ft [182 m] bgs. Data are insufficient at this stage of analysis to be able to quantify the horizontal components of stress and thus distinguish between normal and strike-slip regimes.

Table 2.9. Relation of Principal Stresses to Fault Types (Zoback 2007)

Regime	Stress		
	S_1	S_2	S_3
Normal	S_v	S_{Hmax}	S_{hmin}
Strike-Slip	S_{Hmax}	S_v	S_{hmin}
Reverse	S_{Hmax}	S_{hmin}	S_v

2.4.3 Elastic Moduli and Fracture Gradient

The elastic moduli (or constants) include bulk modulus, Poisson's ratio, shear modulus, and Young's modulus, and characterize the properties of a rock that define how rock deforms when undergoing stress and how the rock recovers after the stress is released.

Fracture pressure is the pressure above which fluid injection will cause a formation to undergo brittle failure, i.e., to fracture hydraulically. Fracture-closing pressure is the pressure required to keep an existing fracture open, or to cause an existing fracture to widen. Fracture gradient is the pressure increase (change) per unit of depth that would initiate the onset of brittle rock failure.

Elastic moduli and fracture gradients were estimated from limited core analysis samples. Triaxial geomechanical tests were conducted on eight vertical core plugs from the cored intervals of the stratigraphic well. Table 2.10 lists the measured and calculated results of elastic moduli for the proposed injection zone and for the Precambrian basement. Table 2.11 shows the resulting calculated fracture gradients. For each table, samples 1 and 2 are from the Lombard member; samples 3 and 4 are from the Elmhurst; samples 5 and 6 are from the uppermost Mount Simon Sandstone; sample 7 is from the basal part of the Mount Simon, and sample 8 is from the Precambrian basement.

For comparison with regional data, Table 2.12 lists fracture gradients and elastic moduli determined for the Mount Simon at the ADM sequestration site at Decatur, Illinois, and at other Illinois Basin locations.

Table 2.10. Elastic Moduli Parameters from Triaxial Tests on Vertical Core Plugs in the Injection Interval and Precambrian Basement

Sample Number	Depth (ft)	Formation	Confining Pressure (psi)	Bulk Density (gm/cm ³)	Compressive Strength (psi)	Young's Modulus (10 ⁶ psi)	Poisson's Ratio
1	3788.10	Lombard member	980	2.41	19,731	4.97	0.22
2	3802.80	Lombard member	1820	2.69	25,605	4.56	0.23
3	3867.90	Elmhurst member	890	2.25	9820	0.88	0.20
4	3887.30	Elmhurst member	750	2.28	7655	1.82	0.21
5	3929.10	Mt Simon SS.	770	2.42	18,076	2.89	0.23
6	3937.40	Mt Simon SS.	840	2.41	11,430	1.54	0.23
7	4401.90	Mt Simon SS.	1100	2.34	11,336	1.49	0.23
8	4434.50	Basement	1320	2.63	40,994	9.11	0.29

Table 2.11. Minimum Horizontal Stress and Fracture Gradient Calculated from Triaxial Tests (the red line represents the injection zone.)

Sample Number	Depth(ft)	Overburden Stress (psi)	Pore Pressure (psi)	Biot's Constant	Min. Horizontal Stress	Fracture Gradient (psi/ft)	Fracture Toughness (psi-in0.5)
1	3788.10	4167	1667	0.69	2533	0.669	1913
2	3802.80	4183	1673	0.70	2579	0.678	1836
3	3867.90	4255	1702	0.66	2502	0.647	802
4	3887.30	4276	1710	0.67	2560	0.659	1156
5	3929.10	4322	1729	0.71	2679	0.682	1464
6	3937.40	4331	1732	0.71	2682	0.681	1069
7	4401.90	4842	1937	0.70	2987	0.679	1050
8	4434.50	4878	1951	0.84	3301	0.744	2642

Table 2.12. Range of Geomechanical Properties (after EPA 2011, unless otherwise noted)

Hydrogeologic Unit	Fracture Gradient (psi/ft)	Young's Modulus (psi)	Poisson's Ratio	Bulk Modulus (psi)	Shear Modulus (psi)
Mount Simon Sandstone	0.57 ^(a) to 0.715 ^(b)	2.33-7.86E6 ^(c)	0.17-0.36 ^(c)	NA	NA

NA = Not available.

(a) EPA (1994).

(b) After EPA 2011 and 40 CFR 146.88.

(c) After Sminchak 2011.

2.4.3.1 Injection Zone Fracture Pressure

Geophysical logs from the stratigraphic well provide general estimates of geomechanical anisotropic elastic properties. Triaxial test data for log calibration are limited to six vertical plugs within the cored intervals, and validation of well-log and core data using mini-frac data or leak-off tests is still required to acquire accurate values for elastic parameters and fracture gradients. Fracture gradient (Table 2.11) ranges for the injection zone were calculated from 0.647 to 0.682 psi/ft. Although no step-rate injection tests or leak-off test data are currently available for the injection zone, these data will be obtained when the injection wells are drilled.

At the CCS#1 well at Decatur, about 65 mi east of the stratigraphic well, a fracture pressure gradient of 0.715 psi/ft was calculated for the base of the Mount Simon Sandstone formation using a step-rate injection test (EPA 2011). Additional comparison of regional fracture gradients is provided in the *Determination of Maximum Injection Pressure for Class I Wells in Region 5* (EPA 1994), which lists a default fracture gradient of 0.57 psi/ft for the Mount Simon Sandstone.

Based on these considerations, a pressure gradient of 0.65 psi/ft is suggested to model the injection-zone fracture gradient.

2.4.3.2 Confining Zone Fracture Pressure

Elastic moduli calculated from triaxial core tests on two vertical core samples from the lowermost Lombard member are presented in Table 2.13, and estimations of minimum horizontal stress and fracture gradient calculated from triaxial tests are presented in Table 2.14. Note that the lower Lombard has lithologies and rock properties that are transitional from the porous and permeable Elmhurst sandstones to lithologies and properties of the actual confining part of the upper Lombard. Thus, these moduli, stress estimates, and fracture gradients are not representative of the confining zone. Although no step-rate tests or leak-off tests are currently available for the primary confining zone in the stratigraphic well and no whole core is currently available from the Proviso member or from the upper part of the Lombard member, these data will be obtained when the injection wells are drilled.

Field analog data may be more representative of confining zone properties. The elastic moduli and fracture gradient for the Eau Claire confining zone at the CCS#1 well at Decatur, Illinois, are presented in Table 2.15.

Table 2.13. Elastic Moduli Parameters from Triaxial Tests of Core from the Lowermost Part of the Lombard Member

Depth (ft)	Member	Confining Pressure (psi)	Bulk Density (gm/cm ³)	Compressive Strength (psi)	Young's Modulus (10 ⁶ psi)	Poisson's Ratio
3788.10	Lombard	980	2.41	19731	4.97	0.22
3802.80	Lombard	1820	2.69	25605	4.56	0.23

Table 2.14. Minimum Horizontal Stress and Fracture Gradient Calculated from Triaxial Tests

Sample Number	Depth(ft)	Overburden Stress (psi)	Pore Pressure (psi)	Biot's Constant	Minimum Horizontal Stress	Fracture Gradient (psi/ft)	Fracture Toughness (psi-in 0.5)
1	3788.10	4167	1667	0.69	2533	0.669	1913
2	3802.80	4183	1673	0.70	2579	0.678	1836

Table 2.15. Range of Eau Claire Geomechanical Properties in the CCS#1 Well, Decatur Illinois (after EPA 2011)

Hydrogeologic Unit	Fracture Gradient (psi/ft)	Young's Modulus (psi)	Poisson's Ratio	Bulk Modulus (psi)	Shear Modulus (psi)
Eau Claire Carbonate/Siltstone (Upper Unit-Proviso)	NA	NA	NA	NA	NA
Eau Claire Siltstone/Shale (Lower Unit 1)	0.93 to 0.98	5.5E6	0.27	3.92E6	2.17E6

NA = Not available.

2.5 Seismic History of Region

In Illinois, most of the seismicity occurs in the southern and southeastern part of the state where two seismic zones (Wabash Valley and New Madrid) are found. Central Illinois is an area that has been historically low in earthquakes or seismicity (Figure 2.20). Statewide, the largest recorded earthquake (magnitude 5.4) occurred on April 18, 2008, in the southeastern part of the state; it caused minor structural damage. The closest known earthquake to the FutureGen 2.0 Project site (Intensity VII, magnitude 4.8 – non-instrumented record) occurred on July 19, 1909, approximately 28 mi (45 km) north of the site; it caused slight damage. Most of the events in Illinois occurred at depths greater than 3 km (1.9 mi) (Figure 2.20).

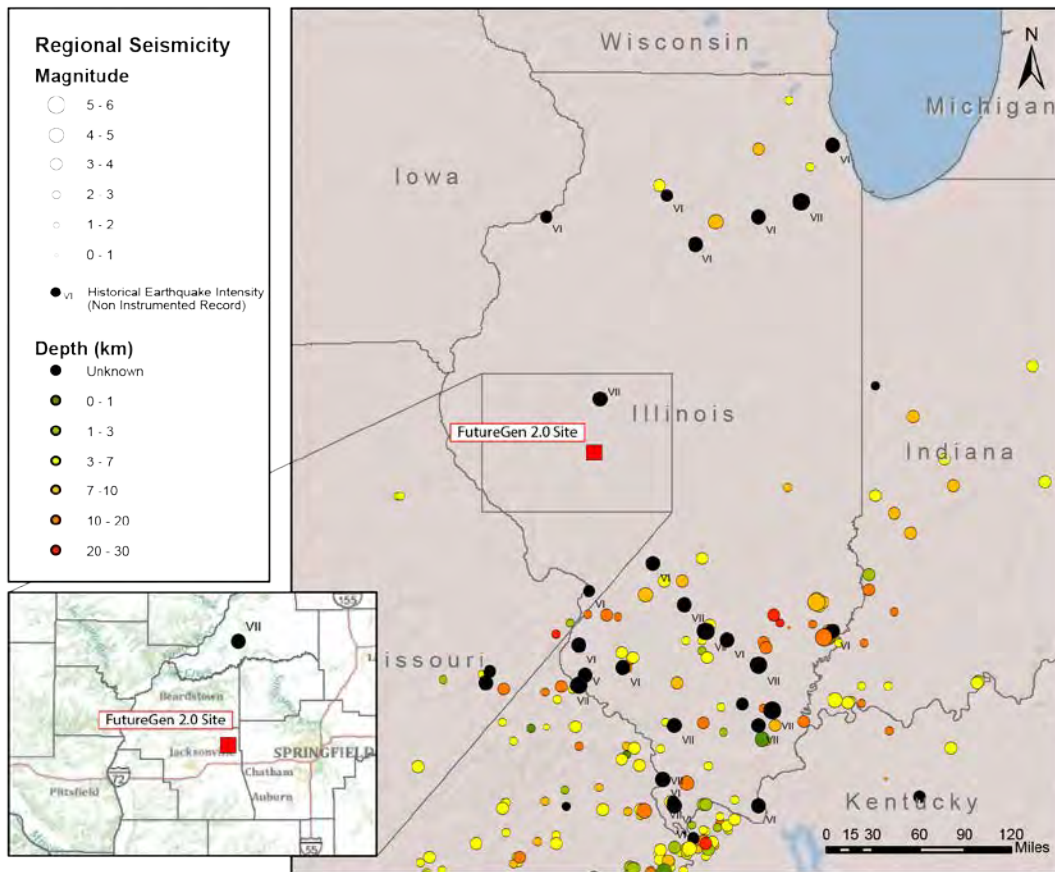


Figure 2.20. Regional Historic Earthquakes (data from USGS 2012a, b)

There is a 2 percent probability that the peak ground acceleration (G) due to seismic activity will exceed 9 percent G within 50 years (Figure 2.21; USGS 2008).

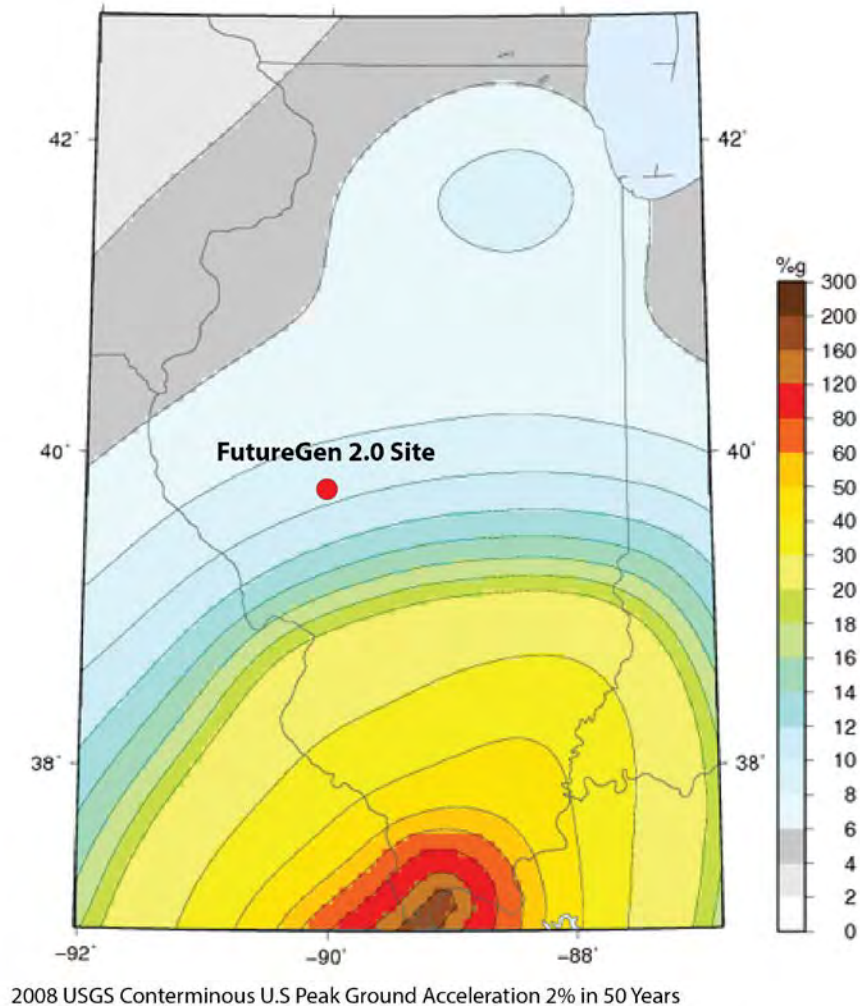


Figure 2.21. Earthquake Risk for Illinois Given as Maximum Accelerations with a 2 Percent Probability of Being Exceeded Within 50 Years (modified from USGS 2008)

The general absence of seismicity in historical times within west-central Illinois suggests a lack of appreciable active faulting in this area.

2.5.1 Regional Topography and Geomorphology

West-central Illinois is located within the low-relief Springfield Plain underlain by pre-last-glacial till (Figure 2.22) of the Glasford Formation. These deposits were laid down during the Illinoian glacial episode more than 120,000 years ago (Kolata and Nimz 2010, p. 223). The Springfield Plain lies beyond the area covered with glaciers during the most recent cycle of glaciation (Wisconsin episode; green area in Figure 2.22). The topography of the region is predominantly farmlands ranging from about 400 ft (122 m) in elevation along the Illinois and Mississippi river valleys to 700 ft (213 m) along some drainage divides to the east.

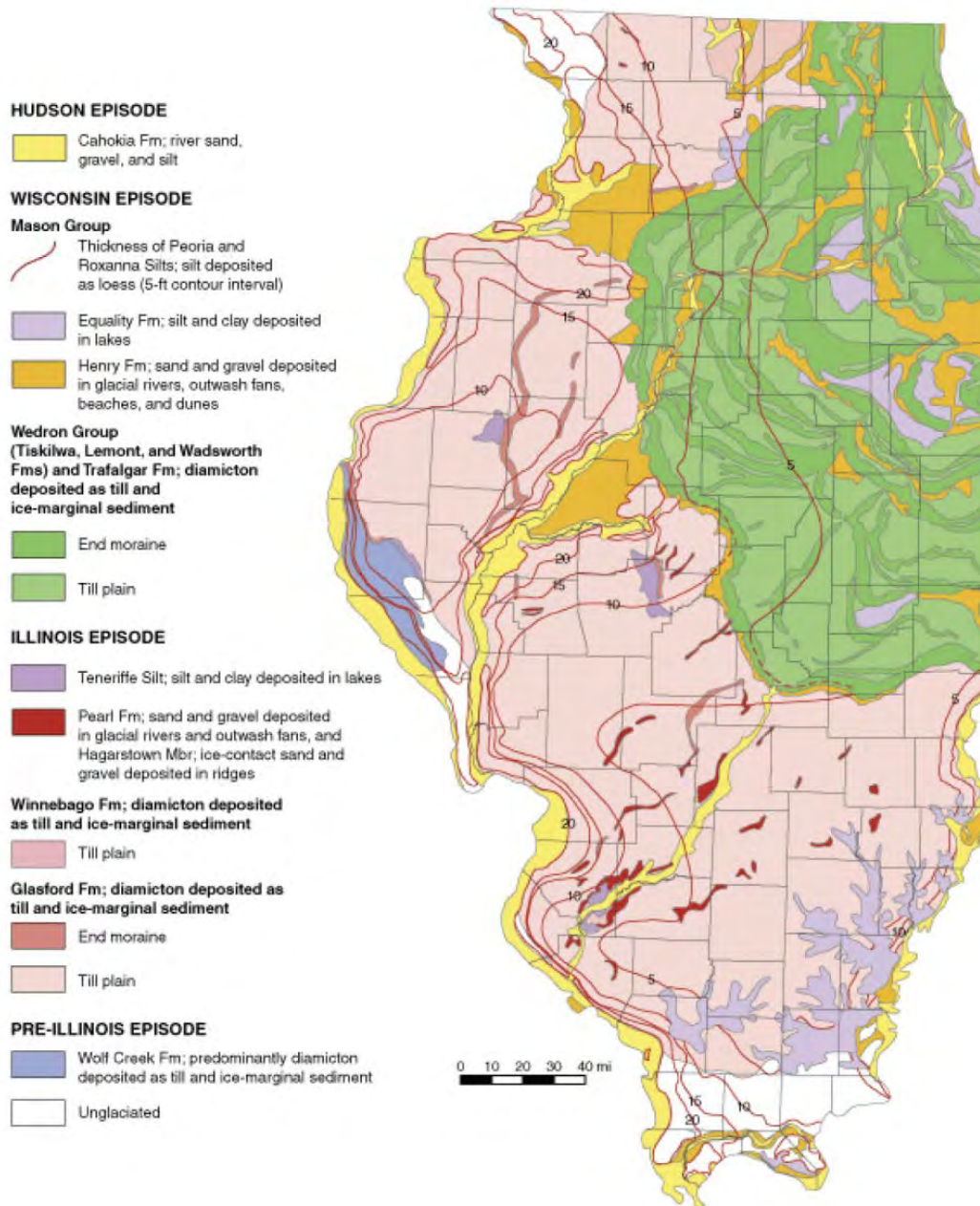


Figure 2.22. Surficial Quaternary Deposits of Illinois (modified from ISGS 2012d)

2.5.2 Site Surface Topography

The surface topography at the proposed Morgan County CO₂ storage site lies between 590 and 620 ft (180 and 189 m) above mean sea level (MSL). Surface drainage is to the north-northeast toward the Illinois River through Indian Creek, the nearest perennial stream (Figure 2.23). About 75 to 125 ft (23 to 38 m) of middle-to-early Pleistocene glacial drift and glaciolacustrine deposits (Glasford Formation) disconformably overlie the Pennsylvanian bedrock in the vicinity of the proposed CO₂ storage site (Figure 2.25 in Section 2.6.1). The uppermost bedrock consists of thinly bedded shale, siltstone, sandstone, limestone, and coal.

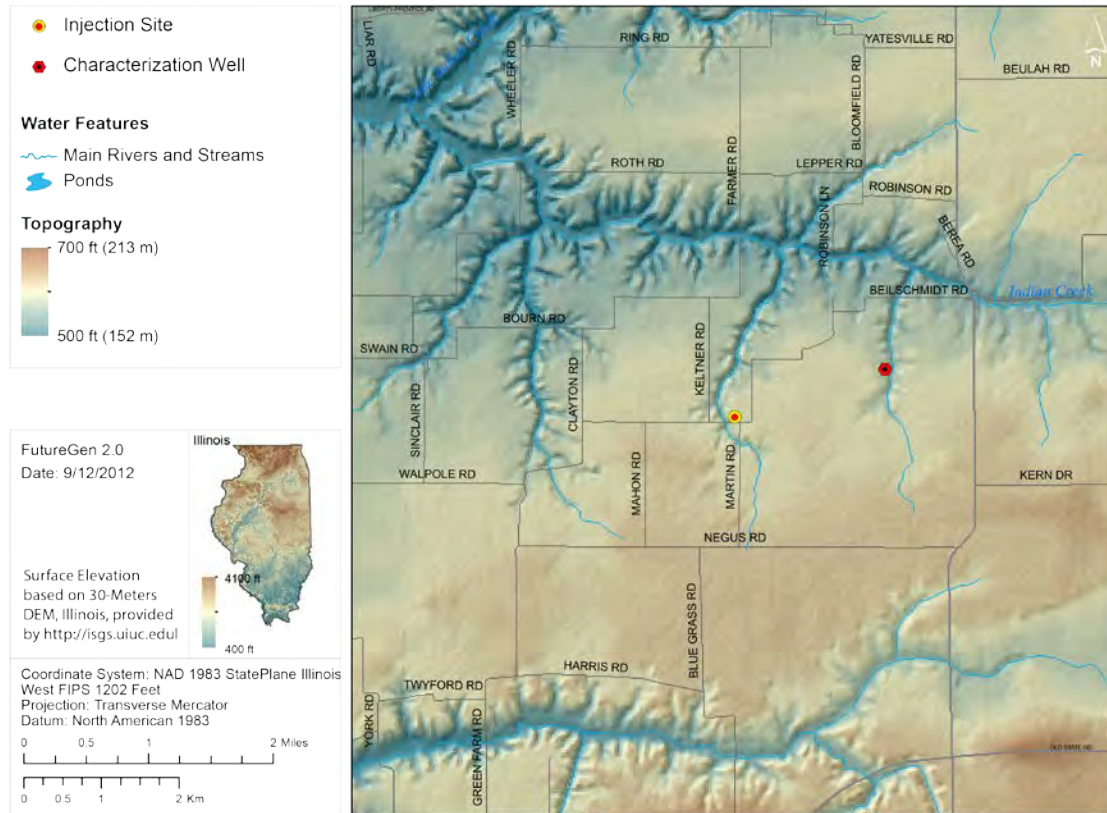


Figure 2.23. Surface Topography and Drainage

2.6 Groundwater

Several aquifers are present at the proposed Morgan County storage site. These aquifers are underground layers of water-bearing permeable rock that are separated from one another by less permeable rock layers. Not all of the aquifers contain potable water and in general the salinity of the aquifers increases with depth. At the proposed Morgan County site, drinking water is developed from the Quaternary-age glacial sediments (approximately 150 ft [46 m] bgs). Although this surficial zone is the hydrogeologic unit from which all known water-supply wells are completed, for the purpose of the permit application, the deeper St. Peter Sandstone is considered the lowermost USDW. The St. Peter Sandstone is considered the lowermost USDW, because the measured TDS content from this unit at the FutureGen stratigraphic well is 3,700 mg/L, which is below the regulatory upper limit of 10,000 mg/L for drinking water aquifers. A summary of both potable and nonpotable and brackish aquifers is presented below.

2.6.1 Surficial Aquifer System

Domestic, municipal, and agricultural water-supply wells in Morgan County typically do not exceed 100 ft (46 m) in depth, and only a few wells are deeper than 75 ft (23 m) bgs. All water-supply wells within a 20-mi² area are from the Quaternary glacially derived sediments that overlie Pennsylvanian bedrock (ISGS 2012b). While much of the Quaternary section consists of fine-grained, low-permeability clay and silt, lenses of glacial outwash sand and gravel are also locally present, particularly within paleo-stream valleys denoted by greater glacial drift thicknesses as shown in Figure 2.24. The variability of the different facies within the Quaternary sediments is illustrated in a cross section in Figure 2.25.

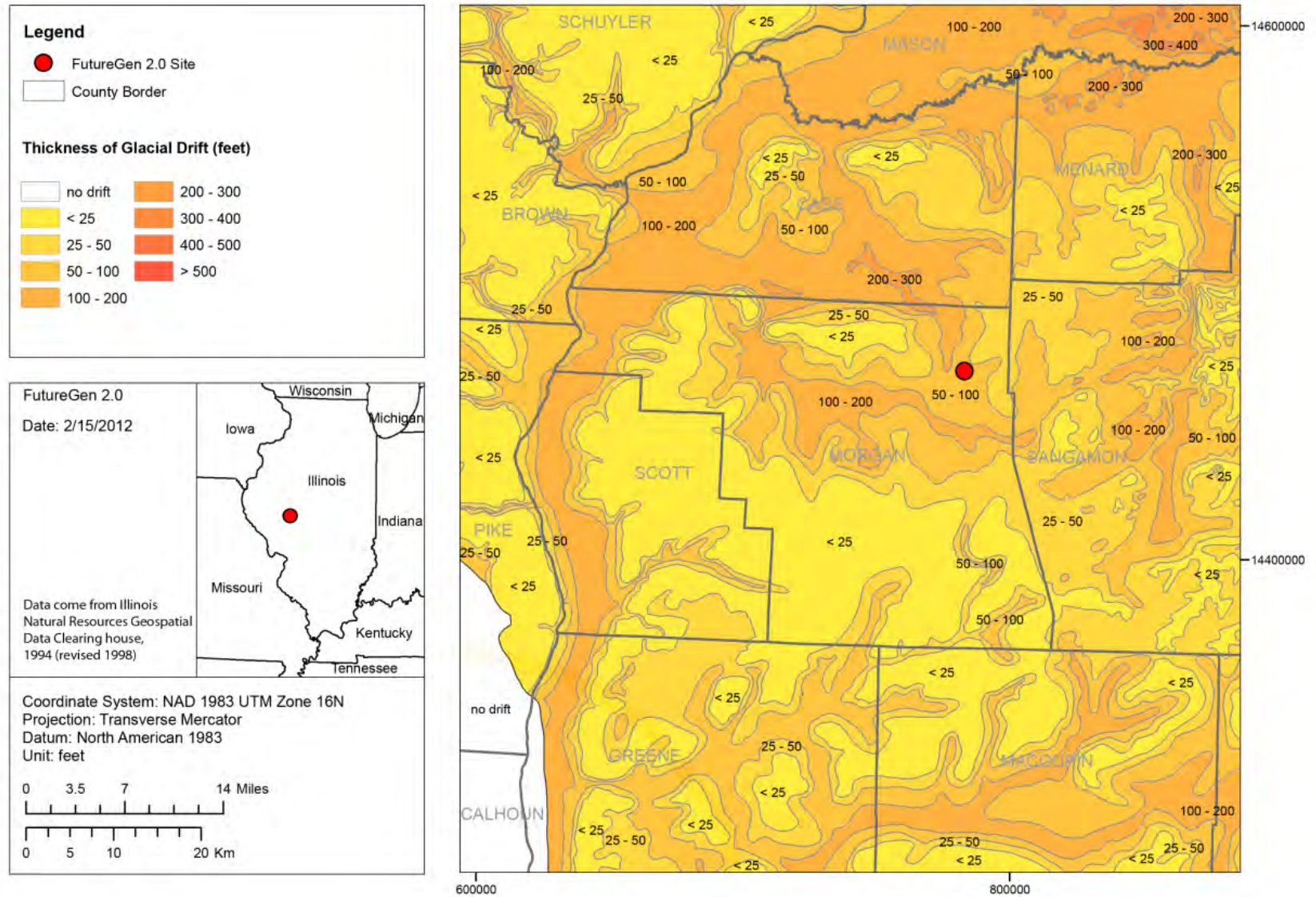


Figure 2.24. Thickness of Unconsolidated Pleistocene Glacial Drift in Morgan and Adjacent Counties (based on data from ISGS 2012b)

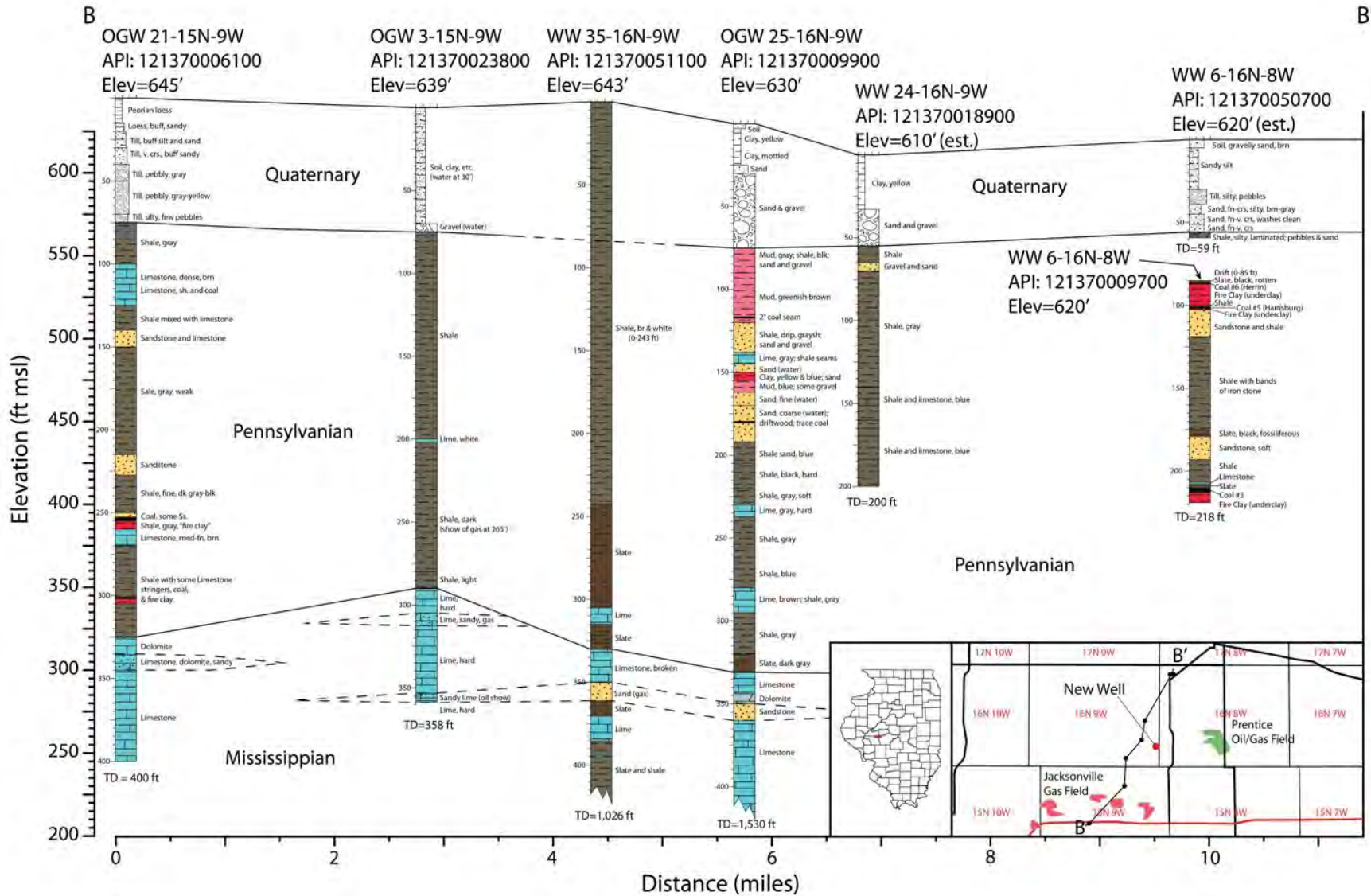


Figure 2.25. Variability of Quaternary Sediments and Shallow Pennsylvanian Rocks in the Vicinity of the Proposed Morgan County CO₂ Storage Site (based on data from ISGS 2011).

Detailed potentiometric surface maps and information about local groundwater flow direction are sparse for the shallow unconfined sand/gravel aquifer system at the Morgan County CO₂ storage site. However, groundwater flow within the shallow surficial aquifer is expected to conform to the local topography and discharge to local surficial drainages and surface bodies of water. Static water-level data available for water-supply wells in northwest Morgan County area indicate that water-table depth varies depending upon local topography and the seasonal variations in recharge and generally ranges between 5 to 30 ft (1.5 to 9 m) bgs (ISGS 2012c).

A shallow groundwater/well sampling investigation was performed in 2011 on 13 surrounding private/domestic water-supply wells within 1.5 mi (2.4 km) of the FutureGen stratigraphic well (FG1) location (Figure 2.26). All of the wells are shallow (14 to 47 ft [4 to 14 m] deep).

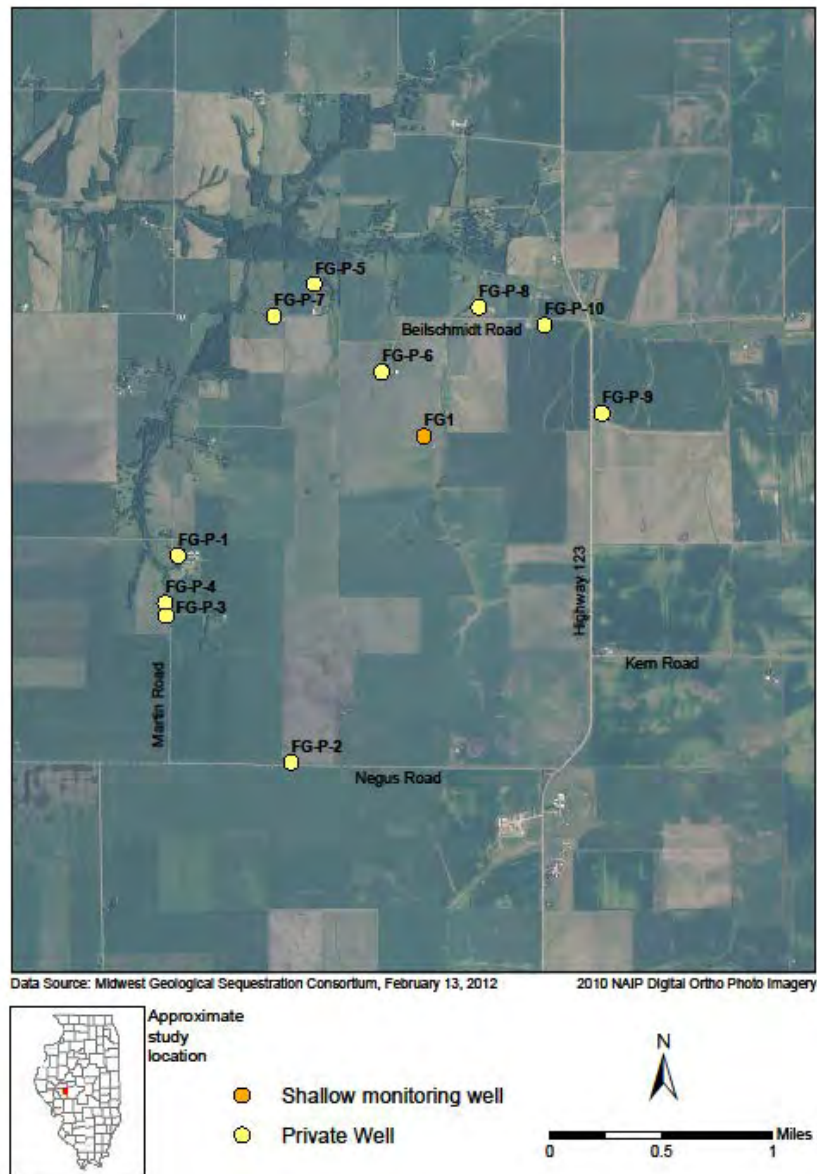


Figure 2.26. Locations of Private/Domestic Water Wells Within 1.5 Mi (2.4 Km) of the Stratigraphic Well (FG1; based on data from ISGS 2012c)

A total of 20 groundwater samples were collected between October 25 and November 10, 2011, including duplicate samples and blanks (Dey et al. in press). General water-quality parameters were measured along with organic and major inorganic constituents. Values of pH ranged from 7.08 to 7.66. Values for specific conductance ranged from 545 to 1,164 $\mu\text{S}/\text{cm}$, with an average of 773 $\mu\text{S}/\text{cm}$. Values of Eh ranged from 105 to 532 mV with an average of 411 mV. Values of dissolved oxygen (DO) ranged from below detection limit to 3.3 mg/L O_2 .

Most dissolved inorganic constituent concentrations are within primary and secondary drinking water standards. However, the constituent concentration in water is elevated with respect to iron (Fe), manganese (Mn), nitrate (NO_3), and TDS. In some cases these constituents exceed the EPA secondary standards.

2.6.2 Upper-Bedrock Aquifer System

The shallow bedrock aquifers are discussed in descending stratigraphic order (i.e., youngest to oldest), and range from Pennsylvanian-aged bedrock units to the older Cambrian-aged Mount Simon Sandstone. The fluid salinity within these formations generally increases with depth and correspondingly their use as potential potable aquifers also diminishes.

Pennsylvanian-aged bedrock units (Kolata 2005) in Morgan County consist principally of shale with occasional sandstone lenses and do not offer potential as sources of groundwater except for the occurrence of discontinuous, thin beds of sandstone or fractured limestone that may yield small, domestic supplies (Woller and Sanderson 1979).

Mississippian-aged strata regionally dip to the east (Figure 2.27) at about 10 to 40 ft/mi in Morgan County (Woller and Sanderson 1979). The Salem and Burlington-Keokuk limestones are the principal, but relatively limited, Mississippian aquifers because their yield capacity depends on the abundance and interconnection of fractures and crevices within the rock that are intersected by the well (Woller and Sanderson 1979). The younger Salem Limestone occurs at a depth ranging from 175 to 650 ft (53 to 198 m) bgs in Morgan County and exhibits marginally adequate yields that become more saline with depth. Data from the Illinois State Water Survey (ISWS)¹ contain water-quality data for three bedrock wells in Morgan County. The TDS concentrations for the three Morgan County wells range from 3,894 to 10,420 mg/L.

A study conducted in 1978, found no water-supply wells were developed within the shallow bedrock aquifers in Morgan County (Woller and Sanderson 1979), although Pennsylvanian and Mississippian bedrock units were reported as water supplies for domestic use in Morgan and adjacent counties (Bergstrom and Zeizel 1957; Selkregg and Kempton 1958; Gibb and O'Hearn 1980).

Lack of primary or secondary porosity appears to be the limiting factor for aquifer development in bedrock shallower than 500 ft (152 m) bgs. No aquifers or aquifer materials have been identified in the Pennsylvanian or Mississippian bedrock near the site and there are no municipal or domestic water-supply wells that develop groundwater from the shallow bedrock aquifers within the preliminary AoR.

¹ Obtained from the ISWS Online Database, <http://www.isws.illinois.edu/data/gwdb>, accessed in April 2011.

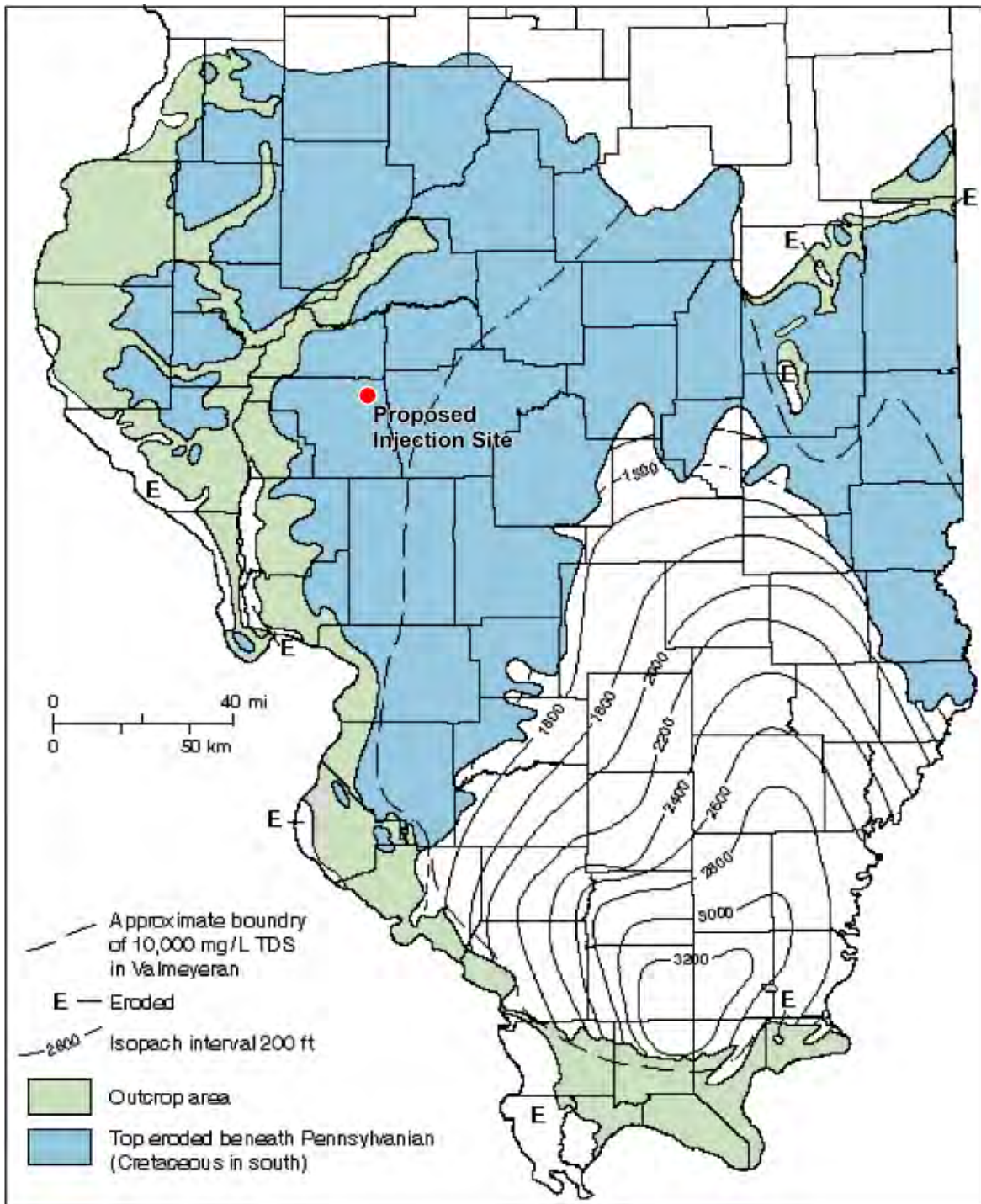


Figure 2.27. Thickness and Distribution of Mississippian Aquifers (after Willman et al. 1975) and the Boundary for 10,000 mg/L TDS in the Middle Mississippian Rocks

2.6.3 Lower-Bedrock Aquifer System

At least four, deep (>500 ft [>152 m]), aquifers are present beneath the proposed Morgan County CO₂ storage site. From youngest to oldest these are the Ordovician St. Peter, New Richmond, Cambrian Ironton-Galesville, and the Elmhurst/Mount Simon Sandstone intervals (see Figure 2.1). Of the four

major lower-bedrock aquifers only the shallowest, the Ordovician St. Peter Sandstone, has been considered for possible, future water-supply use (Kolata and Nimz 2010). None of these deeper, lower-bedrock aquifers below the St. Peter has been used for water supply within or near Morgan County because of elevated salinities, in combination with their depths which limit economic pumping.

Illinois Basin-scale hydrogeologic models (e.g., Bethke and Marshak [1990], Gupta and Bair [1997], and Birkholzer et al. [2007]) indicate elevated freshwater heads within the lower-bedrock aquifer system varying from about 650 ft (198 m) above MSL to 165 ft (50 m) below MSL, with hydraulic head gradients of ~ 0.0003 . Regional approximations of the potentiometric surface (hydraulic head) and generalized flow directions for the deeper lower-bedrock aquifers in the Illinois Basin have also been reported by Visocky et al. (1985) and Mandle and Kontis (1992). However, these studies have focused on the northern portion of Illinois, where extensive water-supply production exists in these deeper bedrock aquifer systems.

2.6.3.1 St. Peter Sandstone

The St. Peter Sandstone has been used for injection and storage of natural gas at the Waverly Storage Field (16 mi [26 km] southeast of the proposed Morgan County CO₂ storage site). At the Waverly Storage Field the groundwater salinity of the St. Peter Sandstone is 2,778 mg/L TDS (Buschbach and Bond 1974; Weiss et al. 2009). A fluid sample collected from this aquifer during installation of the stratigraphic well resulted in a laboratory-measured TDS value of 3,400 mg/L and field parameter values of 7.91 and 5,910 $\mu\text{S}/\text{cm}$ for pH and electrical conductivity, respectively. Because the dissolved solids content near the proposed storage site was measured at below the upper regulatory limit of 10,000 mg/L for potable aquifers, for the purposes of this UIC permit application, the St. Peter Sandstone is considered to be the lowermost federal USDW. The State of Illinois, however, does not recognize the St. Peter Sandstone as a suitable potable water source at this location.

2.6.3.2 New Richmond Sandstone

The New Richmond Sandstone aquifer occurs between a depth of 2,346 and 2,448 ft (715 and 746 m) within the FutureGen stratigraphic well. No fluid samples were collected from this lower-bedrock aquifer unit.

2.6.3.3 Ironton-Galesville Sandstone

The first bedrock aquifer above the Eau Claire confining zone in Morgan County is the Cambrian Ironton-Galesville Sandstone. Although the Ironton-Galesville Sandstone serves as a water source in northern Illinois where it may reach a thickness of 200 ft (61 m) (Buschbach and Bond 1974; Willman et al. 1975), it is not used as a water-supply source in Morgan or surrounding counties. Regionally, this aquifer system includes two separate lithostratigraphic formations—the Galesville and Ironton formations; the former sandy dolomite is in places separated by a minor conformity from the latter overlying dolomitic sandstone (Willman et al. 1975). Within the FutureGen stratigraphic well, the top of the Ironton-Galesville Sandstone occurs at a depth of 3,300 ft (1,006 m) bkb and is 139 ft (42 m) thick. Little information is available about the potentiometric surface of the Ironton-Galesville Sandstone in Morgan County because of the lack of surrounding deep well characterization information.

Although no published data specifically address the salinity of the Ironton-Galesville Sandstone in wells in Morgan County, Lloyd and Lyke (1995) indicate (Figure 2.28) that groundwater within the Ironton-Galesville Sandstone at the proposed Morgan County CO₂ storage site is saline. No fluid samples were collected from this lower-bedrock aquifer unit. Calculated salinities, however, based on wireline resistivity survey results and observed temperature conditions, indicate an average salinity concentration of approximately 15,000 mg/L at the FutureGen stratigraphic well location. Similar calculations based on wireline log response results for the Mount Simon Sandstone indicate an average salinity concentration of a about 52,000 mg/L, which compares to a laboratory-measured TDS value of ~47,500 mg/L. This difference in calculated salinity concentration between the Ironton and Mount Simon sandstones supports regional information that the intervening Eau Claire acts as a hydrologic barrier above the combined Elmhurst/Mount Simon injection zone.

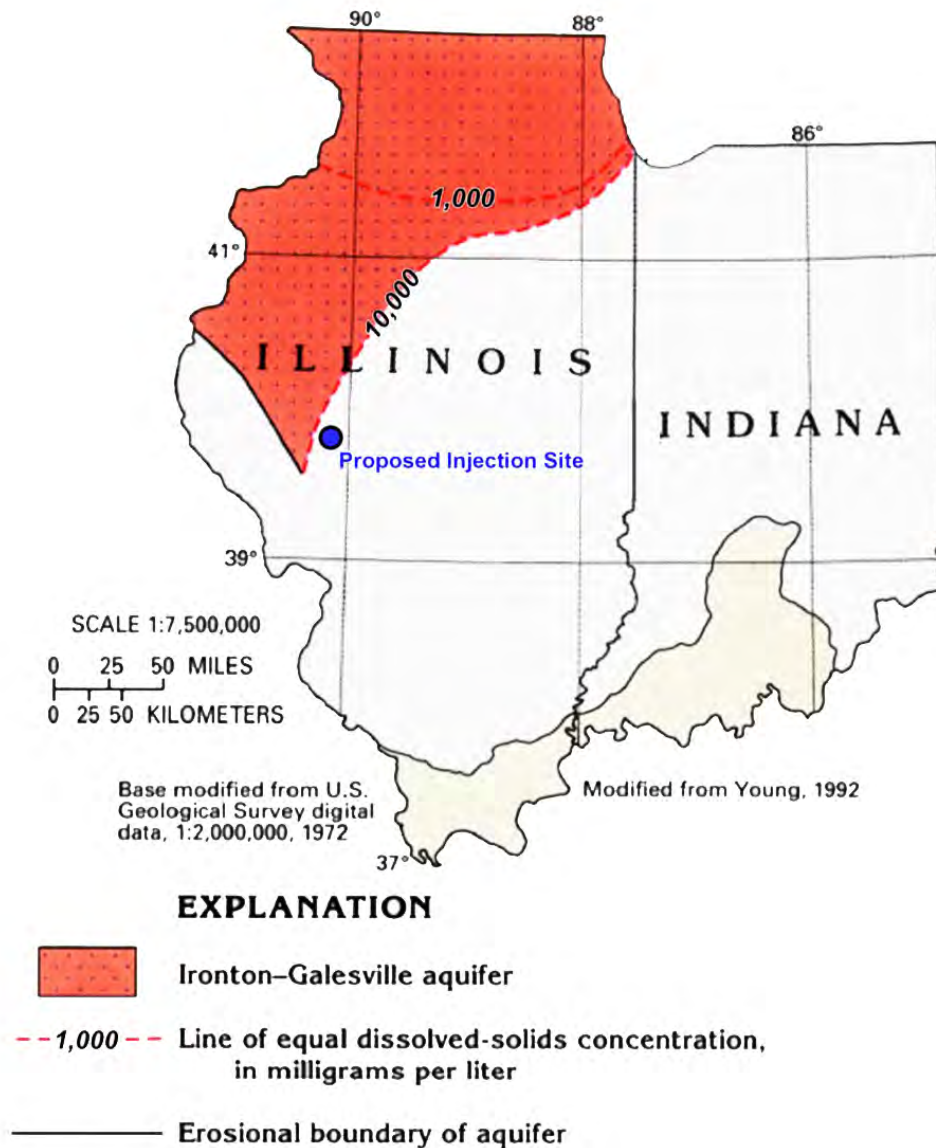


Figure 2.28. Regional Map Showing Limits of Freshwater in the Ironton-Galesville Sandstone Relative to the Proposed Morgan County CO₂ Storage Site (after Lloyd and Lyke 1995)

2.6.3.4 Elmhurst/Mount Simon Sandstone

Visocky et al. (1985) group the overlying Elmhurst member of the Eau Clair Formation with the underlying Mount Simon Sandstone as an individual hydrologic aquifer unit in northern Illinois. In the northern part of the state, the Elmhurst/Mount Simon Sandstone contains fresh groundwater that served as a water supply in northeastern Illinois until the 1970s (Visocky et al. 1985; Young 1992). However, in central Illinois the Mount Simon Sandstone is considered too deep (>3,000 ft [>914 m]) and the groundwater too highly mineralized to be a viable source of drinking water (Kolata and Nimz 2010). Analyses of Mount Simon water samples (Table 2.16) collected in the FutureGen stratigraphic well at a 4,048 ft (1,234 m) with a wireline-deployed formation fluid sampling tool indicated a TDS content of 47,000 mg/L, which is significantly well in excess of the 10,000-mg/L TDS limit recommended for drinking water (40 CFR 144.3). This discrete-depth sample result is consistent with laboratory results obtained from composite sampling of the open borehole Mount Simon section (3,942 to 4,430 ft), which was obtained after significant borehole development (i.e., after pumping >100,000 gal of groundwater from the composite Mount Simon).

Table 2.16. Analyses of Two Formation Fluid Samples from the Mount Simon Sandstone in the Stratigraphic Well

Sample #	Sample Depth (ft bkb)	Elec. Conductivity (μ MHOS/cm)	TDS (mg/L)	Salinity (g/kg)
11	4,048	68,600	47,100	44.3
11	4,048	68,600	47,700	44.2

Regionally, Gupta and Bair (1997) presented borehole drill-stem test (DST) data that indicated hydraulic heads within the Mount Simon Sandstone are near hydrostatic levels. Pressure depth measurements for the Mount Simon at the FutureGen stratigraphic well indicate a similar condition with a pressure gradient of ~0.4375 psi/ft, which is slightly higher than hydrostatic conditions (0.4331 psi/ft). Gupta and Blair (1997) also modeled the seepage velocity and flow direction of groundwater in the Mount Simon Formation across an eight-state area that does not include the Morgan County area, but does include eastern Illinois. They concluded that for deep bedrock aquifers, the lateral flow patterns are away from regional basin high arches, such as the Kankakee Arch, and toward the deeper parts of the Illinois Basin. With respect to vertical groundwater flow, Gupta and Blair (1997) surmised that within the deeper portions of the Illinois Basin, groundwater has the potential to flow vertically upward from the Mount Simon to the Eau Claire, and the vertical velocities are <0.01 in./yr. They estimated that 17 percent of the water recharging the Mount Simon basin-wide migrates regionally into the overlying Eau Claire, while 83 percent flows laterally within the Mount Simon hydrogeologic unit.

Vertical flow potential at the FutureGen site was evaluated based on an analysis of discrete pressure/depth measurements obtained within the pilot characterization borehole over the depth interval of 1,148 to 4,263 ft. Figure 2.29 shows the static pressure/depth measurements obtained within the pilot characterization borehole. Twelve discrete static pressure/depth measurements were obtained using the Schlumberger, wireline conveyed MDT tool, and two static pressure/depth readings were obtained from hydrologic packer tests. As indicated in the figure, representative static pressure measurements over this open pilot borehole interval were obtained for the Silurian Limestone Formation, St. Peter Sandstone, and the Mount Simon Sandstone. For comparison purposes, the normal freshwater hydrostatic pressure

gradient (i.e., 0.4331 psi/ft; $\rho_w = 1.000 \text{ g/cm}^3 \text{ @STP}$) and brine hydrostatic pressure gradient (based on Mount Simon salinity conditions; 0.4478 psi/ft; $\rho_w = 1.033 \text{ g/cm}^3 \text{ @STP}$) are shown for comparison. As indicated in the figure, pressure/depth measurements for both the Silurian and St. Peter test intervals are slightly under-pressured in comparison to the projected, normal freshwater hydrostatic conditions, while pressure/depth measurements exhibit a similar under-pressured relationship in comparison to the projected brine hydrostatic profile.

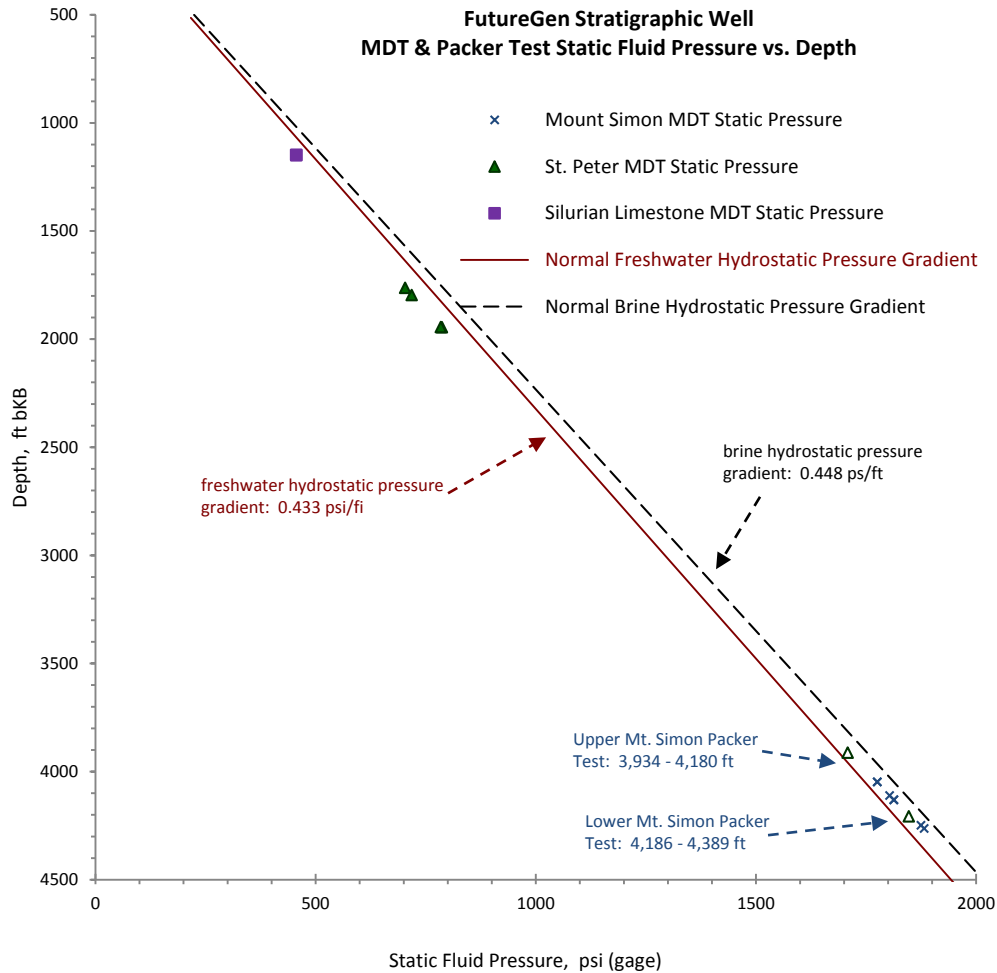


Figure 2.29. Pressure vs. Depth Profile Relationships Within the FutureGen Stratigraphic Well

To assess the vertical flow potential between the Mount Simon and the overlying St. Peter (the lowest USDW) formations, pressure measurements for those two hydrogeologic units were normalized taking into account variations in temperatures and fluid densities and then the calculated, or “observed”, pressure heads were compared. The observed hydraulic head values were calculated using the HEADCO program (Spane and Mercer 1985) and represent the elevation of a water column for the static pressure/depth readings, and for the established formation fluid densities, and prevailing static fluid temperature/depth gradient at the stratigraphic well location (which varies between ~0.01 and 0.02°F/ft for respective depths). Figure 2.30 shows the calculated observed hydraulic head for the St. Peter and several selected Mount Simon pressure/depth measurements. The results indicate that there is a positive head difference

in the Mount Simon that ranges from 47.8 to 61.6 ft above the calculated St. Peter observed static hydraulic head condition (i.e., 491.1 ft above MSL). This positive head difference suggests a natural vertical flow potential from the Mount Simon to the overlying St. Peter if hydraulic communication is afforded (e.g., an open communicative well). It should also be noted, however, that the higher head within the unconsolidated Quaternary aquifer (~611 ft above MSL), indicates a downward vertical flow potential from this surficial aquifer to both underlying St. Peter and Mount Simon bedrock aquifers (Figure 2.30).

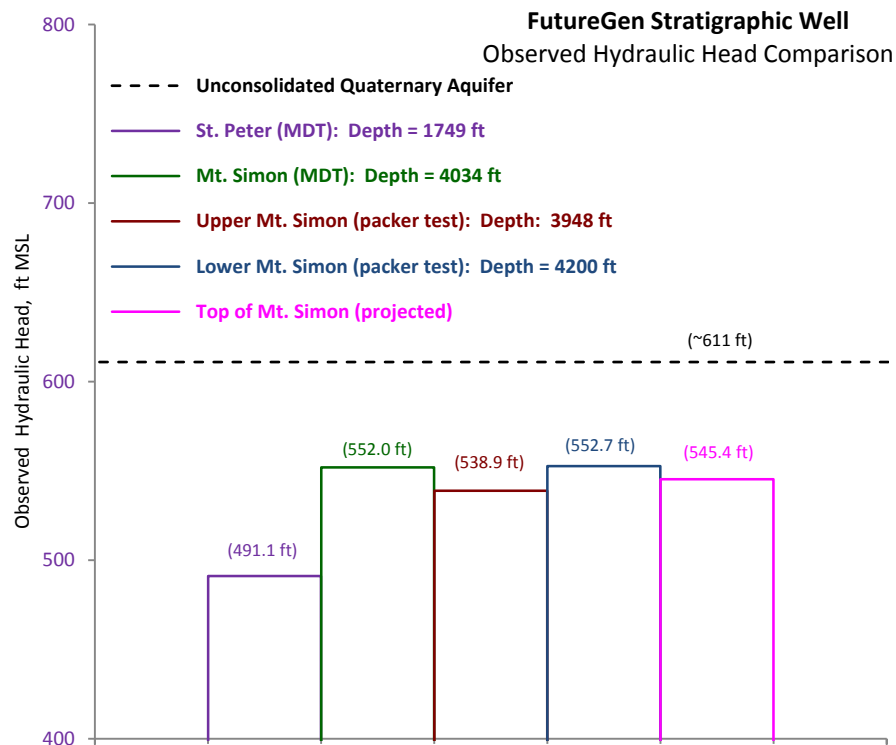


Figure 2.30. Observed Hydraulic Head Comparison Between the Unconsolidated Quaternary Aquifer, St. Peter Sandstone, and Mount Simon Sandstone Within the FutureGen Stratigraphic Well

The disparity in the calculated hydraulic head measurements (together with the significant differences in formation fluid salinity) also suggests that groundwater within the St. Peter and Mount Simon bedrock aquifers is physically isolated from one another. This is an indication that there are no significant conduits (open well bores or fracturing) between these two formations and that the Eau Claire forms an effective confining layer. Because the naturally occurring hydraulic head conditions are higher in the Mount Simon than the hydraulic heads in the St. Peter Formation, which is the lowest most USDW, the standard EPA methodology for determining the AoR pressure front is negated. However, it should also be noted that the upper unconsolidated Quaternary aquifer has a naturally higher hydraulic head than the Mount Simon. In addition, as indicated in Figure 2.30, all the bedrock aquifers, including the Mount Simon, have hydraulic heads lower than the upper unconsolidated Quaternary aquifer, which is the current source of drinking water for the area surrounding the FutureGen site. A discussion of the AoR determination is provided in Section 3.1.9 and a comprehensive monitoring plan that is protective of the USDW is presented in Chapter 5.0.

2.7 Site Evaluation of Mineral Resources

Other subsurface geochemical considerations include the potential for mineral or hydrocarbon resources beneath the proposed CO₂ storage site. While no significant mineral deposits are known to exist within Morgan County, natural gas has been recovered in the region, including at the Prentice and Jacksonville fields located within several miles of the stratigraphic well (Figure 2.31). ISGS oil and gas website data indicate that the Prentice Field contained more than 25 wells drilled during the 1950s; re-exploration occurred in the 1980s.¹ Both oil and gas have been produced from small stratigraphic traps in the shallow Pennsylvanian targets, at depths of 250 to 350 ft (75 to 105 m) bgs. It is important to note that gas produced from these wells may contain around 16 percent CO₂ (Meents 1981).

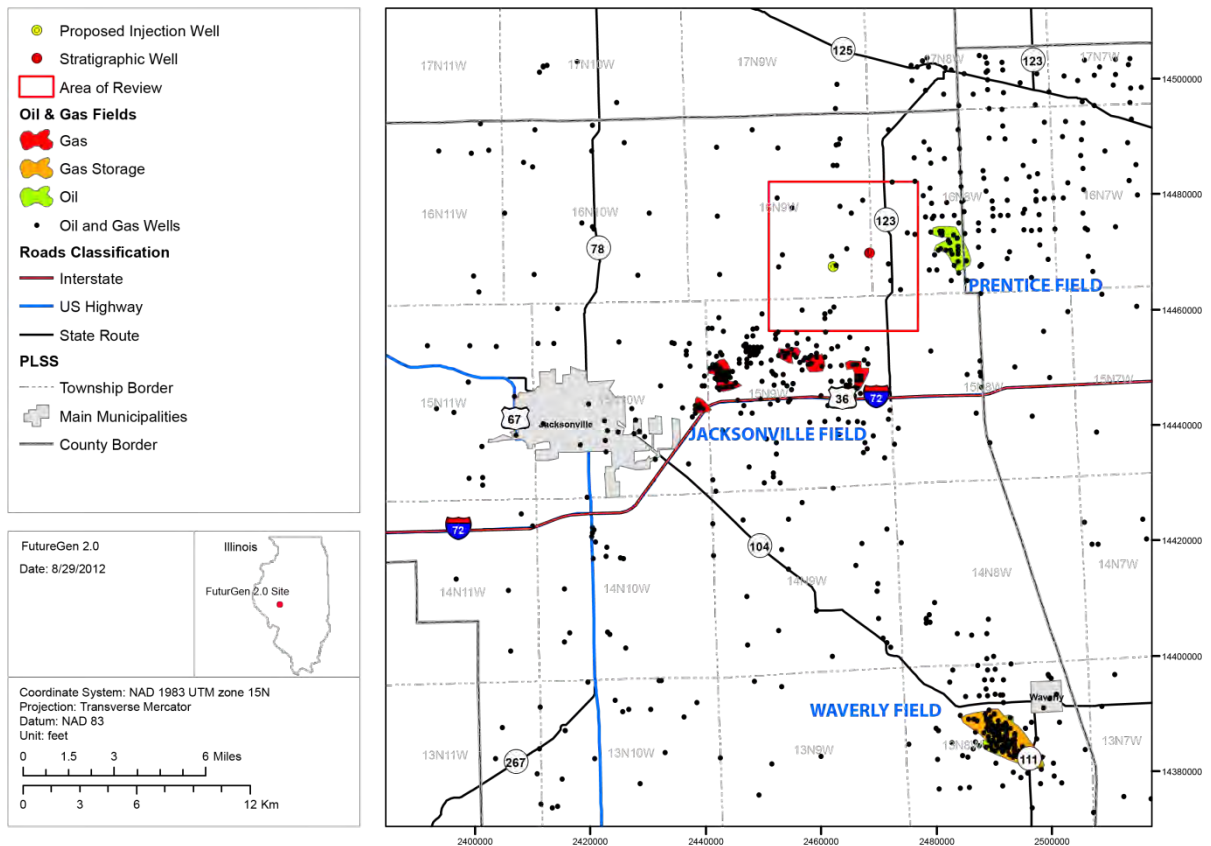


Figure 2.31. Map of Oil and Gas Wells Located Near the Proposed Morgan County CO₂ Storage Site (based on data from ISGS 2011a)

More than 75 wells have been drilled in the Jacksonville Field. Gas was discovered in the Jacksonville Field as early as 1890 (Bell 1927), but most oil and gas production from the Prentice and Jacksonville fields occurred between the late 1920s and late 1980s. The most productive formations in the Illinois Basin (lower Pennsylvanian and Mississippian siliciclastics and Silurian reefs) are not present in Morgan County. Only two boreholes in the vicinity of the Prentice Field and five boreholes near the Jacksonville Field penetrate through the New Albany Shale into Devonian and Silurian limestones.

¹ <http://moulin.igs.uiuc.edu/ILOIL/webapp/ILOIL.html>, accessed on September 20, 2011.

Cumulative production from the Prentice and Jacksonville fields is not available, and both fields are largely abandoned. The Waverly Storage Field natural-gas storage site in the southeast corner of Morgan County originally produced oil from Silurian carbonates. This field no longer actively produces oil, but since 1954 it has been successfully used for natural-gas storage in the St. Peter and the Galesville/Ironton Sandstone formations (Buschbach and Bond 1974).

The nearest active coal mine is approximately 10 mi (16 km) away in Menard County and does not penetrate more than 200 ft (61 m) bgs (ISGS 2012a). A review of the known coal geology within a 5-mi (8-km) radius of the proposed drilling site indicates that the Pennsylvanian coals, the Herrin, Springfield, and Colchester coals, are very thin or are absent from the project area (ISGS 2010, 2011; Hatch and Affolter 2008). During continuous coring of a shallow groundwater monitoring well, immediately adjacent to the stratigraphic well, only a single thin (5-ft [1.5-m]) coal seam was encountered at about 200 ft (61 m) deep.

2.8 Wells Within the Survey Area

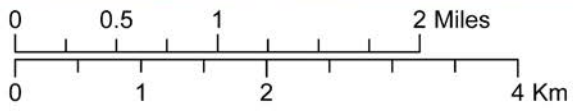
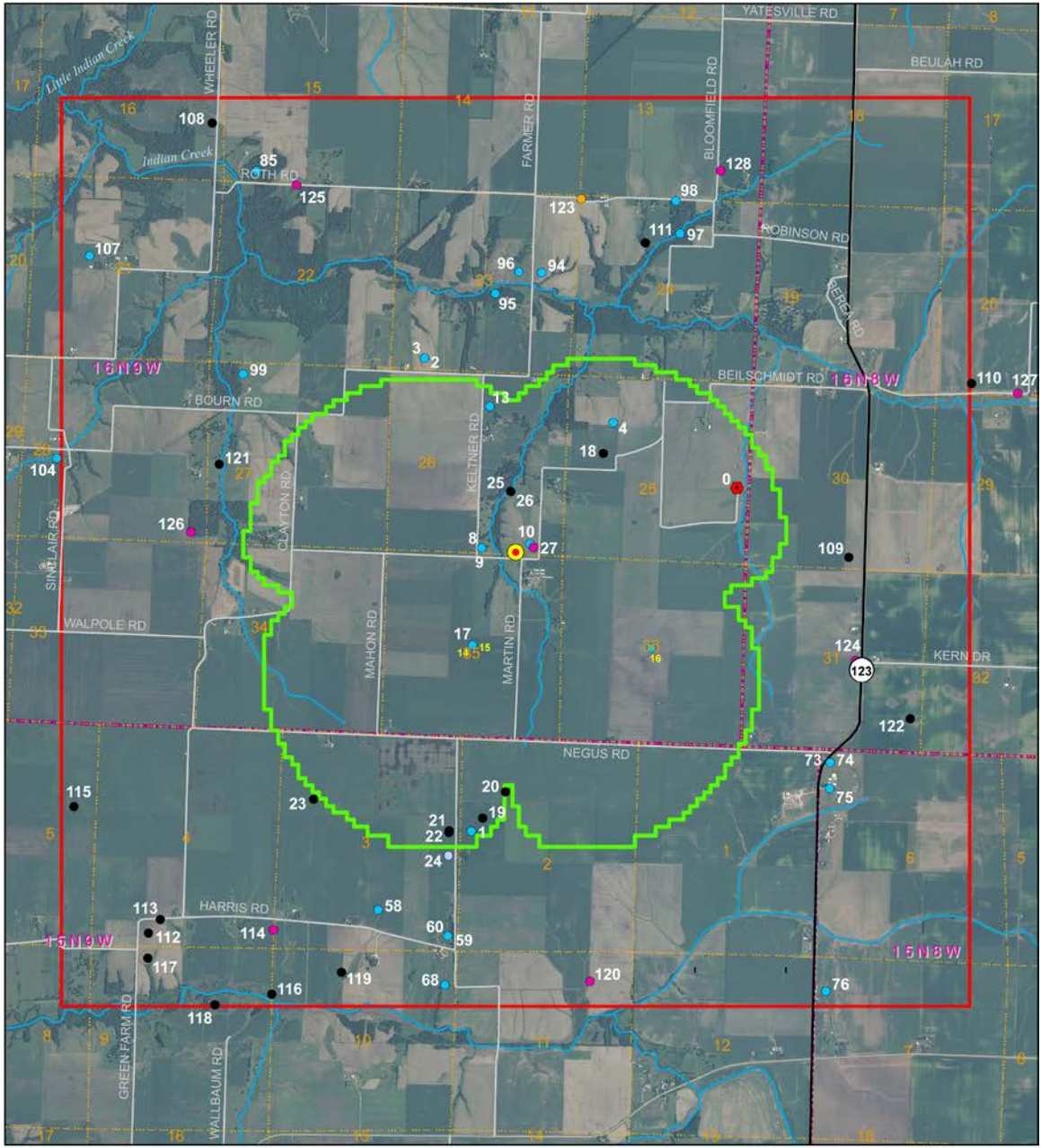
A survey area of 25 mi² (65 km²) that is centered on the proposed injection location and encompasses the area of the expected CO₂ plume (the AoR) is shown in Figure 2.32. Surface bodies of water and other pertinent surface features (including structures intended for human occupancy), administrative boundaries, and roads are shown. There are no subsurface cleanup sites, mines, quarries, or Tribal lands within this area. Although numerous wells are located within a 25-mi² (65-km²) survey area that includes the proposed injection location (Figure 2.32), none but the Alliance's stratigraphic well penetrates the injection zone (Mount Simon Sandstone and the lower Eau Claire [Elmhurst Sandstone Member]), the confining zone (Lombard and Proviso members of the Eau Claire Formation), or the secondary confining zone (Franconia Dolomite).

A total of 129 wells (including stratigraphic well) are within the survey area (see Appendix B); 51 wells are (or are potentially) within the AoR (Table 2.17). Indeed, 24 of these 51 water wells are only identified with a general location (center of a section) in the ISWS database. If the section of those wells intersected the AoR borders, the wells were assumed to be within the AoR even though they could be beyond the border. Those well are indicated with a "potentially" label in the last column of the Table 2.17 but are not shown on the map. Shallow domestic water wells with depths of less than 50 ft (15 m) are the most common well type. Five slightly deeper water wells were identified that range in depths from 110 ft (33 m) to 405 ft (123 m). Other wells include stratigraphic test holes, coal test holes, and oil and gas wells (Figure 2.32). Table 2.17 lists these wells with their unique API (American Petroleum Institute) identification number, ISWS well identification (ID), well location, depth, elevation, completion date, well owner, well type, and identified status.

The map in Figure 2.32 shows the locations of four proposed injection wells for which permits are being sought. It also shows the location of the Alliance's stratigraphic well and abandoned hydrocarbon test holes, coal test holes, oil and gas wells, other plugged and abandoned wells, known water wells, and other surface features within a 25-mi² (65-km²) area centered on the location of the proposed injection wells. Figure 8.1 is a map of residences, water wells, and surface water features within the delineated AoR and survey area.

Table 2.17. List of Wells Located Within the AoR

Map ID	API Number	ISWS ID	Latitude NAD1983	Longitude NAD1983	Public Land Survey System	Total Depth ft	Elev ft	Completion Date	Owner	Well Num	Well Type	Status	Confining Zone Penetration Well	In AoR
0	121372213200		39.806064	-90.052919	T16n,R9w,Sec 25	4812	633	TBD	FutureGen Industrial Alliance, Inc.	1	Monitoring	Active	Yes	Yes
1	121372118200	116519	39.778074	-90.078443	T15N,R9W,Sec 2	25		19780712	A.A. Negus Estate	1	Water	Private Water Well	No	Yes
4	121370018700	115778	39.811025	-90.065241	T16N,R9W,Sec 25	115			Beilschmidt, William H.		Water		No	Yes
8	121370028500	115740	39.800661	-90.078386	T16N,R9W,Sec 26	127		1950	Martin, L. E.	1	Water		No	Yes
9		115741	39.800661	-90.078386	T16N,R9W,Sec 26	127			Martin, L. E.		Water		No	Yes
10	121372128600	115779	39.801129	-90.07342	T16N,R9W,Sec 26	25		19781213	Martin, Marvin & Jean	1	Water	Private Water Well	No	Yes
14		115763	39.792894	-90.078875	T16N,R9W,Sec 35	28			E Clemons		Water		No	Yes
15		115764	39.792894	-90.078875	T16N,R9W,Sec 35	25			B Sister		Water		No	Yes
16		115765	39.792837	-90.060294	T16N,R9W,Sec 36	35			J M Dunlap		Water		No	Yes
17	121370051100		39.792893	-90.078984	T16N,R9W,Sec 35	1056	643		O'Rear, Judge	1	Oil & Gas / Water		No	Yes
18	121370009900		39.808545	-90.06614	T16N,R9W,Sec 25	1530	630	19391001	Beilschmidt, Wm.	1	Oil & Gas	Dry and Abandoned, No Shows	No	Yes
19	121370023500		39.779153	-90.077325	T15N,R9W,Sec 2	338	644	19231101	Conklin	1	Oil & Gas	Dry and Abandoned, No Shows	No	Yes
20	121370023600		39.781298	-90.075082	T15N,R9W,Sec 2	348	646	19231101	Conklin	2	Oil & Gas	Dry and Abandoned, No Shows	No	Yes
21	121370023700		39.778057	-90.080754	T15N,R9W,Sec 3	342	645	19231001	Harris, A. J.	1	Oil & Gas	Gas Producer	No	Yes
22	121370023900		39.7779	-90.080756	T15N,R9W,Sec 3	334	644	19231107	Harris, A. J.	3	Oil & Gas	Gas Producer	No	Yes
25	121370036300		39.805251	-90.075597	T16N,R9W,Sec 26	1205		19670330	Martin	1	Oil & Gas	Dry and Abandoned, No Shows	No	Yes
26	121370036301		39.805251	-90.075597	T16N,R9W,Sec 26	1400		19731029	Martin	1	Oil & Gas	Junked and Abandoned, Plugged	No	Yes
27	121372088500		39.800861	-90.073017	T16N,R9W,Sec 26	302	630				Coal Test		No	Yes
		115735	39.807386	-90.060378	T16N,R9W,Sec 25	27			Beilschmidt, William H.		Water		No	Potentially
		115736	39.807386	-90.060378	T16N,R9W,Sec 25	30			W R Fowler		Water		No	Potentially
		115737	39.807386	-90.060378	T16N,R9W,Sec 25	28			Mason		Water		No	Potentially
		115739	39.807478	-90.079049	T16N,R9W,Sec 26	25			C H Matin		Water		No	Potentially
		115738	39.807478	-90.079049	T16N,R9W,Sec 26	22			T Gondall		Water		No	Potentially
		115650	39.807193	-90.041413	T16N,R8W,Sec 30	19		1930	R Allison		Water		No	Potentially
		115651	39.792765	-90.041512	T16N,R8W,Sec 31	28			W J Huston		Water		No	Potentially
		115652	39.792765	-90.041512	T16N,R8W,Sec 31	28			E Robinson		Water		No	Potentially
		116450	39.777005	-90.052023	T15N,R9W,Sec 1	25			A Harris		Water		No	Potentially
		116453	39.776968	-90.070521	T15N,R9W,Sec 2	32			A Harris		Water		No	Potentially
		116451	39.776968	-90.070521	T15N,R9W,Sec 2	22			W R Conklin		Water		No	Potentially
		116452	39.776968	-90.070521	T15N,R9W,Sec 2	30			B Negus		Water		No	Potentially
		116454	39.77688	-90.088996	T15N,R9W,Sec 3	28			C Negus		Water		No	Potentially
		116455	39.77688	-90.088996	T15N,R9W,Sec 3	30			L B Trotter		Water		No	Potentially
		115727	39.821881	-90.078925	T16N,R9W,Sec 23	30			D Flinn		Water		No	Potentially
		115728	39.821881	-90.078925	T16N,R9W,Sec 23	30			Hazel Dell School		Water		No	Potentially
		115729	39.821881	-90.078925	T16N,R9W,Sec 23	35			K Haneline		Water		No	Potentially
		115733	39.821811	-90.060168	T16N,R9W,Sec 24	30			J L Icenagle		Water		No	Potentially
		115734	39.821811	-90.060168	T16N,R9W,Sec 24	30			G Lewis		Water		No	Potentially
		115775	39.821811	-90.060168	T16N,R9W,Sec 24	200		1944	E C Lewis		Water		No	Potentially
		115742	39.807531	-90.097566	T16N,R9W,Sec 27	23			J Stewart		Water		No	Potentially
		115743	39.807531	-90.097566	T16N,R9W,Sec 27	23			I J Stewart		Water		No	Potentially
		115761	39.792917	-90.097513	T16N,R9W,Sec 34	28			T Harrison		Water		No	Potentially
		115762	39.792917	-90.097513	T16N,R9W,Sec 34	30			J Mahon		Water		No	Potentially



Basemap: Imagery from the National Agriculture Imagery Program (NAIP) - Morgan County, Illinois, 2010, provided by <http://datagateway.nrcs.usda.gov>.

Projection: NAD 1983 UTM zone 16N

05/08/2013

Figure 2.32. Wells Located Within the Survey Area. The map includes surface bodies of water, mines, quarries, faults, and other surface features. Tables of the data used to produce this map are provided in Table 2.17 and Appendix B.

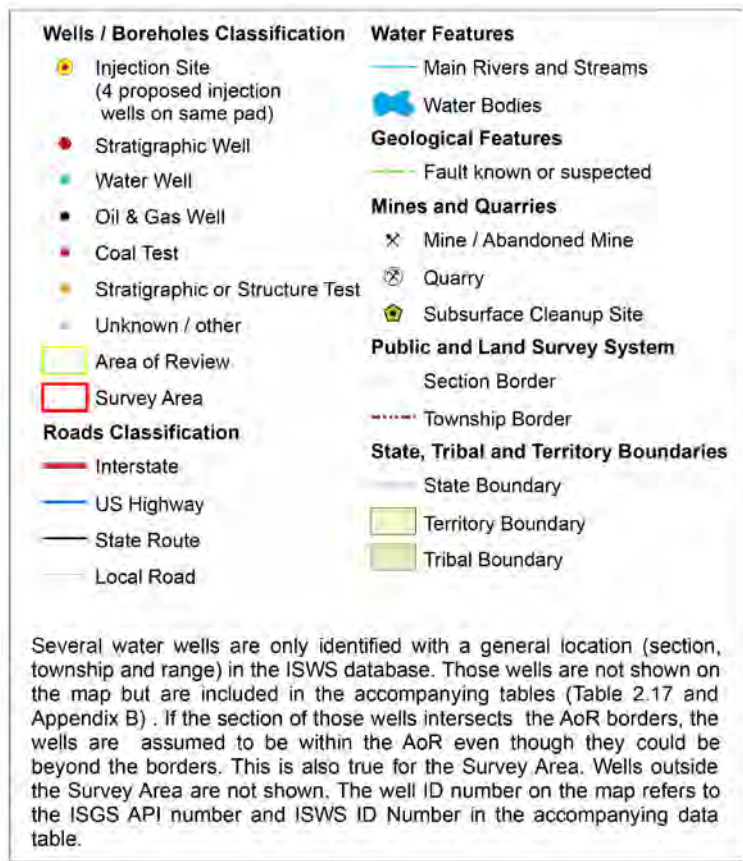


Figure 2.32. (contd)

2.9 Conclusion

The geologic setting of the proposed site indicates that the Mount Simon Sandstone at the site is sufficiently deep, and has sufficient thickness, lateral continuity, porosity, and permeability to store the proposed 22-MMT volume of CO₂. In addition, the Eau Claire Formation at the site is of sufficient thickness, lateral continuity, and has low enough permeabilities to serve as the primary confining zone. The site affords additional containment with several secondary confining zones, including the Franconian Formation. The basement rock was encountered at 4,430 ft and is a rhyolite, which will act as an impermeable lower boundary for the injection zones within the Mount Simon Sandstone. No potential conduits for CO₂ to migrate out of the Mount Simon reservoir were identified at the proposed storage site. Three relatively deep wells are present within the AoR, but none of them penetrates beyond the Maquoketa Shale which is significantly shallower than the primary confining zone. No faults or fractures were identified based on geophysical well logs of the stratigraphic well and from seismic analysis of the site. The rarity of tectonic fractures and lack of large-aperture tension fractures in the stratigraphic well, as determined from the image and sonic logs, indicate that the well is not proximal to normal (tensional) faults that might be close to failure.

Chapter 3.0 uses a conceptual model developed using the appropriate physical and chemical properties determined for the site to simulate the injection of 22 MMT of CO₂ over 20 years using a computational model. The physical and chemical input parameters for the computational model are described in more detail in Chapter 3.0.

2.10 References

- 40 CFR 144.3. Code of Federal Regulations, Title 40, Protection of the Environment, Part 144, "Underground Injection Control Program," Section 3, "Definitions."
- 40 CFR 146.82. Code of Federal Regulations, Title 40, *Protection of Environment*, Part 146, "Underground Injection Control Program: Criteria and Standards," Section 82, "Required Class VI permit information."
- 40 CFR 146.83(a). Code of Federal Regulations, Title 40, *Protection of Environment*, Part 146, "Underground Injection Control Program: Criteria and Standards," Section 83, "Minimum criteria for siting."
- 40 CFR 146.88. Code of Federal Regulations, Title 40, Protection of Environment, Part 146 "Underground Injection Control Program: Criteria and Standards," Section 88, "Injection well operating requirements."
- Bell AH. 1927. *Recent Developments in the Vicinity of Jacksonville*. Illinois Petroleum Report 11, Illinois State Geologic Survey, Urbana, Illinois.
- Bergstrom RE and AJ Zeizel. 1957. *Groundwater Geology in Western Illinois, South Part*. Circular 232, Illinois State Geological Survey, Urbana, Illinois.
- Bethke CM and S Marshak. 1990. "Brine Migrations across North America – The Plate Tectonics of Groundwater." *Annual Review Earth and Planetary Sciences*, 18, 287–315. (Reprinted in WE Dietrich and G Sposito, eds., (1997) *Hydrologic Processes from Catchment to Continental Scales*, Annual Reviews, Inc.)
- Bickford ME, WR Van Schmus, and I Zietz. 1986. "Proterozoic history of the midcontinent region of North America." *Geology* 14(6):492–496.
- Birkholzer JT, Q Zhou, J Rutqvist, P Jordan, K Zhang, and CF Tsang. 2007. *Research Project on CO₂ Geological Storage and Groundwater Resources: Large-Scale Hydrogeological Evaluation and Impact on Groundwater Systems, Annual Report: October 1, 2006 to September 30, 2007*. LBNL-63544, Lawrence Berkeley National Laboratory, Berkeley, California.
- Birkholzer JT, Q Zhou, K Zhang, P Jordan, J Rutqvist, and CF Tsang. 2008. *Research Project on CO₂ Geological Storage and Groundwater Resources Large-Scale Hydrological Evaluation and Modeling of the Impact on Groundwater Systems Annual Report: October 1, 2007, to September 30, 2008*. Lawrence Berkeley National Laboratory, Berkeley, California.
- Bowen BB, R Ochoa, ND Wilkens, J Brophy, TR Lovell, N Fischietto, C Medina, and J Rupp. 2011. "Depositional and Diagenetic Variability Within the Cambrian Mount Simon Sandstone: Implications for Carbon Dioxide Sequestration." *Environmental Geosciences* 18:69-89.
- Buschbach TC and DC Bond. 1974. *Underground Storage of Natural Gas in Illinois – 1973*. Illinois Petroleum 101, Illinois State Geological Survey, Champaign, Illinois.

Buschbach TC and DR Kolata. 1991. "Regional Setting of Illinois Basin." In Leighton MW, Kolata DR, Oltz DF, and Eidel JJ (eds.), *Interior Cratonic Basins. American Association of Petroleum Geologists Memoir 51:29–55.*

Daniels DL, RP Kucks, and PL Hill. 2008. Illinois, Indiana, and Ohio Magnetic and Gravity Maps and Data: A Website for Distribution of Data. U.S. Geological Survey Data Series 321. Available at: <http://pubs.usgs.gov/ds/321/>.

Dey WS, RA Locke, IG Krapac, CG Patterson, and JL Hurry. In press. *Preliminary Hydrogeologic Investigation of the FutureGen 2 Site in Morgan County, Illinois.* Prepared by the Illinois State Geological Survey for Pacific Northwest National Laboratory, Richland, Washington.

Driese SG, CW Byers, and RH Dott. 1981. "Tidal deposition in the basal upper Cambrian Mount Simon Formation in Wisconsin." *Journal of Sedimentary Research 51:367-381.*

EPA (U.S. Environmental Protection Agency). 2011. *Underground Injection Control Permit Application IL-ICCS Project.* Submitted to the EPA Region 5 by Archer Daniels Midland Company, Decatur, Illinois.

EPA (U.S. Environmental Protection Agency). 1994. *Determination of Maximum Injection Pressure for Class I Wells.* Underground Injection Control Section Regional Guidance #7. EPA Region 5, Chicago, Illinois.

Freiburg T and HE Leetaru. 2012. "Controls on Porosity Development and the Potential for CO₂ Sequestration or Waste Water Disposal in the Cambrian Potosi Dolomite (Knox Group): Illinois Basin" (abstract) *AAPG Search and Discovery Article #90154.* AAPG 41st Annual Eastern Section Meeting, September 22-26, 2012, Cleveland, Ohio.
<http://www.searchanddiscovery.com/abstracts/html/2012/90154eastern/abstracts/freib.htm>
Accessed on August 15, 2012.

Gibb JP and M O'Hearn. 1980. *Illinois Ground Water Quality Data Summary.* Contract Report 230, Illinois State Water Survey, Urbana, Illinois.

Goetz LK, JG Tyler, RL Macarevich, D Brewster, and JR Sonnad. 1992. "Deep gas play probed along Rough Creek graben in Kentucky part of Illinois Basin." *Oil and Gas Journal 90:97-101.*

Gupta N and ES Bair. 1997. "Variable-Density Flow in the Midcontinent Basins and Arches Region of the United States." *Water Resources Research 33:1785–1802.*

Hanson GF. 1960. *Summary Statement of Facilities for Underground Storage of Liquid Petroleum Products in Wisconsin.* University of Wisconsin, Wisconsin Geological and Natural History Survey, Madison, Wisconsin.

Hatch JR and RH Affolter. 2008. "Geologic Overview." In Hatch JR and RH Affolter (eds.) Chapter C of *Resource Assessment of the Springfield, Herrin, Danville, and Baker Coals of the Illinois Basin.* U.S. Geological Survey Professional Paper 1625-D, Government Printing Office, Washington D.C.

Helmutz Centre Potsdam – GFZ. 2012. *World Stress Map Project*. Available at <http://dc-app3-14.gfz-potsdam.de/>. Last accessed on 5/9/2012.

Houseknecht DW. 2001. “Earliest Paleozoic stratigraphy and facies, Reelfoot Basin and adjacent craton.” Pp. 27–44, in Gregg, JM, JR Palmer, and VE Krutz (eds.), *Field Guide to the Upper Cambrian of Southeastern Missouri: Stratigraphy, Sedimentology, and Economic Geology*. OFR-01-98-GS, Missouri Department of Natural Resources Open-file Report, Rolla, Missouri.

Hunt LI. 2004. *A Petrophysical and Shallow Geophysical Study to Determine Pathways of Gas Migration Within and Above an Underground Gas Storage Field in North-Central Illinois*. Illinois State University, Normal, Illinois.

IDNR (Iowa Department of Natural Resources). 2012. Iowa Geological and Water Survey GeoSam Database website. Available at: <http://www.igsb.uiowa.edu/webapps/geosam/>.

ISGS (Illinois State Geological Survey). 2012a. Coal Mines, Coal Geology, and Resource Data Online, County Coal Map and Data Series, Morgan County. Available at: <http://www.isgs.uiuc.edu/maps-data-pub/coal-maps/counties/morgan.shtml>. Last accessed January 4, 2012.

ISGS (Illinois State Geological Survey). 2012b. Illinois Natural Resources Geospatial Data Clearinghouse, Glacial Drift Thickness and Character map revised in 1998. Available at: <http://www.isgs.uiuc.edu/nsdihome/>

ISGS (Illinois State Geological Survey). 2012c. ILWATER Interactive Mapping Web Interface. Available at: <http://www.isgs.illinois.edu/maps-data-pub/wwdb/launchims.shtml>. Last accessed on January 4, 2012.

ISGS (Illinois State Geological Survey). 2012d. Surficial Geology and Features Quaternary Deposits Map website. Available at: <http://www.isgs.uiuc.edu/sections/quat/deposit-map.shtml>. Last accessed on February 14, 2012.

ISGS (Illinois State Geological Survey). 2011. Illinois Oil and Gas Resources (ILOIL) Internet Map Service, <http://moulin.isgs.uiuc.edu/ILOIL/webapp/ILOIL.html>. Last accessed on October 8, 2011.

Kisvarsanyi EB. 1979. *Geologic Map of the Precambrian of Missouri*. Contributions to Precambrian Geology No 7, 1:1000000 map, Missouri Department of Natural Resources, Jefferson City, Missouri.

Kolata DR. 2005. Bedrock Geology of Illinois. Illinois Map 14 1:500,000, Illinois State Geological Survey, Urbana, Illinois.

Kolata DR and J Nelson. 1991. “Tectonic History of the Illinois Basin.” Pp. 263–285 in MW Leighton, DR Kolata, DF Oltz, and JJ Eidel (eds.), Interior Cratonic Basins. *Memoir 51, American Association of Petroleum Geologists*. Tulsa, Oklahoma.

Kolata DR and CK Nimz. 2010. *Geology of Illinois*. Illinois State Geologic Survey, Urbana, Illinois.

Leetaru HE and JH McBride. 2009. “Reservoir uncertainty, Precambrian topography, and carbon sequestration in the Mt. Simon Sandstone, Illinois Basin.” *Environmental Geosciences* 16(4):235-243.

Leetaru HE, DG Morse, R Bauer, SM Frailey, D Keefer, DR Kolata, C Korose, E Mehnert, S Rittenhouse, J Drahovzal, S Fisher, JH McBride. 2005. "Saline reservoirs as a sequestration target." In *An Assessment of Geological Carbon Sequestration Options in the Illinois Basin*, Final Report for U.S. DOE Contract: DE-FC26-03NT41994, Principal Investigator: Robert Finley. Midwest Geological Sequestration Consortium, Champaign, Illinois.

Leetaru HE, SM Frailey, D Morse, RJ Finley, JA Rupp, JA Drahovzal, and JH McBride. 2009. "Carbon sequestration in the Mount Simon Sandstone saline reservoir." In Grobe M, JC Pashin, and RL Dodge (eds.), *Carbon dioxide sequestration in geological media—State of the science*, *AAPG Studies in Geology* 59:261-277.

Lidiak EG. 1996. "Geochemistry of subsurface Proterozoic rocks in the eastern Midcontinent of the United States: Further evidence for a within-plate tectonic setting." Pp. 45-66, in van der Pluijm BA and Catacosinos PA (eds.), *Basement and Basins of Eastern North America*. Special Paper 308, Geological Society of America, Boulder, Colorado.

Lloyd OB and WL Lyke. 1995. *Ground Water Atlas of the United States*, Segment 10. United States Geological Survey, U.S. Government Printing Office, Washington D.C.

McBride JH and DR Kolata. 1999. "Upper Crust Beneath Central Illinois Basin, United States". *GSA Bulletin* 111(3):375-394.

MDNR (Missouri Department of Natural Resources). 2012. Missouri Department of Natural Resources Water Resources Center, Geologic Well Logs of Missouri website. Available at: <http://www.dnr.mo.gov/env/wrc/logmain/index.html>.

Meents WF. 1981. *Analysis of Natural Gas in Illinois, Gas, Natural – Illinois*. Illinois State Geological Survey, Urbana, Illinois.

Morse DG and HE Leetaru. 2005. *Reservoir characterization and three-dimensional models of Mt. Simon Gas Storage Fields in the Illinois Basin*. Circular 567, Illinois State Geological Survey, Urbana, Illinois (CD-ROM).

Nelson WJ. 1995. *Structural Features in Illinois*. Bulletin 100, Illinois State Geological Survey, Champaign, Illinois.

Saller AH, J Schwab, S Walden, S Robertson, R Nims, H Hagiwara, and S Mizohata. 2004. "Three-dimensional seismic imaging and reservoir modeling of an upper Paleozoic "reefal" buildup, Reinecke Field, west Texas, United States." Pp. 107-125 in GP Eberli, JL Masferro, and JF Sarg (eds.), *Seismic Imaging of Carbonate Reservoirs and Systems*, Volume 81, American Association of Petroleum Engineers, Tulsa, Oklahoma.

Sargent ML and Z Lasemi. 1993. "Tidally dominated depositional environment for the Mount Simon Sandstone in central Illinois." *Great Lakes Section, Geological Society of America, Abstracts and Programs* 25(3):78.

Selkregg LF and JP Kempton. 1958. *Groundwater Geology in East-Central Illinois*. Circular 248, Illinois State Geological Survey, Urbana, Illinois.

- Sminchak J. 2011. *Conceptual Model Summary Report Simulation Framework for Regional Geologic CO₂ Storage Along Arches Province of Midwestern United States*, Topical Report. Battelle Memorial Institute, Columbus, Ohio.
- Spane FA and RB Mercer. 1985. *HEADCO: A Program for Converting Observed Water Levels and Pressure Measurements to Formation Pressure and Standard Hydraulic Head*. RHO-BW-ST-71P, Rockwell Hanford Operations, Richland, Washington.
- Streit JE and RR Hillis. 2004. "Estimating Fault Stability and Sustainable Fluid Pressures for Underground Storage of CO₂ in Porous Rock." *Energy* 29(9-10):1445-1456.
- USGS (U.S. Geological Survey). 2012a. Illinois – Earthquake History. Available at: <http://earthquake.usgs.gov/earthquakes/states/illinois/history.php>. Last accessed August 29, 2012
- USGS (U.S. Geological Survey). 2012b Earthquake Search. Available at: http://earthquake.usgs.gov/earthquakes/eqarchives/epic/epic_circ.php. Last accessed on August, 29, 2012.
- USGS (U.S Geological Survey). 2008. National Seismic Hazard Mapping Project, Earthquake Hazards Program. Last accessed on September 24, 2012 at <http://earthquake.usgs.gov/hazards/>.
- Weiss WW, X Xie, and JW Weiss. 2009. "Field Test of Wettability Alteration to Increase the Flow Rate from Aquifer Gas Storage Wells." Paper 12567, SPE Eastern Regional Meeting, 23-25 September 2009, Charleston, West Virginia. ISBN 978-1-55563-262-5. Available at: <http://www.onepetro.org/mslib/servlet/onepetropreview?id=SPE-125867-MS>.
- Whiting LL and DL Stevenson. 1965. *The Sangamon Arch*. Circular 383, Illinois State Geological Survey, Urbana, Illinois.
- Wilkens ND, N Fischietto, BB Bowen, and J Rupp. 2011. "Anatomy of a Cambrian Sheet Sand: Depositional Environments in the Mount Simon Sandstone." *GSA Abstracts with Programs* 42(5), Geological Society of America, Boulder, Colorado.
- Willman HB, E Atherton, TC Buschbach, C Collinson, JC Frey, ME Hopkins, JA Lineback, and JA Simon. 1975. *Handbook of Illinois Stratigraphy*. Bulletin 95, Illinois State Geological Survey, Urbana, Illinois.
- Woller DM and EW Sanderson. 1979. "Public Groundwater Supplies in Morgan and Scott Counties." Bulletin 60-27, Illinois State Water Survey, Illinois Institute of Natural Resources, Urbana, Illinois.
- Young HL. 1992. "Hydrogeology of the Cambrian-Ordovician aquifer system in the northern Midwest, United States." Professional Paper 1405-B, U.S. Geological Survey, U.S. Government Printing Office, Washington D.C.
- Zhou Q, JT Birkholzer, E Mehnert, Y-F Lin, and K Zhang. 2010. "Modeling Basin- and Plume-Scale Processes of CO₂ Storage for Full-Scale Deployment." *Ground Water* 48(4):494-514.

Zoback MD, CA Barton, M Brudy, DA Castillo, T Finkbeiner, BR Grollmund, DB Moos, P Peska, CD Ward, and DJ Wiprut. 2003. "Determination of stress orientation and magnitude in deep wells." *International Journal of Rock Mechanics and Mining Sciences* 40(7–8):1049-1076.

Zoback MD. 2007. *Reservoir Geomechanics*, Cambridge University Press, Cambridge, England.

3.0 Area of Review and Corrective Action Plan

This chapter describes how site geologic and hydrologic information were used to delineate the Area of Review (AoR) as it is defined in 40 CFR 146.84(a). This chapter also addresses the extent to which the Alliance needs to undertake corrective actions for features within the AoR that may penetrate the confining zone and how such corrective actions will be taken if needed in the future. Section 3.1 describes the computational model that was used to delineate the AoR, including a description of the simulator and the physical processes modeled, along with a description of the conceptual model and numerical implementation. It also describes the AoR and how the AoR will be reevaluated over time. Section 3.2 describes the Alliance's corrective action plan. Chapter 3.0 is intended to demonstrate compliance with 40 CFR 146.84.

3.1 Area of Review

The EPA GS Rule (75 FR 77230) defines the AoR as “the region surrounding the geologic sequestration project where underground sources of drinking water (USDWs) may be endangered by the injection activity” (40 CFR 146.84). Section 3.1.8 describes delineation of the proposed AoR for the Morgan County CO₂ storage site. All requested data (wells, cleanup sites, surface bodies of water, structures intended for human occupancy, etc.) for this area are provided in this application; the same information is also provided for a larger survey area of 25 mi² to demonstrate conclusively that USDWs will not be endangered by injection activities.

As discussed in Section 2.6, the natural ambient hydraulic head conditions within the proposed injection zone beneath the Morgan County storage site are higher than the hydraulic head conditions measured in the lowermost USDW (St. Peter Formation) of the stratigraphic well. The EPA suggests using a methodology for determining the AoR based either on the maximum extent of the separate-phase plume, or on the maximum extent of the pressure front, whichever is greater. Because the injection zone is overpressured relative to the lowermost USDW at the Morgan County storage site, use of the pressure front methodology would result in an infinite AoR. Therefore, the maximum extent of the separate-phase plume will be the basis for the AoR delineation for the Morgan County site. A discussion of this AoR delineation, and the measures that are being taken to ensure that the FutureGen 2.0 Project is protective of USDW aquifers, is provided in Section 3.1.9.

The GS Rule requires that the AoR “is delineated using computational modeling that accounts for the physical and chemical properties of all phases of the injected carbon dioxide stream and displaced fluids, and is based on available site characterization, monitoring, and operational data” (40 CFR 146.84). Computational modeling comprises two elements: a computer code, or simulator, that implements the mathematics of our scientific understanding, and implementation of the simulator as an analytical tool. These elements result in the ability to predict the quantity and distribution of CO₂ injected into saline reservoirs for storage. This requires solving the mathematical equations that describe the migration and partition behavior of supercritical CO₂ (scCO₂) as it is injected into geologic media for which the pore space is initially filled with an aqueous saline solution (brine). The equations that describe these flow and transport processes are too complex to solve directly. Therefore, the governing flow and transport equations are solved indirectly where space and time are divided into discrete elements. Space discretization involves dividing the reservoir into grid blocks and time discretization involves moving through time using finite steps. The discretization process transforms the governing flow and transport

equations into forms that are solvable on high-speed computers. Both elements of the computational model used to determine the AoR for the Morgan County CO₂ storage site are described in the sections that follow.

3.1.1 Description of Simulator

Numerical simulation of CO₂ injection into deep geologic reservoirs requires the modeling of complex, coupled hydrologic, chemical, and thermal processes, including multi-fluid flow and transport, partitioning of CO₂ into the aqueous phase, and chemical interactions with aqueous fluids and rock minerals. The simulations conducted for this investigation were executed using the STOMP-CO₂ simulator (White et al. 2012; White and Oostrom 2006; White and Oostrom 2000). STOMP-CO₂ was verified against other codes used for simulation of geologic disposal of CO₂ as part of the GeoSeq code intercomparison study (Pruess et al. 2002).

Partial differential conservation equations for fluid mass, energy, and salt mass compose the fundamental equations for STOMP-CO₂. Coefficients within the fundamental equations are related to the primary variables through a set of constitutive relationships. The salt transport equations are solved simultaneously with the component mass and energy conservation equations. The solute and reactive species transport equations are solved sequentially after the coupled flow and transport equations. The fundamental coupled flow equations are solved using an integral volume finite-difference approach with the nonlinearities in the discretized equations resolved through Newton-Raphson iteration. The dominant nonlinear functions within the STOMP-CO₂ simulator are the relative permeability-saturation-capillary pressure (k-s-p) relationships.

The STOMP-CO₂ simulator allows the user to specify these relationships through a large variety of popular and classic functions. Two-phase (gas-aqueous) k-s-p relationships can be specified with hysteretic or nonhysteretic functions or nonhysteretic tabular data. Entrapment of CO₂ with imbibing water conditions can be modeled with the hysteretic two-phase k-s-p functions. Two-phase k-s-p relationships span both saturated and unsaturated conditions. The aqueous phase is assumed to never completely disappear through extensions to the s-p function below the residual saturation and a vapor-pressure lowering scheme. Supercritical CO₂ has the function of a gas in these two-phase k-s-p relationships.

For the range of temperature and pressure conditions present in deep saline reservoirs, four phases are possible: 1) water-rich liquid (aqueous), 2) CO₂-rich vapor (gas), 3) CO₂-rich liquid (liquid-CO₂), and 4) crystalline salt (precipitated salt). The equations of state express 1) the existence of phases given the temperature, pressure, and water, CO₂, and salt concentration; 2) the partitioning of components among existing phases; and 3) the density of the existing phases. Thermodynamic properties for CO₂ are computed via interpolation from a property data table stored in an external file. The property table was developed from the equation of state for CO₂ published by Span and Wagner (1996). Phase equilibria calculations in STOMP-CO₂ use the formulations of Spycher et al. (2003) for temperatures below 100°C and Spycher and Pruess (2010) for temperatures above 100°C, with corrections for dissolved salt provided in Spycher and Pruess (2010). The Spycher formulations are based on the Redlich-Kwong equation of state with parameters fitted from published experimental data for CO₂-H₂O systems. Additional details regarding the equations of state used in STOMP-CO₂ can be found in the guide by White et al. (2012).

A well model is defined as a type of source term that extends over multiple grid cells, where the well diameter is smaller than the grid cell. A fully coupled well model in STOMP-CO₂ was used to simulate the injection of scCO₂ under a specified mass injection rate, subject to a pressure limit. When the mass injection rate can be met without exceeding the specified pressure limit, the well is considered to be flow controlled. Conversely, when the mass injection rate cannot be met without exceeding the specified pressure limit, the well is considered to be pressure controlled and the mass injection rate is determined based on the injection pressure. The well model assumes a constant pressure gradient within the well and calculates the injection pressure at each cell in the well. The CO₂ injection rate is proportional to the pressure gradient between the well and surrounding formation in each grid cell. By fully integrating the well equations into the reservoir field equations, the numerical convergence of the nonlinear conservation and constitutive equations is greatly enhanced.

3.1.2 Physical Processes Modeled

Physical processes modeled in the reservoir simulations included isothermal multi-fluid flow and transport for a number of components (e.g., water, salt, and CO₂) and phases (e.g., aqueous and gas). Isothermal conditions were modeled because it was assumed that the temperature of the injected CO₂ will be similar to the formation temperature. Reservoir salinity is considered in the simulations because salt precipitation can occur near the injection well in higher permeability layers as the rock dries out during CO₂ injection. This can completely plug pore throats, making the layer impermeable, thereby reducing reservoir injectivity and affecting the distribution of CO₂ in the reservoir.

Injected CO₂ partitions in the reservoir between the free (or mobile) gas, entrapped gas, and aqueous phases. Sequestering CO₂ in deep saline reservoirs occurs through four mechanisms: 1) structural trapping, 2) aqueous dissolution, 3) hydraulic trapping, and 4) mineralization. Structural trapping is the long-term retention of the buoyant gas phase in the pore space of the reservoir rock held beneath one or more impermeable caprocks. Aqueous dissolution occurs when CO₂ dissolves in the brine resulting in an aqueous-phase density greater than the ambient conditions. Hydraulic trapping is the pinch-off trapping of the gas phase in pores as the brine re-enters pore spaces previously occupied by the gas phase. Generally, hydraulic trapping only occurs upon the cessation of CO₂ injection. Mineralization is the chemical reaction that transforms formation minerals to carbonate minerals. In the Mount Simon Sandstone, the most likely precipitation reaction is the formation of iron carbonate precipitates. A likely reaction between CO₂ and shale is the dewatering of clays. Laboratory investigations are currently quantifying the importance of these reactions at the Morgan County CO₂ storage site. Therefore, the simulations described here did not include mineralization reactions. However, the STOMP-CO₂ simulator does account for precipitation of salt during CO₂ injection.

The CO₂ stream provided by the plant to the storage site is no less than 97 percent dry basis CO₂, (see Table 4.1 in Chapter 4.0). Because the amount of impurities is small, for the purposes of modeling the CO₂ injection and redistribution for this project, it was assumed that the injectate was pure CO₂.

3.1.3 Conceptual Model

A stratigraphic conceptual model of the geologic layers from the Precambrian basement to ground surface was constructed using the EarthVision® software package (Figure 3.1). The geologic setting and site characterization data described in Chapter 2.0 and later in this chapter were the basis for the Morgan County CO₂ storage site model. Borehole data from the FutureGen 2.0 stratigraphic well and data from

regional boreholes and published regional contour maps were used as input data. However, units below the Shakopee Dolomite and above the Eau Claire Formation were assumed to have a constant thickness based on the stratigraphy observed at the stratigraphic well. There is a regional dip of approximately 0.25 degrees in the east-southeast direction.

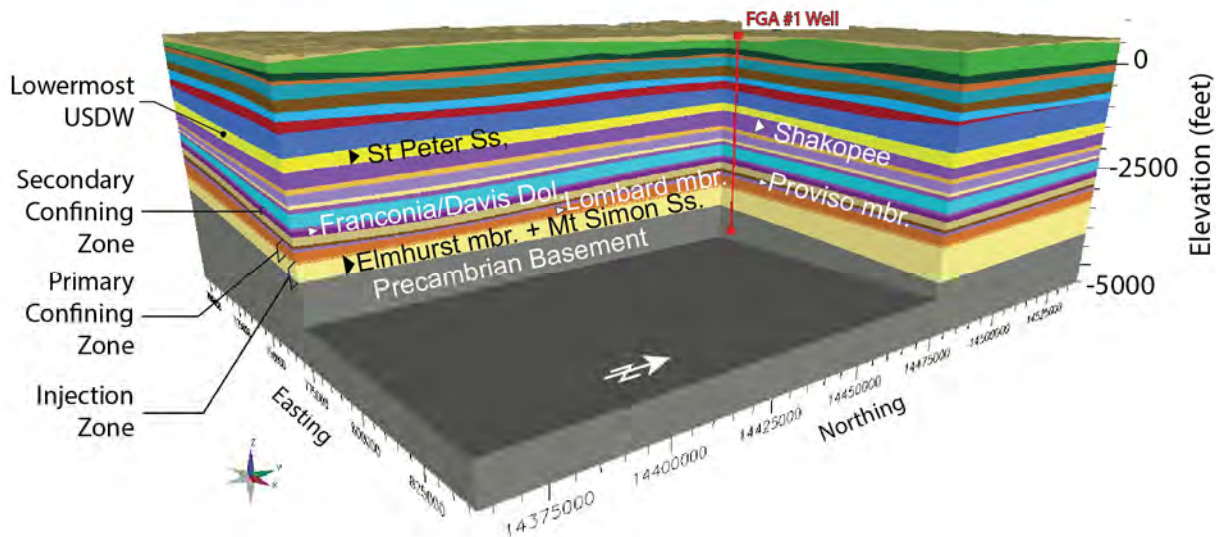


Figure 3.1. EarthVision® Solid Earth Model for the Proposed Morgan County CO₂ Storage Site. View to the southwest. For clarity, only the main formations have been labeled.

An expanded 100- x 100-mi conceptual model was constructed to represent units below the Potosi dolomite interval including the Franconia, Ironton, Eau Claire (Proviso, Lombard, and Elmhurst), Mount Simon, and Precambrian formations. These surfaces were gridded in EarthVision® based on borehole data and regional contour maps and make up the stratigraphic layers of the computational model.

3.1.3.1 Hydrogeologic Layers

The conceptual model hydrogeologic layers were defined for each stratigraphic layer based on zones of similar hydrologic properties. The hydrologic properties (permeability, porosity) were deduced from geophysical well logs and side-wall cores. The lithology, deduced from wireline logs and core data, was also used to subdivide each stratigraphic layer of the model. Based on these data, the Mount Simon Sandstone was subdivided into 17 layers, and the Elmhurst Sandstone (member of the Eau Claire Formation) was subdivided into 7 layers (Figure 3.2). These units form the injection zone. The Lombard and Proviso members of the Eau Claire Formation were subdivided respectively into 14 and 5 layers. The Ironton Sandstone was divided into four layers, the Davis Dolomite into three layers, and the Franconia Formation into one layer (Figure 3.2). One can also note that some layers (“split” label in Figure 3.2) have similar properties but have been subdivided to maintain a reasonable thickness of layers within the injection zone as represented in the computational model.

The thickness of the layers varies from 4 to 172 ft, with an average of 26 ft. The assignment of hydrologic properties to these layers is described in the next sections.

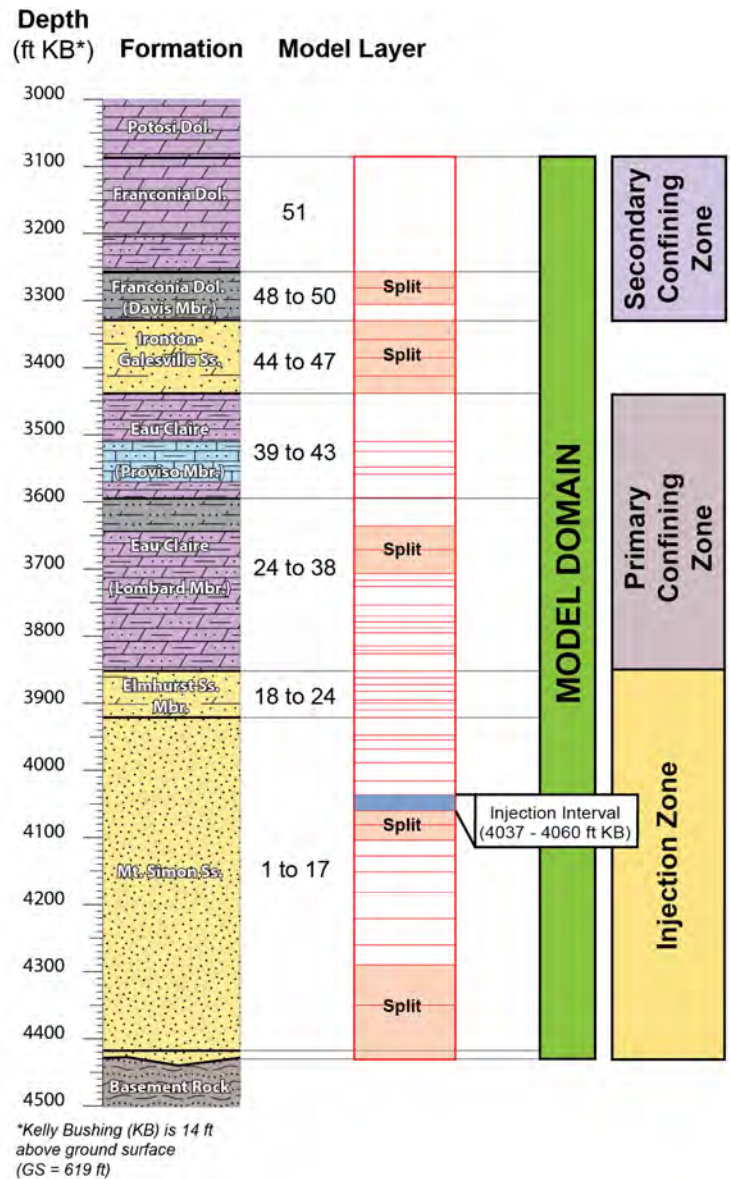


Figure 3.2. Division of Stratigraphic Layers to Create Computational Model Layers

3.1.3.2 Hydrologic and Porous Media Properties

Continuous wireline log results are commonly calibrated using discrete laboratory core measurements to provide a more continuous record for the particular characterization parameter (e.g., permeability, porosity). From these calibrated wireline-survey measurements, statistical or average values for the hydrologic parameter can be assigned to layers used in numerical models for the purpose of predicting fluid movement within targeted reservoirs.

A number of characterization data sources and methods were used to assign hydrologic properties to the various model layers. Available data sources for the Morgan County site include results from continuous wireline surveys (compensated magnetic resonance [CMR], Elemental Analysis [ELAN]), standard and side-wall cores (SWCs), and hydrologic tests (Modular Formation Dynamics Tester [MDT] and packer tests).

Because of differences in lithology and in the borehole construction, the method used to assign properties varied for different vertical zones of the conceptual model.

Horizontal Permeability

Intrinsic permeability is the property of the rock/formation that relates to its ability to transmit fluid, and is independent of the in situ fluid properties. For modeling of sedimentary rock formations, two permeabilities are commonly used: permeability in the horizontal direction, k_h (permeability parallel to sedimentary layering [also K_h]) and permeability in the vertical direction, k_v (permeability perpendicular to layering [also K_v]). The subsequent discussion pertains to assigned horizontal permeability values for the various borehole sections.

Intrinsic permeability data sources for the FutureGen 2.0 stratigraphic well include computed geophysical wireline surveys (CMR and ELAN logs), and where available, laboratory measurements of rotary SWCs, core plugs from the whole core intervals, and hydrologic tests (including wireline [MDT]), and packer tests.

Intrinsic Permeability in the Injection Zone (Mount Simon and Elmhurst Sandstone)

For model layers within the injection reservoir section (i.e., Elmhurst Sandstone and Mount Simon Sandstone; 3,852 to 4,432 ft [1174 to 1350 m]) a correlation/calibration approach was applied. Wireline log CMR- and ELAN-computed permeability model responses were first correlated with and then calibrated to rotary side-wall and core plug permeability results. The correlation process was facilitated using natural gamma ray responses and clay or shale abundance to establish correlation data sets. This calibration provided a continuous permeability estimate over the entire injection reservoir section (curve permKCal). The calibrated permeability response was then slightly adjusted, or scaled, to match the composite results obtained from the hydrologic packer tests over uncased intervals. For injection reservoir model layers within the cased well portion of the model, no hydrologic test data are available, and core-calibrated ELAN log response was used directly in assigning average model layer permeabilities.

The hydraulic packer tests were conducted in two zones of the Mount Simon portion of the reservoir. The Upper Zone (3,948 ft bkb to 4,194 ft bkb) equates to layers 6 through 17 of the model, while the Lower Zone (4,200 ft bkb to 4,512 ft bkb) equates to layers 1 through 5.¹ The most recent ELAN-based permeability-thickness product values are 9,524 mD-ft for the 246-ft-thick section of the upper Mount Simon corresponding to the Upper Zone and 3,139 mD-ft for the 312-ft-thick section of the lower Mount Simon corresponding to the Lower Zone. The total permeability-thickness product for the open borehole Mount Simon is 12,663 mD-ft, based on the ELAN logs. Results of the field hydraulic tests suggest that the upper Mount Simon permeability-thickness product is 9,040 mD-ft and the lower Mount Simon interval permeability-thickness product is 775 mD-ft. By simple direct comparison, the packer test for the upper Mount Simon is nearly equivalent (~95 percent) to the ELAN-predicted value, while the lower Mount Simon represents only ~25 percent of the ELAN-predicted value (Table 3.1).

¹ The layers “MtSimon5” and “MtSimon4” are subdivisions of a single layer. Because the MtSimon5 layer is located between the two testing zones and is more similar in log properties to the lower level, it is assigned as part of the lower zone.

Because no hydrologic test has been conducted in the Elmhurst Sandstone reservoir interval, a conservative scaling factor of 1 has been assigned to this interval, based on ELAN PermKCal data. The scaling factors applied in the model are listed in Table 3.2.

Table 3.1. Comparison of Results from Hydraulic Field Tests and ELAN Data

	Permeability-Thickness Product (mD-ft), T		T _f /T _e
	Field Test, T _f	ELAN, T _e	
Upper Mt. Simon	9,040	9,524	0.949
Lower Mt. Simon	775	3,139	0.247
Overall	9,815	12,663	0.775

Table 3.2. Summary of the Scaling Factors Applied for the Modeling

	Depth (ft bkb) – Based on Model Layers	Scaling Factor
Caprock and Overburden Formations	3,086 to 3,852 ft	1
Elmhurst	3,852 to 3,922 ft	1
Upper Mt. Simon	3,922 to 4,182 ft	0.949
Lower Mt Simon	4,182 to 4,432 ft	0.247

Intrinsic Permeability in the Confining Zones (Franconia to Lombard Formations)

The sources of data are similar to those for the injection zone reservoir, with the exception that no hydrologic or MDT test data are available.

ELAN log-derived permeabilities are unreliable below about 0.01 mD (personal communication from Bob Butsch, Schlumberger, 2012). Because the average log-derived permeabilities (permKCal wireline from ELAN log) for most of the caprock layers are at or below 0.01 mD, an alternate approach was applied. For each model layer the core data were reviewed, and a simple average of the available horizontal Klinkenberg permeabilities was then calculated for each layer. Core samples that were noted as having potential cracks and/or were very small were eliminated if the results appeared to be unreasonable based on the sampled lithology. If no core samples were available and the arithmetic mean of the PermKCal was below 0.01 mD, a default value of 0.01 mD was applied (Lombard9 is the only layer with a 0.01-mD default value).

Because the sandstone intervals of the Ironton-Galesville Sandstone have higher permeabilities that are similar in magnitude to the modeled reservoir layers, the Ironton-Galesville Sandstone model layer permeabilities were derived from the arithmetic mean of the PermKCal permeability curve.

Because no hydraulic test has been conducted in the primary confining zone, the scaling factor was assigned to be 100 percent in this interval and the overburden formations (Table 3.2).

Figure 3.3 shows the depth profile of the horizontal permeability assigned to each layer of the model (actual values assigned are listed in Table 3.8).

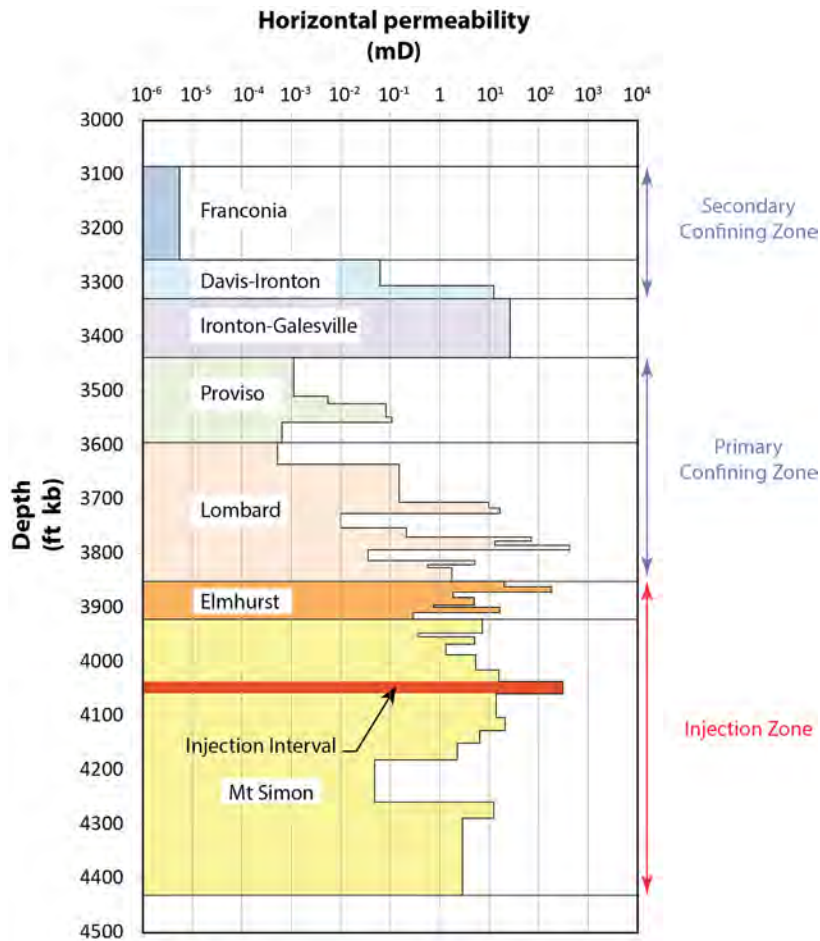


Figure 3.3. Horizontal Permeability Versus Depth in Each Model Layer

Vertical Permeability

Sedimentation can create an intrinsic permeability anisotropy, caused by sediment layering and preferential directions of connected-pore channels. K_v/K_h ratios were successfully determined for 20 vertical/horizontal siliciclastic core plug pairs cut from intervals of whole core from the stratigraphic well. Horizontal permeability data in the stratigraphic well far outnumber vertical permeability data, because vertical permeability could not be determined from rotary SWCs.

Effective vertical permeability in siliciclastic rocks is primarily a function of the presence of mudstone or shale (Ringrose et al. 2005). The siliciclastic lithologies (sandstones, siltstones, mudstones and shales) are heterolithic in the cored interval of the lower Lombard, and in rotary SWCs from the upper Lombard and non-carbonate Proviso. Core plug samples of heterolithic siliciclastics are poorly representative of larger vertical intervals (Meyer and Krause 2006).

Because the anisotropy of the model layers is not likely to be represented by the sparse data from the stratigraphic well, the following lithology-specific permeability anisotropy averages from literature studies representing larger sample sizes are used for the model layers (Table 3.3).

Table 3.3. Lithology-Specific Permeability Anisotropy Averages from Literature

Facies or Lithology	Kv/Kh	Reference
1. Heterolithic, laminated shale/mudstone/siltstone/sandstone	0.1	Meyer and Krause (2006)
2. Herringbone cross-stratified sandstone. Strat dips to 18 degrees	0.4	Meyer and Krause (2006)
3. Paleo weathered sandstone (coastal flat)	0.4	Meyer and Krause (2006)
4. Accretionary channel bar sandstones with minor shale laminations	0.5	Ringrose et al. (2005); Meyer and Krause (2006)
6. Alluvial fan, alluvial braided stream plain to shallow marine sandstones, low clay content	.3	Kerr et al. (1999)
7. Alluvial fan, alluvial plain sandstones, sheet floods, paleosols, higher clay content	0.1	Hornung and Aigner (1999)
8. Dolomite mudstone	0.007	Saller et al. (2004)

The literature-based permeability anisotropy values listed in Table 3.3 were used to assign Kv and Kh to each layer of the model (Table 3.4). Figure 3.4 shows the depth profile of the anisotropy assigned to each layer of the model. Actual values assigned for each layer are listed in Table 3.8.

Table 3.4. Summary of the Kv/Kh Ratios Applied to Model Layers

Model Layer	Kv/Kh
Franconia Carbonate	0.007
Davis-Ironton	0.1
Ironton-Galesville	0.4
Proviso (layers 4 and 5)	0.1
Proviso (layers 1 to 3)	0.007
Lombard	0.1
Elmhurst	0.4
Mount Simon (layers 12, 13, 14, 15, 17)	0.4
Mount Simon (layer 16)	0.1
Mount Simon (layer 11, injection zone)	0.5
Mount Simon (layers 6, 7, 8, 9, 10)	0.3
Mount Simon (layers 1, 2, 3, 4, 5)	0.1

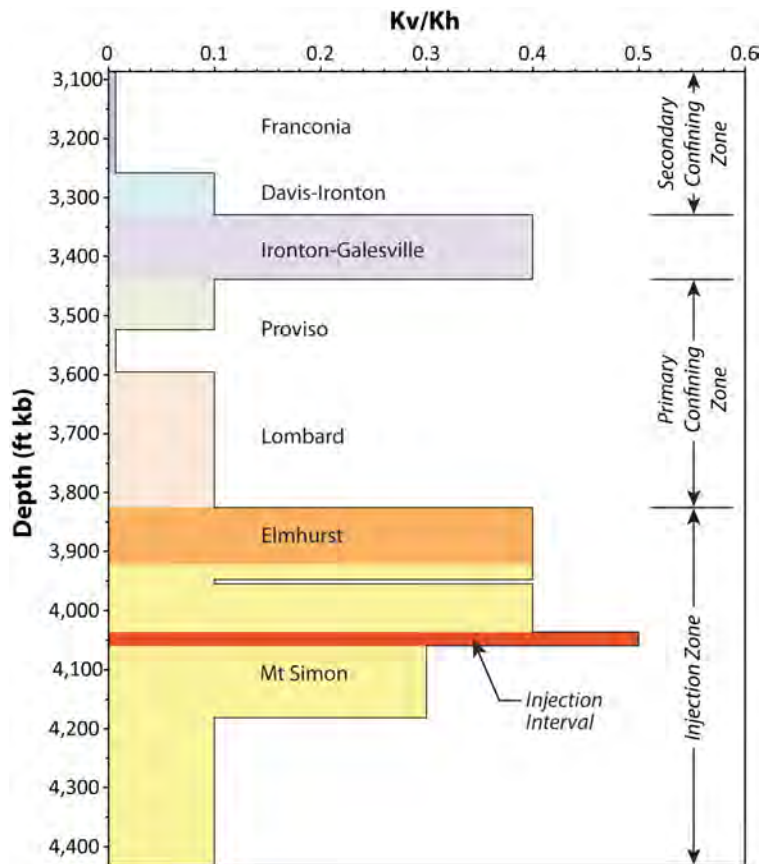


Figure 3.4. Kv/Kh Assigned to Each Model Layer Versus Depth

Porosity

Total (or absolute) porosity is the ratio of void space to the volume of whole rock. Effective porosity is the ratio of interconnected void space to the volume of the whole rock.

As a first step in assigning porosity values for the FutureGen 2.0 numerical model layers, Schlumberger ELAN porosity log results were compared with laboratory measurements of porosity as determined from SWC and core plugs for specific sampling depth within the Mount Simon (Figure 3.5). The Schlumberger ELAN porosity logs examined include PIGN (Gamma-Neutron Porosity), PHIT (Total Porosity), and PIGE (Effective Porosity). Results for PHIT are listed as a total porosity, while PIGN and PIGE results are referred to as “effective porosity” values. The PIGN and PIGE wireline log surveys use different algorithms to identify clay- or mineral-bound fluid/porosity in calculating an effective porosity value. SWC porosity measurements are listed as “total porosity,” but their measurement can be considered to be determinations of “effective porosity,” because the measurement technique (weight measurements of heated/oven-dried core samples) primarily measures the amount of “free” or connected-pore liquid contained within the SWC sample as produced by the heating process. It should be noted that the SWC porosity measurements were determined under ambient pressure conditions. An available porosity measurement data set for a conventional Mount Simon core plug sample taken near the top of the formation (depth 3,926 ft) indicates only minor changes in porosity for measurements taken over a wide range in pressure (i.e., ambient to 1,730 psi). This suggests that ambient SWC porosity measurements of the Mount Simon may be representative of in situ formation pore pressure conditions.

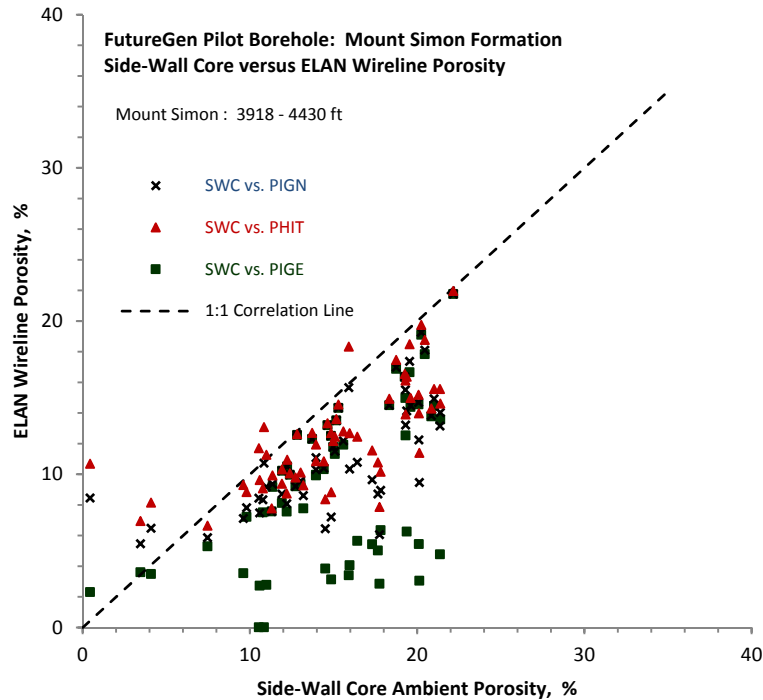


Figure 3.5. Comparison of SWC Porosity Measurements and Associated ELAN Porosity Log Values

As shown in Figure 3.5, the ELAN porosity log results generally underestimate the SWC porosity measured values (i.e., part of the Figure 3.5 plot below the 1:1 Correlation Line), and the PIGE survey measurements exhibit the lowest visual correlation. As a result of the poor visual correlation of the PIGE survey results with SWC measurements, this ELAN log was omitted from subsequent correlation evaluations. To aid in the correlations, the gamma ray survey log (GR) was used as a screening tool for development of linear-regression correlation relationships between ELAN log responses and SWC porosity measurements. This helps account for the shale or clay content that can cause the inclusion of “bound water” porosity. Figure 3.6 shows the visual correlation ellipse between the PIGN and PHIT ELAN logs with SWC porosity measurements for sample depths exhibiting gamma ray readings of <38 gamma API units. As indicated, a parallel offset relationship is exhibited between ELAN and SWC measurements for sample depths meeting this gamma cutoff criterion. This visual correlation suggests that a linear-regression relationship can be developed to calibrate the ELAN survey results to the SWC porosity measurements for sample depths exhibiting low gamma (and presumed low shale volume) criteria.

Similarly, Figure 3.7 shows the visual correlation between the PIGN and PHIT ELAN logs with SWC porosity measurements for sample depths exhibiting natural gamma ray readings within the range of 38 to 64 gamma API units. As indicated, a non-parallel, correlation ellipse relationship is exhibited between ELAN and SWC measurements for sample depths within this gamma range. This visual correlation suggests that a second linear-regression relationship can be developed to calibrate the ELAN survey results to the SWC porosity measurements for these samples. For sample depths exhibiting gamma readings >64 gamma API units, no visual correlation or definitive regression relationships can be developed to calibrate the ELAN survey readings with SWC porosity measurements (Figure 3.8).

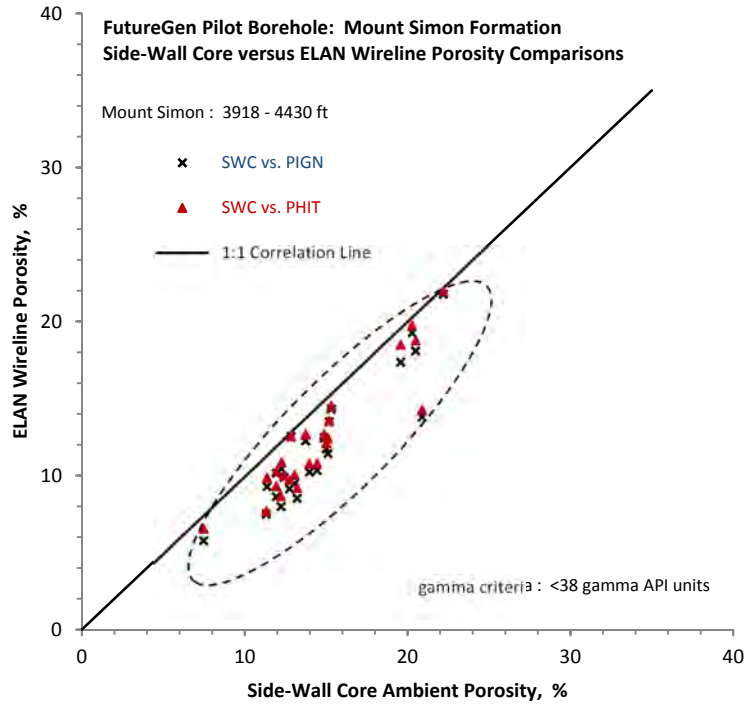


Figure 3.6. Comparison of SWC Porosity Measurements and Associated ELAN Porosity Log Values: <38 Gamma API Units

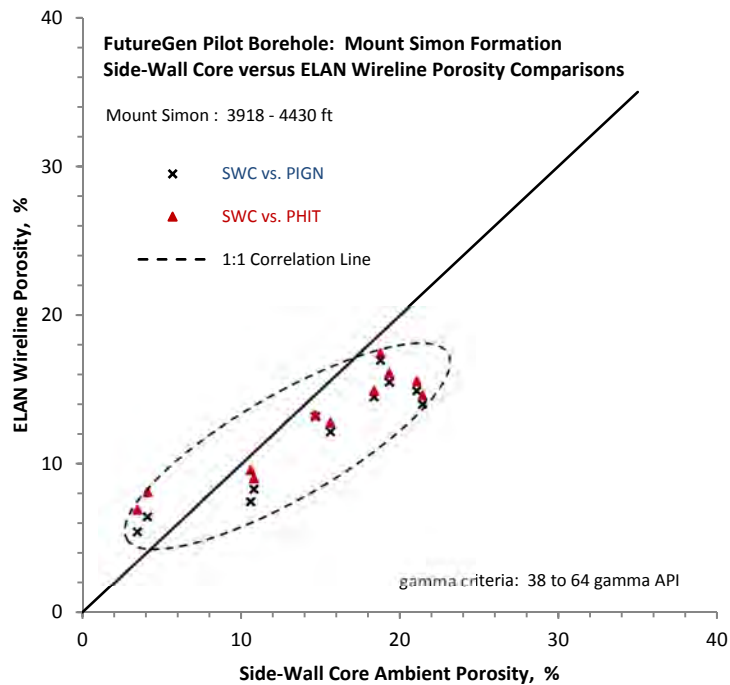


Figure 3.7. Comparison of SWC Porosity Measurements and Associated ELAN Porosity Log Values: 38 to 64 Gamma API Units

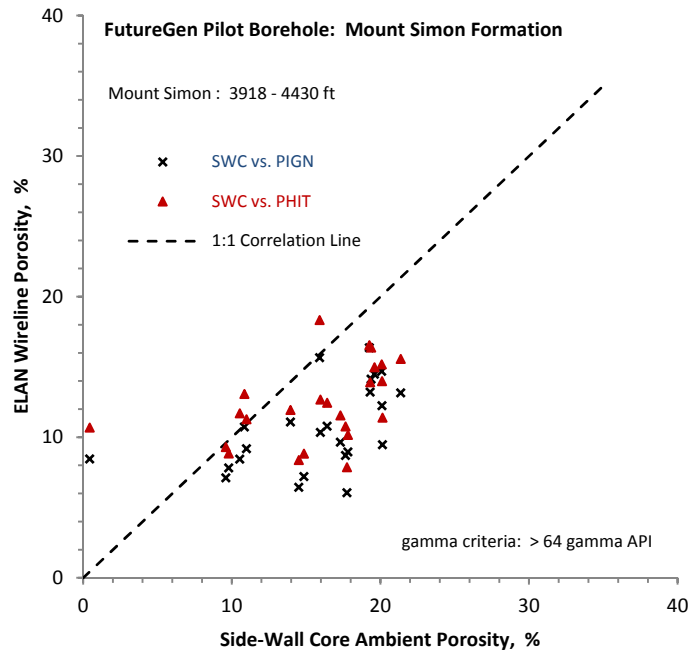


Figure 3.8. Comparison of SWC Porosity Measurements and Associated ELAN Porosity Log Values: >64 Gamma API Units

To calibrate the ELAN porosity log results to SWC measurements, the PIGN and PHIT log values were averaged and two linear regression relationships were developed for the two data sets meeting the gamma cutoffs shown in Figure 3.6 and Figure 3.7 (i.e., <38 and 38 to 64 gamma API units, respectively). These two linear-regression relationships (not shown) were then used to calibrate the ELAN results to the SWC measurements. Figure 3.9 shows the correlation of the regression-calibrated ELAN results to the SWC porosity measurements. As indicated, the calibrated ELAN porosity results fall within a correlation ellipse coincident with the 1:1 correlation line.

To assign model layer porosities, the regression model relationships used to calibrate the ELAN measurement results (Figure 3.9) were applied to the ELAN survey results over the formational depths represented by the Mount Simon (3,918 to 4,430 ft) and overlying Eau Claire-Elmhurst member (3,852 to 3,918 ft) based on the gamma response criteria. The ELAN survey results are reported at 0.5-ft depth intervals. For stratigraphic units above the Elmhurst and/or depth intervals exhibiting gamma readings >64 API units, the uncalibrated, average ELAN log result for that depth interval was used. An average porosity was then assigned to the model layer based on the average of the calibrated ELAN values within the model layer depth range.

Figure 3.10 shows the depth profile of the assigned model layer porosities based on the average of the calibrated ELAN values. The actual values assigned for each layer are listed in Table 3.8.

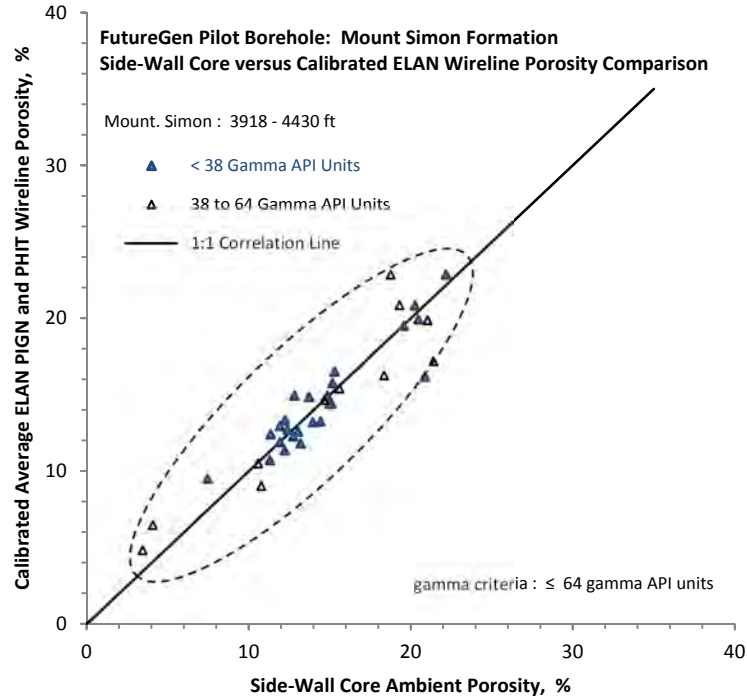


Figure 3.9. Comparison of SWC Porosity Measurements and Regression-Calibrated ELAN Log Porosities: ≤64 Gamma API Units

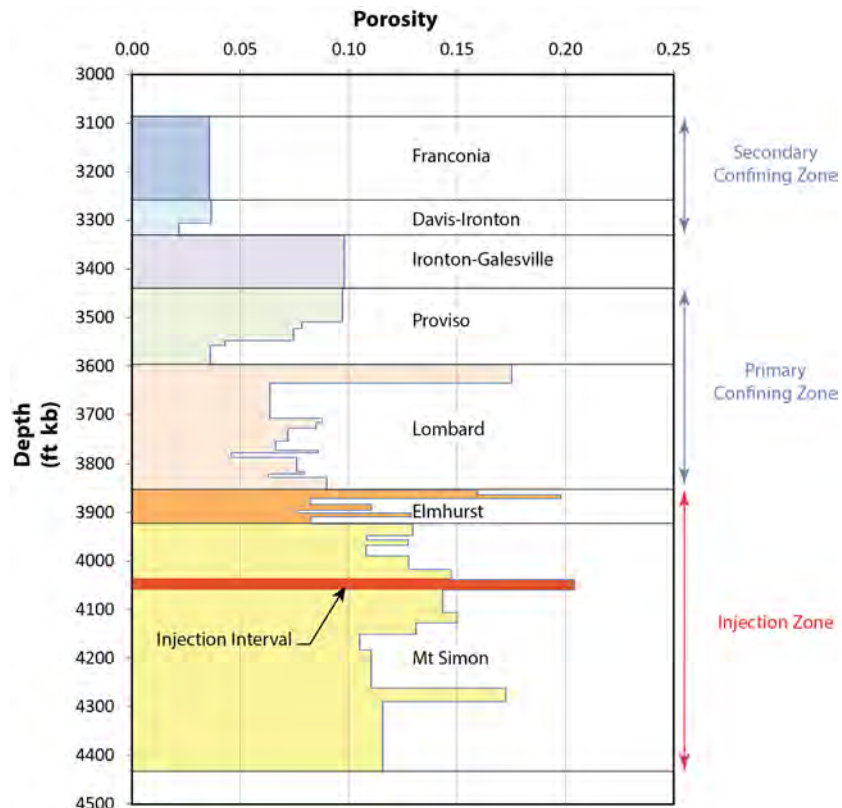


Figure 3.10. Porosity Versus Depth in Each Model Layer

Rock (Bulk) Density and Grain Density

Grain density data were calculated from laboratory measurements of SWCs. The data were then averaged (arithmetic mean) for each main stratigraphic layer in the model. Only the Proviso member (Eau Claire Formation) has been divided in two sublayers to be consistent with the lithology changes. Figure 3.11 shows the calculated grain density with depth. The actual values assigned to each layer of the model are listed in Table 3.8. Grain density is the input parameter specified in the simulation input file, and STOMP-CO₂ calculates the bulk density from the grain density and porosity for each model layer.

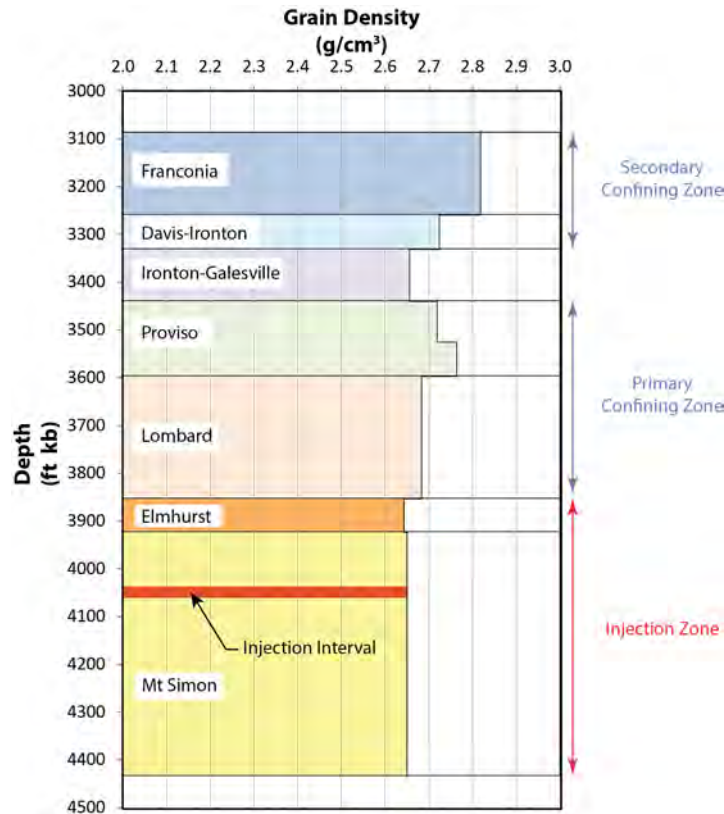


Figure 3.11. Grain Density Versus Depth in Each Model Layer

Capillary Pressure and Saturation Functions

Capillary pressure is the pressure difference across the interface of two immiscible fluids (e.g., CO₂ and water). The entry capillary pressure is the minimum pressure required for an immiscible non-wetting fluid (i.e., CO₂) to overcome capillary and interfacial forces and enter pore space containing the wetting fluid (i.e., saline formation water).

Capillary pressure data determined from site-specific cores were not available at the time the model was constructed. However, tabulated capillary pressure data were available for several Mount Simon gas storage fields in the Illinois Basin. The data for the Manlove Hazen well were the most complete. Therefore, these aqueous saturation and capillary pressure values were plotted and a user-defined curve fitting was performed to generate Brooks-Corey parameters for four different permeabilities (Figure 3.12). These parameters were then assigned to layers based on a permeability range as shown in Table 3.5

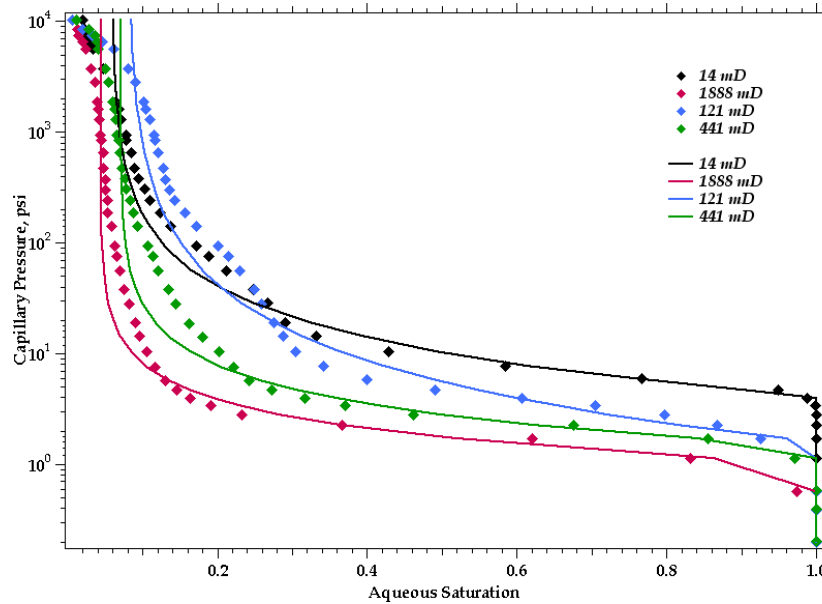


Figure 3.12. Aqueous Saturation Versus Capillary Pressure Based on Mercury Injection Data from the Hazen No. 5 Well at the Manlove Gas Field in Champagne County, Illinois

Table 3.5. Permeability Ranges Used to Assign Brooks-Corey Parameters to Model Layers

Permeability (mD)	Psi (ψ)	Lambda (λ)	Residual Aqueous Saturation
< 41.16	4.116	0.83113	0.059705
41.16 to 231	1.573	0.62146	0.081005
231 to 912.47	1.450	1.1663	0.070762
> 912.47	1.008	1.3532	0.044002

Gas Entry Pressure

No site-specific data were available for gas entry pressure; therefore, this parameter was estimated using the Davies- (1991) developed empirical relationships between air entry pressure, P_e , and intrinsic permeability, k , for different types of rock:

$$P_e = a k^b,$$

where P_e takes the units of MPa and k the units of m^2 , a and b are constants and are summarized below for shale, sandstone, and carbonate (Davies 1991; Table 3.6).

Table 3.6. Values for Constants a and b for Different Lithologies

	Shale	Sandstone	Carbonate
a	7.60E-07	2.50E-07	8.70E-07
b	-0.344	-0.369	-0.336

The dolomite found at the Morgan County site is categorized as a carbonate. The P_e for the air-water system is further converted to that for the CO₂-brine system by multiplying the interfacial tension ratio of a CO₂-brine system β_{cb} to an air-water system β_{aw} . An approximate value of 30 mN/m was used for β_{cb} and 72 mN/m for β_{aw} .

CO₂ Entrapment

The entrapment option available in STOMP-CO₂ was used to allow for entrapment of CO₂ when the aqueous phase is on an imbibition path (i.e., increasing aqueous saturation). Gas saturation can be free or trapped:

$$s_g = 1 - s_l = s_{gf} + s_{gt}$$

where the trapped gas is assumed to be in the form of aqueous occluded ganglia and immobile. The potential effective trapped gas saturation varies between zero and the effective maximum trapped gas saturation as a function of the historical minimum value of the apparent aqueous saturation.

No site-specific data were available for the maximum trapped gas saturation, so this value was taken from the literature. Suekane et al. (2009) used micro-focused x-ray CT to image a chip of Berea Sandstone to measure the distribution of trapped gas bubbles after injection of scCO₂ and then water, under reservoir conditions. Based on results presented in the literature, a value of 0.2 was used in the model, representing the low end of measured values for the maximum trapped gas saturation in core samples.

Formation Compressibility

Limited information about formation (pore) compressibility estimates is available. The best estimate for the Mount Simon Sandstone (Table 3.7) is that back-calculated by Birkholzer et al. (2008) from a pumping test at the Hudson Field natural-gas storage site, found 80 mi (129 km) northeast of the Morgan County CO₂ storage site. The back-calculated pore-compressibility estimate for the Mount Simon of 3.71E-10 Pa⁻¹ was used as a spatially constant value for their basin-scale simulations. In other simulations, Birkholzer et al. (2008) assumed a pore-compressibility value of 4.5E-10 Pa⁻¹ for aquifers and 9.0E-10 Pa⁻¹ for aquitards. Zhou et al. (2010) in a later publication used a pore-compressibility value of 7.42E-10 Pa⁻¹ for both the Eau Claire Formation and Precambrian granite, which were also used for these initial simulations (Table 3.7).

Table 3.7. Formation Compressibility Values Selected from Available Sources

Hydrogeologic Unit	Formation (Pore) Compressibility, Pa ⁻¹
Franconia	7.42E-10 Pa ⁻¹
Davis-Ironton	3.71E-10 Pa ⁻¹
Ironton-Galesville	3.71E-10 Pa ⁻¹
Eau Claire Formation (Lombard and Proviso)	7.42E-10 Pa ⁻¹
Eau Claire Formation (Elmhurst)	3.71E-10 Pa ⁻¹
Mount Simon Sandstone	3.71E-10 Pa ⁻¹

Because the site-specific data are limited to a single reservoir sample, only these two published values have been used for the model. The first value (3.71E-10 Pa⁻¹) has been used for sands that are compressible because of the presence of porosity. The second value (7.42E-10 Pa⁻¹) is assigned for all other rocks that are less compressible (dolomite, limestone, shale, and rhyolite). Table 3.8 lists the hydrologic parameters assigned to each model layer.

Table 3.8. Summary of the Hydrologic Properties Assigned to Each Model Layer

Model Layer	Top Depth (ft bkb)	Top Elevation (ft)	Bottom Elevation (ft)	Thickness (ft)	Porosity	Horizontal Permeability (mD)	Vertical Permeability (mD)	Grain Density (g/cm ³)	Compressibility (1/Pa)
Primary Conf. Zone	Franconia	3086.00	-2453	172	0.0358	5.50E-06	3.85E-08	2.82	7.42E-10
	Davis-Ironton3	3258.00	-2625	24	0.0367	6.26E-02	6.26E-03	2.73	3.71E-10
	Davis-Ironton2	3282.00	-2649	24	0.0367	6.26E-02	6.26E-03	2.73	3.71E-10
	Davis-Ironton1	3306.00	-2673	24	0.0218	1.25E+01	1.25E+00	2.73	3.71E-10
Primary Confining Zone	Ironton-Galesville4	3330.00	-2697	28	0.0981	2.63E+01	1.05E+01	2.66	3.71E-10
	Ironton-Galesville3	3358.00	-2725	27	0.0981	2.63E+01	1.05E+01	2.66	3.71E-10
	Ironton-Galesville2	3385.00	-2752	27	0.0981	2.63E+01	1.05E+01	2.66	3.71E-10
	Ironton-Galesville1	3412.00	-2779	27	0.0981	2.63E+01	1.05E+01	2.66	3.71E-10
	Proviso5	3439.00	-2806	71	0.0972	1.12E-03	1.12E-04	2.72	7.42E-10
	Proviso4	3510.00	-2877	14	0.0786	5.50E-03	5.50E-04	2.72	7.42E-10
	Proviso3	3524.00	-2891	25	0.0745	8.18E-02	5.73E-04	2.77	7.42E-10
	Proviso2	3548.50	-2916	10	0.0431	1.08E-01	7.56E-04	2.77	7.42E-10
Primary Confining Zone	Proviso1	3558.50	-2926	38	0.0361	6.46E-04	4.52E-06	2.77	7.42E-10
	Lombard14	3596.00	-2963	40	0.1754	5.26E-04	5.26E-05	2.68	7.42E-10
	Lombard13	3636.00	-3003	35	0.0638	1.53E-01	1.53E-02	2.68	7.42E-10
	Lombard12	3671.00	-3038	35	0.0638	1.53E-01	1.53E-02	2.68	7.42E-10
	Lombard11	3706.00	-3073	11	0.0878	9.91E+00	9.91E-01	2.68	7.42E-10
	Lombard10	3717.00	-3084	10	0.0851	1.66E+01	1.66E+00	2.68	7.42E-10
	Lombard9	3727.00	-3094	27	0.0721	1.00E-02	1.00E-03	2.68	7.42E-10
	Lombard8	3753.50	-3121	17	0.0663	2.13E-01	2.13E-02	2.68	7.42E-10
	Lombard7	3770.50	-3138	8	0.0859	7.05E+01	7.05E+00	2.68	7.42E-10
	Lombard6	3778.00	-3145	8	0.0459	1.31E+01	1.31E+00	2.68	7.42E-10
	Lombard5	3785.50	-3153	9	0.0760	4.24E+02	4.24E+01	2.68	7.42E-10
	Lombard4	3794.00	-3161	20	0.0604	3.56E-02	3.56E-03	2.68	7.42E-10
Lombard3	3814.00	-3181	8	0.0799	5.19E+00	5.19E-01	2.68	7.42E-10	
Lombard2	3821.50	-3189	5	0.0631	5.71E-01	5.71E-02	2.68	7.42E-10	
Lombard1	3826.50	-3194	26	0.0900	1.77E+00	1.77E-01	2.68	7.42E-10	

Table 3.8. (contd)

Model Layer	Top Depth (ft bkb)	Top Elevation (ft)	Bottom Elevation (ft)	Thickness (ft)	Porosity	Horizontal Permeability (mD)	Vertical Permeability (mD)	Grain Density (g/cm ³)	Compressibility (1/Pa)
Elmhurst7	3852.00	-3219	-3229	10	0.1595	2.04E+01	8.17E+00	2.64	3.71E-10
Elmhurst6	3862.00	-3229	-3239	10	0.1981	1.84E+02	7.38E+01	2.64	3.71E-10
Elmhurst5	3872.00	-3239	-3249	10	0.0822	1.87E+00	1.87E-01	2.64	3.71E-10
Elmhurst4	3882.00	-3249	-3263	14	0.1105	4.97E+00	1.99E+00	2.64	3.71E-10
Elmhurst3	3896.00	-3263	-3267	4	0.0768	7.52E-01	7.52E-02	2.64	3.71E-10
Elmhurst2	3900.00	-3267	-3277	10	0.1291	1.63E+01	6.53E+00	2.64	3.71E-10
Elmhurst1	3910.00	-3277	-3289	12	0.0830	2.90E-01	2.90E-02	2.64	3.71E-10
MtSimon17	3922.00	-3289	-3315	26	0.1297	7.26E+00	2.91E+00	2.65	3.71E-10
MtSimon16	3948.00	-3315	-3322	7	0.1084	3.78E-01	3.78E-02	2.65	3.71E-10
MtSimon15	3955.00	-3322	-3335	13	0.1276	5.08E+00	2.03E+00	2.65	3.71E-10
MtSimon14	3968.00	-3335	-3355	20	0.1082	1.33E+00	5.33E-01	2.65	3.71E-10
MtSimon13	3988.00	-3355	-3383	28	0.1278	5.33E+00	2.13E+00	2.65	3.71E-10
MtSimon12	4016.00	-3383	-3404	21	0.1473	1.59E+01	6.34E+00	2.65	3.71E-10
MtSimon11 (injection Interval)	4037.00	-3404	-3427	23	0.2042	3.10E+02	1.55E+02	2.65	3.71E-10
MtSimon10	4060.00	-3427	-3449	22	0.1434	1.39E+01	4.18E+00	2.65	3.71E-10
MtSimon9	4082.00	-3449	-3471	22	0.1434	1.39E+01	4.18E+00	2.65	3.71E-10
MtSimon8	4104.00	-3471	-3495	24	0.1503	2.10E+01	6.29E+00	2.65	3.71E-10
MtSimon7	4128.00	-3495	-3518	23	0.1311	6.51E+00	1.95E+00	2.65	3.71E-10
MtSimon6	4151.00	-3518	-3549	31	0.1052	2.26E+00	6.78E-01	2.65	3.71E-10
MtSimon5	4182.00	-3549	-3588	39	0.1105	4.83E-02	4.83E-03	2.65	3.71E-10
MtSimon4	4221.00	-3588	-3627	39	0.1105	4.83E-02	4.83E-03	2.65	3.71E-10
MtSimon3	4260.00	-3627	-3657	30	0.1727	1.25E+01	1.25E+00	2.65	3.71E-10
MtSimon2	4290.00	-3657	-3717	60	0.1157	2.87E+00	2.87E-01	2.65	3.71E-10
MtSimon1	4350.00	-3717	-3799	82	0.1157	2.87E+00	2.87E-01	2.65	3.71E-10

Injection Zone

3.1.3.3 Reservoir Properties

Fluid Pressure

An initial fluid sampling event from the Mount Simon Formation was conducted on December 14, 2011 in the stratigraphic well during the course of conducting open-hole logging. Sampling was attempted at 22 discrete depths using the MDT tool in the Quicksilver Probe configuration and from one location using the conventional (dual-packer) configuration. Pressure data were obtained at 7 of the 23 attempted sampling points, including one duplicated measurement at a depth of 4,048 ft bkb (Table 3.9).

Table 3.9. Pressure Data Obtained from the Mount Simon Formation Using the MDT Tool. (Red line delimits the samples within the injection zone.)

Sample Number	Sample Depth (ft bkb)	Absolute Pressure (psia)
7	4130	1828
8	4131	1827.7
9	4110.5	1818.3
11	4048	1790.2
17	4048 (duplicated)	1790.3
21	4248.5	1889.2
22	4246	1908.8
23	4263	1896.5 ^(a)

(a) Sample affected by drilling fluids (not representative)

Temperature

The best fluid temperature depth profile was performed on February 9, 2012 as part of the static borehole flow meter/fluid temperature survey that was conducted prior to the constant-rate injection flow meter surveys. Two confirmatory discrete probe depth measurements that were taken prior to the active injection phase (using colder brine) corroborate the survey results. The two discrete pressure probe temperature measurements have been plotted on the temperature/depth profile plot (Figure 3.13).

The discrete static measurement for the depth of 3,712 ft is a pressure probe temperature gauge that has been installed below the tubing packer used to facilitate running of the dynamic flow meter survey. It is in the well casing so there is very little to no vertical movement of fluid and we have static measurements at this depth for more than 12 hours before starting any testing within the borehole. The value for this depth (3,712 ft) was 95.9°F. This value plots exactly on the static, continuous fluid temperature survey results for this depth.

The second discrete static probe temperature measurement is from the MDT probe for the successful sampling interval of 4,048 ft. This sample is perhaps less “static” in that fluid was produced through the tool for a period of time as part of the sampling process; however, it does provide a consistent value with the continuous fluid temperature survey. So the bottom line is that the static fluid temperature of February 9, 2012 looks to be a valid representation of well fluid column conditions.

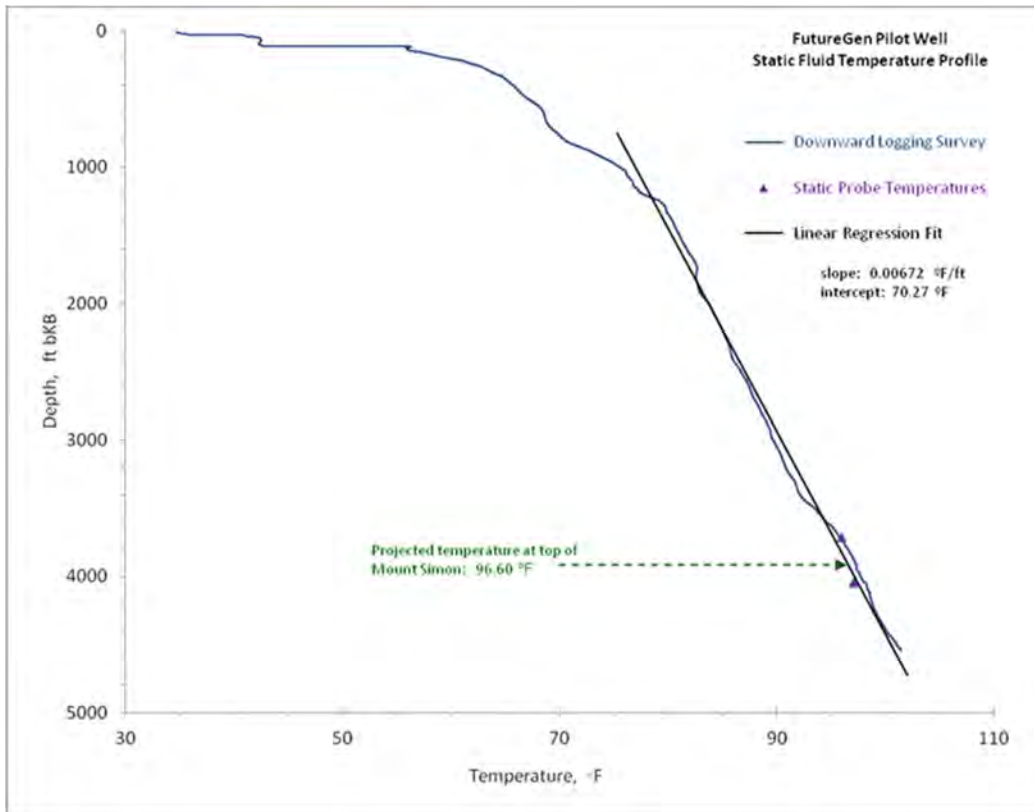


Figure 3.13. Static Fluid Temperature Profile Performed on February 9, 2012 in the Stratigraphic Well

Based on that conclusion, a linear-regression temperature/depth relationship was developed for use by modeling. The regression data set analyzed was for temperature data over the depth interval of 1,300 to 4,547 ft. Based on this regression a projected temperature for the reference datum at the top of the Mount Simon (3,918 ft bkb) of 96.60°F is indicated. A slope (gradient) of 6.72⁻³ °F/ft and intercept of 70.27°F is also calculated from the regression analysis.

Brine Density

Although this parameter is determined by the simulator using pressure, temperature, and salinity, based on the upper and lower Mount Simon reservoirs tests, the calculated in situ reservoir fluid density is 1.0315 g/cm³.

Salinity

During the process of drilling the well, fluid samples were obtained from discrete-depth intervals in the St. Peter Formation and the Mount Simon Formation using wireline-deployed sampling tools (MDTs) on December 14, 2011. After the well had been drilled, additional fluid samples were obtained from the open borehole section of the Mount Simon Formation by extensive pumping using a submersible pump.

The assigned salinity value for the Mount Simon (upper zone) 47,500 ppm is as indicated by both the MDT sample (depth 4,048 ft) and the multiple samples collected during extensive composite pumping of the open borehole section.

3.1.3.4 Chemical Properties

The EPA (2011a) identified a number of chemical properties as relevant parameters for multiphase flow modeling. These include the aqueous diffusion coefficient, aqueous solubility, and solubility in CO₂. The properties change significantly relative to temperature, pressure, salinity, and other variables, and are predicted by equations of state used by the model to calculate properties at conditions encountered in the simulation as they change with location and time (White et al. 2012)

3.1.3.5 Fracture Pressure in the Injection Zone

Hubbert and Willis (1957) established that the orientation of a hydraulic fracture is controlled by the orientation of the least principal stress and the pressure needed to propagate a hydraulic fracture is controlled by the magnitude of the least principal stress. Hydraulic fracturing (mini-frac, leak-off tests) is commonly used to determine the magnitude of the least principal stress (Haimson and Cornet 2003; Zoback et al. 2003). In situ determination of the fracture pressure using these methods provides the best estimation of the fracture pressure of both the injection and the confining zones. However no hydraulic fracturing test has been conducted in the stratigraphic well and no site-specific fracture pressure values are available for the confining zone and the reservoir. Other approaches (listed below) have thus been chosen to determine an appropriate value for the fracture pressure.

- The geomechanical uncalibrated anisotropic elastic properties log from Schlumberger performed in the stratigraphic well could give information about the minimum horizontal stress. However, several assumptions are made and a calibration with available mini-fracs or leak-off tests is usually required to get accurate values of these elastic parameters for the studied site. These data will not be considered here.
- Triaxial tests were also conducted on eight samples from the stratigraphic well (see Table 2.11 in Chapter 2.0). Samples 3 to 7 are located within the injection zone. Fracture gradients were estimated to range from 0.647 to 0.682 psi/ft, which cannot directly be compared to the fracture pressure gradient required for the permit. Triaxial tests alone cannot provide accurate measurement of fracture pressure.
- Existing regional values. Similar carbon storage projects elsewhere in Illinois (in Macon and Christian counties) provide data for fracture pressure in a comparable geological context. In Macon County (CCS#1 well at Decatur), about 65 mi east of the FutureGen 2.0 proposed site, a fracture pressure gradient of 0.715 psi/ft was obtained at the base of the Mount Simon Sandstone Formation using a step-rate injection test (EPA 2011b). In Christian County, a “conservative” pressure gradient of 0.65 psi/ft was used for the same injecting zone (EPA 2011c). No site-specific data were available.
- Last, the regulation relating to the “Determination of Maximum Injection Pressure for Class I Wells” in EPA Region 5 is based on the fracture closure pressure, which has been chosen to be 0.57 psi/ft for the Mount Simon Sandstone (EPA 1994).

Based on all of these considerations, a fracture pressure gradient of 0.65 psi/ft was chosen. The EPA GS Rule requires that “Except during stimulation, the owner or operator must ensure that injection pressure does not exceed 90 percent of the fracture pressure of the injection zone(s) so as to ensure that the injection does not initiate new fractures or propagate existing fractures in the injection zone(s)...” Therefore, a value of .585 psi/ft (90% of 0.65 psi/ft) was used in the model to calculate the maximum injection pressure.

3.1.4 Numerical Model Implementation

As described above, the model domain for the Morgan County CO₂ storage site consists of the injection zone (Mount Simon and Elmhurst), the primary confining zone (Lombard and Proviso), the Ironton-Galesville, and the secondary confining zone (Davis-Ironton and the Franconia). Preliminary simulations were conducted to determine the extent of the model domain so that lateral boundaries were distant enough from the injection location so as not to influence the model results. The three-dimensional, boundary-fitted numerical model grid was designed to have constant grid spacing with higher resolution in the area influenced by the CO₂ injection (3- by 3-mi area), with increasingly larger grid spacing moving out in all lateral directions toward the domain boundary.

Figure 3.14 shows the numerical model grid for the entire 100- by 100-mi domain and also for the 3- by 3-mi area with higher grid resolution and uniform grid spacing of 200 ft by 200 ft. The model grid contains 125 nodes in the x-direction, 125 nodes in the y-direction, and 51 nodes in the z-direction for a total number of nodes equal to 796,875. The expanded geologic model was queried at the node locations of the numerical model to determine the elevation of each surface for the stratigraphic units at the numerical model grid cell centers (nodes) and cell edges. Then each of those layers was subdivided into the model layers by scaling the thickness to preserve the total thickness of each stratigraphic unit. Once the vertical layering was defined, material properties were mapped to each node in the model. Figure 3.15 shows the distribution of horizontal and vertical permeability as it was assigned to the numerical model grid.

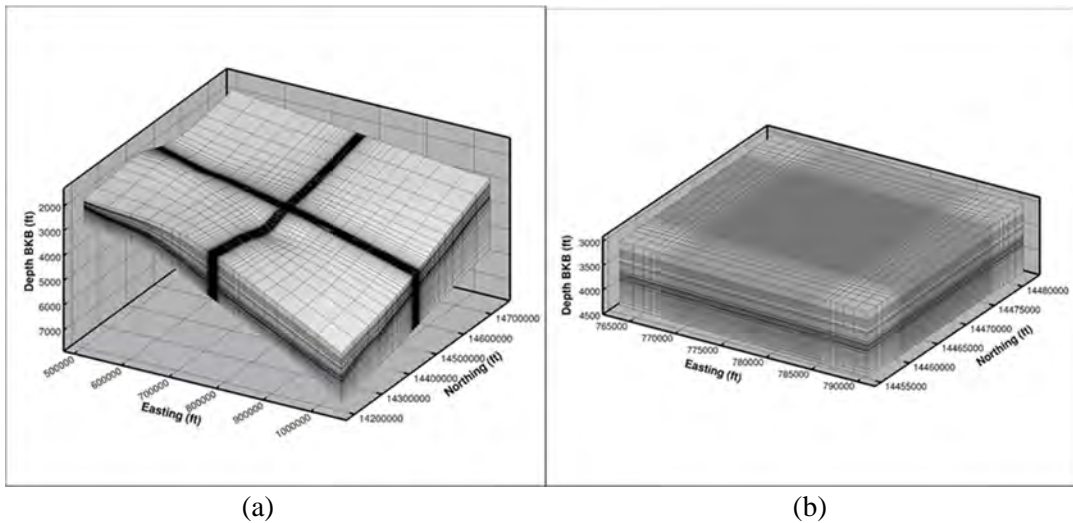


Figure 3.14. Numerical Model Grid for a) Full Domain, and b) Finer Resolution Area Containing the Injection Wells

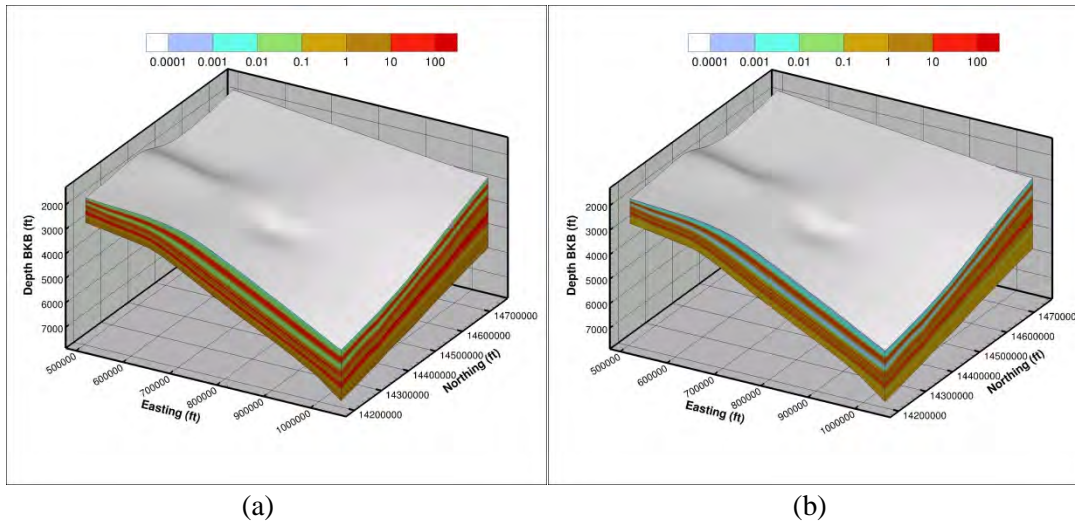


Figure 3.15. Permeability Assigned to Numerical Model a) Horizontal Permeability; b) Vertical Permeability

3.1.4.1 Initial Conditions

The reservoir is assumed to be under hydrostatic conditions with no regional or local flow conditions. Therefore the hydrologic flow system is assumed to be at steady state until the start of injection. To achieve this with the STOMP-CO₂ simulator one can either run an initial simulation (executed for a very long time period until steady-state conditions are achieved) to generate the initial distribution of pressure, temperature, and salinity conditions in the model from an initial guess, or one can specify the initial conditions at a reference depth using the hydrostatic option, allowing the simulator to calculate and assign the initial conditions to all the model nodes. Site-specific data were available for pressure, temperature, and salinity, and therefore the hydrostatic option was used to assign initial conditions. A temperature gradient was specified based on the geothermal gradient, but the initial salinity was considered to be constant for the entire domain. A summary of the initial conditions is presented in Table 3.10.

Table 3.10. Summary of Initial Conditions

Parameter	Reference Depth (bkb)	Value
Reservoir Pressure	4,048 ft	1,790.2 psi
Aqueous Saturation		1.0
Reservoir Temperature	3,918 ft	96.6 °F
Temperature Gradient		0.00672 °F/ft
Salinity		47,500 ppm

3.1.4.2 Boundary Conditions

Boundary conditions were established with the assumption that the reservoir is continuous throughout the region and that the underlying Precambrian unit is impermeable. Therefore, the bottom boundary was set as a no-flow boundary for aqueous fluids and for the CO₂-rich phase. The lateral and top boundary conditions were set to hydrostatic pressure using the initial condition with the assumption that each of these boundaries is distant enough from the injection zone to have minimal to no effect on the CO₂ plume migration and pressure distribution.

3.1.4.3 Simulation Time Period

The EPA GS Rule requires that owners or operators must “Predict, using existing site characterization, monitoring and operational data, and computational modeling, the projected lateral and vertical migration of the CO₂ plume and formation fluids in the subsurface from the commencement of injection activities until the plume movement ceases, until pressure differentials sufficient to cause the movement of injected fluids or formation fluids into a USDW are no longer present, or until the end of a fixed time period as determined by the Director.” Simulations were conducted to determine the total simulation time needed to satisfy the required conditions, and those results are presented in this section.

Figure 3.16 shows the plume area over time relative to the extent at 20 years, with the plume area being defined as the areal extent containing 99.0 percent of the separate-phase (supercritical) CO₂ mass. While the CO₂ is still redistributing long after injection ceases, it can be seen that the change in the areal extent of the plume becomes insignificant after the end of the injection period. The pressure differential on the other hand dissipates much more slowly. Therefore, based on measured pressures in the alluvial aquifer system and the injection zone, it was determined that the pressure differential needed to force fluids from the injection zone into the surficial alluvial aquifer system through a hypothetical conduit was 31.45 psi. Therefore, once the pressure differential in the injection zone falls below this value, the simulation time period conditions are satisfied. The preliminary simulations show that by year 60 the pressure differential is below 30 psi at the location of the injection well (Figure 3.17). Hence, the final representative case simulations were executed for a period of 100 years.

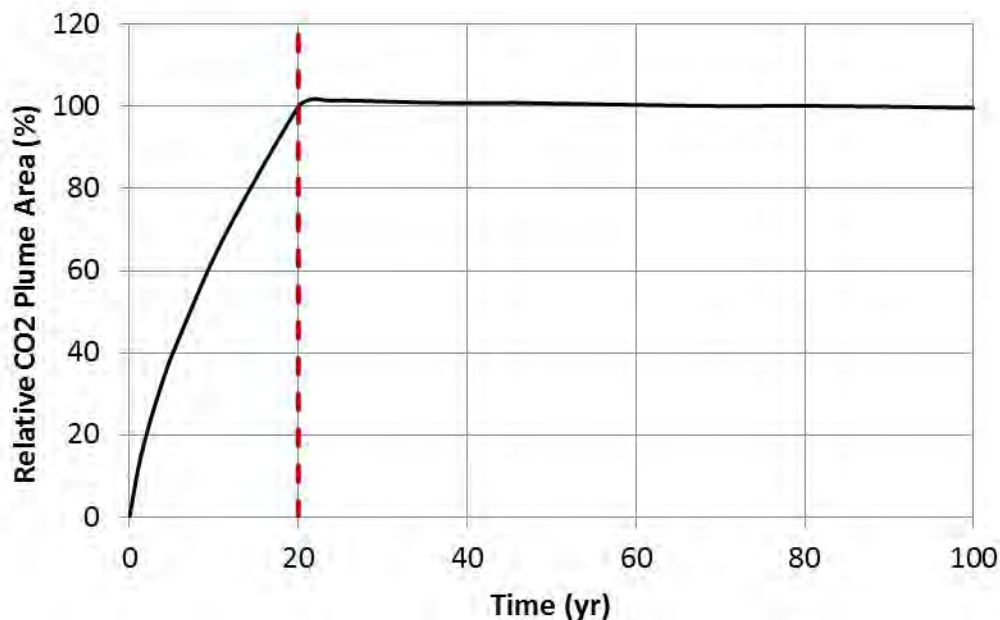


Figure 3.16. CO₂ Plume Area Versus Time Relative to Plume Extent at End of Injection Period (20 Years). Areal plume extent is defined by 99.0 percent of separate-phase scCO₂ mass.

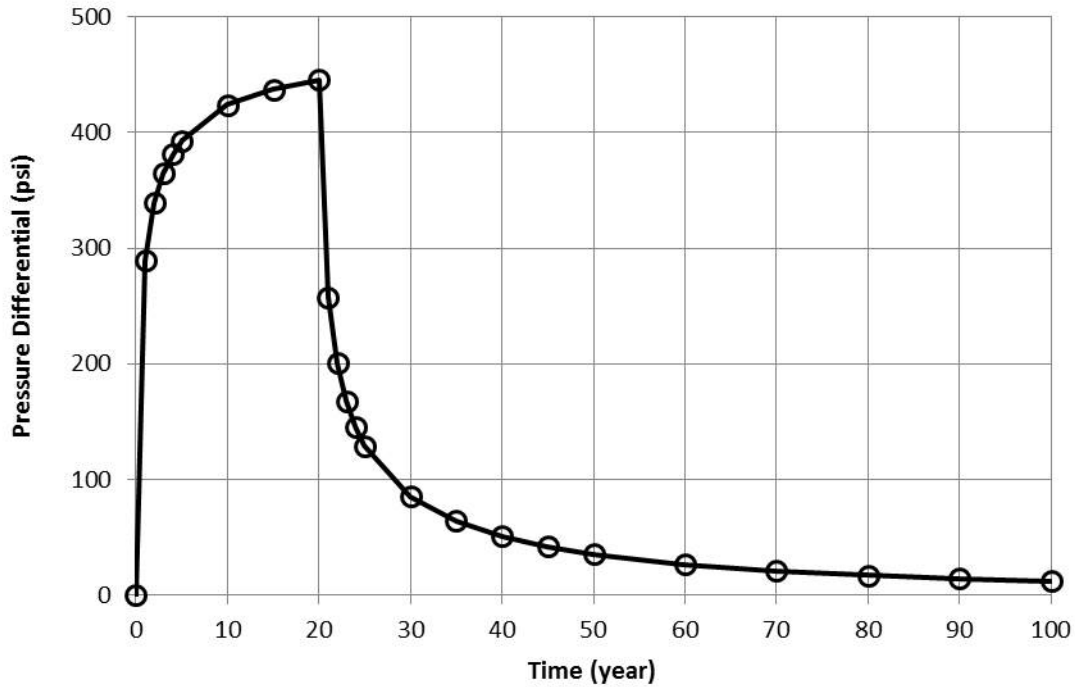


Figure 3.17. Pressure Differential (relative to initial formation pressure) Versus Time at the Injection Well

3.1.5 Representative Case Scenario Description

The representative case presented here focuses on CO₂-driven fluid–rock interactions in the injection zone and considers the proposed well design to define the operational parameters in the model. The conceptual model implemented under this scenario is described in Section 3.1.3 and the additional numerical model parameters are described in Section 3.1.4. Figure 3.18 shows the well design for the representative case for the refined area of the model domain in plan view and in 3D view. Injection into four lateral wells with a well-bore radius of 4.5 in. was modeled with the lateral leg of each well being located within the best layer of the injection zone to maximize injectivity. Only the non-cased open sections of the wells are specified in the model input file because only those sections are delivering CO₂ to the formation. The well design modeled in this case is the open borehole design, therefore part of the curved portion of each well is open and thereby represented in the model in addition to the lateral legs. The orientation and lateral length of the wells, as well as CO₂ mass injection rates, were chosen so that the resulting modeled CO₂ plume would avoid sensitive areas.

The CO₂ mass injection rate was distributed among the four injection wells as shown in Table 3.11 for a total injection rate of 1.1 MMT/yr for 20 years. The injection rate was assigned to each well according to the values in Table 3.11. A maximum injection pressure of 2,252.3 psi was assigned at the top of the open interval (depth of 3,850 ft bgs), based on 90 percent of the fracture gradient described in Section 3.1.3.5 (0.65 psi/ft).

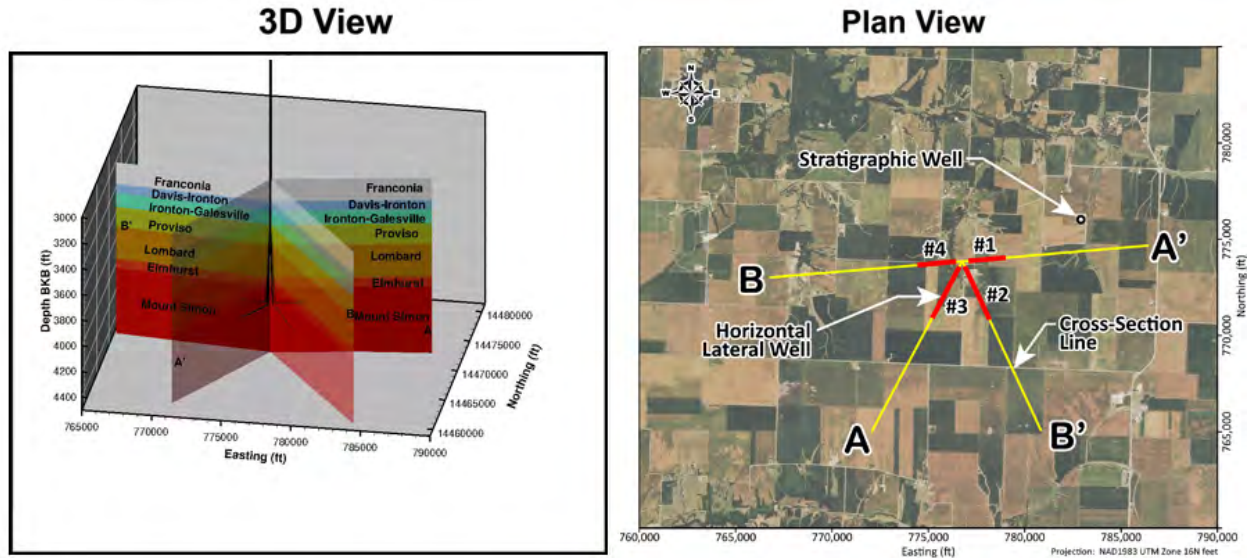


Figure 3.18. Operational Well Design for Representative Case Scenario as Implemented in the Numerical Model. The lateral legs of the injection wells are shown in red and the cross-section lines are shown in yellow.

Table 3.11. Mass Rate of CO₂ Injection for Each of the Four Lateral Injection Wells

Well	Length of Lateral leg (ft)	Mass Rate of CO ₂ Injection (MMT/yr)
Injection well #1	1,500	0.2063
Injection well #2	2,500	0.3541
Injection well #3	2,500	0.3541
Injection well #4	1,500	0.1856

3.1.6 Computational Model Results

The representative case scenario described in Section 3.1.5 was simulated for a total time of 100 years to predict the migration of CO₂ and formation fluids. Figure 3.19 shows the mass of injected CO₂ over time, demonstrating that the injection rate of 1.1 MMT/yr can be attained with the four lateral injection wells. The trapped gas (3.4 MMT) shown in Figure 3.19 exists in the CO₂-rich phase and is therefore included in the mass of CO₂ in the CO₂-rich phase (22.0 MMT) shown in the plot. Most of the CO₂ mass occurs in the CO₂-rich (or separate-) phase, with 20 percent occurring in the dissolved phase at the end of the simulation period. Note that residual trapping begins to take place once injection ceases, resulting in about 15 percent of the total CO₂ mass being immobile at the end of 100 years.

The injection pressure at each of the four wells is shown in Figure 3.20. Injection pressure is reported at the top of the open interval and once injection ceases reflects the formation pressure at the node within which the well is located.

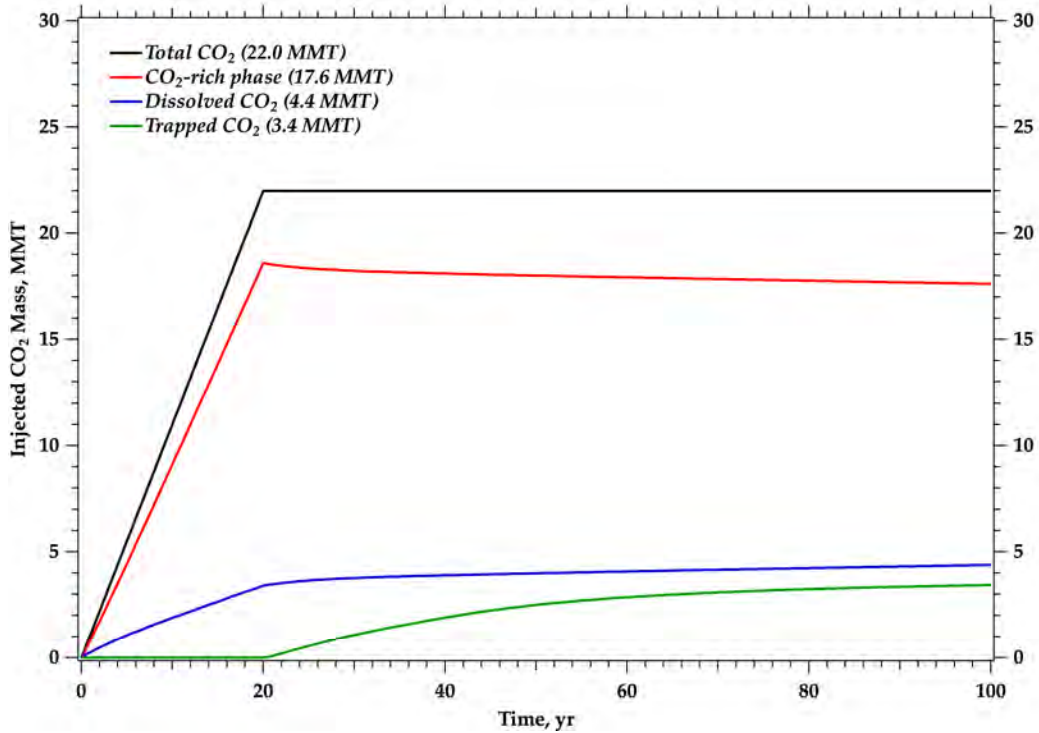


Figure 3.19. Mass of Injected CO₂ over Time Integrated over the Entire Model Domain. CO₂-rich phase mass includes both free (mobile) and trapped (immobile) CO₂ mass.

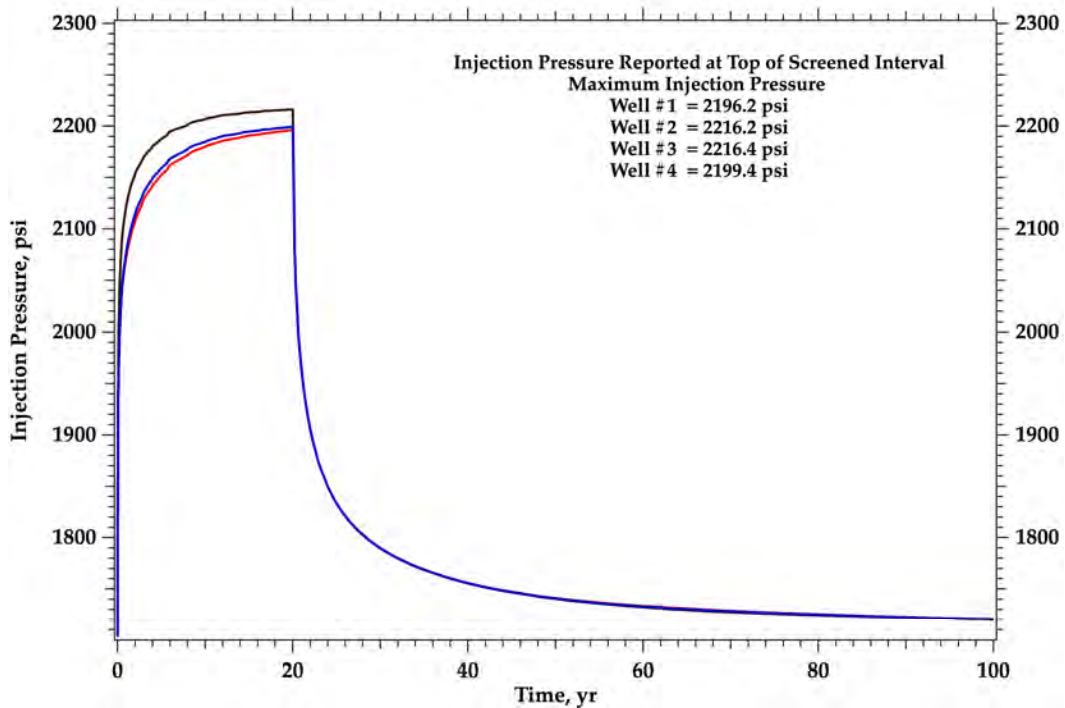


Figure 3.20. Injection Pressure Versus Time for All Four Injection Wells. Injection pressure is reported at the top of the open interval.

Reservoir conditions are such that the CO₂ remains in the supercritical state throughout the domain and for the entire simulation period. The CO₂-rich (or separate-) phase saturation is presented for selected time planes in Figure 3.21. The CO₂ plume forms a cloverleaf pattern as a result of the four lateral-injection-well design. A cross-sectional view of the CO₂ plume is presented as slices through the well centers and along the well trace (see Figure 3.18 for location of cross sections). Figure 3.22 and Figure 3.23 show the CO₂-rich (or separate) phase saturation for selected times for slices A-A' and B-B', respectively. The pressure differential across the model domain for selected times is shown in Figure 3.24. The pressure differential at 70 years is not shown because the maximum pressure differential at that time is below 30 psi. The plume grows both laterally and vertically as injection continues. Most of the CO₂ resides in the Mount Simon Sandstone. A small amount of CO₂ enters into the Elmhurst and the lower part of the primary confining zone (Lombard). When injection ceases at 20 years, the lateral growth becomes negligible but the plume continues to move slowly primarily upward. Once CO₂ reaches the low-permeability zone in the upper Mount Simon it begins to move laterally. There is no additional CO₂ entering the confining zone from the injection zone after injection ceases.

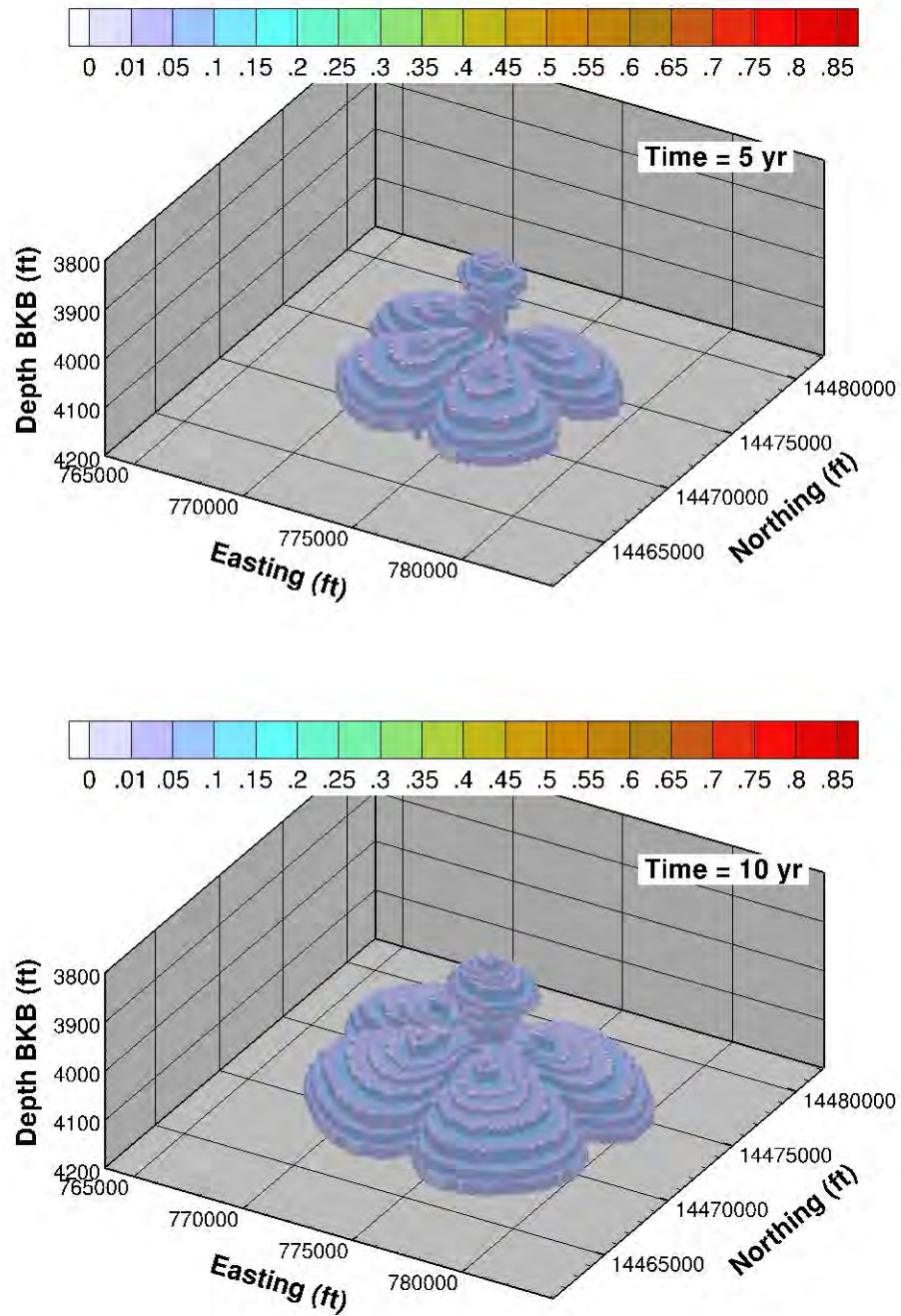


Figure 3.21. CO₂-Rich Phase Saturation for the Representative Case Scenario Simulations Shown at Selected Times (5 Years, 10 Years, 20 Years, and 70 Years)

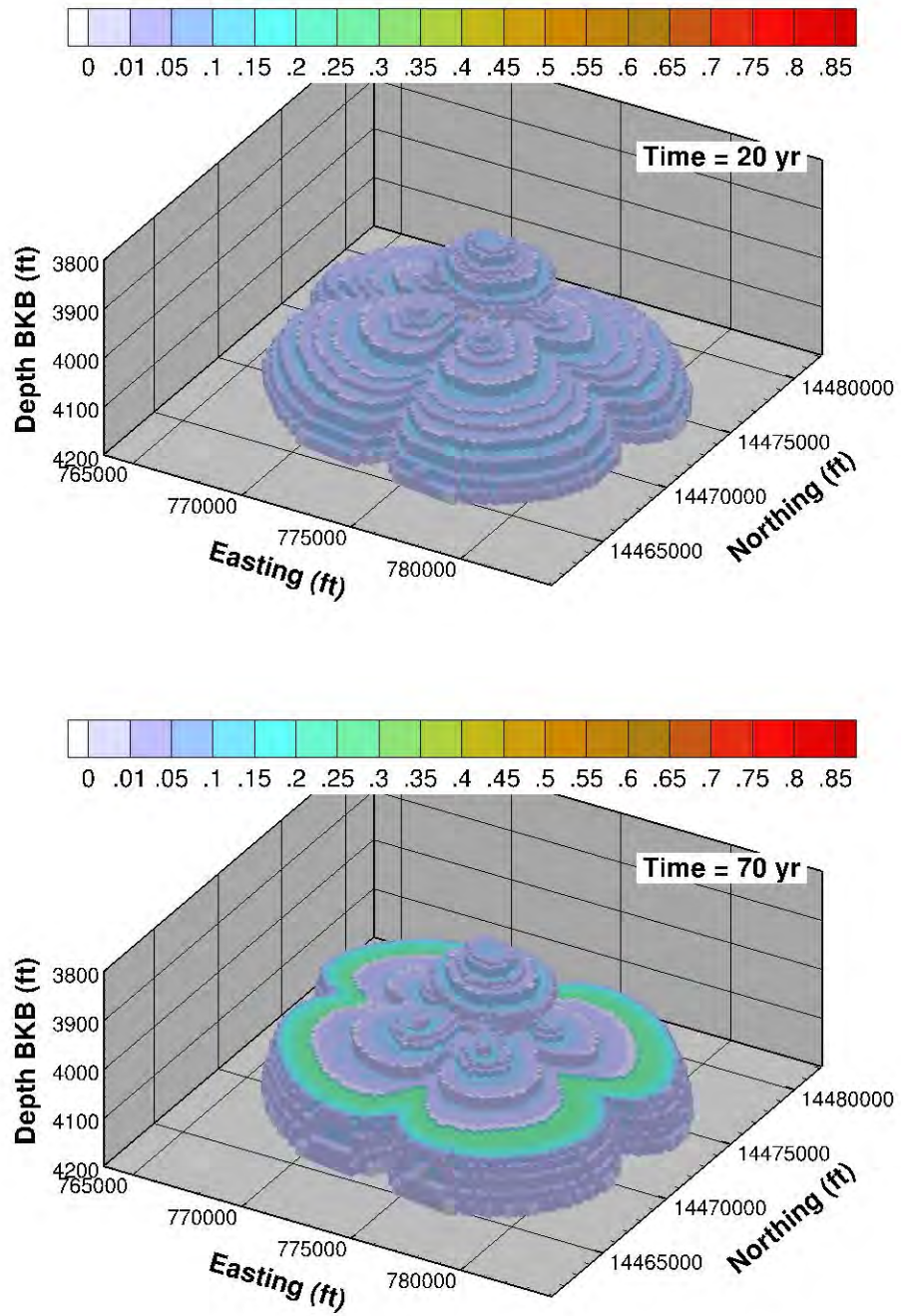


Figure 3.21. (contd)

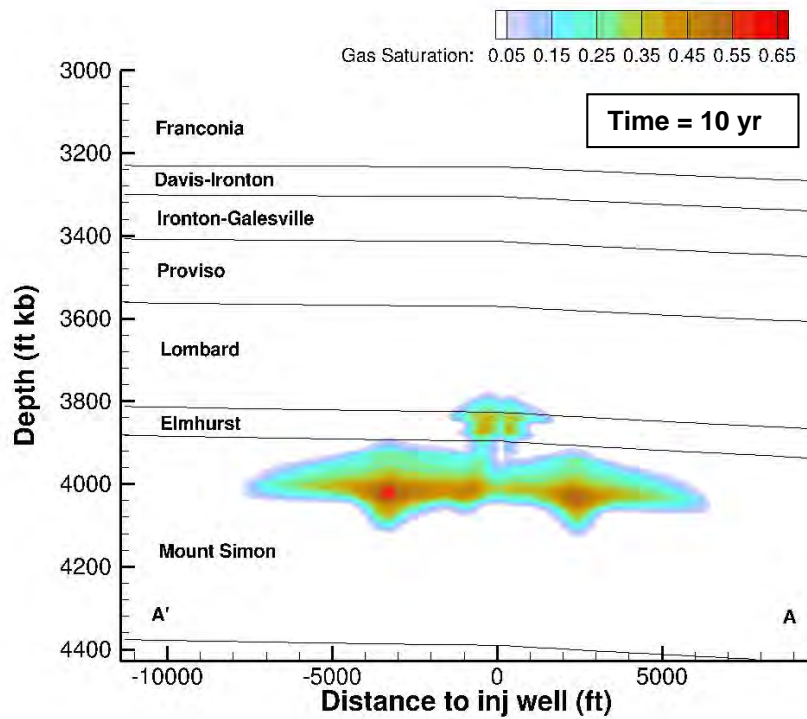
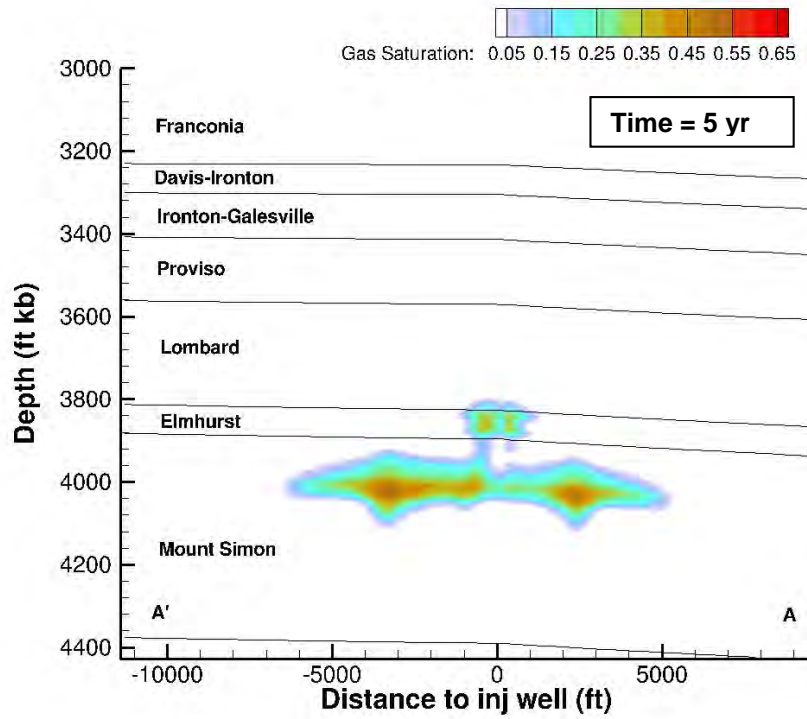


Figure 3.22. Cutaway View of CO₂-Rich Phase Saturation Along A-A' (Wells 1 and 3) for Selected Times (5 Years, 10 Years, 20 Years, and 70 Years)

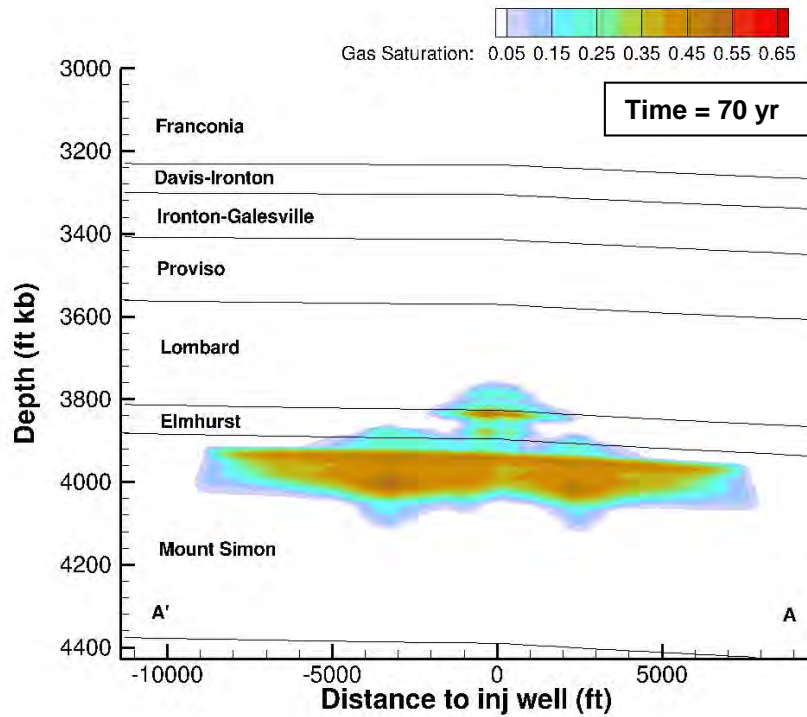
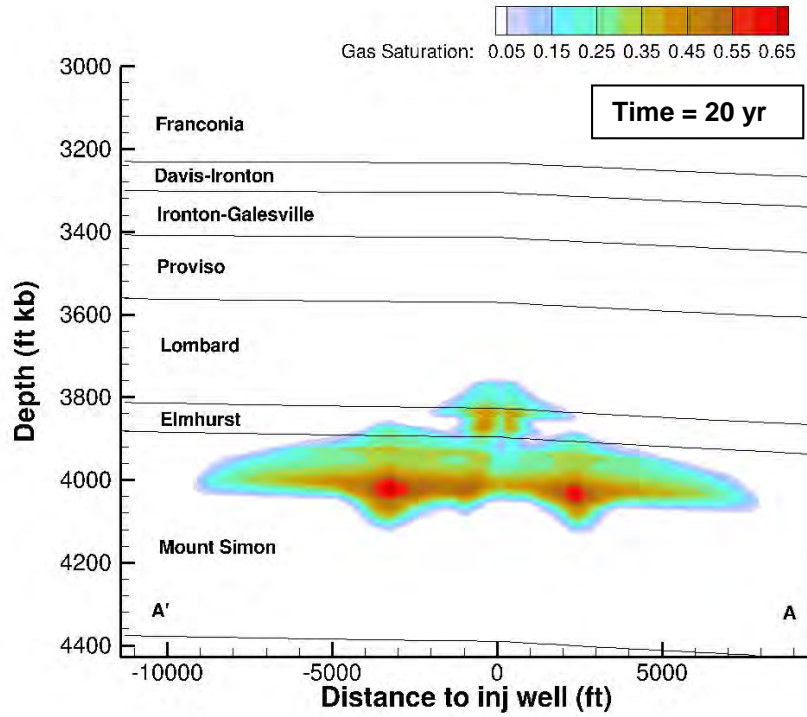


Figure 3.22. (contd)

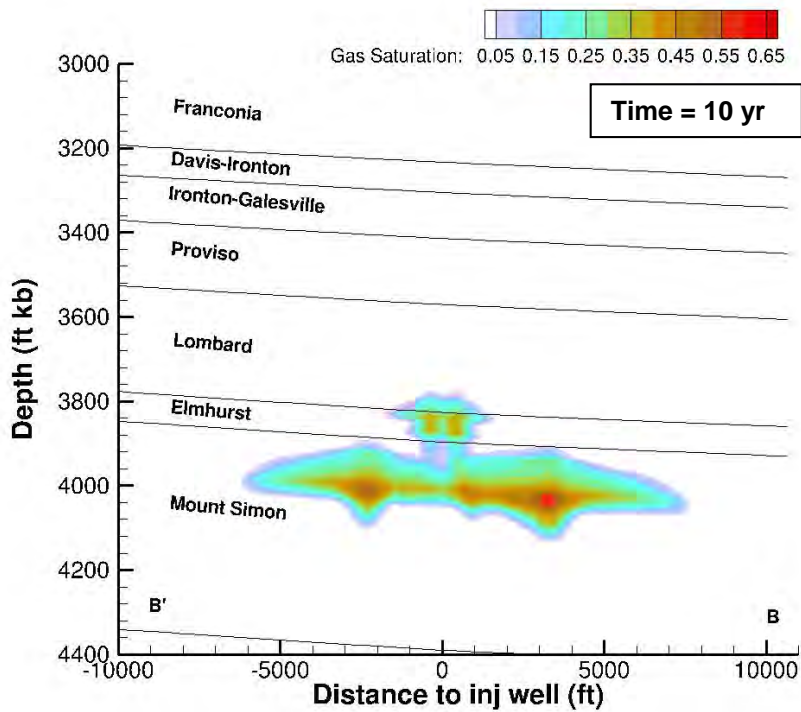
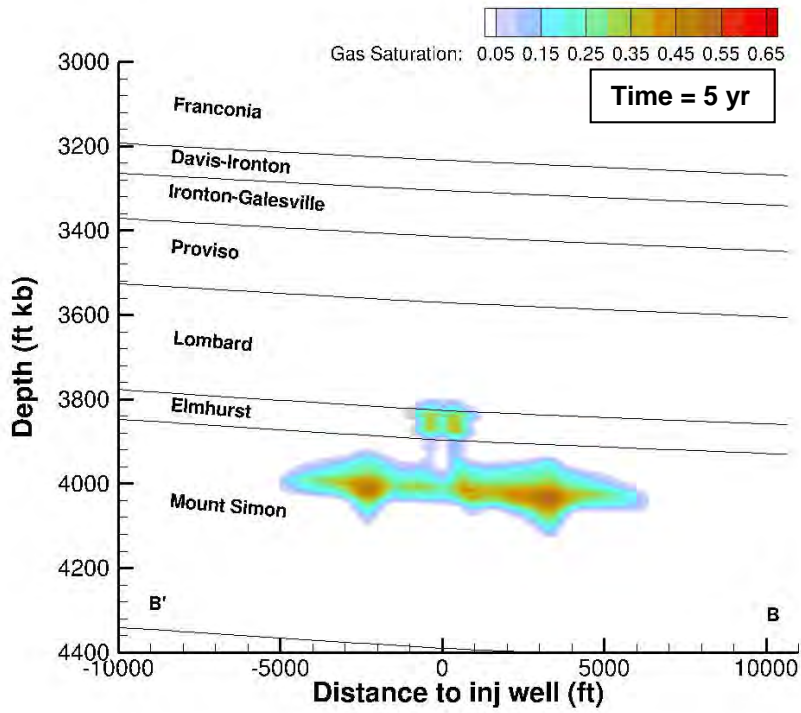


Figure 3.23. Cutaway View CO₂-Rich Phase Saturation Along B-B' (Wells 2 and 4) for Selected Times (5 Years, 10 Years, 20 Years, and 70 Years)

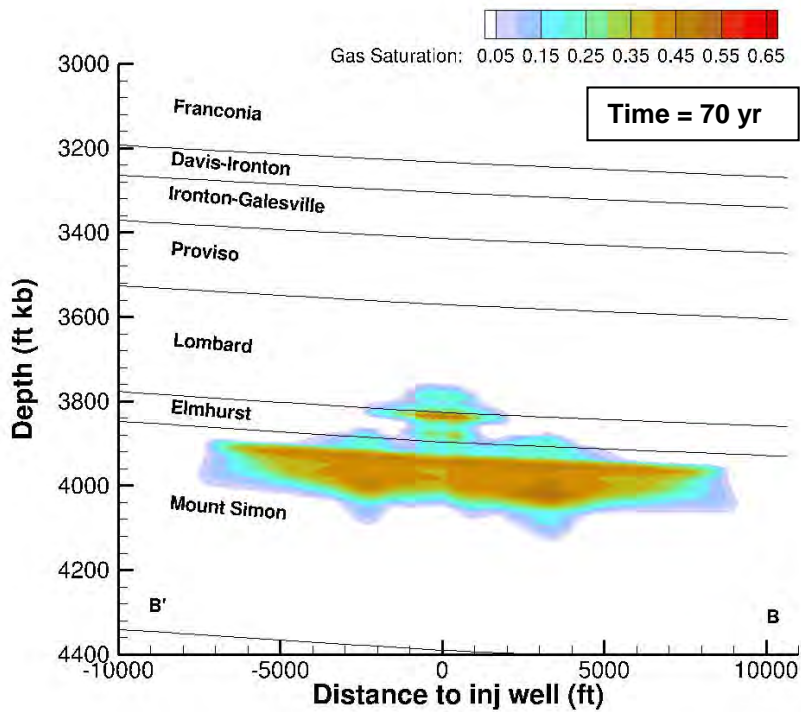
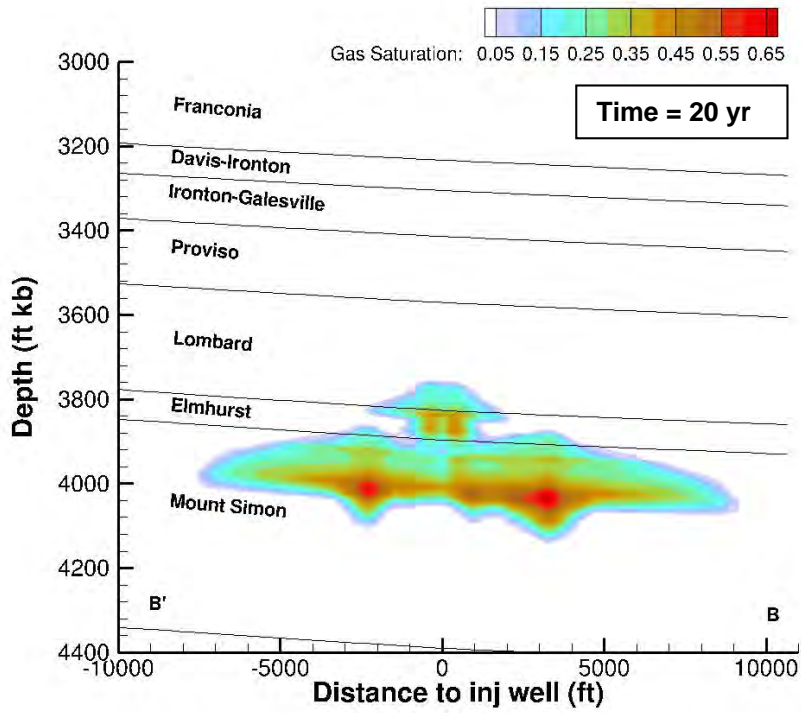


Figure 3.23. (contd)

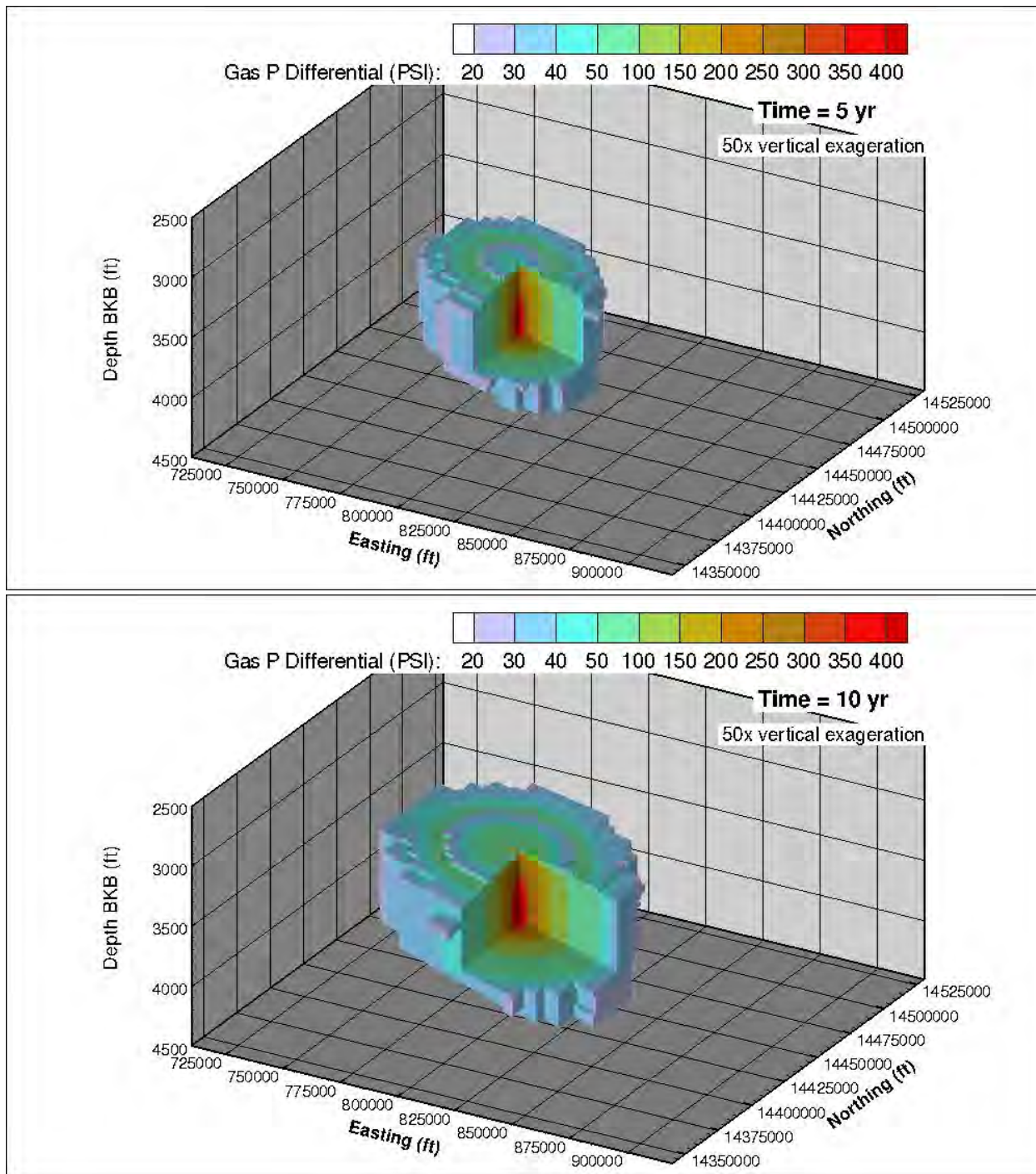


Figure 3.24. Cross-Sectional View of Pressure Differential at Selected Times (5 Years, 10 Years, 20 Years. Note that no year 70 figure is provided because the differential pressure decreases to less than 20 psi and the figure would be “blank.” It returns to near pre-injection conditions.)

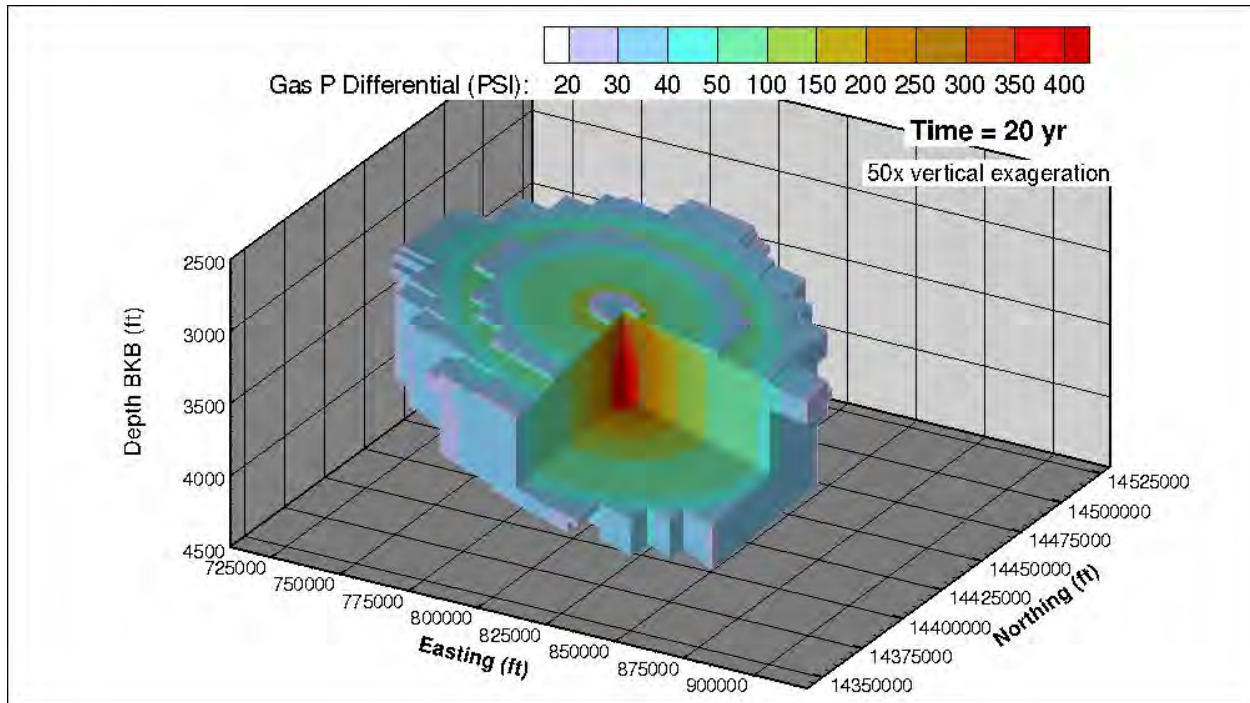


Figure 3.24. (contd)

3.1.7 Method for Delineating the AoR from Model Results

Generally, most of the CO₂ injected for storage exists in the subsurface in the supercritical phase, assuming appropriate injection zone pressure and temperature. Some of the CO₂ dissolves in the aqueous phase. Using the CO₂-rich phase saturation as a defining parameter for the CO₂ plume extent is subject to overprediction due to numerical model choices such as grid spacing. Therefore, to accurately delineate the plume size, a methodology that used the vertically integrated mass per unit area (VIMPA) of CO₂ was developed.² This ensures that the plume extent is defined based on the distribution of the mass of CO₂ in the injection zone. The VIMPA is calculated as follows:

$$VIMPA_{i,j} = \sum_k \frac{M_{i,j,k}}{A_{i,j,k}}$$

where

- M = the total CO₂ mass in a cell,
- A = the horizontal cross-sectional area of a cell,
- i and j = cell indices in the horizontal directions, and
- k = the index in the vertical direction.

² White SK, ZF Zhang, TJ Gilmore, PD Thorne, and MD White. 2011. "Quantifying the Predicted Extent of the CO₂ plume for Delineating the Area of Review." Presented by Fred Zhang at American Geophysical Union's 2011 Fall Meeting, San Francisco, CA on December 7, 2011. PNWD-SA-9683, Pacific Northwest National Laboratory, Richland, Washington.

The VIMPA may be calculated for the CO₂-rich phase or the dissolved CO₂, or the total CO₂ for the entire vertical depth or for a specific layer or layers (e.g., the injection zone). The VIMPA distributes non-uniformly in the horizontal plane. Generally, the VIMPA is larger near the injection well and decreases gradually away from the well. For certain geologic conditions, the plume size defined by the area that contains all of the CO₂ mass can be very large, while in fact, most of the mass may reside in a subregion of that area. For the purposes of AoR determination, the extent of the plume is defined as the contour line of VIMPA, within which 99.0 percent of the CO₂-rich phase (separate-phase) mass is contained. The acreage (areal extent in acres) of the plume is calculated by integrating all cells within the plume extent. Therefore, the CO₂ plume referred to in this document is defined as the area containing 99.0 percent of the separate phase CO₂ mass.

3.1.8 Delineation of the AoR

The AoR for the Morgan County site is based on the predicted areal extent encompassing 99.0 percent of the separate phase CO₂ mass after 20 years of injection and 2 years of shut-in (being temporarily sealed) (see Section 3.1). A larger, 25-mi² area that represents an expanded search area used to identify the existence of any confining zone penetrations (see Section 3.2.1) is also identified. As described in Section 3.1, the site conditions result in an infinite AoR when using the EPA-suggested methodology for calculating a pressure front based on the lowermost USDW. Planned control measures will be implemented by the Monitoring, Verification, and Accounting Program to ensure that the FutureGen 2.0 Project is protective of USDWs and in addition natural geologic features will help mitigate impacts on USDWs in the event that an unforeseen injection zone containment loss were to occur. These control measures and natural geologic features that protect the USDW include the following:

- planned early detection monitoring within the interval immediately above the primary confining zone (Ironton Sandstone)
- planned development of an environmental release model, which will encompass the overburden materials between the injection zone and ground surface and will be used to predict vertical CO₂ and/or brine migration under various containment-loss scenarios, and to assess the potential for impacts on shallow USDWs.
- the disparity in the calculated hydraulic head measurements (together with the significant formation fluid salinity differences), which suggests that groundwaters within the St. Peter and Mount Simon bedrock aquifers are naturally and physically isolated from one another, providing indication that there are no significant conduits (open well bores or fracturing) between these two formations and that the Eau Claire forms an effective confining layer
- the presence of secondary confining zones and the relatively high-permeability Potosi dolomite interval, which would both act to limit vertical migration to USDWs if primary containment were lost

After 20 years of injection and 2 years of shut-in, the areal extent of the separate-phase CO₂ plume no longer increases significantly. Therefore, the AoR, shown in Figure 3.25, is delineated based on the predicted areal extent of the separate-phase CO₂ plume at 22 years.

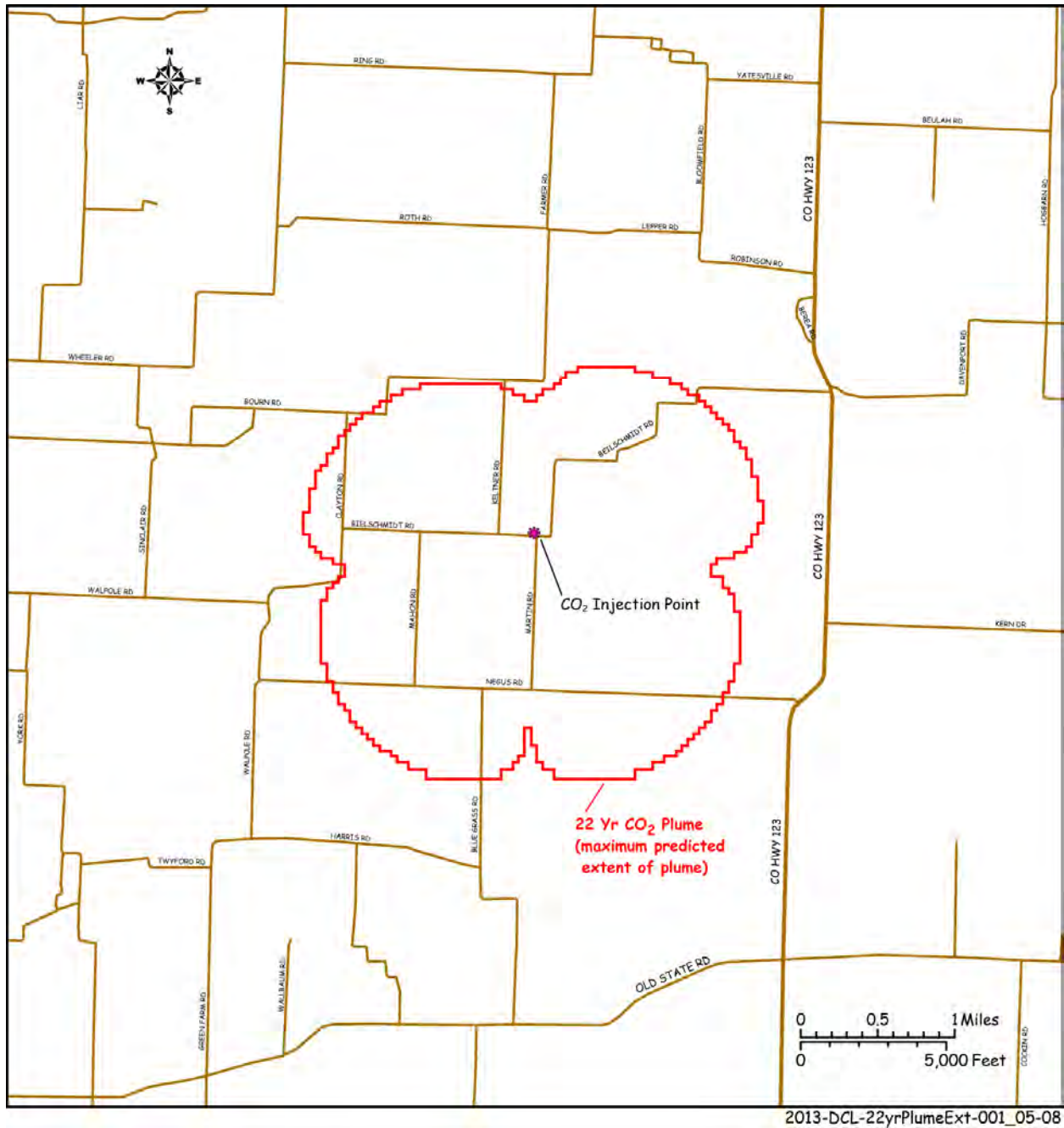


Figure 3.25. Area of Review for the Morgan County CO₂ Storage Site

3.1.9 Periodic Reevaluation of AoR

This section describes the planned frequency of reevaluation of the AoR, the conditions that would warrant reevaluation prior to the next scheduled reevaluation, and how monitoring and operational data would be used to inform a reevaluation.

3.1.9.1 Minimum Frequency

The Alliance will reevaluate the AoR, at a minimum, every 5 years after issuance of a UIC Class VI permit and initiation of injection operations, as required by 40 CFR 146.84(b)(2)(i). The reevaluation will be based on site-specific information as described in the following sections. Although the Alliance will reevaluate the AoR every 5 years, some conditions would warrant reevaluation prior to the next scheduled reevaluation. These conditions include 1) a significant change in operations such as a prolonged increase or decrease in the CO₂ injection rates at the injections wells, 2) a significant difference between simulated and observed pressure and CO₂ arrival response at site monitoring wells, or 3) newly collected characterization data that have a significant effect on the site computational model. If any of these conditions occurs, the Alliance will reevaluate the AoR as described below.

3.1.9.2 Operational and Monitoring Data and Model Calibration

As discussed in the Chapter 5.0 (Testing and Monitoring Plan), the monitoring program will adopt 1) both direct and indirect monitoring methodologies for assessing CO₂ fate and transport within the injection zone, 2) direct monitoring of the lowermost USDW, and 3) other near-surface-monitoring technologies (as needed to meet project or regulatory requirements), including soil-gas, atmospheric, and ecological monitoring.

Ongoing direct and indirect monitoring data, which provide relevant information for understanding the development and evolution of the CO₂ plume, will be used to support reevaluation of the AoR. These data include 1) the chemical and physical characteristics of the CO₂ injection stream based on sampling and analysis; 2) continuous monitoring of injection mass flow rate, pressure, temperature, and fluid volume; 3) measurements of pressure response at all site monitoring wells; and 4) CO₂ arrival and transport response at all site monitoring wells based on direct aqueous measurements and selected indirect monitoring method(s). The Alliance will compare these observational data with predicted responses from the computational model and if significant discrepancies between the observed and predicted responses exist, the monitoring data will be used to recalibrate the model (Figure 3.26). In cases where the observed monitoring data agree with model predictions, an AoR reevaluation will consist of a demonstration that monitoring data are consistent with modeled predictions.

As additional characterization data are collected, the site conceptual model will be revised and the modeling steps described above will be repeated to incorporate new knowledge about the site.

3.1.9.3 Report of the AoR Reevaluation

The Alliance will submit a report notifying the UIC Program Director of the results of this reevaluation. At that time, the Alliance will either 1) submit the monitoring data and modeling results to demonstrate that no adjustment to the AoR is required, or 2) modify its Corrective Action, Emergency and Remedial Response and other plans to account for the revised AoR. All modeling inputs and data used to support AoR reevaluations will be retained by the Alliance for 10 years.

To the extent that the reevaluated AoR is different from the one identified in this supporting documentation, the Alliance will identify all active and abandoned wells and underground mines that penetrate the confining zone (the Eau Claire Formation) in the reevaluated AoR and will perform corrective actions on those wells in the manner described in Section 3.2.2. As needed, the Alliance will revise all other plans, such as the Emergency and Remedial Response Plan, to take into account the reevaluated AoR and will submit those plans to the UIC Program Director for review and approval.

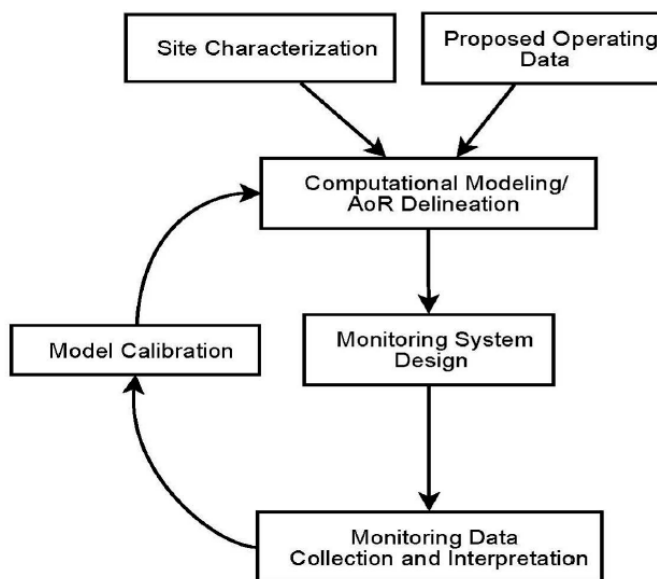


Figure 3.26. AoR Correction Action Plan Flowchart (from EPA 2011a)

To date, the Alliance has successfully negotiated access to land for access roads, a stratigraphic well, and pre-injection monitoring activities such as groundwater sampling, a gravity survey, and a weather station. The Alliance’s proven ability to work with local landowners to obtain access to surface and subsurface areas for activities related to the FutureGen 2.0 Project should be sufficient to demonstrate the Alliance’s ability to obtain access for corrective actions if they are necessary (although, as noted above, extremely unlikely) in the future. Moreover, it can be anticipated that, if corrective actions were required, affected property owners would be cooperative.

3.1.10 Parameter Sensitivity and Uncertainty

Modeling underground CO₂ storage involves many conceptual and quantitative uncertainties, including CO₂ leakage and brine displacement and infiltration into drinking water aquifers far from the storage site. The major problem for determining injection zone suitability is the uncertainty in parameters such as permeability and porosity, and the geologic description of the injection zone and confining zone. To address these uncertainties, Monte Carlo simulation was conducted. Because the model results serve as a basis for calculating the AoR, the sensitivity analysis focuses on a parsimonious set of parameters that strongly influence the AoR calculation.

The effects of scaling factors associated with porosity, permeability, and fracture gradient were evaluated. The three scaling factors are independent variables, while the rock type and other mechanical/hydrological properties for the geological layers are dependent variables, which vary according to scaling.

The sensitivity of selected output variables, including the percent of CO₂ mass injected, the acreage of the plume, the acreage of the projected plume, and the percent variation of plume area relative to the representative case, was analyzed. The projected acreage of the plume is calculated for cases where less than 100 percent of the CO₂ mass was injected, providing a normalization of the plume area for direct comparison across cases. Both marginal (individual) and joint (combined) effects were evaluated.

Whether a response curve (two-dimensional [2D]) or response surface (three-dimensional [3D] or higher dimension) is representative or reliable depends on the efficiency of the sampling approach. A good sampling approach should be able to explore the parameter space without clumping or gapping. As can be seen in Figure 3.27, our quasi Monte Carlo (QMC) approach (right), with controlled locations of the samples, has better scatters than regular Monte Carlo (left) and Latin-hypercube samples (right).

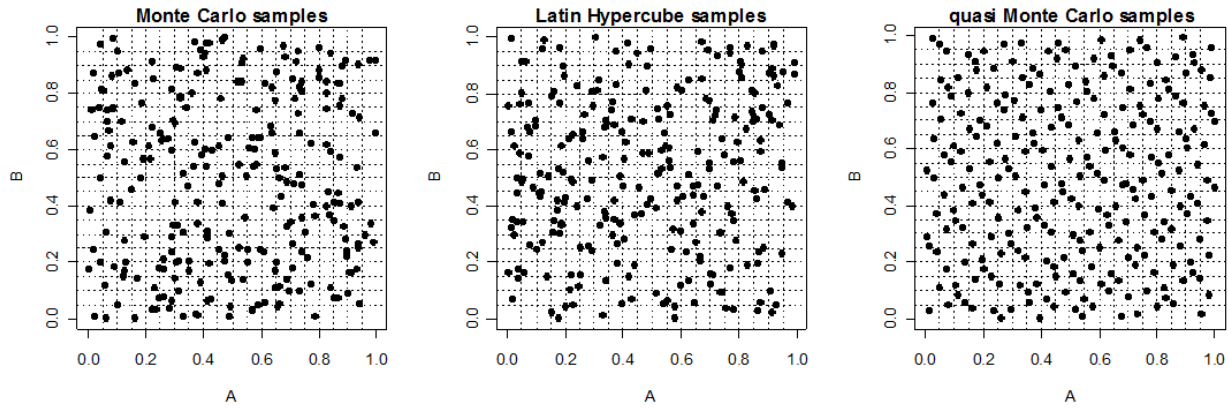


Figure 3.27. Scatter Plots of Monte Carlo, Latin-Hypercube, and QMC Samples. QMC samples are well dispersed in the parameter space and therefore are exploratory and efficient without clumping points and gapping.

The scaling factors used for generating these samples were based on an evaluation of the site characterization data to determine reasonable bounding values. These scaling factors are shown in Table 3.12.

Table 3.12. Scaling Factors Evaluated for Parameter Sensitivity Analysis

Parameter	Minimum	Representative Case	Maximum
Porosity	.75	1.0	1.25
Permeability	.75	1.0	1.25
Fracture Gradient	.88	1.0	1.10

Thirty-two cases were defined from the representative case model using the QMC sampling technique to represent a statistical distribution of possible cases based on the parameters varied. All other inputs were the same as in the representative case.

Simulation results indicate that increasing the porosity produced a smaller predicted plume area. Varying the permeability also resulted in a smaller plume area, but with a slightly weaker effect, primarily because in this case only a narrow range of permeability values across layers was considered. As expected, increasing the fracture gradient (and therefore, the maximum injection pressure) resulted in an increase in the plume area.

A generalized linear model analysis was performed for the simulated CO₂ plume area and the final model was obtained through AIC (Akaike information criterion) -based step-wise backward removal approach and the statistical t-values and P-values were obtained (Akaike 1974; Hou et al. 2012; Venables and Ripley 2002). When a P-value is larger than the significance level (e.g., 0.05), one can say the corresponding variable (input parameter) is relatively insignificant. Considering only the marginal linear

effects, the fracture gradient and porosity are the most significant parameters for determining plume size. However, when the interactions are included, the combination of permeability and fracture gradient becomes significant.

The injectivity varied from the representative base case by about 50 percent for cases either with low permeability, low fracture gradient, or a combination of both. Because the injection rate was specified as a maximum rate, it was not possible to determine if, in some cases, more than 100 percent of the mass could be injected and if so, how much more. The predicted plume area varied from the representative case by about 80 to 120 percent, which is approximately the same as the variation in permeability and porosity.

3.2 Corrective Action Plan

With the AoR identified using computational modeling, EPA Class VI regulations require the identification of all confining zone penetrations within the AoR that may become a preferential pathway for leakage of CO₂ and/or formation brine fluids out of the injection zone, and if necessary, performance of corrective actions to prevent leakage that could potentially cause endangerment to a USDW. The following sections discuss the findings of an evaluation that was performed to 1) identify existing penetrations within a 25-mi² region that extends beyond the AoR (see Figure 3.28); 2) determine if any penetrations extend below the primary confining zone, thereby presenting a risk of leakage that may require corrective actions; and 3) identify corrective actions and define the approach that will be taken to prevent leakage that could endanger a USDW.

3.2.1 Identification of Primary Confining Zone Penetrations

The potential for the presence of natural primary confining zone penetrations (i.e., faults and fracture zones) was evaluated by reviewing existing maps and publications to identify any available information about local geologic structures, faults, and seismicity. Additional site-specific information was obtained from 2D seismic lines acquired within the project AoR and from preliminary borehole geophysical log data acquired from the FutureGen 2.0 stratigraphic well. Artificial penetrations (i.e., wells) were initially identified using data available online from the ISGS interactive map tools (ISGS 2012a, 2011), followed by a detailed review of historical well log records obtained from the ISGS Geologic Records Unit (ISGS 2012b).

Based on the information evaluated during this review and with the exception of the stratigraphic well, no natural or artificial penetrations have been identified within the AoR that penetrate the primary confining zone or the injection zone. The closest wells identified that penetrate the primary confining zone are approximately 16 mi south-southwest of the proposed Morgan County storage site (Figure 3.28). Although these wells are well outside the AoR, they are within the region where increased pressures in the injection zone are expected and were therefore considered for additional review. The well records obtained during this review suggest that all primary confining zone penetrations found have been properly constructed, plugged, and/or are currently in use, and do not present a risk for direct leakage and migration of fluids out of the injection zone, and will therefore not be considered for corrective action.

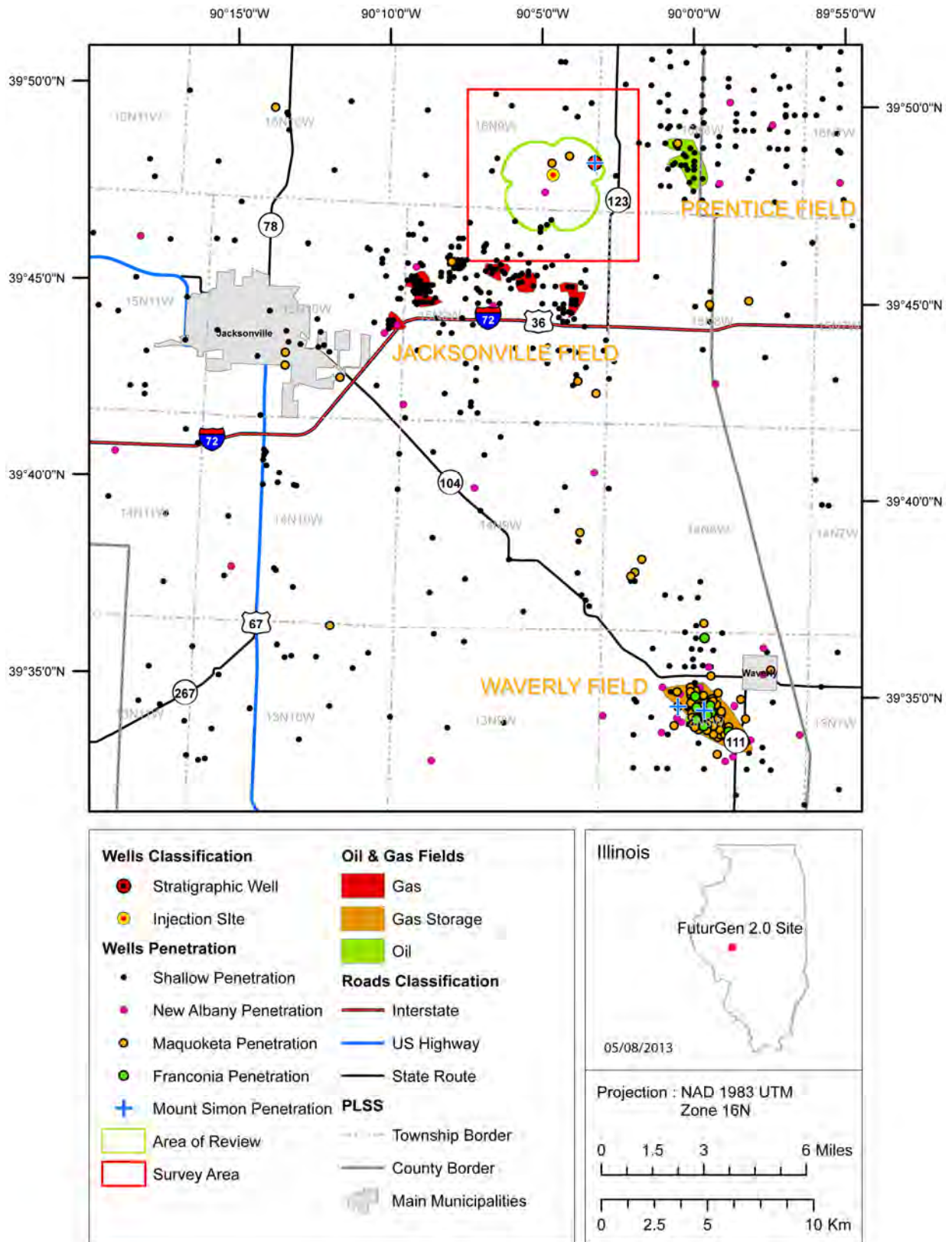


Figure 3.28. Location of the Well Penetrations in the Area Surrounding the Storage Site. The survey area encompasses the AoR.

A more detailed discussion of the geologic features of the confining zones and local geologic structures, faulting, seismicity, and available geomechanical information is presented in Chapter 2.0.

With the exception of the stratigraphic well, the nearest wells that have penetrated through the primary confining zone (Eau Claire Formation) and into the injection zone (Mount Simon Sandstone) are more than 16 mi away in the Waverly Storage Field (Figure 3.28), south-southwest of the proposed storage site, and are not in the AoR. The two boreholes, the Criswell #1-16 (API number 121370034900) and Whitlock #7-15 (API number 121370034601), are part of the Waverly Storage Field, which is an active natural-gas storage facility that is currently operated by Panhandle Eastern Pipeline Company. The primary storage reservoir used at the Waverly Storage Field is the St. Peter Sandstone. However, several wells were drilled into the underlying Ironton-Galesville Sandstone and two test wells were drilled into the Mount Simon Sandstone. The Ironton-Galesville Sandstone was selected as a second storage reservoir and received natural-gas exchange beginning in 1968 (Buschbach and Bond 1974).

Well construction details obtained from available records for the Criswell #1-16 and Whitlock #7-15 wells are presented in Figure 3.29 and Figure 3.30, respectively. The Criswell #1-16 well was drilled approximately 133 ft into the Mount Simon Sandstone to a total depth of 4,253 ft. A cement plug was placed in the bottom of the well and the casing was perforated within the Ironton/Galesville Sandstone, presumably for natural-gas storage. In 1978, the well was reconfigured as an observation well by isolating the original perforations with a bridge plug, and recompleting the well with additional perforations above the primary storage reservoir (St. Peter Sandstone) within the Joachim “B” horizon.

Records available for the Whitlock #7-15 well indicate that it was drilled to a total depth of 4,250 ft in 1965 and completed as a saltwater disposal well in 1966. However, the depth interval or reservoir used for saltwater disposal was not determined from available records. In 1997, the well was reconfigured as an observation well and completed below the primary (St. Peter Sandstone) storage reservoir with perforations across the Oneota Dolomite and Potosi Dolomite.

Both wells are believed to have been sufficiently plugged and recompleted, and are not considered to represent a risk of providing a preferential pathway for leakage of formation brine to surface or near-surface environments. Subsequently, no direct monitoring and/or corrective action will be performed.

3.2.2 Corrective Actions

Based on information obtained for the FutureGen 2.0 UIC permit application, no wells have been identified within the AoR that require corrective action. If corrective actions are warranted after reevaluation of the AoR (see Section 3.1.9, the UIC Program Director will be officially notified and the Alliance will take the following actions:

- Identify all wells within the AoR that may require corrective action (e.g., plugging).
- Perform an investigation to establish the condition of the well(s).
- Identify the appropriate level of corrective action for the well(s).
- Prioritize corrective actions to be performed.
- Conduct corrective actions in an expedient manner to minimize risk of CO₂ leakage to a USDW.

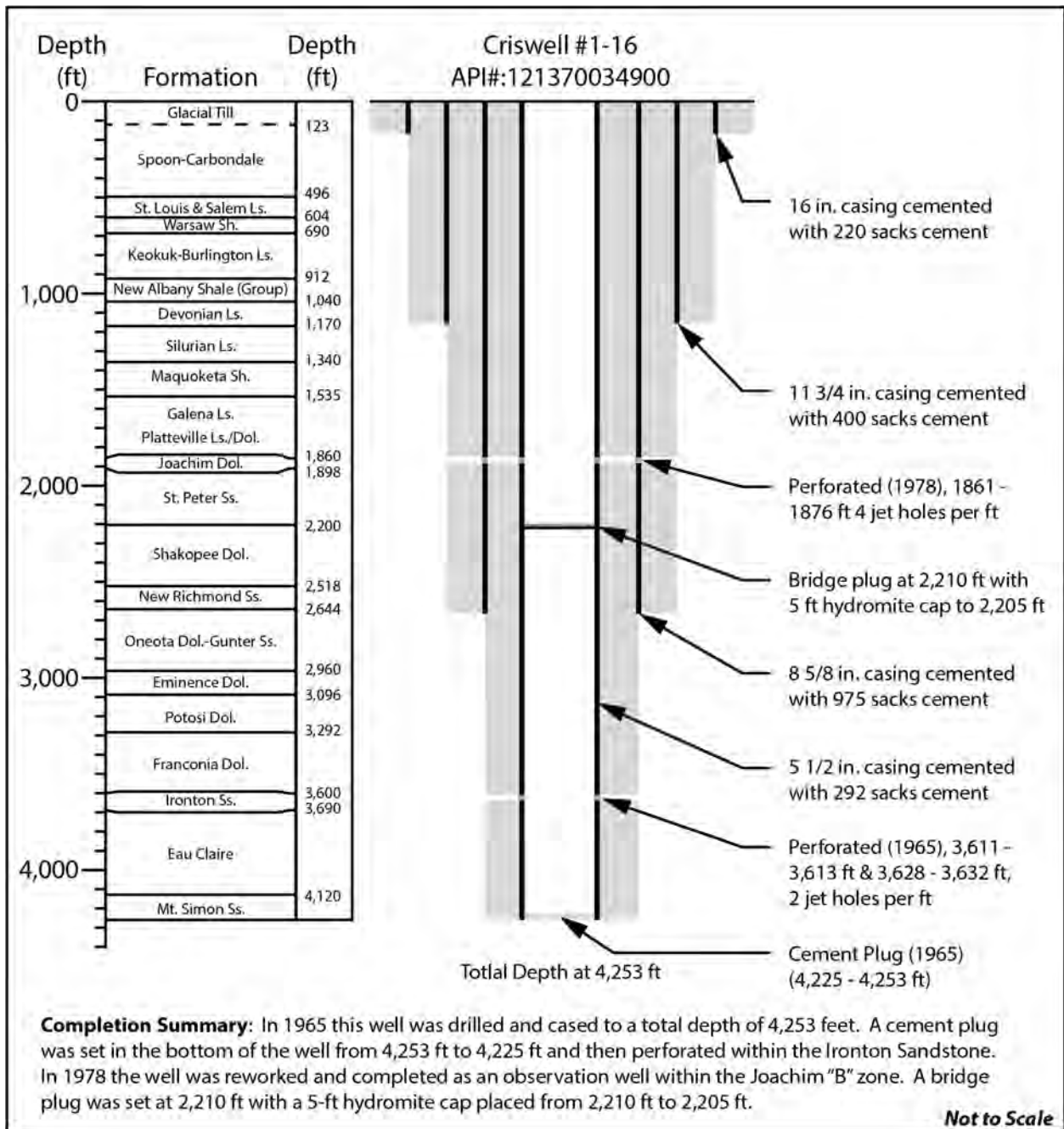


Figure 3.29. Well Construction Diagram for a Deep Borehole (API# 121370034900) in Morgan County that Penetrates the Target Reservoir for CO₂ Sequestration (i.e., Mount Simon Sandstone). Well completion information obtained from ISGS well records (ISGS 2012b).

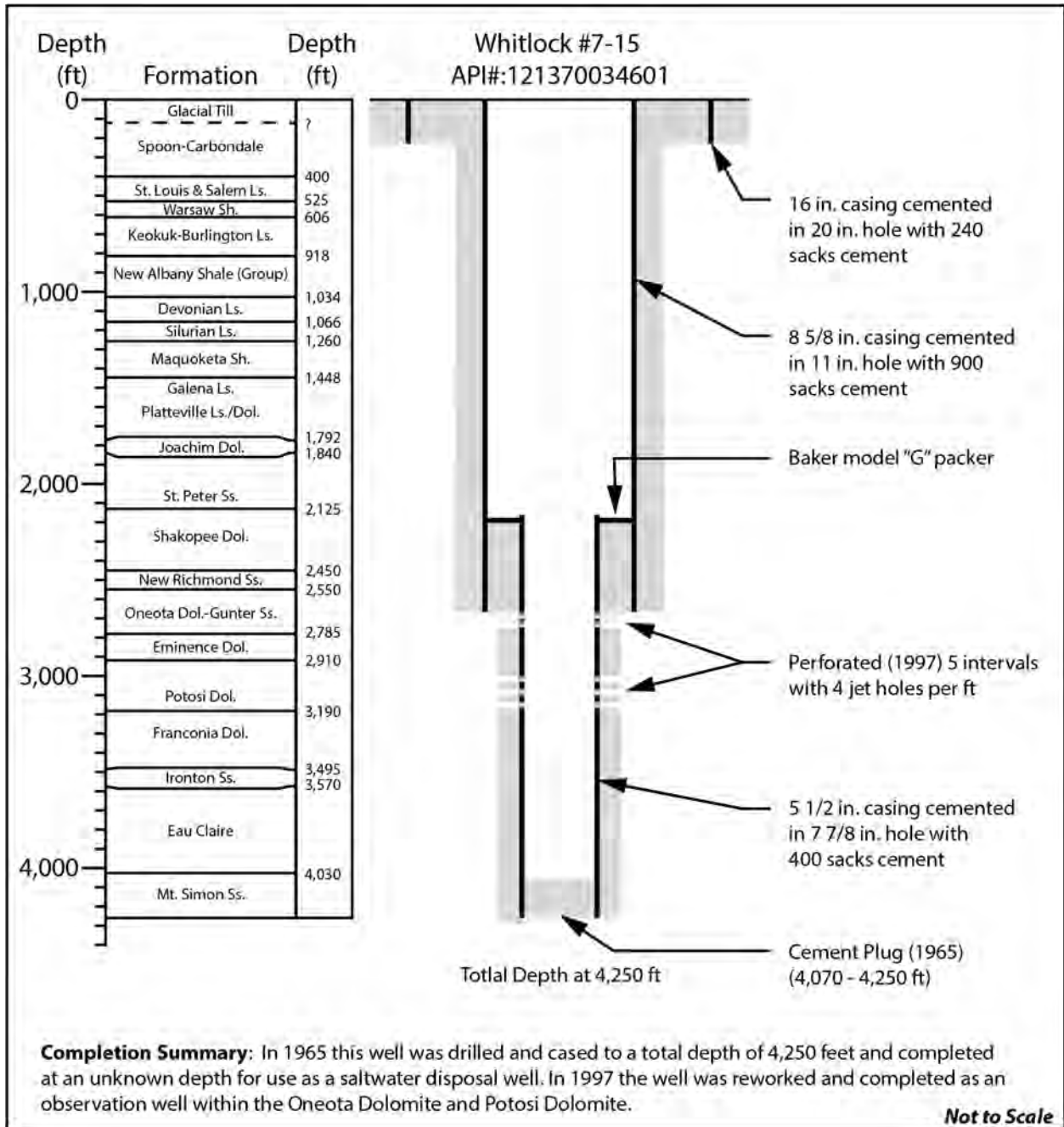


Figure 3.30. Well Construction Diagram for a Deep Borehole (API# 121370034601) in Morgan County that Penetrates the Target Reservoir for CO₂ Sequestration (i.e., Mount Simon Sandstone). Well completion information obtained from ISGS well records (ISGS 2012b).

3.3 References

40 CFR 146.84. Code of Federal Regulations, Title 40, *Protection of Environment*, Part 146, "Underground Injection Control Program: Criteria and Standards." Section 84, "Area of review and corrective action."

75 FR 77230. December 10, 2010. "Federal Requirements Under the Underground Injection Control (UIC) Program for Carbon Dioxide (CO₂) Geologic Sequestration (GS) Wells." *Federal Register*. Environmental Protection Agency.

Akaike H. 1974. "A New Look at Statistical-Model Identification." *IEEE Automat. Contr.* Ac19(6):716-723.

Birkholzer JT, J Apps, L Zhenge, Y Zhang, T Xu and C Tzang. 2008. *Research Project on CO₂ Geological Storage and Groundwater Resources: Large-Scale Hydrological Evaluation and Modeling of the Impact on Groundwater Systems Annual Report: October 1, 2007, to September 30, 2008*. Lawrence Berkeley National Laboratory, Berkeley, California.

Buschbach TC and DC Bond. 1974. *Underground Storage of Natural Gas in Illinois – 1973*. Illinois Petroleum 101, Illinois State Geological Survey, Champaign, Illinois.

Davies PB. 1991. *Evaluation of the Role of Threshold Pressure in Controlling Flow of Waste-Generated Gas into Bedded Salt at the Waste Isolation Pilot Plant (WIPP)*. SAND 90-3246, Sandia National Laboratory, Albuquerque, New Mexico.

EPA (U.S. Environmental Protection Agency). 2011a. *Draft Underground Injection Control (UIC) Program Class VI Well Area of Review Evaluation and Corrective Action Guidance for Owners and Operators*. EPA 816-D-10-007, EPA Office of Water, Washington, D.C.

EPA (U.S. Environmental Protection Agency). 2011b. "Underground Injection Control Permit Application IL-ICCS Project." Administrative Record for Underground Injection Control Permit Application from Archer Daniels Midland Company, EPA Region 5, Chicago Illinois.

EPA (U.S. Environmental Protection Agency). 2011c. "Underground Injection Control Permit Application IL-ICCS Project." Administrative Record for Underground Injection Control Permit Application from Christian County Generation, LLC of Taylorville, EPA Region 5, Chicago Illinois.

EPA (U.S. Environmental Protection Agency). 1994. "Determination of Maximum Injection Pressure for Class I Wells." Underground Injection Control Section Regional Guidance #7. EPA Region 5, Chicago, Illinois.

Haimson BC and FH Cornet. 2003. "ISRM Suggested Methods for rock stress estimation—Part 3: hydraulic fracturing (HF) and/or hydraulic testing of pre-existing fractures (HTPF)." *International Journal of Rock Mechanics and Mining Sciences* 40(7–8):1011-1020.

Hornung J and T Aigner. 1999. "Reservoir and aquifer characterization of fluvial architectural elements: Stubensandstein, Upper Triassic, southwest Germany." *Sedimentary Geology* 129(3–4):215-280.

Hou Z, ML Rockhold, and CJ Murray. 2012. "Evaluating the impact of caprock and reservoir properties on potential risk of CO₂ leakage after injection." *Environmental Earth Sciences* 66(8):2403-2415, doi:10.1007/s12665-011-1465-2.

Hubbert MK and DG Willis. 1957. "Mechanics of hydraulic fracturing." *Petroleum Transactions, AIME*, 210:153-168.

- ISGS (Illinois State Geological Survey). 2012a. ILWATER Interactive Mapping Web Interface. Last accessed on January 4, 2012 at <http://www.isgs.illinois.edu/maps-data-pub/wwdb/launchims.shtml>.
- ISGS (Illinois State Geological Survey). 2012b. Geologic Records Unit (GRU) Website. Last accessed on February 16, 2012 at <http://www.isgs.uiuc.edu/sections/oil-gas/launchims.shtml>.
- ISGS (Illinois State Geological Survey). 2011. Illinois Oil and Gas Resources (ILOIL) Internet Map Service. Last accessed on October 8, 2011 at <http://moulin.isgs.uiuc.edu/ILOIL/webapp/ILOIL.html>
- Kerr DR, L Ye, A Bahar, BM Kelkar, and S Montgomery. 1999. "Glenn Pool Field, Oklahoma: A Case of Improved Production from a Mature Reservoir." *American Association of Petroleum Geologists Bulletin* 83(1):1-18.
- Meyer R and FF Krause. 2006. "Permeability Anisotropy and Heterogeneity of a Sandstone Reservoir Analogue: An Estuarine to Shoreface Depositional System in the Virgelle Member, Milk River Formation, Writing-On-Stone Provincial Park, Southern Alberta." *Bulletin of Canadian Petroleum Geology* 54(4):301-318.
- Pruess K, J Garcia, T Kavscek, C Oldenburg, J Rutqvist, C Steefel, and T Xu. 2002. *Intercomparison of Numerical Simulation Codes for Geologic Disposal of CO₂*. LBNL-51813, Lawrence Berkeley National Laboratory, Berkeley, California.
- Ringrose P, K Nordahl, and RJ Wen. 2005. "Vertical permeability estimation in heterolithic tidal deltaic sandstones." *Petroleum Geoscience* 11(1):29-36.
- Saller AH, J Schwab, S Walden, S Robertson, R Nims, H Hagiwara, and S Mizohata. 2004. "Three-dimensional seismic imaging and reservoir modeling of an upper Paleozoic "reefal" buildup, Reinecke Field, west Texas, United States." Pp. 107-125 in GP Eberli, JL Masferro, and JF Sarg (eds.), *Seismic Imaging of Carbonate Reservoirs and Systems*, Volume 81, American Association of Petroleum Geologists, Tulsa, Oklahoma.
- Span R and W Wagner. 1996. "A New Equation of State for Carbon Dioxide Covering the Fluid Region from the Triple-Point Temperature to 1100 K at Pressures Up to 800 MPa." *J Phys Chem Ref Data* 25:1509-1596.
- Spycher N and K Pruess. 2010. "A Phase-Partitioning Model for CO₂-Brine Mixtures at Elevated Temperatures and Pressures: Application to CO₂-Enhanced Geothermal Systems." *Transport in Porous Media* 82:173-196. doi:10.1007/s11242-009-9425-y.
- Spycher N, K Pruess, and J Ennis-King. 2003. "CO₂-H₂O mixtures in geological sequestration of CO₂. I. Assessment and calculation of mutual solubilities from 12 to 100°C and up to 600 bar." *Geochimica et Cosmochimica Acta* 67(16):3015-3031. doi:10.1016/s0016-7037(03)00273-4.
- Suekane T, NH Thanh, T Matsumoto, M Matsuda, M Kiyota, and A Ousaka. 2009. "Direct measurement of trapped gas bubbles by capillarity on the pore scale." *Energy Procedia* 1(1):3189-3196, doi:10.1016/j.egypro.2009.02.102.

Venables WN and BD Ripley. 2002. *Modern applied statistics with S*. Springer Science+Business Media, New York, New York.

White MD, DH Bacon, BP McGrail, DJ Watson, SK White, and ZF Zhang. 2012. *STOMP Subsurface Transport Over Multiple Phases: STOMP-CO₂ and STOMP-CO₂e Guide, Version 1.0*. PNNL-21268, Pacific Northwest National Laboratory, Richland, Washington.

White MD and M Oostrom. 2006. *STOMP Subsurface Transport Over Multiple Phases, Version 4: User's Guide*. PNNL-15782, Pacific Northwest National Laboratory, Richland, Washington.

White MD and M Oostrom. 2000. *STOMP Subsurface Transport Over Multiple Phases: Theory Guide*. PNNL-12030, Pacific Northwest National Laboratory, Richland, Washington.

Zhou Q, JT Birkholzer, E Mehnert, Y-F Lin, and K Zhang. 2010. "Modeling basin- and plume-scale processes of CO₂ storage for full-scale deployment." *Ground Water* 48(4):494–514.

Zoback MD, CA Barton, M Brudy, DA Castillo, T Finkbeiner, BR Grollimund, DB Moos, P Peska, CD Ward, and DJ Wiprut. 2003. "Determination of stress orientation and magnitude in deep wells." *International Journal of Rock Mechanics and Mining Sciences* 40(7–8):1049-1076.